Quantum Critical Phenomena of Relativistic Fermions in $1+1$d and $2+1$d

by

Hanqing Liu

Department of Physics
Duke University

Date: _____

Approved:

_____
Shailesh Chandrasekharan, Advisor

_____
Ribhu Kaul

_____
Thomas Mehen

_____
Ashutosh Kotwal

_____
Iman Marvian

Dissertation submitted in partial fulfillment of the requirements for the degree of
Doctor of Philosophy in the Department of Physics
in the Graduate School of Duke University
2022

Abstract

Quantum Critical Phenomena of Relativistic Fermions in $1+1$d and $2+1$d

by

Hanqing Liu

Department of Physics
Duke University

Date: _____

Approved:

_____
Shailesh Chandrasekharan, Advisor

_____
Ribhu Kaul

_____
Thomas Mehen

_____
Ashutosh Kotwal

_____
Iman Marvian

An abstract of a dissertation submitted in partial fulfillment of the requirements for the degree of Doctor of Philosophy in the Department of Physics in the Graduate School of Duke University
2022

Abstract

In this dissertation, we study the phase structures and the quantum critical phenomena of relativistic lattice fermions with $\mathrm{O}(2N_f)$ symmetry in one and two spatial dimensions, motivated by the ability to perform efficient Monte Carlo simulations. Close to a quantum critical point, physics is universal and can be described by continuum quantum field theories. We perform a perturbative analysis of all independent four-fermion interactions allowed by the $\mathrm{O}(2N_f)$ symmetry near the free-fermion fixed point. We then analyze the resulting continuum field theories using various techniques. In one spatial dimension, we use the powerful tools from conformal field theory and non-abelian bosonization to understand the renormalization group flows, the correlation functions, and the spectra. In the case of $N_f = 2$, we find that by tuning a Hubbard coupling, our model undergoes a second-order phase transition, which can be described by an $\mathrm{SU}(2)_1$ Wess-Zumino-Witten model perturbed by a marginal coupling. We confirm these results using the meron-cluster algorithm, and locate the critical point precisely using exact diagonalization based on the spectrum of the Wess-Zumino-Witten model. In two spatial dimensions, we analyze the model using ε expansion, large N_f expansion and effective potential methods. In the case of $N_f = 2$, we find a novel critical point where the anti-ferromagnetic order and superconducting-CDW order become simultaneously quantum critical, which seems to have been missed in literature. We compare these predictions with the numerical results obtained using the fermion-bag algorithm by Emilie Huffman.

Dedication

Dedicated to my mother, and in memory of my father and grandparents.

Contents

List of Tables

List of Figures

List of Abbreviations and Symbols

Symbols

d	Spatial dimension
$c_i, c_i^\dagger$	Lattice Dirac fermions
γ_i	Lattice Majorana fermions
$\psi(x)$	Continuum Dirac fermions
$\xi(x)$	Continuum Majorana fermions
$\varepsilon_{\mu\nu}$	Levi-Civita symbol defined with $\varepsilon_{01} = 1$
tr, det	Trace and determinant over matrices or local Hilbert space
Tr, Det	Trace and determinant over full Hilbert space

Abbreviations

AFM	anti-ferromagnetic
BSS	Blankenbecler-Scalapino-Sugar
CDW	charge density wave
CFT	conformal field theory
DMRG	density matrix renormalization group
GN	Gross-Neveu
GNY	Gross-Neveu-Yukawa
IR	infrared
irrep	irreducible representation

LGW	Landau-Ginzburg-Wilson
LSM	Lieb-Schultz-Mattis
MC	Monte Carlo
OPE	operator product expansion
QFT	quantum field theory
RG	renormalization group
SPT phase	symmetry-protected topological phase
UV	ultraviolet
VBS	valance-bond solid
VEV	vacuum expectation value
WZW	Wess-Zumino-Witten

Acknowledgements

First and foremost, I would like to express my deep and sincere gratitude to my advisor Shailesh Chandrasekharan, without whom this dissertation would not be possible. He not only guides me through the research, but also is very supportive both academically and in life. I would also like to thank the committee members Ribhu Kaul, Ashutosh Kotwal, Iman Marvian, and Thomas Mehen for reading this dissertation and giving feedback.

I also learned quite a lot from my co-advisors Iman Marvian and Ribhu Kaul. For example, from Iman I learned to keep asking questions for true understanding, and from Ribhu, I learned to be skeptical about things you do not truly understand and the importance of knowing experiments. I am also grateful to my collaborator Emilie Huffman for the numerical works.

The constant discussion with Mendel Nguyen and Hersh Singh across many areas in physics has been a treasure of my whole graduate study. I have also benefited from numerous conversations with my fellow graduate students Austin Hulse, Peifan Liu, Zhe Wang, Xiaojun Yao, Xin Zhang, and Yiqiu Zhao, as well as professors Paul Aspinwall, Hubert Bray, Ronen Plesser, Arya Roy, Yuya Tanizaki, and Mithat Ünsal. I am grateful to professors Jian-Guo Liu, Thomas Mehen, Roxanne Springer, and Stephen Teitsworth for their encouragement and support.

I would also like to thank Professor Robert Parkins for teaching me organ with extreme patience for almost five years.

My graduate study has been supported by the U.S. Department of Energy, Office of Science, Nuclear Physics program under Award No.DE-FG02-05ER41368, the Duke Graduate School travel award, and the Fritz London Fellowship from the Duke physics department, as well as the support from the summer schools at RPI and Cargèse, France.

1

Introduction

All happy families are alike; each unhappy family is unhappy in its own way.
—Lev Tolstoy, *Anna Karenina*

1.1 Quantum phase transitions and quantum critical phenomena

Nature is complex. Classifying matter into phases and studying the phase transitions between them have been a fruitful way to understand nature. While most familiar phases and phase transitions occur at finite temperatures, many exotic ones only arise at zero temperature, which are known as quantum phases and quantum phase transitions [1]. The study of them has led to insights into exotic phases of matter in both condensed matter physics and high energy physics, from quantum Hall effect and high-temperature superconductivity, to quark-gluon plasma and color superconductivity inside neutron stars.

A quantum phase transition is most exciting when it is second order, where the quantum fluctuations, usually swept away by thermal fluctuations at finite temperatures, become dominant. At the point in parameter space where such a transition

occurs, known as a quantum critical point, the correlation length measured in the unit of microscopic length scale diverges, and therefore the long-distance physics of the system becomes scale-invariant. In most cases, the long-range physics can be described by a handful of quantities. The way these quantities depend on the scales is known as scaling relations, and can be characterized by the so-called critical exponents. The critical exponents are not sensitive to the details of the microscopic structures, or in other words, they are universal. From the perspective of the renormalization group (RG), universality arises because long-range physics is characterized by a unique fixed point, and the number of relevant operators at the fixed point is usually quite limited.

The most successful approach to understanding phase transitions is through spontaneous symmetry breaking and RG, known as the Landau-Ginzburg-Wilson (LGW) approach [2, 3, 4, 5]. The idea behind the LGW approach is that the phases of matter should be classified by how the symmetries are presented, and in particular, whether the symmetries are spontaneously broken or not. In this approach, the physics of the quantum critical point is usually described by the fluctuation of the order parameters. In this dissertation, this is the approach we will adopt to understand quantum critical points in lattice fermion systems.

While the traditional LGW approach has been very successful, in recent decades, many new types of quantum phase transitions have been discovered that seem cannot be described by it. These second-order phase transitions usually separate gapped phases indistinguishable through their symmetry properties, or in some instances break distinct symmetries, both of which are forbidden in the LGW paradigm. Here a gapped quantum phase means a phase with a finite energy gap between the ground states and excited states in the thermodynamic limit. From a modern perspective, gapped quantum phases can be viewed as equivalent classes of gapped ground states connected by local adiabatic changes without closing the gap [6, 7]. This point of

view means that there can exist different gapped phases with the same symmetry, if they can only be distinguished by non-local properties, such as the ground state entanglement properties. Topological invariants are also valuable properties, which are integers that cannot change in any adiabatic process, but can change when crossing phase boundaries, such as winding number, linking number, and in many cases, simply ground state degeneracy.

A gapped phase with a nondegenerate ground state is called a trivially gapped phase. Of more interest are the many non-trivially gapped phases, for example, phases with topological order [8], which are gapped phases with long-range entanglement [7], and symmetry-protected topological (SPT) phases [9, 10], which are phases that are only distinguishable under symmetry-preserving Hamiltonians, and are characterized by short-range entangled degenerate ground states and edge states that represent an anomaly associated with the symmetry group [11]. It has also been shown recently that fermion masses can be generated by strong four-fermion interactions without spontaneous symmetry breaking [12, 13, 14, 15, 16], which has a deep connection to the SPT phases [17].

In addition to these phases that are indistinguishable by symmetries, there are also quantum critical points that immediately separate phases breaking distinct symmetries, such as the so-called deconfined quantum critical points, whose quantum fluctuation is described by an emergent gauge field, rather than the ordinary order parameters [18, 19, 20, 21, 22]. Nonetheless, there have been attempts recently to fit all these exotic quantum phases and quantum phase transitions into a generalized LGW paradigm using generalized symmetries [23], including higher-form symmetries [24, 25] and non-invertible symmetries [26, 27, 28]. For example, topological orders can be understood through the spontaneous breaking of higher-form symmetries [29].

Another valuable tool to understand quantum phases is anomaly, or more precisely, 't Hooft anomaly. An anomaly is preserved in any symmetry-preserving de-

formation of the theory and in particular, is RG invariant. Therefore it can create substantial restrictions on the infrared (IR) physics through 't Hooft anomaly matching [30]. In particular, if a theory has a 't Hooft anomaly in the ultraviolet (UV), then the IR theory cannot be trivially gapped [25]. Instead, it can only be either gapless or non-trivially gapped, including spontaneously breaking certain symmetry or topologically ordered [31, 23]. A famous example is the Lieb-Schultz-Mattis (LSM) theorem [32, 33, 34], in which the symmetries of a lattice Hamiltonian, being UV properties, can impose constraints on the ground state degeneracy, which is in the deep IR. This is an old theorem but recently received new insights in terms of a mixed 't Hooft anomaly between spin rotation symmetry and lattice translation symmetry [35, 31, 36, 37, 38, 39]. Later in this dissertation, we will use similar arguments to understand the ground state degeneracy of our lattice models.

1.2 Quantum critical phenomena of lattice fermions

In this dissertation, we are interested in the quantum critical phenomena arising in interacting lattice fermion models, which will help us understand strongly coupled quantum field theories (QFTs). The strongly coupled QFTs are usually poorly understood analytically because they are beyond the capability of perturbative analysis. However, when a lattice regularization for such strongly coupled QFT exists, it is possible to recover the continuum physics near a quantum critical point on a lattice model. In fact, this can be viewed as a way to define a strongly coupled QFT non-perturbatively. One powerful first principle method to study the lattice models is the Monte Carlo (MC) method [40]. Unfortunately, Monte Carlo studies of quantum critical phenomena involving lattice fermions suffer from the notorious sign problem [41]. Therefore designing lattice fermion models that contain interesting quantum critical points while being free of the sign problems is an important area of research.

One such model that is amenable to efficient Monte Carlo simulations is given by

the following Hamiltonian

$$H_\kappa = -\sum_{\langle i,j\rangle} \exp\left(\kappa\eta_{ij} \sum_{\alpha=1}^{N_f} c_i^{\alpha\dagger} c_j^{\alpha} + c_j^{\alpha\dagger} c_i^{\alpha}\right), \tag{1.1}$$

where i and j are lattice sites on a bipartite lattice and the sum is over all the nearest-neighbor pairs of sites $\langle i,j\rangle$, $c_i^{\alpha\dagger}$ and c_i^{α} are the usual fermionic creation and annihilation operators, $\alpha = 1, \cdots, N_f$ is the flavor index, η_{ij} is the π flux phase which renders relativistic fermions in the continuum, and κ is the coupling of the model. In particular, when κ is small, the Hamiltonian is very close to the Hamiltonian of staggered fermions [42], which describes free massless fermions at low energies. When κ gets larger, new and interesting phases may appear, and by tuning κ, we can study the quantum phase transitions that turn out to be second order. For generic κ, this Hamiltonian can be simulated efficiently using the fermion bag algorithm [43, 44]. In the limit $\kappa \to \infty$, it can be simulated even more efficiently with the meron-cluster algorithm [45, 46, 47].

An interesting feature of the above lattice model is that it preserves all the symmetries of the free lattice fermions, in particular, the O($2N_f$) symmetry. As we will show in the next chapter, together with lattice translation symmetry, this O($2N_f$) symmetry leads to an interesting degeneracy of spectrum when the lattice size is a multiple of four. Actually, from the mixed 't Hooft anomaly between the lattice translation symmetry and the particle number symmetry U(1), which is a subgroup of the O($2N_f$) symmetry, we already know that the model cannot be trivially gapped in the continuum limit. However, with the additional O($2N_f$) symmetry, the ground states of the model are degenerate even in a finite volume.

We also note that the case of $N_f = 2$ is special for several reasons. First, the two components in this case can be viewed as the spins of a spin-half particle, like an electron, and therefore the critical phenomena might be observed in real materials.

Furthermore, the adjoint representation of SO(4) is reducible, because it can be viewed as spin and charge symmetries $\mathrm{SU}(2)_s \times \mathrm{SU}(2)_c$. Therefore we can have independent spin and charge couplings if the O(4) symmetry is broken down to SO(4) by some interactions. One such interaction is the well-known Hubbard interaction,

$$H_U = U \sum_j (n_j^1 - 1/2)(n_j^2 - 1/2), \tag{1.2}$$

where $n_j^\alpha = c_j^{\alpha\dagger} c_j^\alpha$ is the particle number operator. The improper part of the O(4) symmetry can be identified as a spin-charge flip symmetry $\mathbb{Z}_2^{sc}$, which plays an important role at the quantum critical point. Our Monte Carlo results mainly focus on the case of $N_f = 2$, and in this dissertation, we will refer to the sum of Eq. (1.1) and Eq. (1.2) as "our lattice model".

1.3 Continuum QFTs of our lattice fermion models

Near the quantum critical points, the leading correlation length of the lattice model diverges in the lattice unit, and the long-distance physics can be described by a continuum QFT [48, 49]. One of the main goals of this dissertation is to identify and study the continuum QFTs that emerge in the vicinity of the quantum critical point of our Hamiltonian H_κ. In this process, the $\mathrm{O}(2N_f)$ symmetry and other lattice symmetries of our microscopic models play a crucial role because they are RG invariant.

In order to identify the emergent QFTs, we adopt a perturbative approach by starting from the weak coupling regime, which is close to the free-fermion fixed point. Then we analyze all the four-fermion interactions allowed by the $\mathrm{O}(2N_f)$ symmetry, which are the most relevant interactions near the free-fermion fixed point. Field theories with four-fermion interactions originated from high energy physics a long time ago [50, 51, 52], but recently they have also gained popularity in the condensed

matter literature as a description of low-energy physics of Dirac semi-metals, with graphene as the most prominent example [53, 54, 55].

All relativistically invariant four-fermion interactions can be built out of mass terms and currents, known as Gross-Neveu (GN) type [51, 56] and Thirring type [52] respectively. Here mass terms [57] and currents are fermion bilinears that are relativistically invariant and covariant respectively, but are allowed to transform non-trivially under the internal non-abelian symmetry. In general, these two types of interactions can behave quite differently. For example, by tuning the four-fermion couplings, the Gross-Neveu model in two spatial dimensions undergoes a phase transition from a massless phase to a massive phase with spontaneously broken parity symmetry for arbitrary N_f. In contrast, such transition occurs in the Thirring model only when N_f is below a critical value N_{crit}, whose precise value is still controversial [58, 59, 60, 61, 62, 63]. However, as we will show in this dissertation later, in the presence of the $\mathrm{O}(2N_f)$ symmetry, Gross-Neveu type and Thirring type interactions are equivalent. In fact, only one independent four-fermion interaction is allowed by the $\mathrm{O}(2N_f)$ symmetry in one spatial dimension, while there are four in two spatial dimensions, all of which can be chosen as Gross-Neveu type. Furthermore, in the case of $N_f = 2$ with SO(4) symmetry, one more Gross-Neveu type interaction is allowed in both cases.

Gross-Neveu type interactions built out of mass terms transforming under different representations of the non-abelian symmetry groups usually have different symmetry breaking patterns, leading to different universality classes at the quantum critical points. For example, in two spatial dimensions, some of these universality classes are known in the literature as "chiral-Ising", "chiral-XY" and "chiral-Heisenberg" universality class, although there is really no chiral symmetry in these cases. One of the main results of this dissertation is that in the case of $N_f = 2$ in two spatial dimensions, the presence of $\mathbb{Z}_2^{sc}$ symmetry leads to a new university class,

where the anti-ferromagnetic (AFM) order parameter and superconducting-CDW order parameter become simultaneously quantum critical, which we dubbed the name "chiral spin-charge symmetric" university class. To the best of our knowledge, this universality class has not been explored in the literature before.

The remaining chapters of this dissertation are organized as follows. In Chapter 2, we give more details of our lattice fermion Hamiltonians and discuss their symmetries. We also prove an interesting theorem regarding the degeneracy of the spectrum, and discuss its relation to anomaly and implications for the ground states of our models. In Chapter 3, we derive the continuum limit of the free lattice fermions in one and two spatial dimensions. We also discuss the (emergent) symmetries of the continuum theory and how the lattice symmetries are embedded in the continuum symmetries. In Chapter 4, we analyze all the four-fermion interactions allowed by the lattice symmetries, especially the $\mathrm{O}(2N_f)$ symmetry. We also discuss the special case of $N_f = 2$ with SO(4) symmetry. In Chapter 5, we analyze the physics of our model in one spatial dimension using techniques from 2d conformal field theory (CFT) and bosonization. In particular, we use operator product expansions (OPEs) to calculate the β functions and the correlation functions of observables on the lattice. In Chapter 6, we study the physics of our model with $N_f = 2$ in two spatial dimensions. We study the phases of the model by calculating the effective potential, the β functions and critical exponents in $4 - \varepsilon$ space-time dimensions [64, 65]. Our predictions are then compared with Monte Carlo and other numerical results in Chapter 7.

2

The Lattice Model

This chapter introduces the Hamiltonian lattice fermion models we study in this dissertation. These models lead to interesting relativistic Dirac fermions in the continuum limit, which we will discuss in the following chapters. We first discuss free lattice fermions to motivate our lattice models and point out an $\mathrm{O}(2N_f)$ symmetry. We then introduce our models, which are essentially strongly interacting versions of the free models with the same $\mathrm{O}(2N_f)$ symmetry. Interestingly, this $\mathrm{O}(2N_f)$ symmetry implies that the degeneracy of all energy eigenstates is an even number under some reasonable assumptions, which is presented as a theorem at the end of this chapter. We also discuss the implication of this degeneracy for our model and its connection to 't Hooft anomaly matching.

2.1 Free lattice fermions

One standard way to construct free massless fermions in d spatial dimension on the lattice is through staggered fermions [42]. We begin with a d dimensional cubic lattice with periodic boundary conditions, and the Hamiltonian of N_f staggered fermions is

given by

$$H_0 = -t \sum_{\alpha=1}^{N_f} \sum_i \sum_\mu \eta_{i,\mu} c_i^{\alpha\dagger} c_{i+e_\mu}^{\alpha} + \text{H.c.}, \tag{2.1}$$

where $c_i^{\alpha\dagger}$ and c_i^{α} are the usual fermionic creation and annihilation operators, $\alpha = 1, \cdots, N_f$ is the flavor index, i is summed over all the sites on the d dimensional lattice, e_μ is the unit vector of the lattice in the μ direction and $\mu = 1, \cdots, d$. The phase factor $\eta_{i,\mu} = (-1)^{\sum_{\nu=1}^{\mu-1} i_\nu}$, where i_ν is the coordinate of i in the e_ν direction. When $d = 1$, the Hamiltonian can be simply written as

$$H_0 = -t \sum_{j,\alpha} c_j^{\alpha\dagger} c_{j+1}^{\alpha} + c_{j+1}^{\alpha\dagger} c_j^{\alpha}, \tag{2.2}$$

and when $d = 2$, we can write

$$H_0 = -t \sum_{n_1 n_2, \alpha} c_{n_1 n_2}^{\alpha\dagger} c_{n_1+1 n_2}^{\alpha} + (-1)^{n_1} c_{n_1 n_2}^{\alpha\dagger} c_{n_1 n_2+1}^{\alpha} + \text{H.c.}. \tag{2.3}$$

Note that in the case of 2 spatial dimensions, there is another lattice with relativistic dispersion relation, i.e., the honeycomb lattice, which is of much interest in the condensed matter literature [66].

2.1.1 Symmetries of the free lattice fermions

These lattice fermions have a set of standard discrete symmetries. The most obvious one is the symmetry group of d-dimensional cubic lattice: translations by one lattice spacing in the e_μ direction T_a^μ, and the hyperoctahedral group B_d, which is the symmetry group of a d-dimensional hypercube containing parity P. In addition, it also has time reversal symmetry Θ and charge conjugation symmetry C.

In one spatial dimension, $B_1 \cong \mathbb{Z}_2$ is simply the parity P. These symmetry

transformations act on the fermion operators as

$$\text{unit translation:} \quad T_a c_j T_a^{-1} = c_{j+1}, \tag{2.4}$$

$$\text{parity:} \quad P c_j P^{-1} = c_{-j}, \tag{2.5}$$

$$\text{time reversal:} \quad \Theta c_j \Theta^{-1} = c_j, \quad \Theta \mathrm{i} \Theta^{-1} = -\mathrm{i}, \tag{2.6}$$

$$\text{charge conjugation:} \quad C c_j C^{-1} = (-1)^j c_j^\dagger. \tag{2.7}$$

In two spatial dimensions B_2 is isomorphic to the dihedral group $D_4 \cong \mathbb{Z}_4 \rtimes \mathbb{Z}_2$, generated by $\frac{\pi}{2}$ rotation R and parity P. These symmetry transformations act on the fermion operators as

$$\text{translation by } e_1\text{:} \quad T_1 c_{n_1 n_2} T_1^{-1} = (-1)^{n_2} c_{n_1+1, n_2}, \tag{2.8}$$

$$\text{translation by } e_2\text{:} \quad T_2 c_{n_1 n_2} T_2^{-1} = c_{n_1, n_2+1}, \tag{2.9}$$

$$\frac{\pi}{2} \text{ spatial rotation:} \quad R c_{n_1 n_2} R^{-1} = (-1)^{n_1 n_2} c_{-n_2, n_1}, \tag{2.10}$$

$$\text{parity:} \quad P c_{n_1 n_2} P^{-1} = c_{-n_1, n_2}, \tag{2.11}$$

$$\text{time reversal:} \quad \Theta c_{n_1 n_2} \Theta^{-1} = c_{n_1 n_2}, \quad \Theta \mathrm{i} \Theta^{-1} = -\mathrm{i}, \tag{2.12}$$

$$\text{charge conjugation:} \quad C c_{n_1 n_2} C^{-1} = (-1)^{n_1+n_2} c_{n_1 n_2}^\dagger. \tag{2.13}$$

In addition to these lattice symmetries, since the lattices are bipartite, free lattice fermions also have an $\mathrm{O}(2N_f)$ internal symmetry. This internal symmetry is easily observed in the Majorana representation. Consider a simple hopping term $c_i^{\alpha\dagger} c_j^\alpha + c_j^{\alpha\dagger} c_i^\alpha$, where i and j are on different sublattices. We define two Majorana operators $\gamma_j^{2\alpha-1}$ and $\gamma_j^{2\alpha}$ from each c_j^α operator through the following relations

$$c_j^\alpha =: \frac{\mathrm{i}^j}{2}(\gamma_j^{2\alpha-1} - \mathrm{i}\gamma_j^{2\alpha}), \quad c_j^{\alpha\dagger} =: \frac{(-\mathrm{i})^j}{2}(\gamma_j^{2\alpha-1} + \mathrm{i}\gamma_j^{2\alpha}), \tag{2.14}$$

where γ_j^α satisfies $\{\gamma_i^\alpha, \gamma_j^\beta\} = 2\delta_{ij}\delta_{\alpha\beta}\mathbb{1}$. Then we have

$$\sum_{\alpha=1}^{N_f} c_i^{\alpha\dagger} c_j^\alpha + c_j^{\alpha\dagger} c_i^\alpha = \sum_{\alpha=1}^{2N_f} \frac{\mathrm{i}^{j-i}}{2} \gamma_i^\alpha \gamma_j^\alpha. \tag{2.15}$$

Notice that both sides are symmetric under $i \leftrightarrow j$ as desired. Clearly this term has $\mathrm{O}(2N_f)$ symmetry generated by the operators $\Gamma^{\alpha\beta} := \mathrm{i}\sum_j \gamma_j^\alpha \gamma_j^\beta$, under which γ_i^α transforms as an $\mathrm{O}(2N_f)$ vector.

Free fermion Hamiltonians are quadratic in the fermion creation/annihilation operators and translationally invariant, and therefore can be diagonalized in the momentum space. We obtain the energy of single-particle excitations over the vacuum state as a function of momentum, giving the dispersion relation of the low-energy particles. When considering excitations with wavelengths much larger than the lattice spacing, we can focus on modes near the Fermi points. Using these low-energy modes, we can derive the effective Hamiltonian in the continuum. We will discuss the details in the next chapter.

2.2 Interacting lattice Hamiltonians with $\mathrm{O}(2N_f)$ symmetry

We now wish to construct an interacting lattice Hamiltonian with all the symmetries of the free lattice Hamiltonian. Our choice will be

$$H_\kappa = -\sum_{\langle i,j\rangle} \exp\left(\kappa\eta_{ij} \sum_{\alpha=1}^{N_f} (c_i^{\alpha\dagger} c_j^\alpha + c_j^{\alpha\dagger} c_i^\alpha)\right), \tag{re 1.1}$$

which is motivated by the fact that it is sign-problem-free [67] and can be simulated efficiently using the fermion bag algorithm [43, 44]. Since each bond of this Hamiltonian only depends on the free Hamiltonian bond $\sum_\alpha c_i^{\alpha\dagger} c_j^\alpha + c_j^{\alpha\dagger} c_i^\alpha$, clearly it has all the symmetries of the free lattice fermion, and in particular, it has the $\mathrm{O}(2N_f)$ internal symmetry. Note that $\kappa > 0$ is a free parameter in the theory, and as we will discuss below, it will play the role of a tunable coupling. When κ is small, the theory is almost free.

2.2.1 The conventional form of our lattice model

In order to understand the role of κ, it is helpful to express the lattice Hamiltonian Eq. (1.1) in a more conventional form. Since the hopping term at different layers commute, we can expand the exponential and write

$$H_\kappa = -\sum_{\langle i,j\rangle}\prod_{\alpha=1}^{N_f}\exp\left(\kappa\eta_{ij}(c_i^{\alpha\dagger}c_j^{\alpha}+c_j^{\alpha\dagger}c_i^{\alpha})\right). \tag{2.16}$$

As in the free theory, the $\mathrm{O}(2N_f)$ symmetry is manifest in the Majorana language, which is also useful for rewriting the Hamiltonian in a more conventional form,

$$H_\kappa = -\sum_{\langle i,j\rangle}\prod_{\alpha=1}^{2N_f}\exp\left(\kappa\eta_{ij}\frac{\mathrm{i}^{j-i}}{2}\gamma_i^{\alpha}\gamma_j^{\alpha}\right) = -\sum_{\langle i,j\rangle}\prod_{\alpha=1}^{2N_f}\Big(\cosh\frac{\kappa}{2}+\sinh\frac{\kappa}{2}\eta_{ij}\mathrm{i}^{j-i}\gamma_i^{\alpha}\gamma_j^{\alpha}\Big), \tag{2.17}$$

Focusing on a single Dirac flavor on a single bond, we have

$$\begin{aligned}
&\exp\left(\kappa\eta_{ij}(c_i^{\alpha\dagger}c_j^{\alpha}+c_j^{\alpha\dagger}c_i^{\alpha})\right)\\
&=\cosh\frac{\kappa}{2}\sinh\frac{\kappa}{2}\eta_{ij}\mathrm{i}^{j-i}(\gamma_i^{2\alpha-1}\gamma_j^{2\alpha-1}+\gamma_i^{2\alpha}\gamma_j^{2\alpha})+\Big(\sinh\frac{\kappa}{2}\Big)^2\gamma_i^{2\alpha-1}\gamma_i^{2\alpha}\gamma_j^{2\alpha-1}\gamma_j^{2\alpha}+\Big(\cosh\frac{\kappa}{2}\Big)^2\\
&=2\cosh\frac{\kappa}{2}\sinh\frac{\kappa}{2}\eta_{ij}(c_i^{\alpha\dagger}c_j^{\alpha}+c_j^{\alpha\dagger}c_i^{\alpha})-4\Big(\sinh\frac{\kappa}{2}\Big)^2\Big(n_i^{\alpha}-\frac{1}{2}\Big)\Big(n_j^{\alpha}-\frac{1}{2}\Big)+\Big(\cosh\frac{\kappa}{2}\Big)^2.
\end{aligned} \tag{2.18}$$

Multiplying these terms from all the flavors, we obtain a highly complicated set of multi-fermion interactions. It is well known that multi-fermion interactions are highly irrelevant perturbatively at the free fermion fixed point in one spatial dimension and higher, and only quadratic and quartic terms are important. Up to these orders, the Hamiltonian can be written as

$$\begin{aligned}
H_\kappa \approx &-\sum_{\langle i,j\rangle}\sum_{\alpha=1}^{N_f}t\eta_{ij}(c_i^{\alpha\dagger}c_j^{\alpha}+c_j^{\alpha\dagger}c_i^{\alpha})-2t\tanh\frac{\kappa}{2}\Big(n_{i\alpha}-\frac{1}{2}\Big)\Big(n_{j\alpha}-\frac{1}{2}\Big)\\
&+\sum_{\alpha<\beta}2t\tanh\frac{\kappa}{2}(c_i^{\alpha\dagger}c_j^{\alpha}+c_j^{\alpha\dagger}c_i^{\alpha})(c_i^{\beta\dagger}c_j^{\beta}+c_j^{\beta\dagger}c_i^{\beta}),
\end{aligned} \tag{2.19}$$

where $t = 2(\cosh\frac{\kappa}{2})^{2N_f-1}\sinh\frac{\kappa}{2}$. Notice that

$$\Big(n_{i\alpha}-\frac{1}{2}\Big)\Big(n_{j\alpha}-\frac{1}{2}\Big) = -\frac{1}{2}(c_i^{\alpha\dagger}c_j^{\alpha}+c_j^{\alpha\dagger}c_i^{\alpha})^2-\frac{1}{4}, \tag{2.20}$$

and therefore, we can rewrite

$$H_\kappa \approx -\sum_{\langle i,j\rangle}\Big(\sum_{\alpha=1}^{N_f} t\eta_{ij}(c_i^{\alpha\dagger}c_j^{\alpha}+c_j^{\alpha\dagger}c_i^{\alpha}) + t\tanh\frac{\kappa}{2}\Big(\sum_{\alpha=1}^{N_f} c_i^{\alpha\dagger}c_j^{\alpha}+c_j^{\alpha\dagger}c_i^{\alpha}\Big)^2\Big), \tag{2.21}$$

Here we would like to point out that the quadratic and quartic terms of our Hamiltonian are identical to the one studied recently in [68], when we set $J = 4t\tanh\frac{\kappa}{2}$ in their notation. We will also use $\mathbf{g} := 2\tanh\frac{\kappa}{2}$ later for convenience. Notice that when $\kappa\to\infty$, i.e., $\mathbf{g}=2$, our model can be simulated very efficiently using the meron-cluster algorithm [46].

Later in Chapter 7, we will discuss the model at $\kappa\to\infty$ (i.e., $\mathbf{g}=2$) and $N_f=2$ extensively. In this limit, the exponential operator of a single Dirac flavor on a single bond can be written as

$$\exp\big(\kappa\eta_{ij}(c_i^{\alpha\dagger}c_j^{\alpha}+c_j^{\alpha\dagger}c_i^{\alpha})\big) \propto \eta_{ij}(c_i^{\alpha\dagger}c_j^{\alpha}+c_j^{\alpha\dagger}c_i^{\alpha}) - 2\Big(n_i^{\alpha}-\frac{1}{2}\Big)\Big(n_j^{\alpha}-\frac{1}{2}\Big)+\frac{1}{2}. \tag{2.22}$$

2.2.2 The case of $N_f = 2$ with SO(4) symmetry

It is also interesting to ask what if we relax the $\mathrm{O}(2N_f)$ symmetry to $\mathrm{SO}(2N_f)$. An interaction that is invariant under $\mathrm{SO}(2N_f)$ transformations but not $\mathrm{O}(2N_f)$ necessarily transforms as the determinant of the $\mathrm{O}(2N_f)$ transformations, and the simplest choice is $\sum_j \gamma^1\gamma^2\cdots\gamma^{2N_f}$. When $N_f\geq 3$, this term would be highly irrelevant at the free fermion fixed point. On the other hand, when $N_f=2$, this is a four-fermion interaction, also known as a Hubbard interaction,

$$H_U = -\frac{U}{4}\sum_j \gamma_j^1\gamma_j^2\gamma_j^3\gamma_j^4 = U\sum_j\Big((n_j^1-1/2)(n_j^2-1/2)+1/4\Big). \tag{2.23}$$

Our lattice model, Eq. (2.23) together with Eq. (1.1), can be simulated efficiently using both fermion-bag and meron-cluster algorithms. By tuning κ (or equivalently $\mathbf{g}$) and U, we can reach interesting quantum critical points in both one spatial dimension and two spatial dimensions. We will discuss these quantum phase transitions in detail later.

We end this chapter with an observation that lattice fermion models with an $\mathrm{O}(2N_f)$ symmetry, like the ones we study here, have a degenerate energy spectrum. In the next section, we will prove this result.

2.3 Degeneracy of the spectrum under $\mathrm{O}(2N_f)$ symmetry

In this section, we prove that under certain assumptions, the degeneracy of all energy eigenvalues of a fermionic lattice model with $\mathrm{O}(2N_f)$ symmetry is always an even number. In particular, the ground state is doubly degenerate. The essence of the proof is already contained in the case $N_f = 1$, where the O(2) symmetry can be understood as a semidirect product of a U(1) particle number symmetry and a $\mathbb{Z}_2$ particle-hole symmetry. In this case, the result can be formulated as the following theorem:

Theorem 1. *Consider a Hamiltonian of a single-flavor Dirac fermion on a bipartite lattice with the periodic boundary condition. If the Hamiltonian has translation symmetry,* U(1) *particle number symmetry and particle-hole symmetry, then the degeneracy of all energy eigenvalues is an even number when the size of at least one side of the lattice is a multiple of four.*

Although this result holds in arbitrary dimension, it is sufficient to prove it in one spatial dimension, because the translation operator T_a in the following proof can be easily generalized to higher dimensions.

Proof. Let the lattice size be $L = Na$ where N is the number of sites and a is the

lattice spacing. For a bipartite lattice N must be an even number. Let $c_i^\dagger$ and c_i be the creation and annihilation operators on site i. Then the Hamiltonian commutes with the U(1) particle number operator $\mathcal{N} = \sum_i c_i^\dagger c_i$, and the lattice translation operator

$$T_a = \exp\Big(- \mathrm{i}a \sum_k k \; d_k^\dagger d_k \Big), \tag{2.24}$$

where

$$d_k = \frac{1}{\sqrt{N}} \sum_k c_j \, \mathrm{e}^{\mathrm{i}kaj}, \quad k = \frac{2\pi n}{L}, \quad n = -\frac{N}{2} + 1, \cdots, \frac{N}{2}. \tag{2.25}$$

Most importantly, H also commutes with the particle-hole transformation

$$C = \prod_{i=1}^{N} (c_i + (-1)^i c_i^\dagger), \tag{2.26}$$

which only exists on a bipartite lattice, and satisfies $C = C^\dagger$ and

$$C c_i C^\dagger = (-1)^i c_i^\dagger, \quad C d_k C^\dagger = d_{\frac{\pi}{a}-k}^\dagger, \tag{2.27}$$

Therefore we have

$$C \mathcal{N} C^\dagger = \sum_i c_i c_i^\dagger = \sum_i (1 - c_i^\dagger c_i) = N - \mathcal{N}, \tag{2.28}$$

and

$$\begin{aligned} C T_a C^\dagger &= \exp\Big(- \mathrm{i}a \sum_k k \; d_{\frac{\pi}{a}-k} d_{\frac{\pi}{a}-k}^\dagger \Big) \\ &= \exp\Big(- \mathrm{i}a \sum_k \big(\frac{\pi}{a} - k\big) \; (1 - d_k^\dagger d_k) \Big) \\ &= (-1)^{N-\mathcal{N}-1} T_a = -(-1)^{\mathcal{N}} T_a, \end{aligned} \tag{2.29}$$

where we have use the fact that $\sum_k k = \frac{\pi}{a}$ and $(-1)^N = 1$, both because N must be an even number.

Since $H, T_a, \mathcal{N}$ commute with each other, we can label the energy eigenstates by $|E, k, n, q\rangle$, where $E, \mathrm{e}^{-\mathrm{i}ak}, n$ are eigenvalues of $H, T_a, \mathcal{N}$, and q denote possible additional quantum numbers. Using Eqs. (2.28) and (2.29) we can show that

$$C|E, k, n, q\rangle \propto |E, k + (n+1)\frac{\pi}{a}, N - n, q\rangle, \tag{2.30}$$

from which we can pair up the degenerate states in a unique way. When $n \neq \frac{N}{2}$, states $|E, k, n, q\rangle$ and $|E, k+(n+1)\frac{\pi}{a}, N-n, q\rangle$ form a degenerate pair. On the other hand, when $n = \frac{N}{2}$, C mixes the states $|E, k, \frac{N}{2}, q\rangle$ and $|E, k + (\frac{N}{2}+1)\frac{\pi}{a}, \frac{N}{2}, q\rangle$. When $\frac{N}{2}$ is odd, these two states are identical and C cannot be used to pair degenerate states in this case. However, when $\frac{N}{2}$ is even, C mixes $|E, k, \frac{N}{2}, q\rangle$ with $|E, k + \frac{\pi}{a}, \frac{N}{2}, q\rangle$, and the whole spectrum has even degeneracy. This completes the proof. □

In the case of N_f flavor of Dirac fermions, the $\mathrm{O}(2N_f)$ symmetry implies that the particle number of each flavor is conserved, i.e., $[H, \mathcal{N}^\alpha] = 0$, where

$$\mathcal{N}^\alpha = \sum_i c_i^{\alpha\dagger} c_i^\alpha, \quad \alpha = 1, \cdots, N_f, \tag{2.31}$$

and clearly $[\mathcal{N}^\alpha, \mathcal{N}^\beta] = 0$. Actually, $\mathcal{N}^\alpha$ can be viewed as a Cartan subalgebra of $\mathrm{O}(2N_f)$ represented on the fermion Hilbert space. The lattice translation operator in this case can be written as

$$T_a = \prod_\alpha T_a^\alpha = \prod_\alpha \exp\Big(- \mathrm{i}a \sum_k k \; d_k^{\alpha\dagger} d_k^\alpha \Big). \tag{2.32}$$

Furthermore, the particle-hole transformation on a single flavor α

$$C^\alpha = \prod_{i=1}^{N} (c_i^\alpha + (-1)^i c_i^{\alpha\dagger}) \tag{2.33}$$

can be identified as an improper $\mathrm{O}(2N_f)$ transformation, which is not present if the system only has $\mathrm{SO}(2N_f)$ or $\mathrm{U}(N_f)$ symmetry. In the case of $N_f = 2$, C^α can be

identified with the spin-charge flip transformation $\mathbb{Z}_2^{sc}$. On the fermion operators, C^α acts as

$$C^\alpha c_i^\alpha C^{\alpha\dagger} = (-1)^i c_i^{\alpha\dagger}, \quad C^\alpha d_k^\alpha C^{\alpha\dagger} = d_{\frac{\pi}{a}-k}^{\alpha\dagger}, \tag{2.34}$$

while it commutes with fermion operators of other flavors, which implies

$$C^\alpha \mathcal{N}^\alpha C^{\alpha\dagger} = N - \mathcal{N}^\alpha, \tag{2.35}$$

$$C^\alpha T_a C^{\alpha\dagger} = -(-1)^{\mathcal{N}^\alpha} T_a. \tag{2.36}$$

Using these relations together with a similar argument used in the above proof, we have the following corollary,

Corollary 1. *Consider a Hamiltonian of N_f flavors of Dirac fermions on a bipartite lattice with the periodic boundary condition. If the Hamiltonian has translation symmetry and $\mathrm{O}(2N_f)$ internal symmetry, then the degeneracy of all energy eigenvalues is an even number when the size of at least one side of the lattice is a multiple of four.*

Note that these theorems have the flavor of the Kramers theorem, where the particle-hole symmetry plays the role of the time reversal symmetry. Clearly, states away from half-filling will change to another state under the particle-hole transformation. However, here we show that when the lattice size is a multiple of four, even at half-filling, the state will also change because the momentum is shifted by $\frac{\pi}{a}$.

From the proof, we also see that the entire $\mathrm{O}(2N_f)$ symmetry is not necessary; instead, we only need the U(1) particle number subgroup and an improper $\mathbb{Z}_2$ subgroup of $\mathrm{O}(2N_f)$ symmetry, i.e., particle-hole transformation on a single flavor. In particular, the improper $\mathbb{Z}_2$ subgroup of $\mathrm{O}(2N_f)$ plays an important role in the proof. For example, in the case of $N_f = 2$, the Hubbard interaction only has SO(4) symmetry and is odd under the improper $\mathbb{Z}_2^{sc}$ subgroup, and it can be checked numerically that the ground state is non-degenerate.

In the following, we will briefly discuss the implication of this theorem to the gapped phases of our lattice model and its connection to 't Hooft anomaly.

2.3.1 Implications for our lattice models

Let us focus on the gapped phase of our model, and assume that the lattice size is a multiple of 4. Since our model has the symmetries in Corollary 1, the ground state is degenerate. Assuming no topological order, then it is reasonable that certain 0-form symmetry is spontaneously broken in the infinite volume limit. Due to the particle-hole symmetry, the ground states are usually at half-filling, and one ground state should have momentum 0, denoted as $|0\rangle$. $C^1|0\rangle$ is another ground state, which has momentum $\frac{\pi}{a}$ and can be denoted as $|\pi\rangle$. In the ground state subspace spanned by $|0\rangle$ and $|\pi\rangle$, we have $C^1 = \sigma^1$ and $T_a = \sigma^3$, satisfying

$$C^1 T_a = -T_a C^1, \tag{2.37}$$

as a special case of Eq. (2.36). Since C^1 and T_a do not commute, the ground states cannot be simultaneous eigenstates of both symmetries. Therefore at least one of the symmetries must be spontaneously broken in the infinite volume limit. Indeed, as we will see from the numerical results in Chapter 7, in the massive phases, it is T_a that is spontaneously broken in one spatial dimension, while in two spatial dimensions, it is C^1, which is nothing but the spin-charge flip symmetry $\mathbb{Z}_2^{sc}$ in the case of $N_f = 2$, is spontaneously broken.

2.3.2 Connection to 't Hooft anomaly matching

Our theorem excludes the possibility of the ground state being trivially gapped in the presence of certain microscopic symmetries. This sounds very similar to the LSM theorem and 't Hooft anomaly matching, which states that if a theory has a 't Hooft anomaly in the UV, then the IR physics cannot be trivially gapped. Indeed, in one spatial dimension, there is a 't Hooft anomaly between the particle number

symmetry and lattice translation symmetry in our model. The anomaly can be seen clearly in the continuum limit, where the particle number symmetry is the U(1) vector symmetry, and the lattice translation symmetry is mapped to a discrete chiral symmetry, as we will see in the next chapter. It is well-known that when we gauge the U(1) vector symmetry, the discrete chiral symmetry is no longer a symmetry [69, 70, 71, 72], which means there is a mixed 't Hooft anomaly between them. This anomaly implies that our model cannot be trivially gapped. It may seem that the particle-hole symmetry in our theorem is not necessary. However, here we want to emphasize that anomaly can only teach us the physics in the continuum limit, while the additional particle-hole symmetry leads to degenerate ground states even on a finite lattice. Actually, our theorem holds even on a lattice with four sites.

One may have heard the statement that symmetries on a lattice cannot be anomalous. However, it is important to remember that this statement only holds for "on-site" lattice symmetries: the lattice translation symmetry is not an "on-site" symmetry [36]. In particular, if the low-energy sector has fractional filling $\nu = \frac{p}{q}$, with p, q being coprime, then in the low-energy limit, the lattice translation symmetry effectively becomes a $\mathbb{Z}_q$ chiral symmetry [36]. From an alternative point of view, the fractional filling leads to an effective fractional charge per site, which can be viewed as a "projective representation" of the U(1) particle number symmetry, also being related to the 't Hooft anomaly [35].

3

Continuum Limit of Free Lattice Fermions

In this chapter, we study the continuum limit of free lattice fermions. By continuum limit, we mean the physics that emerges at low energies and long distances compared to the lattice spacing. We will analyze the symmetries of the continuum theory and understand how the lattice symmetries are embedded in the continuum symmetries. Since the flavor index α will be necessary only when we analyze the internal symmetries, i.e., the transformations that mix the index α, we will omit it in our analysis and introduce it only when necessary.

3.1 One spatial dimension

We begin with a finite lattice with N sites labeled with $j = 1, \cdots, N$ and consider the free lattice Hamiltonian

$$H_0 = -t \sum_j c_j^\dagger c_{j+1} + c_{j+1}^\dagger c_j. \tag{3.1}$$

Let us first understand the continuum limit of this Hamiltonian.

3.1.1 Continuum limit

We introduce a as the lattice spacing, meaning that the lattice describes a physical box of length $L = Na$. Since the Hamiltonian is quadratic and translationally invariant, it can be diagonalized in the momentum space. Fourier transforming to the momentum space

$$c_j = \frac{1}{\sqrt{N}} \sum_k d_k \, \mathrm{e}^{-\mathrm{i}kaj}, \quad k = \frac{2\pi n}{L}, \quad n = -\frac{N}{2} + 1, \cdots, \frac{N}{2}, \tag{3.2}$$

where d_k is the fermion annihilation operator at momentum k, and inserting this back into the Hamiltonian above, we have

$$H_0 = -2t \sum_k \cos ak \; d_k^\dagger d_k. \tag{3.3}$$

The dispersion relation of this Hamiltonian is plotted in Fig. 3.1

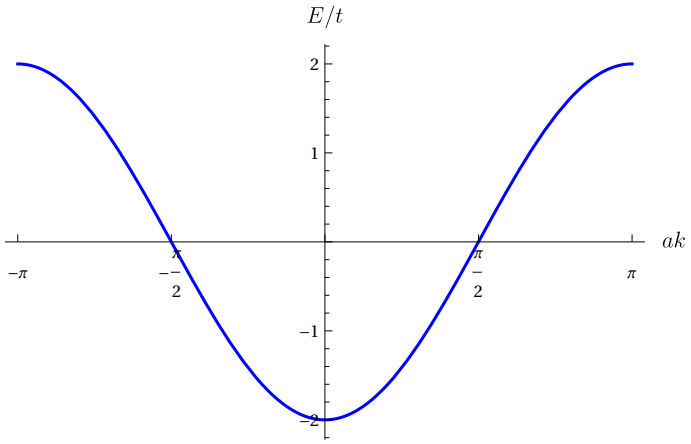

FIGURE 3.1: The single-particle dispersion relation of free lattice fermions in one spatial dimension.

We can find expressions valid on an infinite lattice by taking the limit $N \to \infty$, keeping a fixed. This implies that the physical size $L \to \infty$ and the momentum space becomes continuous. Then we can replace the momentum sums with integrals,

$$\frac{1}{N} \sum_k \longrightarrow \frac{a}{2\pi} \int_{-\frac{\pi}{a}}^{\frac{\pi}{a}} \mathrm{d}k. \tag{3.4}$$

We then define $d(k) := \sqrt{\frac{Na}{2\pi}} d_k$ as the continuum version of d_k, and we have

$$\frac{1}{\sqrt{a}} c_j = \frac{1}{\sqrt{2\pi}} \int_{-\frac{\pi}{a}}^{\frac{\pi}{a}} \mathrm{d}k \; d(k) \, \mathrm{e}^{-\mathrm{i}kaj} \, . \tag{3.5}$$

In order to understand the continuum limit, we focus on low energies where only modes near the two Fermi momenta $k = \mp k_F$ are important. Therefore we replace

$$\begin{aligned} \frac{1}{\sqrt{a}} c_j &\approx \frac{1}{\sqrt{2\pi}} \int_{-k_F-\Lambda}^{-k_F+\Lambda} \mathrm{d}k \; d(k) \, \mathrm{e}^{-\mathrm{i}kaj} + \frac{1}{\sqrt{2\pi}} \int_{k_F-\Lambda}^{k_F+\Lambda} \mathrm{d}k \; d(k) \, \mathrm{e}^{-\mathrm{i}kaj} \\ &= \frac{1}{\sqrt{2\pi}} \, \mathrm{e}^{\mathrm{i}k_F aj} \int_{-\Lambda}^{\Lambda} \mathrm{d}k \; d(k - k_F) \, \mathrm{e}^{-\mathrm{i}kaj} + \frac{1}{\sqrt{2\pi}} \, \mathrm{e}^{-\mathrm{i}k_F aj} \int_{-\Lambda}^{\Lambda} \mathrm{d}k \; d(k + k_F) \, \mathrm{e}^{-\mathrm{i}kaj} \, . \end{aligned} \tag{3.6}$$

Based on this relation we define

$$\frac{1}{\sqrt{a}} c_j =: \mathrm{e}^{\mathrm{i}k_F aj} \, \Psi_+(aj) + \mathrm{e}^{-\mathrm{i}k_F aj} \, \Psi_-(aj), \tag{3.7}$$

where we have introduced continuum fields $\Psi_\pm(x)$ as smooth left(right)-moving fields. These two fields can be combined into a two-component field $\Psi(x)$ defined as

$$\Psi := \begin{pmatrix} \Psi_+ \\ \Psi_- \end{pmatrix} . \tag{3.8}$$

Inserting Eq. (3.7) into H_0, we can expand in powers of lattice spacing a to obtain the leading low-energy effective Hamiltonian in the continuum. In the following we assume the system is at half-filling, i.e., $k_F = \frac{\pi}{2a}$. Then we have

$$\begin{aligned} \frac{1}{a} c_j^\dagger c_{j+1} &= \mathrm{i}\Psi_+^\dagger(aj)\Psi_+(a(j+1)) - \mathrm{i}\Psi_-^\dagger(aj)\Psi_-(a(j+1)) \\ &\quad + \mathrm{i}(-1)^j(-\Psi_+^\dagger(aj)\Psi_-(a(j+1)) + \Psi_-^\dagger(aj)\Psi_+(a(j+1))). \end{aligned} \tag{3.9}$$

The second term oscillates at the lattice scale and will be dropped as not contributing to the effective continuum Hamiltonian. Taylor expanding the fields at $j+1$,

$$\frac{1}{a} c_j^\dagger c_{j+1} = \mathrm{i}\Psi_+^\dagger(aj)(\Psi_+(aj) + a\partial\Psi_+(aj)) - \mathrm{i}\Psi_-^\dagger(aj)(\Psi_-(aj) + a\partial\Psi_-(aj)) \tag{3.10}$$

and adding the Hermitian conjugate term we obtain

$$\frac{1}{a}c_j^\dagger c_{j+1} + \text{H.c.} \approx 2a\mathrm{i}\Psi_+^\dagger(aj)\partial\Psi_+(aj) - 2a\mathrm{i}\Psi_-^\dagger(aj)\partial\Psi_-(aj)$$

$$= 2a\mathrm{i}\Psi^\dagger(aj)\sigma^3\partial\Psi(aj) \tag{3.11}$$

Finally, we construct the effective continuum Hamiltonian as

$$H = -2a^2t\sum_j \mathrm{i}\Psi^\dagger(aj)\sigma^3\partial\Psi(aj) = -2at\int \mathrm{d}x\ \mathrm{i}\Psi^\dagger(x)\sigma^3\partial\Psi(x), \tag{3.12}$$

which is the well-known continuum Dirac Hamiltonian in one spatial dimension.

In order to understand the symmetries of the continuum model and to perform analytic calculations, it is helpful to construct its Lagrangian. Using Grassmann coherent state fermion path integral (see Appendix A), we can map the continuum Hamiltonian Eq. (3.12), into the following Euclidean space-time Lagrangian

$$\mathcal{L} = \bar{\psi}\gamma^\mu\partial_\mu\psi, \tag{3.13}$$

where ψ is a two-component Grassmann-valued field, $\bar{\psi} = \psi^\dagger\gamma^0$ but should be treated as an independent field in Euclidean space-time [1], and $\mu = 0, 1$. $\gamma^0 = \sigma^1, \gamma^1 = -\sigma^2, \gamma^3 = \mathrm{i}\gamma^1\gamma^2 = \sigma^3$ are three 2×2 Hermitian matrices satisfying the Clifford algebra $\{\gamma^i, \gamma^j\} = 2\delta^{ij}\mathbb{1}_2$. In terms of single component Weyl fermions $\psi_\pm$, the Lagrangian can be written as

$$\mathcal{L} = \psi^\dagger(\partial_0 - \mathrm{i}\sigma^3\partial_1)\psi = \psi_+^\dagger\partial_-\psi_+ + \psi_-^\dagger\partial_+\psi_-, \tag{3.14}$$

where $\partial_\pm = \partial_0 \pm \mathrm{i}\partial_1$.

3.1.2 Symmetries of the continuum theory

Now let us consider the theory with N_f flavors of lattice fermions, whose Lagrangian is given by

$$\mathcal{L} = \sum_{\alpha=1}^{N_f} \bar{\psi}^\alpha\gamma^\mu\partial_\mu\psi^\alpha, \tag{3.15}$$

[1] A hand-waving argument is that under imaginary time evolution $\psi^\dagger(x,t) = \mathrm{e}^{-tH}\,\psi^\dagger(x,0)\,\mathrm{e}^{tH} \neq \left(\mathrm{e}^{-tH}\,\psi(x,0)\,\mathrm{e}^{tH}\right)^\dagger$ is no longer the $\dagger$ of $\psi(t)$.

and understand its symmetries. The easiest way to analyze the symmetry is by writing the Lagrangian in terms of single-component Weyl fermions,

$$\mathcal{L} = \sum_{\alpha=1}^{N_f} \psi_+^{\alpha\dagger}\partial_-\psi_+^{\alpha} + \psi_-^{\alpha\dagger}\partial_+\psi_-^{\alpha}. \tag{3.16}$$

This form manifests the $\mathrm{U}(N_f)_+ \times \mathrm{U}(N_f)_-$ symmetry. However, the theory actually has $\mathrm{O}(2N_f)_+ \times \mathrm{O}(2N_f)_-$ symmetry because of the existence of Majorana-Weyl fermions. To see this, we define

$$\psi_\pm^{\alpha} = \frac{1}{\sqrt{2}}(\xi_\pm^{2\alpha-1} - \mathrm{i}\xi_\pm^{2\alpha}), \quad \psi_\pm^{\alpha\dagger} = \frac{1}{\sqrt{2}}(\xi_\pm^{2\alpha-1T} + \mathrm{i}\xi_\pm^{2\alpha T}), \tag{3.17}$$

and write the Lagrangian in terms of Majorana-Weyl fermions $\xi_\pm^{\alpha}, \alpha = 1, 2, \cdots, 2N_f$,

$$\mathcal{L} = \frac{1}{2}\sum_{\alpha=1}^{2N_f} \xi_+^{\alpha T}\partial_-\xi_+^{\alpha} + \xi_-^{\alpha T}\partial_+\xi_-^{\alpha}, \tag{3.18}$$

from which it can be clearly seen that the theory has $\mathrm{O}(2N_f)_+ \times \mathrm{O}(2N_f)_-$ symmetry.

It is also possible to analyze the symmetries directly using the two-component Majorana fermions, which will be useful in the next chapter when analyzing fermion bilinears and four-fermion interactions. To see the $\mathrm{O}(2N_f)_+ \times \mathrm{O}(2N_f)_-$ symmetry directly from two-component Majorana fermions, we need to understand Majorana fermions better. In Appendix B we discuss some of the subtleties of the various definitions of Majorana fermions. For our purpose, by defining

$$\psi^{\alpha} = \frac{1}{\sqrt{2}}(\xi^{2\alpha-1} - \mathrm{i}\xi^{2\alpha}), \quad \bar{\psi}^{\alpha} = \frac{1}{\sqrt{2}}(\xi^{2\alpha-1T}\mathcal{C}^T + \mathrm{i}\xi^{2\alpha T}\mathcal{C}^T), \tag{3.19}$$

we can write the Lagrangian as

$$\mathcal{L} = \frac{1}{2}\sum_{\alpha=1}^{2N_f} \xi^{\alpha T}\mathcal{C}^T\gamma^{\mu}\partial_{\mu}\xi^{\alpha}, \tag{3.20}$$

where $\mathcal{C}$ is the charge conjugation matrix. In one spatial dimension, $\mathcal{C}$ can either satisfy the Majorana condition Eq. (B.18), if we choose $\mathcal{C} = \gamma^1$, or the pseudo-

Majorana condition Eq. (B.19), if we choose $\mathcal{C} = \gamma^0$. In either case, the Majorana-Weyl condition Eq. (B.29) is satisfied. Since we are working with free massless fermions, these two conditions are equivalent, and here we will choose $\mathcal{C} = \gamma^0$ for convenience. The justification of this choice when interactions are added will be discussed in the next chapter.

With this choice of $\mathcal{C}$, we can write down the $2\binom{2N_f}{2}$ generators of the $\mathrm{O}(2N_f)_+ \times \mathrm{O}(2N_f)_-$ symmetry explicitly,

$$A \otimes \frac{1}{2}(\mathbb{1}_2 + \gamma^3), \quad A \otimes \frac{1}{2}(\mathbb{1}_2 - \gamma^3), \tag{3.21}$$

where A are $2N_f \times 2N_f$ anti-symmetric matrices acting on the Majorana flavor space. There is a conserved current associated with each symmetry generator, which will be discussed in the next chapter.

3.1.3 Embedding of lattice symmetries in the continuum

We now wish to understand how the lattice symmetries discussed in Chapter 2 are embedded in the continuum. In one spatial dimension, the lattice symmetries are translations generated by T_a, parity P, time reversal Θ and charge conjugation C, given in Eqs. (2.4) to (2.7). These lattice transformations induce transformations on the continuum fields according to Eq. (3.7),

$$\frac{1}{\sqrt{a}} c_j \approx \mathrm{i}^j \Psi_+(aj) + \mathrm{i}^{-j} \Psi_-(aj). \tag{re 3.7}$$

For example, under translations by one lattice spacing, Eq. (3.7) goes to

$$\frac{1}{\sqrt{a}} c_{j+1} \approx \mathrm{i}^{j+1} \Psi_+(aj + a) + \mathrm{i}^{-j-1} \Psi_-(aj + a). \tag{3.22}$$

In the continuum limit, $\Psi_\pm(aj + a) \approx \Psi_\pm(aj)$ at leading order. Therefore comparing with Eq. (3.7), we learn that T_a induces the following transformation on the continuum fields:

$$\Psi(x) \mapsto \mathrm{i}\sigma^3 \Psi(x) = \mathrm{i}\gamma^3 \Psi(x). \tag{3.23}$$

Here we would like to point out that a finite translation by a distance $x = Na$ in the continuum is obtained by an N site translation on the lattice where N is a multiple of 4 and $N \to \infty$ when $a \to 0$, which is clear from Eq. (3.22).

Using similar techniques, we can derive the embedding of all lattice symmetry transformations on the continuum fields. In terms of the space-time fields $\psi(t,x)$ and $\xi(t,x)$, the results are tabulated in Table 3.1.

Table 3.1: The action of lattice symmetries on the continuum fields in one spatial dimension.

	c_j	$\psi(t,x)$	$\xi(t,x)$
T_a	c_{j+1}	$\mathrm{i}\gamma^3\psi(t,x)$	$\mathrm{i}\sigma^2\otimes\gamma^3\xi(t,x)$
P	c_{-j}	$\gamma^0\psi(t,-x)$	$\mathbb{1}_2\otimes\gamma^0\xi(t,-x)$
Θ	c_j	$\gamma^0\psi(-t,x)$	$\mathbb{1}_2\otimes\gamma^0\xi(-t,x)$
C	$(-1)^j c_j^\dagger$	$\psi^{\dagger T}(t,x) = \mathcal{C}^{-1}\bar{\psi}^T$	$(\sigma^3\otimes\mathbb{1}_2)\ \xi(t,x)$

Notice that, while P and Θ are space-time symmetries in the continuum as on the lattice, T_a and C are subgroups of $\mathrm{O}(2N_f)_+ \times \mathrm{O}(2N_f)_-$ and therefore are internal symmetries, which is clear in the Majorana language. Furthermore, since the internal $\mathrm{O}(2N_f)$ symmetry acts the same way on $\psi_\pm$, it corresponds to the diagonal subgroup of the $\mathrm{O}(2N_f)_+ \times \mathrm{O}(2N_f)_-$ symmetry.

3.1.4 The continuum limit of local lattice fermion bilinears

Observables on the lattice are usually fermion bilinears. In this subsection, we derive the continuum limit of various lattice fermion bilinears obtained from a single lattice site, which will be useful later.

Consider the case of N_f flavors. Using the relation Eq. (3.7), we can write

$$\frac{1}{a} c_j^{\alpha\dagger} c_j^\beta \to \psi^{\alpha\dagger}\psi^\beta + (-1)^j \bar{\psi}^\alpha \psi^\beta. \tag{3.24}$$

Notice that the lattice fermion bilinears on even and odd sites map to different continuum operators due to the factor $(-1)^j$. We can perform a particle-hole trans-

formation and obtain

$$\frac{1}{a}(-1)^j c_j^\alpha c_j^\beta \to \psi^{\alpha T}\psi^\beta + (-1)^j \psi^{\alpha T}\gamma^0\psi^\beta,$$

$$\frac{1}{a}(-1)^j c_j^{\alpha\dagger} c_j^{\beta\dagger} \to \psi^{\alpha\dagger}\psi^{\beta\dagger T} + (-1)^j \bar{\psi}^\alpha\gamma^0\bar{\psi}^{\beta T}. \tag{3.25}$$

We can also write these relations in terms of Majorana fermions. Reversing the relations in Eq. (2.14), we get

$$\gamma_j^{2\alpha-1} = (-\mathrm{i})^j c_j^\alpha + \mathrm{i}^j c_j^{\alpha\dagger}, \quad \gamma_j^{2\alpha} = (-\mathrm{i})^{j-1} c_j^\alpha + \mathrm{i}^{j-1} c_j^{\alpha\dagger}. \tag{3.26}$$

Then using the relations Eqs. (3.7) and (3.19), we can relate lattice Majorana fermions to the continuum Majorana fermions as

$$\begin{aligned}
\frac{1}{\sqrt{a}}\gamma_j^{2\alpha-1} &\to (\psi_+^\alpha + \psi_+^{\alpha\dagger T}) + (-1)^j(\psi_-^\alpha + \psi_-^{\alpha\dagger T}) = \sqrt{2}\xi_+^{2\alpha-1} + (-1)^j\sqrt{2}\xi_-^{2\alpha-1} \\
\frac{1}{\sqrt{a}}\gamma_j^{2\alpha} &\to \mathrm{i}(\psi_+^\alpha - \psi_+^{\alpha\dagger T}) + (-1)^j\mathrm{i}(\psi_-^\alpha - \psi_-^{\alpha\dagger T}) = \sqrt{2}\xi_+^{2\alpha} + (-1)^j\sqrt{2}\xi_-^{2\alpha}.
\end{aligned} \tag{3.27}$$

These two lines can be combined into a single relation

$$\frac{1}{\sqrt{2a}}\gamma_j^\alpha \to \xi_+^\alpha + (-1)^j\xi_-^\alpha \quad \text{for } \alpha = 1, \cdots, 2N_f. \tag{3.28}$$

Therefore we obtain

$$\frac{1}{2a}\gamma_j^\alpha\gamma_j^\beta \to \xi^{\alpha T}\xi^\beta + (-1)^j\xi^{\alpha T}\mathcal{C}\xi^\beta. \tag{3.29}$$

We will use these relations in Chapter 5 to study the correlation functions of lattice observables.

3.2 Two spatial dimension

We can extend the above results to free fermions in two spatial dimensions. We consider a two-dimensional square lattice with sites labeled by (n_1, n_2), where $n_i =$

$1, 2, \cdots, N_i$. The total number of sites would then be $N := N_1 N_2$. The staggered lattice Hamiltonian can be written as

$$H = -t \sum_{n_1 n_2} c^\dagger_{n_1 n_2} c_{n_1+1 n_2} + (-1)^{n_1} c^\dagger_{n_1 n_2} c_{n_1 n_2+1} + \text{H.c.} \tag{3.30}$$

Let us first understand the continuum limit of this Hamiltonian.

3.2.1 Continuum limit

Again we introduce a as the lattice spacing, and the lattice describes a two-dimensional box with lengths $L_i = N_i a$ in each direction. In order to construct the continuum limit we first Fourier transform $c_{n_1 n_2}$ to the momentum space fermion operators $d_{k_1 k_2}$,

$$c_{n_1 n_2} = \frac{1}{\sqrt{N}} \sum_{k_1 k_2} d_{k_1 k_2} \, \mathrm{e}^{-\mathrm{i}(k_1 a n_1 + k_2 a n_2)}, \quad k_i = -\frac{\pi}{a} + \frac{2\pi}{N_i a}, \cdots, \frac{\pi}{a}. \tag{3.31}$$

Substituting this into the Hamiltonian we obtain

$$\begin{aligned}
H &= -\frac{t}{N} \sum_{k_1 k_2} \sum_{k_1' k_2'} \mathrm{e}^{-\mathrm{i}a k_1'} \, d^\dagger_{k_1 k_2} d_{k_1' k_2'} \sum_{n_1 n_2} \mathrm{e}^{\mathrm{i}((k_1 - k_1')a n_1 + (k_2 - k_2')a n_2)} \\
&\quad - \frac{t}{N} \sum_{k_1 k_2} \sum_{k_1' k_2'} \mathrm{e}^{-\mathrm{i}a k_2'} \, d^\dagger_{k_1 k_2} d_{k_1' k_2'} \sum_{n_1 n_2} \mathrm{e}^{\mathrm{i}((k_1 - k_1' + \pi/a)a n_1 + (k_2 - k_2')a n_2)} + \text{H.c.} \\
&= -t \sum_{k_1 k_2} \mathrm{e}^{-\mathrm{i}a k_1} \, d^\dagger_{k_1 k_2} d_{k_1 k_2} + \mathrm{e}^{-\mathrm{i}a k_2} \, d^\dagger_{k_1 k_2} d_{k_1 + \frac{\pi}{a} k_2} + \text{H.c.} \\
&= -2t \sum_{0 < k_1 \le \frac{\pi}{a}, k_2} \begin{pmatrix} d^\dagger_{k_1 k_2} & d^\dagger_{k_1 + \frac{\pi}{a} k_2} \end{pmatrix} \begin{pmatrix} \cos a k_1 & \cos a k_2 \\ \cos a k_2 & -\cos a k_1 \end{pmatrix} \begin{pmatrix} d_{k_1 k_2} \\ d_{k_1 + \frac{\pi}{a} k_2} \end{pmatrix} \\
&= -2t \sum_{0 < k_1 \le \frac{\pi}{a}, k_2} \begin{pmatrix} d^\dagger_{k_1 k_2} & d^\dagger_{k_1 + \frac{\pi}{a} k_2} \end{pmatrix} (\sigma^3 \cos a k_1 + \sigma^1 \cos a k_2) \begin{pmatrix} d_{k_1 k_2} \\ d_{k_1 + \frac{\pi}{a} k_2} \end{pmatrix}.
\end{aligned} \tag{3.32}$$

Diagonalizing this Hamiltonian, we obtain the dispersion relation as shown in Fig. 3.2. Notice that although we have shown four Dirac cones in the plot, there are actually only two Dirac cones because $0 < k_1 \le \frac{\pi}{a}$ in the summation, and $d_{k_1 k_2}, d_{k_1 + \frac{\pi}{a} k_2}$ together form a single Dirac cone. They can be viewed as the Fourier modes of the continuum Dirac field with spin.

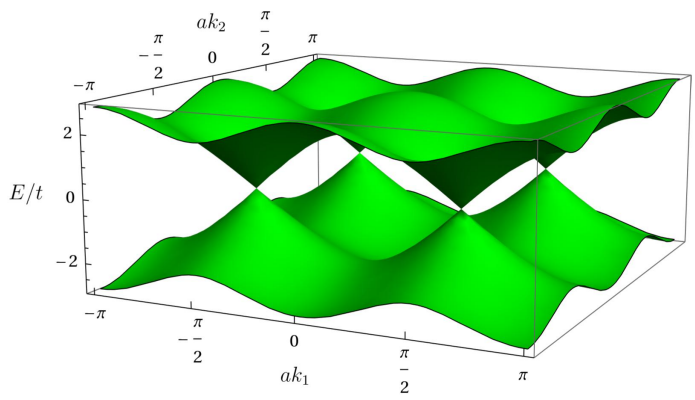

FIGURE 3.2: The single-particle dispersion relation of free lattice fermion on a two-dimensional square lattice.

When $N_1, N_2 \to \infty$, we can replace the momentum sums with integrals,

$$\frac{1}{N}\sum_{k_1 k_2} \longrightarrow \frac{a^2}{(2\pi)^2}\int_{-\frac{\pi}{a}}^{\frac{\pi}{a}} \mathrm{d}k_1 \int_{-\frac{\pi}{a}}^{\frac{\pi}{a}} \mathrm{d}k_2. \tag{3.33}$$

We then define $d(k_1, k_2) := \frac{\sqrt{N}a}{2\pi} d_{k_1 k_2}$ as the continuum version of d_k, and we have

$$\frac{1}{a} c_{n_1 n_2} = \frac{1}{2\pi}\int_{-\frac{\pi}{a}}^{\frac{\pi}{a}} \mathrm{d}k_1 \int_{-\frac{\pi}{a}}^{\frac{\pi}{a}} \mathrm{d}k_2 \; d(k_1, k_2)\, \mathrm{e}^{-\mathrm{i}(k_1 a n_1 + k_2 a n_2)}\,. \tag{3.34}$$

At low energies, only the modes near the four points $(k_1, k_2) = (\pm\frac{\pi}{2a}, \pm\frac{\pi}{2a})$ are important, and we can approximate

$$\begin{aligned}\frac{1}{a} c_{n_1 n_2} \approx \frac{a}{2\pi}\int_{-\Lambda}^{\Lambda} \mathrm{d}k_1 \mathrm{d}k_2 \; \mathrm{e}^{-\mathrm{i}(k_1 a n_1 + k_2 a n_2)} \Big(&\mathrm{i}^{-n_1-n_2} d(\frac{\pi}{2a}+k_1, \frac{\pi}{2a}+k_2) + \mathrm{i}^{n_1-n_2} d(-\frac{\pi}{2a}+k_1, \frac{\pi}{2a}+k_2) \\ &+ \mathrm{i}^{n_1+n_2} d(-\frac{\pi}{2a}+k_1, -\frac{\pi}{2a}+k_2) + \mathrm{i}^{-n_1+n_2} d(\frac{\pi}{2a}+k_1, -\frac{\pi}{2a}+k_2)\Big).\end{aligned} \tag{3.35}$$

Based on this relation, we can define four smooth continuum fields as

$$\frac{1}{a} c_{n_1 n_2} =: \mathrm{i}^{-n_1-n_2}\Psi_{-\uparrow} + \mathrm{i}^{n_1-n_2}\Psi_{-\downarrow} + \mathrm{i}^{n_1+n_2}\Psi_{+\uparrow} + \mathrm{i}^{-n_1+n_2}\Psi_{+\downarrow}. \tag{3.36}$$

The components $\Psi_{\pm\updownarrow}$ can be combined into a single four-component fermion field

$$\Psi = \begin{pmatrix}\Psi_+ \\ \Psi_-\end{pmatrix} = \begin{pmatrix}\Psi_{+\uparrow} \\ \Psi_{+\downarrow} \\ \Psi_{-\uparrow} \\ \Psi_{-\downarrow}\end{pmatrix}. \tag{3.37}$$

Similar to the $1+1$d case, we can now substitute this back into the Hamiltonian and keep only the leading non-oscillating terms,

$$\begin{aligned}\frac{1}{a^2}c^\dagger_{n_1n_2}c_{n_1+1n_2}+\text{H.c.} &= 2ai(-\Psi^\dagger_{-\uparrow}\partial_1\Psi_{-\uparrow}+\Psi^\dagger_{-\downarrow}\partial_1\Psi_{-\downarrow}+\Psi^\dagger_{+\uparrow}\partial_1\Psi_{+\uparrow}-\Psi^\dagger_{+\downarrow}\partial_1\Psi_{+\downarrow})\\ &= 2ai(-\Psi^\dagger_-\sigma^3\partial_1\Psi_-+\Psi^\dagger_+\sigma^3\partial_1\Psi_+)\\ &= 2ai\Psi^\dagger\sigma^3\otimes\sigma^3\partial_1\Psi, \end{aligned} \tag{3.38}$$

$$\begin{aligned}\frac{1}{a^2}(-1)^{n_1}c^\dagger_{n_1n_2}c_{n_1n_2+1}+\text{H.c.} &= 2ai(-\Psi^\dagger_{-\uparrow}\partial_2\Psi_{-\downarrow}-\Psi^\dagger_{-\downarrow}\partial_2\Psi_{-\uparrow}+\Psi^\dagger_{+\uparrow}\partial_2\Psi_{+\downarrow}+\Psi^\dagger_{+\downarrow}\partial_2\Psi_{+\uparrow})\\ &= 2ai(-\Psi^\dagger_-\sigma^1\partial_2\Psi_-+\Psi^\dagger_+\sigma^1\partial_2\Psi_+)\\ &= 2ai\Psi^\dagger\sigma^3\otimes\sigma^1\partial_2\Psi. \end{aligned} \tag{3.39}$$

This then leads to the continuum Hamiltonian for four-component Dirac fermions

$$H=-2a^3t\sum \mathrm{i}\Psi^\dagger\sigma^3\otimes(\sigma^3\partial_1+\sigma^1\partial_2)\Psi=2at\int \mathrm{d}^2x\ \mathrm{i}\Psi^\dagger(\Gamma^1\partial_1+\Gamma^2\partial_2)\Psi, \tag{3.40}$$

where $\Gamma^1=-\sigma^3\otimes\sigma^3$ and $\Gamma^2=-\sigma^3\otimes\sigma^1$. This result shows that a single flavor of staggered lattice fermion is equivalent to a four-component Dirac fermion in the continuum.

Using Grassmann coherent state fermion path integral, we can map the Hamiltonian in Euclidean time into the following Euclidean Lagrangian density

$$\mathcal{L}=\bar\psi\gamma^\mu\partial_\mu\psi, \tag{3.41}$$

where ψ is a four-component Grassmann-valued field, $\bar\psi=\psi^\dagger\gamma^0$ but should be treated as an independent field in Euclidean space-time, and $\mu=0,1,2$. In this mapping we define five 4×4 Hermitian matrices $\gamma^{0,1,2,3,5}$ satisfying the Clifford algebra $\{\gamma^i,\gamma^j\}=2\delta^{ij}\mathbb{1}_4$. We will choose $\gamma^{0,3,5}$ to be real, and $\gamma^{1,2}$ to be imaginary. One choice that is consistent with $\Gamma^{1,2}$ that naturally arises from the lattice structure is

$$\gamma^0=\sigma^1\otimes\mathbb{1},\ \gamma^1=-\sigma^2\otimes\sigma^3,\ \gamma^2=-\sigma^2\otimes\sigma^1,\ \gamma^3=\sigma^3\otimes\mathbb{1},\ \gamma^5=\gamma^0\gamma^1\gamma^2\gamma^3=\sigma^2\otimes\sigma^2. \tag{3.42}$$

3.2.2 Symmetries of the continuum theory

We now show that the continuum theory that emerges from N_f flavors of lattice fermions has an O($4N_f$) internal symmetry. The continuum Euclidean Lagrangian density is

$$\mathcal{L} = \sum_{\alpha=1}^{N_f} \bar{\psi}^\alpha \gamma^\mu \partial_\mu \psi^\alpha \qquad \text{(re 3.41)}$$

The easiest way to analyze the internal symmetries of the theory is by writing the Lagrangian in terms of two-component fermions. In this case, it is more convenient to work in a different spinor basis where γ^0 and γ^5 are flipped. This can be accomplished by a unitary transformation $\psi \mapsto \tilde{\psi} = U\psi$ and $\bar{\psi} \mapsto \bar{\tilde{\psi}} = \bar{\psi}U^\dagger$ where $U = \exp(\frac{\pi}{4}\gamma^0\gamma^5)$. If we define $\tilde{\gamma}^i := U\gamma^i U^\dagger$,

$$\tilde{\gamma}^0 = -\sigma^2 \otimes \sigma^2,\ \tilde{\gamma}^1 = -\sigma^2 \otimes \sigma^3,\ \tilde{\gamma}^2 = -\sigma^2 \otimes \sigma^1,\ \tilde{\gamma}^3 = \sigma^3 \otimes \mathbb{1},\ \tilde{\gamma}^5 = \sigma^1 \otimes \mathbb{1}, \quad (3.43)$$

then the form of the Lagrangian is unchanged,

$$\mathcal{L} = \sum_{\alpha=1}^{N_f} \bar{\tilde{\psi}}^\alpha \tilde{\gamma}^\mu \partial_\mu \tilde{\psi}^\alpha. \qquad (3.44)$$

In particular, we notice that

$$\tilde{\gamma}^0\tilde{\gamma}^0 = \mathbb{1}, \quad \tilde{\gamma}^0\tilde{\gamma}^1 = \mathrm{i}\mathbb{1} \otimes \sigma^1, \quad \tilde{\gamma}^0\tilde{\gamma}^2 = -\mathrm{i}\mathbb{1} \otimes \sigma^3, \qquad (3.45)$$

are diagonal in the $\pm$ space. Therefore in terms of two-component Grassmann fields, the Lagrangian can be written as

$$\mathcal{L} = \sum_{\alpha=1}^{N_f} \bar{\tilde{\psi}}_+^\alpha \gamma_{(2)}^\mu \partial_\mu \tilde{\psi}_+^\alpha + \bar{\tilde{\psi}}_-^\alpha \gamma_{(2)}^\mu \partial_\mu \tilde{\psi}_-^\alpha, \qquad (3.46)$$

where $\bar{\tilde{\psi}}_\pm^\alpha = \tilde{\psi}_\pm^{\alpha\dagger}\gamma_{(2)}^0$ and $\gamma_{(2)}^0 = \sigma^2$, $\gamma_{(2)}^1 = \sigma^3$, $\gamma_{(2)}^3 = \sigma^1$. From this expression, we can clearly read the U($2N_f$) symmetry. To see the O($4N_f$) symmetry, we need to express the Lagrangian in terms of Majorana fermions.

From the discussion in Appendix B we know that although it is not possible to choose all $\gamma^{\mu}_{(2)}$ to be real in 3d Euclidean space, it is still possible to define "physical" Majorana fermions in the following way

$$\tilde{\psi}^{\alpha}_{+} = \frac{1}{\sqrt{2}}(\xi^{4\alpha-3}_{(2)} - \mathrm{i}\xi^{4\alpha-2}_{(2)}), \quad \bar{\tilde{\psi}}^{\alpha} = \frac{1}{\sqrt{2}}(\xi^{4\alpha-3T}_{(2)}\mathcal{C}^{T}_{(2)} + \mathrm{i}\xi^{4\alpha-2T}_{(2)}\mathcal{C}^{T}_{(2)}),$$

$$\tilde{\psi}^{\alpha}_{-} = \frac{1}{\sqrt{2}}(\xi^{4\alpha-1}_{(2)} - \mathrm{i}\xi^{4\alpha}_{(2)}), \qquad \bar{\tilde{\psi}}^{\alpha} = \frac{1}{\sqrt{2}}(\xi^{4\alpha-1T}_{(2)}\mathcal{C}^{T}_{(2)} + \mathrm{i}\xi^{4\alpha T}_{(2)}\mathcal{C}^{T}_{(2)}), \tag{3.47}$$

where $\xi^{\alpha}_{(2)}$ are two-component Majorana fermions, and the charge conjugation matrix $\mathcal{C}_{(2)}$ satisfies

$$\mathcal{C}^{T}_{(2)} = -\mathcal{C}_{(2)}, \quad \mathcal{C}_{(2)}\gamma^{\mu}_{(2)}\mathcal{C}^{-1}_{(2)} = -\gamma^{\mu T}_{(2)}. \tag{3.48}$$

In this case $\mathcal{C}_{(2)}$ can be chosen to be σ^2. Then the Lagrangian can be written as

$$\mathcal{L} = \frac{1}{2}\sum_{\alpha=1}^{4N_f} \xi^{\alpha T}_{(2)}\mathcal{C}^{T}_{(2)}\gamma^{\mu}_{(2)}\partial_{\mu}\xi^{\alpha}_{(2)}. \tag{3.49}$$

In this case, although it is impossible to implement all space-time rotations by real matrices, they still act as identity on the Majorana flavor space, as explained in Appendix B. Therefore the theory has $\mathrm{O}(4N_f)$ symmetry.

It is also possible to see the $\mathrm{O}(4N_f)$ symmetry directly from four-component Majorana fermions, which will be useful in the next chapter. As discussed in Appendix B, by defining

$$\psi^{\alpha} = \frac{1}{\sqrt{2}}(\xi^{2\alpha-1} - \mathrm{i}\xi^{2\alpha}), \quad \bar{\psi}^{\alpha} = \frac{1}{\sqrt{2}}(\xi^{2\alpha-1T}\mathcal{C}^{T} + \mathrm{i}\xi^{2\alpha T}\mathcal{C}^{T}). \tag{3.50}$$

we can write the Lagrangian as

$$\mathcal{L} = \frac{1}{2}\sum_{\alpha=1}^{2N_f} \xi^{\alpha T}\mathcal{C}^{T}\gamma^{\mu}\partial_{\mu}\xi^{\alpha}, \tag{3.51}$$

where $\mathcal{C}$ is the charge conjugation matrix. Since 4 dimensional representation of the Clifford algebra $\mathrm{Cl}(3,0)$ is reducible, it turns out that $\mathcal{C}$ can satisfy both Majorana

condition Eq. (B.18) and pseudo-Majorana condition Eq. (B.19). For example, $\mathcal{C} = \gamma^0\gamma^3$ or $\mathcal{C} = \gamma^0\gamma^5$ satisfies the Majorana condition, while $\mathcal{C} = \gamma^0$ satisfies the pseudo-Majorana condition. Since we are working with free massless fermions, these two conditions are equivalent, and here we will choose $\mathcal{C} = \gamma^0$ for later convenience. The justification of this choice when interactions are added will be discussed in the next chapter.

With this choice of $\mathcal{C}$, we can write down the $\binom{4N_f}{2}$ generators of the $\mathrm{O}(4N_f)$ symmetry explicitly,

$$A \otimes \mathbb{1}_4, \quad A \otimes \gamma^3, \quad A \otimes \gamma^5, \quad S \otimes \mathrm{i}\gamma^3\gamma^5, \tag{3.52}$$

where A and S are $2N_f \times 2N_f$ anti-symmetric and symmetric matrices respectively, acting on the Majorana flavor space. Although these generators depend on the Dirac space, they commute with space-time rotations, and therefore generate internal symmetries. There is a conserved current associated with each symmetry generator, which will be discussed in the next chapter.

3.2.3 Lattice symmetries and their embedding in the continuum

We now wish to understand how the lattice symmetries discussed in Chapter 2 are embedded in the continuum. In two spatial dimension the lattice symmetries are translations generated by T_1 and T_2, parity P, spatial rotation R, time reversal Θ and charge conjugation C, given in Eqs. (2.8) to (2.13). As in one dimension, spatial symmetries map to a mixture of internal and spatial symmetries in the continuum. These lattice transformations induce transformations of the continuum fields according to the map Eq. (3.36),

$$\frac{1}{a}c_{n_1 n_2} \approx \mathrm{i}^{n_1+n_2}\Psi_{+\uparrow} + \mathrm{i}^{-n_1+n_2}\Psi_{+\downarrow} + \mathrm{i}^{-n_1-n_2}\Psi_{-\uparrow} + \mathrm{i}^{n_1-n_2}\Psi_{-\downarrow}. \tag{re 3.36}$$

Since the derivation of the continuum embedding of lattice rotations by $\frac{\pi}{2}$ is a

bit tricky, we explain it in detail below. Using the relation

$$(-1)^{n_1 n_2} = \frac{1}{2}\big(1 + (-1)^{n_1} + (-1)^{n_2} - (-1)^{n_1+n_2}\big), \tag{3.53}$$

we can write

$$\begin{aligned}
(-1)^{n_1 n_2} c_{-n_2,n_1} = \frac{1}{2}\big(1 + (-1)^{n_1} + (-1)^{n_2} - (-1)^{n_1+n_2}\big) \\
\big(\mathrm{i}^{-n_2+n_1}\Psi_{+\uparrow} + \mathrm{i}^{n_2+n_1}\Psi_{+\downarrow} + \mathrm{i}^{n_2-n_1}\Psi_{-\uparrow} + \mathrm{i}^{-n_2-n_1}\Psi_{-\downarrow}\big) \\
= \frac{1}{2}\big(\mathrm{i}^{n_1-n_2}\Psi_{+\uparrow} + \mathrm{i}^{n_1+n_2}\Psi_{+\downarrow} + \mathrm{i}^{-n_1+n_2}\Psi_{-\uparrow} + \mathrm{i}^{-n_1-n_2}\Psi_{-\downarrow} \\
+ \mathrm{i}^{-n_1-n_2}\Psi_{+\uparrow} + \mathrm{i}^{-n_1+n_2}\Psi_{+\downarrow} + \mathrm{i}^{n_1+n_2}\Psi_{-\uparrow} + \mathrm{i}^{n_1-n_2}\Psi_{-\downarrow} \\
+ \mathrm{i}^{n_1+n_2}\Psi_{+\uparrow} + \mathrm{i}^{n_1-n_2}\Psi_{+\downarrow} + \mathrm{i}^{-n_1-n_2}\Psi_{-\uparrow} + \mathrm{i}^{-n_1+n_2}\Psi_{-\downarrow} \\
- \mathrm{i}^{-n_1+n_2}\Psi_{+\uparrow} - \mathrm{i}^{-n_1-n_2}\Psi_{+\downarrow} - \mathrm{i}^{n_1-n_2}\Psi_{-\uparrow} - \mathrm{i}^{n_1+n_2}\Psi_{-\downarrow}\big).
\end{aligned} \tag{3.54}$$

Therefore

$$R\begin{pmatrix}\Psi_{+\uparrow}\\ \Psi_{+\downarrow}\\ \Psi_{-\uparrow}\\ \Psi_{-\downarrow}\end{pmatrix}R^{-1} = \frac{1}{2}\begin{pmatrix}1 & 1 & 1 & -1\\ -1 & 1 & 1 & 1\\ 1 & -1 & 1 & 1\\ 1 & 1 & -1 & 1\end{pmatrix}\begin{pmatrix}\Psi_{+\uparrow}\\ \Psi_{+\downarrow}\\ \Psi_{-\uparrow}\\ \Psi_{-\downarrow}\end{pmatrix}. \tag{3.55}$$

This transformations can be written as $\mathrm{e}^{\mathrm{i}\frac{\pi}{4}(\mathbb{1}\otimes\sigma^2 - \sigma^1\otimes\sigma^2)} = \mathrm{e}^{\mathrm{i}\frac{\pi}{4}(-\mathrm{i}\gamma^1\gamma^2 - \mathrm{i}\gamma^3\gamma^5)}$. Indeed we can check

$$\mathrm{e}^{-\mathrm{i}\frac{\pi}{4}(-\mathrm{i}\gamma^1\gamma^2-\mathrm{i}\gamma^3\gamma^5)}\,\gamma^0\gamma^1\,\mathrm{e}^{\mathrm{i}\frac{\pi}{4}(-\mathrm{i}\gamma^1\gamma^2-\mathrm{i}\gamma^3\gamma^5)} = \gamma^0\gamma^1\,\mathrm{e}^{\mathrm{i}\frac{\pi}{2}(-\mathrm{i}\gamma^1\gamma^2)} = \gamma^0\gamma^2 \tag{3.56}$$

$$\mathrm{e}^{-\mathrm{i}\frac{\pi}{4}(-\mathrm{i}\gamma^1\gamma^2-\mathrm{i}\gamma^3\gamma^5)}\,\gamma^0\gamma^2\,\mathrm{e}^{\mathrm{i}\frac{\pi}{4}(-\mathrm{i}\gamma^1\gamma^2-\mathrm{i}\gamma^3\gamma^5)} = \gamma^0\gamma^2\,\mathrm{e}^{\mathrm{i}\frac{\pi}{2}(-\mathrm{i}\gamma^1\gamma^2)} = -\gamma^0\gamma^1 \tag{3.57}$$

as desired. Similarly, the continuum embedding of the other lattice symmetry transformations can be derived, and the results are tabulated in Table 3.2.

Notice that while P and Θ are space-time symmetries in the continuum as on the lattice, R is a mixture of space-time and internal symmetries, and T_1, T_2 and C belong to a subgroup of $\mathrm{O}(4N_f)$ and therefore are internal symmetries, which are clear in the Majorana language. Furthermore, the internal $\mathrm{O}(2N_f)$ symmetry of the lattice model is embedded in $\mathrm{O}(4N_f)$ as $A \otimes \mathbb{1}_4$ in Eq. (3.52).

Table 3.2: The action of the lattice symmetries on the continuum fields in two spatial dimensions.

	$c_{n_1n_2}$	$\psi(t,x_1,x_2)$	$\xi(t,x_1,x_2)$
T_1	$(-1)^{n_2}c_{n_1+1,n_2}$	$-\mathrm{i}\gamma^5\psi(t,x_1,x_2)$	$-\mathrm{i}\sigma^2\otimes\gamma^5\xi(t,x_1,x_2)$
T_2	c_{n_1,n_2+1}	$\mathrm{i}\gamma^3\psi(t,x_1,x_2)$	$\mathrm{i}\sigma^2\otimes\gamma^3\xi(t,x_1,x_2)$
R	$(-1)^{n_1n_2}c_{-n_2,n_1}$	$\mathrm{e}^{\mathrm{i}\frac{\pi}{4}(-\mathrm{i}\gamma^1\gamma^2-\mathrm{i}\gamma^3\gamma^5)}\,\psi(t,-x_2,x_1)$	$\mathbb{1}_2\otimes\mathrm{e}^{\mathrm{i}\frac{\pi}{4}(-\mathrm{i}\gamma^1\gamma^2-\mathrm{i}\gamma^3\gamma^5)}\,\xi(t,-x_2,x_1)$
P	c_{-n_1,n_2}	$\mathrm{i}\gamma^1\gamma^5\psi(t,-x_1,x_2)$	$\mathbb{1}_2\otimes\mathrm{i}\gamma^1\gamma^5\xi(t,-x_1,x_2)$
Θ	c_{n_1,n_2}	$\gamma^0\psi(-t,x_1,x_2)$	$\mathbb{1}_2\otimes\gamma^0\xi(-t,x_1,x_2)$
C	$(-1)^{n_1+n_2}c^\dagger_{n_1n_2}$	$\psi^{\dagger T}(t,x_1,x_2)=\mathcal{C}^{-1}\bar\psi^T$	$\sigma^3\otimes\mathbb{1}_2\xi(t,x_1,x_2)$

3.2.4 The continuum limit of local lattice fermion bilinears

The continuum limit of the lattice fermion bilinears is very similar to the case of one spatial dimension. Consider the case of N_f flavors of lattice fermions. Using the relation Eq. (3.7), we have

$$\frac{1}{a^2}c^{\alpha\dagger}_{n_1n_2}c^{\beta}_{n_1n_2}\to(-1)^{n_1+n_2}\bar\psi^\alpha\psi^\beta-(-1)^{n_2}\bar\psi^\alpha\gamma^1\gamma^5\psi^\beta+(-1)^{n_1}\bar\psi^\alpha\gamma^2\gamma^3\psi^\beta+\psi^{\alpha\dagger}\psi^\beta. \tag{3.58}$$

As in one spatial dimension, the linear combination of continuum fields is site-dependent. Performing a particle-hole transformation, we have

$$\begin{aligned}\frac{1}{a^2}(-1)^{n_1+n_2}c^{\alpha}_{n_1n_2}c^{\beta}_{n_1n_2}&\to(-1)^{n_1+n_2}\psi^{\alpha T}\gamma^0\psi^\beta-(-1)^{n_2}\psi^{\alpha T}\gamma^0\gamma^1\gamma^5\psi^\beta\\&\quad+(-1)^{n_1}\psi^{\alpha T}\gamma^0\gamma^2\gamma^3\psi^\beta+\psi^\alpha\psi^\beta,\\\frac{1}{a^2}(-1)^{n_1+n_2}c^{\alpha\dagger}_{n_1n_2}c^{\beta\dagger}_{n_1n_2}&\to(-1)^{n_1+n_2}\bar\psi^\alpha\gamma^0\bar\psi^{\beta T}-(-1)^{n_2}\bar\psi^\alpha\gamma^1\gamma^5\gamma^0\bar\psi^{\beta T}\\&\quad+(-1)^{n_1}\bar\psi^\alpha\gamma^2\gamma^3\gamma^0\bar\psi^{\beta T}+\psi^{\alpha\dagger}\psi^{\beta\dagger T}.\end{aligned} \tag{3.59}$$

We can also write these relations in terms of Majorana fermions. The 2d version of Eq. (3.26) is

$$\gamma^{2\alpha-1}_{n_1n_2}=(-\mathrm{i})^{n_1+n_2}c^\alpha_{n_1n_2}+\mathrm{i}^{n_1+n_2}c^{\alpha\dagger}_{n_1n_2},\quad \gamma^{2\alpha}_{n_1n_2}=(-\mathrm{i})^{n_1+n_2-1}c^\alpha_{n_1n_2}+\mathrm{i}^{n_1+n_2-1}c^{\alpha\dagger}_{n_1n_2}. \tag{3.60}$$

Then using the relations Eqs. (3.36) and (3.50), we can relate lattice Majorana fermions to the continuum Majorana fermions as

$$\frac{1}{\sqrt{2}a}\gamma^{\alpha}_{n_1 n_2} \to \xi^{\alpha}_{+\uparrow} + (-1)^{n_1}\xi^{\alpha}_{+\downarrow} + (-1)^{n_1+n_2}\xi^{\alpha}_{-\uparrow} + (-1)^{n_2}\xi^{\alpha}_{-\downarrow} \tag{3.61}$$

for $\alpha = 1, \cdots, 2N_f$. Therefore

$$\begin{aligned}\frac{1}{2a^2}\gamma^{\alpha}_{n_1 n_2}\gamma^{\beta}_{n_1 n_2} \to (-1)^{n_1+n_2}\xi^{\alpha T}\mathcal{C}\xi^{\beta} - (-1)^{n_2}\xi^{\alpha T}\mathcal{C}\gamma^1\gamma^5\xi^{\beta} \\ + (-1)^{n_1}\xi^{\alpha T}\mathcal{C}\gamma^2\gamma^3\xi^{\beta} + \xi^{\alpha T}\xi^{\beta}.\end{aligned} \tag{3.62}$$

4

Continuum Limit of Interacting Lattice Fermions

In this chapter, we analyze all the independent four-fermion interactions in the continuum allowed by the symmetries of free lattice fermions. In order to do so, we analyze all fermion bilinears, including space-time (pseudo-)scalars, i.e., masses, and space-time (pseudo-)vectors, i.e., currents, and determine how they transform under the lattice symmetries. Then all symmetric four-fermion interactions can be constructed out of them. We will use this analysis to propose the possible continuum limits of our interacting lattice models in one and two spatial dimensions introduced in Chapter 2.

4.1 One spatial dimension

Recall that the Euclidean Lagrangian density of N_f-flavor free Dirac fermions is given by

$$\mathcal{L} = \sum_{\alpha=1}^{N_f} \bar{\psi}^{\alpha} \gamma^{\mu} \partial_{\mu} \psi^{\alpha}, \tag{4.1}$$

where $\bar{\psi} = \psi^\dagger \gamma^0$, $\mu = 0, 1$ and $\gamma^0 = \sigma^1, \gamma^1 = -\sigma^2, \gamma^3 = \sigma^3$. We also showed that this free Lagrangian could be written in terms of Majorana fermions,

$$\mathcal{L} = \frac{1}{2} \sum_{\alpha=1}^{2N_f} \xi^{\alpha T} \mathcal{C} \gamma^\mu \partial_\mu \xi^\alpha. \tag{4.2}$$

where $\mathcal{C} = \gamma^0$, satisfying the pseudo-Majorana condition Eq. (B.19). Note that since we will analyze all possible fermion bilinears with insertion of $\mathbb{1}$ and γ^3, the pseudo-Majorana condition is equivalent to the Majorana condition for the purpose of analyzing all the possible fermion bilinears and interactions.

As we discussed, this Lagrangian is invariant under $\mathrm{O}(2N_f)_+ \times \mathrm{O}(2N_f)_-$ transformations in addition to the usual space-time symmetries. On the other hand, the lattice Hamiltonian is invariant only under lattice translation T_a, parity P, time reversal Θ, charge conjugation C and the diagonal $\mathrm{O}(2N_f)$ symmetry. Thus, the effective continuum theory in the presence of interactions only needs to be invariant under these lattice symmetries, and we learned how they are embedded in the continuum symmetries in Table 3.1 and the discussion following it.

In order to analyze four-fermion interactions that respect these lattice symmetries, let us first construct all fermion bilinears, and determine how they transform under the diagonal $\mathrm{O}(2N_f)$ symmetry. The other symmetries are all $\mathbb{Z}_2$ symmetries and will be satisfied automatically by the four-fermion interactions. Since each Majorana fermion ξ^α has two components, we have a total of $4N_f$ single-component Majorana fermions, from which we can construct $\binom{4N_f}{2}$ fermion bilinears. The most general fermion bilinears can be written as $\xi^T (T \otimes \mathcal{C}\Gamma) \xi$, where Γ can be any one of the 4 elements in the Clifford algebra, T is a $2N_f \times 2N_f$ matrix in the Majorana flavor space, but $T \otimes \mathcal{C}\Gamma$ must be a $4N_f \times 4N_f$ anti-symmetric matrix.

4.1.1 Mass terms

Here fermion mass terms are defined as local fermion bilinears transforming as (pseudo-)scalars under space-time rotations, but are allowed to rotate non-trivially under internal symmetry transformations. This means, among the general fermion bilinears $\xi^T(T \otimes \mathcal{C}\Gamma)\xi$, the matrix Γ is required to satisfy $[\Gamma, \gamma^0\gamma^1] = 0$, with solutions $\Gamma = \mathbb{1}, \mathrm{i}\gamma^3$. Since $T \otimes \mathcal{C}\Gamma$ has to be anti-symmetric, the possible mass terms are $\xi^T(A \otimes \mathcal{C})\xi$ where A is anti-symmetric and $\xi^T(S \otimes \mathrm{i}\mathcal{C}\gamma^3)\xi$ with S symmetric. Therefore there are a total of $N_f(2N_f - 1) + N_f(2N_f + 1) = 4N_f^2$ mass terms. Recall that the diagonal $\mathrm{O}(2N_f)$ transformations and axial $\mathrm{O}(2N_f)_+ \times \mathrm{O}(2N_f)_- / \mathrm{O}(2N_f)$ transformations are generated by

$$A \otimes \mathbb{1}_2, \quad A \otimes \gamma^3. \tag{4.3}$$

and it is easy to verify that the two kinds of mass terms do not mix under the diagonal $\mathrm{O}(2N_f)$ transformations, but they do mix under the axial transformations.

The $4N_f^2$ mass terms decompose into three irreducible representations (irreps)

$$\mathbf{4N_f^2 = adj + sym + triv} \tag{4.4}$$

of the diagonal $\mathrm{O}(2N_f)$ symmetry. If we define A^a as a basis of all anti-symmetric Hermitian matrices satisfying $\mathrm{tr}(A^a A^b) = \frac{1}{2}\delta^{ab}$, the adjoint mass terms $M^a_{\mathbf{adj}} := \xi^T(A^a \otimes \mathcal{C})\xi$ transform in the adjoint representation **adj** (or equivalently, the anti-symmetric representation). The usual mass term $\bar{\psi}\psi = \frac{1}{2}\xi^T(A \otimes \mathcal{C})\xi$ with $A = \mathbb{1}_{N_f} \otimes \sigma^2$ lives in this space. If we define S^a as a basis of all traceless symmetric Hermitian matrices that satisfy $\mathrm{tr}(S^a S^b) = \frac{1}{2}\delta^{ab}$, the symmetric mass terms $M^a_{\mathbf{sym}} := \xi^T(S^a \otimes \mathrm{i}\mathcal{C}\gamma^3)\xi$ transform in the traceless symmetric representation **sym**. Finally, the term $M_{\mathbf{triv}} := \frac{1}{2}\xi^T(\mathbb{1}_{2N_f} \otimes \mathrm{i}\mathcal{C}\gamma^3)\xi$ transforms in the trivial representation **triv**. Actually, this term is the chiral mass $\bar{\psi}\mathrm{i}\gamma^3\psi$.

4.1.2 Currents

Currents are defined as local fermion bilinears transforming as (pseudo-)vectors under space-time rotations. In a covariant notation, they are labeled with an index μ, the direction of the current. Similar to the mass terms, there are two classes of rotationally covariant currents $\xi^T(T \otimes \mathcal{C}\gamma^\mu)\xi$ and $\xi^T(T \otimes \mathrm{i}\mathcal{C}\gamma^3\gamma^\mu)\xi$. However, due to the identity $\mathrm{i}\gamma^3\gamma^\mu = \varepsilon^{\mu\nu}\gamma^\nu$, where $\varepsilon^{01} = 1$, these two currents are not independent. We can choose $\xi^T(T\otimes\mathcal{C}\gamma^\mu)\xi$ to be the independent ones, and since $\mathcal{C}\gamma^\mu$ is symmetric, T must be a $2N_f \times 2N_f$ anti-symmetric matrix. Therefore we have $\binom{2N_f}{2}$ distinct currents denoted as $J^{a\mu} := \xi^T(A^a\otimes\mathcal{C}\gamma^\mu)\xi$, where the basis of anti-symmetric matrices A^a was introduced above. The currents split under the full $\mathrm{O}(2N_f)_+\times\mathrm{O}(2N_f)_-$ chiral symmetry, which is clear if we define

$$J^a_\pm := \frac{1}{2}(J^{a0} \pm \mathrm{i}J^{a1}) = \xi^T_\pm A^a \xi_\pm. \tag{4.5}$$

These are the conserved currents associated with the full $\mathrm{O}(2N_f)_+ \times \mathrm{O}(2N_f)_-$ chiral symmetry. Clearly each $J^a_\pm$ transform independently under the adjoint representation of $\mathrm{O}(2N_f)_\pm$, and the $2N_f(2N_f-1)$ current terms decompose into

$$\mathbf{2N_f(2N_f-1) = adj_+ + adj_-}. \tag{4.6}$$

When we choose $A = \mathbb{1}_{N_f} \otimes \sigma^2$, we obtain the traditional current $\bar\psi\gamma^\mu\psi = \frac{1}{2}\xi^T(A \otimes \mathcal{C}\gamma^\mu)\xi$. In particular, $\bar\psi(\gamma^0 \pm \mathrm{i}\gamma^1)\psi$ lives in $\mathbf{adj}_\pm$.

If we count all the mass terms and the currents, we obtain

$$4N_f^2 + \binom{2N_f}{2} \times 2 = \binom{4N_f}{2} \tag{4.7}$$

fermion bilinears as expected.

It is useful to understand how these mass terms and currents transform under the discrete lattice symmetries T_a, P, Θ, and C, which can be achieved using the transformations we derived in Table 3.1. Some bilinears do not mix with others and

behave like eigenvectors under these transformations. The corresponding eigenvalues are summarized in Table 4.1. Under parity, a current can transform as a vector (v) or a pseudo-vector (p).

Table 4.1: Internal symmetries and transformation properties under lattice symmetries of some fermion bilinears in one spatial dimension.

Bilinears	Internal symmetry	$T_a = \mathrm{i}\gamma^3$	$P = \gamma^0$	$\Theta = \gamma^0 K$	C
$\bar{\psi}\psi$	$\mathrm{U}(N_f)$	-1	$+1$	$+1$	-1
$\bar{\psi}\mathrm{i}\gamma^3\psi$	$\mathrm{O}(2N_f)$	-1	-1	$+1$	$+1$
$\bar{\psi}\gamma^\mu\psi$	$\mathrm{U}(N_f)_+ \times \mathrm{U}(N_f)_-$	$+1$	v	$+1$	-1

4.1.3 Allowed four-fermion interactions

Knowing how the fermion bilinears transform under the symmetry transformations, we can construct four-fermion interactions that are invariant under these transformations. For example, by contracting the fermion bilinears in each irrep of the diagonal $\mathrm{O}(2N_f)$ we can construct four-fermion interactions that are invariant under the lattice $\mathrm{O}(2N_f)$ transformations. When the fermion bilinears are mass terms, we get Gross-Neveu type interactions $(M^a_{\mathbf{adj}})^2$, $(M^a_{\mathbf{sym}})^2$ and $(M_{\mathbf{triv}})^2$. On the other hand, when the fermion bilinears are currents, we get the Thirring interaction $(J^{a\mu})^2$. Although the currents transform under the full $\mathrm{O}(2N_f)_+ \times \mathrm{O}(2N_f)_-$ chiral symmetry, the Thirring interaction is only invariant under the diagonal $\mathrm{O}(2N_f)$ symmetry when $N_f > 1$, because

$$(J^{a\mu})^2 = 4J^a_+ J^a_-. \tag{4.8}$$

Using the Fierz identity and other identities, the three Gross-Neveu interactions and the Thirring interaction can be shown to be proportional to each other,

$$(M_{\mathbf{triv}})^2 = (M^a_{\mathbf{adj}})^2 = -\frac{N_f}{N_f+1}(M^a_{\mathbf{sym}})^2 = -\frac{1}{2}(J^{a\mu})^2, \tag{4.9}$$

where $(M_{\mathbf{triv}})^2 = (\bar{\psi}\mathrm{i}\gamma^3\psi)^2$ is the chiral mass Gross-Neveu interaction. In the case of $N_f = 1$, the above identity reduces to the familiar relation

$$(\bar{\psi}\mathrm{i}\gamma^3\psi)^2 = (\bar{\psi}\psi)^2 = -\frac{1}{2}(\bar{\psi}\gamma^\mu\psi)^2. \tag{4.10}$$

Furthermore, since the adjoint representation is the same as the trivial representation for O(2), $J^a_\pm$ transforms trivially under $\mathrm{O}(2)_+ \times \mathrm{O}(2)_-$, and $(\bar{\psi}\gamma^\mu\psi)^2$ has the full chiral symmetry.

4.1.4 The case of $N_f = 2$ with SO(4) symmetry

Although the above analysis holds for any $N_f \geq 1$, the case of $N_f = 2$ is special if the system only has $\mathrm{SO}(2N_f)$ symmetry instead of $\mathrm{O}(2N_f)$ symmetry. In this case, there are more independent interactions, because SO(4) is not a simple Lie group; therefore, the adjoint representation of SO(4) is not an irrep. More concretely, there are self-dual and anti-self-dual conditions [1] which are preserved under an SO(4) transformation, but are flipped under an improper O(4) transformation. For any 4×4 anti-symmetric matrix A, it is said to be self-dual (or anti-self-dual) if it satisfies the following condition

$$A_{\alpha\beta} = \pm\varepsilon_{\alpha\beta\gamma\delta}A_{\gamma\delta}. \tag{4.11}$$

Without loss of generality, we can assume A to be self-dual in the following argument. Under an O(4) transformation O, $A_{\alpha\beta} \mapsto A'_{\alpha\beta} = O_{\alpha\alpha'}O_{\beta\beta'}A_{\alpha'\beta'}$, and we have

$$\begin{aligned} A'_{\alpha\beta} &= O_{\alpha\alpha'}O_{\beta\beta'}\varepsilon_{\alpha'\beta'\gamma'\delta'}A_{\gamma'\delta'} \\ &= O_{\alpha\alpha'}O_{\beta\beta'}\varepsilon_{\alpha'\beta'\gamma'\delta'}O^{-1}_{\gamma'\gamma}O^{-1}_{\delta'\delta}A'_{\gamma\delta} \\ &= O_{\alpha\alpha'}O_{\beta\beta'}O_{\gamma\gamma'}O_{\delta\delta'}\varepsilon_{\alpha'\beta'\gamma'\delta'}A'_{\gamma\delta} \\ &= \det(O)\varepsilon_{\alpha\beta\gamma\delta}A'_{\gamma\delta}. \end{aligned} \tag{4.12}$$

[1] They are called "dual" because we can associate each anti-symmetric matrix with a 2-form, and the dual operation here corresponds to Hodge dual on differential forms.

Therefore the self-dual condition is preserved if $\det(O) = 1$, i.e., $O \in \mathrm{SO}(4)$, and is flipped to the anti-self-dual condition if $\det(O) = -1$, i.e., O belongs to the improper part of O(4). This means that the adjoint representation is an irrep of O(4), but not an irrep of SO(4).

Since both self-dual and anti-self-dual matrices are fully determined by the matrix elements A_{12}, A_{13} and A_{14}, they both form three-dimensional spaces. The basis of the self-dual matrices can be chosen to be three charge matrices A_c^i, and the basis of the anti-self-dual matrices can be chosen to be three spin matrices A_s^i, where $i = 1, 2, 3$, as is shown in the following,

$$2A_s^1 = -\mathrm{i} \begin{pmatrix} 0 & 0 & 0 & 1 \\ 0 & 0 & -1 & 0 \\ 0 & 1 & 0 & 0 \\ -1 & 0 & 0 & 0 \end{pmatrix} = -J_3 + K_3 = \sigma^1 \otimes \sigma^2 \tag{4.13}$$

$$2A_s^2 = -\mathrm{i} \begin{pmatrix} 0 & 0 & 1 & 0 \\ 0 & 0 & 0 & 1 \\ -1 & 0 & 0 & 0 \\ 0 & -1 & 0 & 0 \end{pmatrix} = -J_2 + K_2 = \sigma^2 \otimes \mathbb{1} \tag{4.14}$$

$$2A_s^3 = -\mathrm{i} \begin{pmatrix} 0 & 1 & 0 & 0 \\ -1 & 0 & 0 & 0 \\ 0 & 0 & 0 & -1 \\ 0 & 0 & 1 & 0 \end{pmatrix} = -J_1 + K_1 = \sigma^3 \otimes \sigma^2, \tag{4.15}$$

and

$$2A_c^1 = -\mathrm{i}\begin{pmatrix} 0 & 0 & 0 & -1 \\ 0 & 0 & -1 & 0 \\ 0 & 1 & 0 & 0 \\ 1 & 0 & 0 & 0 \end{pmatrix} = -J_3 - K_3 = -\sigma^2 \otimes \sigma^1 \tag{4.16}$$

$$2A_c^2 = -\mathrm{i}\begin{pmatrix} 0 & 0 & -1 & 0 \\ 0 & 0 & 0 & 1 \\ 1 & 0 & 0 & 0 \\ 0 & -1 & 0 & 0 \end{pmatrix} = -J_2 - K_2 = -\sigma^2 \otimes \sigma^3 \tag{4.17}$$

$$2A_c^3 = -\mathrm{i}\begin{pmatrix} 0 & -1 & 0 & 0 \\ 1 & 0 & 0 & 0 \\ 0 & 0 & 0 & -1 \\ 0 & 0 & 1 & 0 \end{pmatrix} = -J_1 - K_1 = -\mathbb{1} \otimes \sigma^2, \tag{4.18}$$

where J_i and K_i satisfy the Lie algebra $[J_i, J_j] = \mathrm{i}\varepsilon_{ijk}J_k$, $[J_i, K_j] = \mathrm{i}\varepsilon_{ijk}K_k$ and $[K_i, K_j] = \mathrm{i}\varepsilon_{ijk}J_k$. The matrices A_s^i and A_c^i are called spin and charge matrices because they can also be viewed as the defining representation of $\mathrm{SO}(4) \cong \mathrm{SU}(2)\times\mathrm{SU}(2)/\mathbb{Z}_2$, and the two SU(2)'s can be identified as spin rotations and charge rotations of the Dirac fermions. In order to see this, we can arrange the Majorana fermions as a 2×2 matrix-valued field,[2]

$$\Psi = \xi^1\mathbb{1}_2 - \mathrm{i}\xi^2\sigma^3 - \mathrm{i}\xi^3\sigma^2 - \mathrm{i}\xi^4\sigma^1 = \begin{pmatrix} \xi^1 - \mathrm{i}\xi^2 & -\xi^3 - \mathrm{i}\xi^4 \\ \xi^3 - \mathrm{i}\xi^4 & \xi^1 + \mathrm{i}\xi^2 \end{pmatrix} = \begin{pmatrix} \psi^1 & -\psi^{2\dagger} \\ \psi^2 & \psi^{1\dagger} \end{pmatrix}. \tag{4.19}$$

Then a spin SO(4) transformation $\xi \mapsto \mathrm{e}^{\mathrm{i}\theta A_s^i}\,\xi$ corresponds to $\Psi \mapsto \mathrm{e}^{\mathrm{i}\frac{\theta}{2}\sigma^i}\,\Psi$, while a charge SO(4) transformation $\xi \mapsto \mathrm{e}^{\mathrm{i}\theta A_c^i}\,\xi$ corresponds to $\Psi \mapsto \Psi\,\mathrm{e}^{-\mathrm{i}\frac{\theta}{2}\sigma^i}$.

Using the above insight, we can split the six adjoint masses $M^a_{\mathbf{adj}}$ into three spin mass terms $M_s^i := \frac{1}{2}\xi^T A_s^i \otimes \mathcal{C}\xi$ and three charge mass terms $M_c^i := \frac{1}{2}\xi^T A_c^i \otimes \mathcal{C}\xi$. When written in terms of Dirac fermions, they are

$$M_s^i = \frac{1}{2}\bar{\psi}\sigma^i\psi, \quad M_c^3 = -\frac{1}{2}\bar{\psi}\psi, \tag{4.20}$$

[2] In general, there are many ways to contract four components of ξ with $\mathbb{1}_2$ and σ^i. Our choice is fixed by the following two requirements: the first column of Ψ is $(\psi^1, \psi^2)^T$, and $-\mathrm{i}\sigma^1, -\mathrm{i}\sigma^2, -\mathrm{i}\sigma^3$ can be identified as quaternions.

which are the spin and charge order parameters. The other two charge matrices can be viewed as superconducting order parameters,

$$M_c^1 = \frac{1}{2}(\psi_1^T \mathcal{C} \psi_2 + \bar{\psi}_2 \mathcal{C} \bar{\psi}_1^T), \quad M_c^2 = -\frac{\mathrm{i}}{2}(\psi_1^T \mathcal{C} \psi_2 - \bar{\psi}_2 \mathcal{C} \bar{\psi}_1^T). \tag{4.21}$$

Recall that the self-dual and anti-self-dual conditions are flipped under improper O(4) rotations. In particular, under one such improper rotation, $O = \mathrm{diag}(-1, 1, 1, 1)$, we can see that the matrices A_s^i and A_c^i are flipped into each other. Hence we will refer to this improper O(4) rotation as a spin-charge flip transformation $\mathbb{Z}_2^{sc}$. In terms of Majorana fermions, this flip implies $\xi^1 \mapsto -\xi^1$ and $M_s^i \leftrightarrow M_c^i$. This spin-charge flip transformation can also be implemented on the matrix-valued field in Eq. (4.19) as $\Psi \leftrightarrow -\Psi^\dagger$, or equivalently, on Dirac fermions as $\psi^1 \leftrightarrow -\psi^{1\dagger}$. Therefore, the $\mathbb{Z}_2$ spin-charge flip can be understood as a particle-hole transformation on a single flavor. The above analysis for masses can also be extended to currents and the adjoint currents can be split into spin currents $J_s^{i\mu} := \frac{1}{2}\xi^T A_s^i \otimes \mathcal{C}\gamma^\mu \xi$, and charge currents $J_c^{i\mu} := \frac{1}{2}\xi^T A_c^i \otimes \mathcal{C}\gamma^\mu \xi$. The spin-charge flip transformation will flip between these two.

This split of spin and charge under SO(4) transformations implies that there could possibly be more independent four-fermion interactions. As we argued before, there is only one independent interaction with O(4) symmetry. On the other hand, if we only require SO(4) symmetry, the four-fermion interactions that arise from adjoint representation split into spin and charge parts [3]

$$(M_{\mathbf{adj}}^a)^2 = 2(M_s^i)^2 + 2(M_c^i)^2, \quad (J^{a\mu})^2 = 2(J_s^{i\mu})^2 + 2(J_c^{i\mu})^2, \tag{4.22}$$

and each of them will be invariant under SO(4) transformations, which means we have possibly more independent interactions. It turns out that $(J_s^{i\mu})^2$ and $(J_c^{i\mu})^2$ are indeed independent of each other, and $(M_s^i)^2$ and $(M_c^i)^2$ are dependent on $(J_s^{i\mu})^2$ and

[3] The additional factor of 2 in Eq. (4.22) is due to that we normalized A^a as $\mathrm{tr}(A^a A^b) = \frac{1}{2}\delta^{ab}$, but normalized $\frac{1}{2}A_s^i$ as $\mathrm{tr}(\frac{1}{2}A_s^i \frac{1}{2}S^j) = \frac{1}{4}\delta^{ij}$ and similarly for $\frac{1}{2}A_c^i$.

$(J_c^{i\mu})^2$ through the relations,

$$\begin{pmatrix}(M_s^i)^2\\(M_c^i)^2\end{pmatrix} = \frac{1}{4}\begin{pmatrix}1 & -3\\-3 & 1\end{pmatrix}\begin{pmatrix}(J_s^{i\mu})^2\\(J_c^{i\mu})^2\end{pmatrix}. \tag{4.23}$$

Therefore we have two independent interactions in the case of $N_f = 2$ with SO(4) symmetry.

4.2 Two spatial dimensions

In order to understand the allowed continuum interactions in two spatial dimensions, we begin with the Lagrangian density of N_f flavor Dirac fermions derived in Eq. (3.44). We will drop the tildes in the definition in this chapter and simply write it as

$$\mathcal{L} = \sum_{\alpha=1}^{N_f} \bar{\psi}^\alpha \gamma^\mu \partial_\mu \psi^\alpha, \tag{4.24}$$

where $\bar{\psi} = \psi^\dagger \gamma^0$ and $\mu = 0, 1, 2$. Note that the definition of γ matrices is the same as Eq. (3.43),

$$\gamma^0 = -\sigma^2 \otimes \sigma^2,\ \gamma^1 = -\sigma^2 \otimes \sigma^3,\ \gamma^2 = -\sigma^2 \otimes \sigma^1,\ \gamma^3 = \sigma^3 \otimes \mathbb{1},\ \gamma^5 = \sigma^1 \otimes \mathbb{1}, \tag{4.25}$$

but without the tildes. In terms of Majorana fermions

$$\psi^\alpha = \frac{1}{\sqrt{2}}(\xi^{2\alpha-1} - \mathrm{i}\xi^{2\alpha}), \quad \bar{\psi}^\alpha = \frac{1}{\sqrt{2}}(\xi^{2\alpha-1T}\mathcal{C} + \mathrm{i}\xi^{2\alpha T}\mathcal{C}), \tag{4.26}$$

the Lagrangian can be written as

$$\mathcal{L} = \frac{1}{2}\sum_{\alpha=1}^{2N_f} \xi^{\alpha T}\mathcal{C}\gamma^\mu \partial_\mu \xi^\alpha, \tag{4.27}$$

where $\mathcal{C} = \gamma^0$, satisfying the pseudo-Majorana condition Eq. (B.19). Similar to the one spatial dimension case, since we will analyze all possible fermion bilinears with insertions of $\mathbb{1}$, γ^3, γ^5 and $\mathrm{i}\gamma^3\gamma^5$, the pseudo-Majorana condition is in fact equivalent

to the Majorana condition for the purpose of analyzing all possible fermion bilinears and interactions.

While this continuum Lagrangian has the $\mathrm{O}(4N_f)$ symmetry and the usual space-time symmetries, the lattice symmetries of our model are rather restricted. In Table 3.2 we derived how the lattice symmetries are embedded within the continuum symmetries. We also discussed after Table 3.2 that the generators of the $\mathrm{O}(2N_f)$ symmetry of the lattice model are embedded as $A \otimes \mathbb{1}_4$ among the generators of the $\mathrm{O}(4N_f)$ symmetry in Eq. (3.52). Furthermore, the $\mathbb{Z}_4$ lattice rotation symmetry is enhanced in the continuum to an $\mathrm{SO}(2)_R$ symmetry. This is because the $\mathbb{Z}_4$ transformation mixes two different fermion bilinears, and four-fermion interactions that preserve the $\mathbb{Z}_4$ symmetry would automatically preserve the $\mathrm{SO}(2)_R$ symmetry.

In order to analyze four-fermion interactions that respect these lattice symmetries, let us first construct all fermion bilinears, and determine how they transform under the lattice $\mathrm{O}(2N_f) \times \mathrm{SO}(2)_R$ symmetry. We can then use these bilinears to construct four-fermion interactions that are invariant under all the lattice symmetries. Since each Majorana fermion field ξ^α has four components and α takes $2N_f$ values, we have a total of $8N_f$ single-component Majorana fermions, from which we can construct $\binom{8N_f}{2}$ fermion bilinears. These fermion bilinears are of the form $\xi^T(T \otimes \mathcal{C}\Gamma)\xi$, where Γ can be any one of the 16 elements in the Clifford algebra, T is a $2N_f \times 2N_f$ matrix in the Majorana flavor space, but $T \otimes \mathcal{C}\Gamma$ must be an $8N_f \times 8N_f$ anti-symmetric matrix.

4.2.1 Mass terms

Since fermion mass terms are local fermion bilinears which are invariant under space-time rotations, we can write them as $\xi^T(T \otimes \mathcal{C}\Gamma)\xi$ with the condition that $[\Gamma, \gamma^\mu\gamma^\nu] = 0$. This gives us the constraint that $\Gamma = \mathbb{1}, \mathrm{i}\gamma^3, \mathrm{i}\gamma^5, \mathrm{i}\gamma^3\gamma^5$. Note that the i's are inserted such that $\mathcal{C}\Gamma$ are four Hermitian matrices, and therefore they rotate into

each other under $\mathrm{O}(4N_f)$ transformations. Since $T \otimes \mathcal{C}\Gamma$ has to be anti-symmetric, the possible mass terms turn out to be

$$\xi^T(A \otimes \mathcal{C})\xi, \quad \xi^T(S \otimes \mathrm{i}\mathcal{C}\gamma^3)\xi, \quad \xi^T(S \otimes \mathrm{i}\mathcal{C}\gamma^5)\xi, \quad \xi^T(S \otimes \mathrm{i}\mathcal{C}\gamma^3\gamma^5)\xi, \tag{4.28}$$

where A and S are anti-symmetric and symmetric $2N_f \times 2N_f$ matrices respectively. Therefore we have a total of $N_f(2N_f - 1) + 3N_f(2N_f + 1) = 2N_f(4N_f + 1)$ mass terms. Notice that $2N_f(4N_f + 1) = \binom{4N_f+1}{2}$ is the number of $4N_f \times 4N_f$ symmetric matrices, which is not coincidental. In fact, in our basis, we have

$$\mathcal{C} = -\sigma^2 \otimes \sigma^2, \quad \mathrm{i}\mathcal{C}\gamma^3 = \sigma^1 \otimes \sigma^2, \quad \mathrm{i}\mathcal{C}\gamma^5 = -\sigma^3 \otimes \sigma^2, \quad \mathrm{i}\mathcal{C}\gamma^3\gamma^5 = \mathbb{1} \otimes \sigma^2. \tag{4.29}$$

We see that all $\mathcal{C}\Gamma$ are of the form $\mathcal{C}\Gamma = \Gamma_{(2)} \otimes \sigma^2$, where $\Gamma_{(2)}$ are 2×2 matrices forming $\mathrm{Cl}(2, 0)$. Therefore the mass terms are all of the form $\xi^T(T \otimes \Gamma_{(2)} \otimes \sigma^2)\xi$. $T \otimes \Gamma_{(2)} \otimes \sigma^2$ being anti-symmetric implies that $T \otimes \Gamma_{(2)}$ is symmetric, and since $\Gamma_{(2)}$ spans all 2×2 matrices, the space of $T \otimes \Gamma_{(2)}$ is the space of all $4N_f \times 4N_f$ symmetric matrices, which is $\binom{4N_f+1}{2}$ dimensional.

Recall that in our basis, the $\mathrm{O}(4N_f)$ symmetry is generated by

$$A \otimes \mathbb{1}_4, \quad A \otimes \gamma^3, \quad A \otimes \gamma^5, \quad S \otimes \gamma^3\gamma^5, \tag{re 3.52}$$

where $A \otimes \mathbb{1}_4$ generates the $\mathrm{O}(2N_f)$ transformation that is preserved by the lattice. It can be checked that while the four kinds of mass terms in Eq. (4.28) mix with each other under the full $\mathrm{O}(4N_f)$ symmetry, they do not mix under the lattice $\mathrm{O}(2N_f)$ transformations. On the other hand, under the $\mathrm{SO}(2)_R$ symmetry generated by $\mathbb{1} \otimes \gamma^3\gamma^5$, the two mass terms $\xi^T(S \otimes \mathrm{i}\mathcal{C}\gamma^3)\xi$ and $\xi^T(S \otimes \mathrm{i}\mathcal{C}\gamma^5)\xi$ rotate into each other.

The $\binom{4N_f+1}{2}$ mass terms form seven irreps of the $\mathrm{O}(2N_f)$ symmetry, and we can write

$$\binom{\mathbf{4N_f + 1}}{\mathbf{2}} = \mathbf{adj} + (\mathbf{sym} + \mathbf{triv}) \times 3. \tag{4.30}$$

To make this more explicit, we introduce A^a and S^a as before and denote the seven

irreps as

$$M^a_{\mathbf{adj}} := \xi^T(A^a \otimes \mathcal{C})\xi,$$

$$M^a_{\mathbf{sym3}} := \xi^T(S^a \otimes \mathrm{i}\mathcal{C}\gamma^3)\xi, \quad M_{\mathbf{triv}3} := \frac{1}{2}\xi^T(\mathbb{1}_{2N_f} \otimes \mathrm{i}\mathcal{C}\gamma^3)\xi = \bar{\psi}\mathrm{i}\gamma^3\psi,$$

$$M^a_{\mathbf{sym5}} := \xi^T(S^a \otimes \mathrm{i}\mathcal{C}\gamma^5)\xi, \quad M_{\mathbf{triv}5} := \frac{1}{2}\xi^T(\mathbb{1}_{2N_f} \otimes \mathrm{i}\mathcal{C}\gamma^5)\xi = \bar{\psi}\mathrm{i}\gamma^5\psi,$$

$$M^a_{\mathbf{sym35}} := \xi^T(S^a \otimes \mathrm{i}\mathcal{C}\gamma^3\gamma^5)\xi, \quad M_{\mathbf{triv}35} := \frac{1}{2}\xi^T(\mathbb{1}_{2N_f} \otimes \mathrm{i}\mathcal{C}\gamma^3\gamma^5)\xi = \bar{\psi}\mathrm{i}\gamma^3\gamma^5\psi. \quad (4.31)$$

The usual mass term $\bar{\psi}\psi = \frac{1}{2}\xi^T(A \otimes \mathcal{C})\xi$ with $A = \mathbb{1}_{N_f} \otimes \sigma^2$ is part of $M^a_{\mathbf{adj}}$.

4.2.2 Currents

Currents are defined as local fermion bilinears transforming as (pseudo-)vectors under space-time rotations, and in a covariant notation, they can be written as

$$\xi^T(A \otimes \mathrm{i}\mathcal{C}\gamma^\mu)\xi, \quad \xi^T(A \otimes \mathrm{i}\mathcal{C}\gamma^3\gamma^\mu)\xi, \quad \xi^T(A \otimes \mathrm{i}\mathcal{C}\gamma^5\gamma^\mu)\xi, \quad \xi^T(S \otimes \mathcal{C}\gamma^3\gamma^5\gamma^\mu)\xi, \quad (4.32)$$

where A and S are $2N_f \times 2N_f$ anti-symmetric and symmetric matrices respectively. Therefore we have a total of $3N_f(2N_f-1) + N_f(2N_f+1) = 2N_f(4N_f-1)$ currents. In contrast to the mass terms, $2N_f(4N_f-1) = \binom{4N_f}{2}$ is the number of $4N_f \times 4N_f$ anti-symmetric matrices, which is again not coincidental. In our basis, we have

$$\begin{aligned}
&\mathrm{i}\mathcal{C}\gamma^0 = \mathrm{i}\mathbb{1} \otimes \mathbb{1}, \quad \mathrm{i}\mathcal{C}\gamma^3\gamma^0 = -\mathrm{i}\sigma^3 \otimes \mathbb{1}, \quad \mathrm{i}\mathcal{C}\gamma^5\gamma^0 = -\mathrm{i}\sigma^1 \otimes \mathbb{1}, \quad \mathcal{C}\gamma^3\gamma^5\gamma^0 = -\mathrm{i}\sigma^2 \otimes \mathbb{1},\\
&\mathrm{i}\mathcal{C}\gamma^1 = -\mathbb{1} \otimes \sigma^1, \quad \mathrm{i}\mathcal{C}\gamma^3\gamma^1 = \sigma^3 \otimes \sigma^1, \quad \mathrm{i}\mathcal{C}\gamma^5\gamma^1 = \sigma^1 \otimes \sigma^1, \quad \mathcal{C}\gamma^3\gamma^5\gamma^1 = \sigma^2 \otimes \sigma^1,\\
&\mathrm{i}\mathcal{C}\gamma^2 = \mathbb{1} \otimes \sigma^3, \quad \mathrm{i}\mathcal{C}\gamma^3\gamma^2 = -\sigma^3 \otimes \sigma^3, \quad \mathrm{i}\mathcal{C}\gamma^5\gamma^2 = -\sigma^1 \otimes \sigma^3, \quad \mathcal{C}\gamma^3\gamma^5\gamma^2 = -\sigma^2 \otimes \sigma^3.
\end{aligned} \quad (4.33)$$

We see that all $\mathcal{C}\Gamma\gamma^\mu$ are of the form $\mathcal{C}\Gamma\gamma^\mu = \Gamma_{(2)} \otimes \sigma$, where $\sigma = \mathbb{1}, \sigma^1, \sigma^3$, and therefore the currents are all of the form $\xi^T(T \otimes \Gamma_{(2)} \otimes \sigma)\xi$. Since σ are all symmetric, $T \otimes \Gamma_{(2)} \otimes \sigma$ being anti-symmetric implies that $T \otimes \Gamma_{(2)}$ is anti-symmetric, and since $\Gamma_{(2)}$ spans all 2×2 matrices, the space of $T \otimes \Gamma_{(2)}$ is the space of all $4N_f \times 4N_f$

anti-symmetric matrices, which is $\binom{4N_f}{2}$ dimensional. In fact, each term exactly corresponds to the conserved current associated with each generator of the $\mathrm{O}(4N_f)$ symmetry.

Like the mass terms, the four types of currents in Eq. (4.32) also do not mix with each other under the $\mathrm{O}(2N_f)$ transformations generated by $A \otimes \mathbb{1}_4$, but do mix under the full $\mathrm{O}(4N_f)$ transformations. Furthermore, under the $\mathrm{SO}(2)_R$ symmetry generated by $\mathbb{1} \otimes \gamma^3\gamma^5$, the two currents $\xi^T(S \otimes \mathrm{i}\mathcal{C}\gamma^3\gamma^\mu)\xi$ and $\xi^T(S \otimes \mathrm{i}\mathcal{C}\gamma^5\gamma^\mu)\xi$ rotate into each other.

These $\binom{4N_f}{2}$ currents form five irreps of the $\mathrm{O}(2N_f)$ symmetry that can be summarized in the relation

$$\binom{\mathbf{4N_f}}{\mathbf{2}} = \mathbf{adj} \times 3 + \mathbf{sym} + \mathbf{triv}. \tag{4.34}$$

These irreps include

$$J^{a\mu}_{\mathbf{adj}0} := \xi^T(A^a \otimes \mathrm{i}\mathcal{C}\gamma^\mu)\xi, \quad J^{a\mu}_{\mathbf{adj}3} := \xi^T(A^a \otimes \mathrm{i}\mathcal{C}\gamma^3\gamma^\mu)\xi, \quad J^{a\mu}_{\mathbf{adj}5} := \xi^T(A^a \otimes \mathrm{i}\mathcal{C}\gamma^5\gamma^\mu)\xi$$

$$J^{a\mu}_{\mathbf{sym}} := \xi^T(S^a \otimes \mathcal{C}\gamma^3\gamma^5\gamma^\mu)\xi, \quad J^{\mu}_{\mathbf{triv}} := \frac{1}{2}\xi^T(\mathbb{1}_{2N_f} \otimes \mathcal{C}\gamma^3\gamma^5\gamma^\mu)\xi = \bar{\psi}\gamma^3\gamma^5\gamma^\mu\psi \tag{4.35}$$

The usual current $\bar{\psi}\gamma^\mu\psi = \frac{1}{2}\xi^T(A \otimes \mathcal{C}\gamma^\mu)\xi$ with $A = \mathbb{1}_{N_f} \otimes \sigma^2$ lives in the adjoint representation.

If we count all the mass terms and the currents, we obtain

$$\binom{4N_f+1}{2} + \binom{4N_f}{2} \times 3 = \binom{8N_f}{2} \tag{4.36}$$

fermion bilinears as expected.

We can also determine how each of these fermion bilinears transforms under the discrete symmetries of the lattice. The transformation properties of some important mass terms and currents under the discrete lattice symmetries are summarized in Table 4.2. In all these examples, the fermion bilinears are eigenvectors of the $\mathbb{Z}_2$ symmetries, except that under parity, a current transforms as a vector (v) or a pseudo-vector (p).

Table 4.2: Symmetries of the fermion bilinears in 2d.

Fermion bilinears	Internal symmetry	$T_a^1 = -\mathrm{i}\gamma^5$	$T_a^2 = \mathrm{i}\gamma^3$	$P = \mathrm{i}\gamma^1\gamma^5$	$\Theta = \gamma^0 K$	C
$\bar{\psi}\psi$	$\mathrm{U}(N_f) \times \mathrm{U}(N_f)$	-1	-1	$+1$	$+1$	-1
$\bar{\psi}\mathrm{i}\gamma^3\psi$	$\mathrm{O}(2N_f) \times \mathrm{O}(2N_f)$	$+1$	-1	$+1$	$+1$	$+1$
$\bar{\psi}\mathrm{i}\gamma^5\psi$	$\mathrm{O}(2N_f) \times \mathrm{O}(2N_f)$	-1	$+1$	-1	$+1$	$+1$
$\bar{\psi}\mathrm{i}\gamma^3\gamma^5\psi$	$\mathrm{O}(4N_f)$	$+1$	$+1$	-1	-1	$+1$
$\bar{\psi}\gamma^\mu\psi$	$\mathrm{U}(2N_f)$	$+1$	$+1$	v	$+1$	-1
$\bar{\psi}\mathrm{i}\gamma^3\gamma^\mu\psi$	$\mathrm{U}(N_f) \times \mathrm{U}(N_f)$	-1	$+1$	v	$+1$	-1
$\bar{\psi}\mathrm{i}\gamma^5\gamma^\mu\psi$	$\mathrm{U}(N_f) \times \mathrm{U}(N_f)$	$+1$	-1	p	$+1$	-1
$\bar{\psi}\mathrm{i}\gamma^3\gamma^5\gamma^\mu\psi$	$\mathrm{U}(2N_f)$	-1	-1	p	-1	$+1$

4.2.3 Allowed four-fermion interactions

We can now construct all the four-fermion interactions allowed by the lattice symmetries. Like the one-dimensional case, contracting the fermion bilinears in each irrep will give us a four-fermion interaction that is invariant under the $\mathrm{O}(2N_f)$ transformation. We obtain seven Gross-Neveu type interactions from the mass terms

$$(M^a_{\mathbf{adj}})^2,\ (M^a_{\mathbf{sym}3})^2,\ (M_{\mathbf{triv}3})^2,\ (M^a_{\mathbf{sym}5})^2,\ (M_{\mathbf{triv}5})^2,\ (M^a_{\mathbf{sym}35})^2,\ (M_{\mathbf{triv}35})^2, \quad (4.37)$$

and five Thirring type interactions from the currents

$$(J^{a\mu}_{\mathbf{adj}0})^2,\ (J^{a\mu}_{\mathbf{adj}3})^2,\ (J^{a\mu}_{\mathbf{adj}5})^2,\ (J^{a\mu}_{\mathbf{sym}})^2,\ (J^{\mu}_{\mathbf{triv}})^2. \quad (4.38)$$

Due to Fierz identity and other identities, these 12 four-fermion interactions are not independent. Among the Gross-Neveu type interactions, there are four independent interactions, which can be chosen as

$$(M^a_{\mathbf{adj}})^2, \quad (M_{\mathbf{triv}3})^2, \quad (M_{\mathbf{triv}5})^2, \quad (M_{\mathbf{triv}35})^2 \quad (4.39)$$

for simplicity, where $(M_{\mathbf{triv}3})^2 = (\bar{\psi}\mathrm{i}\gamma^3\psi)^2$, $(M_{\mathbf{triv}5})^2 = (\bar{\psi}\mathrm{i}\gamma^5\psi)^2$, and $(M_{\mathbf{triv}35})^2 = (\bar{\psi}\mathrm{i}\gamma^3\gamma^5\psi)^2$. The remaining three Gross-Neveu interactions can be related to these four through the relations

$$\begin{pmatrix} (M^a_{\mathbf{sym}3})^2 \\ (M^a_{\mathbf{sym}5})^2 \\ (M^a_{\mathbf{sym}35})^2 \end{pmatrix} = - \begin{pmatrix} 1 & \frac{1}{N_f} & -1 & 1 \\ 1 & -1 & \frac{1}{N_f} & 1 \\ -1 & 1 & 1 & \frac{1}{N_f} \end{pmatrix} \begin{pmatrix} (M^a_{\mathbf{adj}})^2 \\ (M^a_{\mathbf{triv}3})^2 \\ (M^a_{\mathbf{triv}5})^2 \\ (M^a_{\mathbf{triv}35})^2 \end{pmatrix}. \quad (4.40)$$

Interestingly, the Thirring type interactions turn out to be not independent and can be expressed in terms of the four independent Gross-Neveu type interactions as

$$\begin{pmatrix} (J^{a\mu}_{\mathbf{adj}0})^2 \\ (J^{a\mu}_{\mathbf{adj}3})^2 \\ (J^{a\mu}_{\mathbf{adj}5})^2 \\ (J^{a\mu}_{\mathbf{sym}})^2 \\ (J^{\mu}_{\mathbf{triv}})^2 \end{pmatrix} = \begin{pmatrix} 1 & 1 & 1 & 2 \\ -1 & -1 & 2 & 1 \\ -1 & 2 & -1 & 1 \\ \frac{N_f-2}{N_f} & -\frac{2N_f-1}{N_f} & -\frac{2N_f-1}{N_f} & \frac{2N_f-1}{N_f} \\ 2 & -1 & -1 & 1 \end{pmatrix} \begin{pmatrix} (M^a_{\mathbf{adj}})^2 \\ (M^a_{\mathbf{triv}3})^2 \\ (M^a_{\mathbf{triv}5})^2 \\ (M^a_{\mathbf{triv}35})^2 \end{pmatrix} \tag{4.41}$$

Since the lattice also preserves the $\mathrm{SO}(2)_R$ transformation that is generated by

$$\mathbb{1}_{2N_f} \otimes \mathrm{i}\gamma^3\gamma^5, \tag{4.42}$$

under which $(M^a_{\mathbf{triv}3})^2$ mixes with $(M^a_{\mathbf{triv}5})^2$, $(M^a_{\mathbf{sym}3})^2$ mixes with $(M^a_{\mathbf{sym}5})^2$, and $(J^{a\mu}_{\mathbf{adj}3})^2$ mixes with $(J^{a\mu}_{\mathbf{adj}5})^2$, we only have 3 independent interactions which can be chosen as $(M^a_{\mathbf{adj}})^2$, $(M_{\mathbf{triv}3})^2 + (M_{\mathbf{triv}5})^2$, and $(M_{\mathbf{triv}35})^2$.

4.2.4 The case of $N_f = 2$

Similar to the discussion in one spatial dimension, the case of $N_f = 2$ is also exceptional in two spatial dimensions if the system only has $\mathrm{SO}(2N_f)$ symmetry instead of $\mathrm{O}(2N_f)$ symmetry. In this case, there can be more independent interactions, because the interactions transforming in the adjoint representation split into spin and charge sectors through the relations

$$\begin{aligned} (M^a_{\mathbf{adj}})^2 &= 2(M^i_s)^2 + 2(M^i_c)^2, \\ (J^{a\mu}_{\mathbf{adj}0})^2 &= 2(J^{i\mu}_{s0})^2 + 2(J^{i\mu}_{c0})^2, \\ (J^{a\mu}_{\mathbf{adj}3})^2 &= 2(J^{i\mu}_{s3})^2 + 2(J^{i\mu}_{c3})^2, \\ (J^{a\mu}_{\mathbf{adj}5})^2 &= 2(J^{i\mu}_{s5})^2 + 2(J^{i\mu}_{c5})^2, \end{aligned} \tag{4.43}$$

where $M^i_s = \frac{1}{2}\xi^T A^i_s \otimes \mathcal{C}\xi$, $M^i_c = \frac{1}{2}\xi^T A^i_c \otimes \mathcal{C}\xi$, $J^{i\mu}_{s0} = \frac{1}{2}\xi^T A^i_s \otimes \mathrm{i}\mathcal{C}\gamma^\mu\xi$, $J^{i\mu}_{c0} = \frac{1}{2}\xi^T A^i_c \otimes \mathrm{i}\mathcal{C}\gamma^\mu\xi$, etc. This splitting then increases the allowed Gross-Neveu type interactions from seven to eight (see Eq. (4.37) and Thirring type interactions from five to eight (see

Eq. (4.38)). However, only five of these sixteen interactions are independent, which can be chosen as

$$(M_s^i)^2,\ (M_c^i)^2,\ (M_{\mathbf{triv}3})^2,\ (M_{\mathbf{triv}5})^2,\ (M_{\mathbf{triv}35})^2. \tag{4.44}$$

The other spin and charge interactions can be related to them via the relations Eq. (4.40), Eq. (4.41), and

$$\begin{pmatrix} (J_{S0}^{a\mu})^2 \\ (J_{Q0}^{a\mu})^2 \\ (J_{S3}^{a\mu})^2 \\ (J_{Q3}^{a\mu})^2 \\ (J_{S5}^{a\mu})^2 \\ (J_{Q5}^{a\mu})^2 \end{pmatrix} = \frac{1}{4} \begin{pmatrix} 0 & 4 & 1 & 1 & 2 \\ 4 & 0 & 1 & 1 & 2 \\ 0 & -4 & -1 & 2 & 1 \\ -4 & 0 & -1 & 2 & 1 \\ 0 & -4 & 2 & -1 & 1 \\ -4 & 0 & 2 & -1 & 1 \end{pmatrix} \begin{pmatrix} (M_s^a)^2 \\ (M_c^a)^2 \\ (M_{\mathbf{triv}3}^a)^2 \\ (M_{\mathbf{triv}5}^a)^2 \\ (M_{\mathbf{triv}35}^a)^2 \end{pmatrix} \tag{4.45}$$

If we impose $\mathrm{SO}(2)_R$ symmetry, there are now four independent interactions that can be chosen as $(M_s^i)^2$, $(M_c^i)^2$, $(M_{\mathbf{triv}3})^2 + (M_{\mathbf{triv}5})^2$ and $(M_{\mathbf{triv}35})^2$.

5

Physics in One Spatial Dimension

From the analysis in the previous chapter, we learned that up to quartic order, the most general continuum Euclidean Lagrangian that preserves the symmetries of the free lattice fermion could be written as

$$\mathcal{L} = \sum_{\alpha=1}^{N_f} \bar{\psi}^\alpha \gamma^\mu \partial_\mu \psi^\alpha - \frac{\lambda}{2} (\bar{\psi}^\alpha \mathrm{i}\gamma^3 \psi^\alpha)^2. \tag{5.1}$$

This field theory is invariant under the $\mathrm{O}(2N_f)$ lattice symmetry as required. When $\lambda \neq 0$, we can view it as a perturbation of the free massless fermion theory, which is a conformal field theory. For relativistic theories in two space-time dimensions, techniques from the conformal field theory [73] and bosonization [74, 75] turn out to be powerful analytical tools. In this chapter, We will use these tools to understand the lattice theory's phase structures and correlation functions.

5.1 The current algebra

Although it is possible to derive the β function of our field theory directly using diagrammatic expansions, here we will use techniques from CFT, which will be very

helpful for calculating correlation functions. In the CFT analysis, it is convenient to write the Lagrangian in terms of chiral fields, and rewrite the Gross-Neveu type interaction in terms of current-current interactions using Eq. (4.9),

$$\begin{aligned}\mathcal{L} = \mathcal{L}_0 + \mathcal{L}_{\text{int}} &= \sum_{\alpha=1}^{N_f} \psi_+^{\alpha\dagger}\partial_-\psi_+^\alpha + \psi_-^{\alpha\dagger}\partial_+\psi_-^\alpha - \frac{\lambda}{2}(\bar\psi^\alpha \mathrm{i}\gamma^3\psi^\alpha)^2 \\ &= \frac{1}{2}\sum_{\alpha=1}^{2N_f} \xi_+^{\alpha T}\partial_-\xi_+^\alpha + \xi_-^{\alpha T}\partial_+\xi_-^\alpha + \lambda\sum_a J_+^a J_-^a, \end{aligned} \tag{5.2}$$

where $J_\pm^a = \xi_\pm^\alpha T_{\alpha\beta}^a \xi_\pm^\beta$, and T^a form a basis of all $2N_f \times 2N_f$ anti-symmetric Hermitian matrices and satisfy

$$\mathrm{tr}(T^a T^b) = \frac{1}{2}\delta^{ab}, \quad [T^a, T^b] = \mathrm{i} f^{abc} T^c. \tag{5.3}$$

First, we focus on the free Lagrangian $\mathcal{L}_0$ and derive its current algebras. Let us denote $z = x^0 + \mathrm{i}x^1$ and $\bar z = x^0 - \mathrm{i}x^1$, then $\partial_- = 2\partial_z$ and $\partial_+ = 2\partial_{\bar z}$. Therefore the fields satisfy

$$\partial_z \xi_+^\alpha = 0, \quad \partial_{\bar z}\xi_-^\alpha = 0, \tag{5.4}$$

which means ξ_- is only a function of z, and ξ_+ is only a function of $\bar z$. Then the correlation functions satisfy

$$-\mathrm{i}\partial_{\bar z}\langle \xi_-^\alpha(z)\xi_-^\beta(w)\rangle = \delta^{\alpha\beta}\delta(z-w)\delta(\bar z - \bar w), \tag{5.5}$$

and using the identity $\partial_{\bar z}\frac{1}{z} = 2\pi\mathrm{i}\delta(z)\delta(\bar z)$, we have

$$\langle \xi_-^\alpha(z)\xi_-^\beta(w)\rangle = \frac{\delta^{\alpha\beta}}{2\pi(z-w)}, \quad \langle \xi_+^\alpha(\bar z)\xi_+^\beta(\bar w)\rangle = \frac{\delta^{\alpha\beta}}{2\pi(\bar z - \bar w)}. \tag{5.6}$$

In order to take advantage of the CFT results, we will work in the operator formulation, where the Dirac fermions satisfy the usual equal-time commutation relations

$$\{\psi_\pm^{\alpha\dagger}(x), \psi_\pm^\beta(y)\} = \delta^{\alpha\beta}\delta(x-y), \quad \{\psi_\pm^{\alpha\dagger}(x), \psi_\pm^{\beta\dagger}(y)\} = \{\psi_\pm^\alpha(x), \psi_\pm^\beta(y)\} = 0, \tag{5.7}$$

which implies that the Majorana fermions satisfy

$$\{\xi_{\pm}^{\alpha}(x), \xi_{\pm}^{\beta}(y)\} = \delta^{\alpha\beta}\delta(x-y). \tag{5.8}$$

Furthermore, Eq. (5.6) implies that the fermions satisfy the following operator product expansions

$$\begin{aligned}
\xi_{-}^{\alpha}(z)\xi_{-}^{\beta}(w) &= \frac{\delta^{\alpha\beta}}{2\pi(z-w)} + :\xi_{-}^{\alpha}(z)\xi_{-}^{\beta}(w):, \\
\xi_{+}^{\alpha}(\bar{z})\xi_{+}^{\beta}(\bar{w}) &= \frac{\delta^{\alpha\beta}}{2\pi(\bar{z}-\bar{w})} + :\xi_{+}^{\alpha}(\bar{z})\xi_{+}^{\beta}(\bar{w}):,
\end{aligned} \tag{5.9}$$

where $:\cdots:$ denotes normal ordering. Using these relations, we will be able to derive the current algebra. Since ξ_+ and ξ_- work similarly, we will focus on ξ_- and drop the subscript temporarily in the following.

In the operator formulation, operator products usually diverge when the operators approach the same point, as we observed in Eq. (5.9). Therefore, in order to define the current operators, we need to remove the divergent piece by normal ordering the operators

$$J_{-}^{a}(z) =: \xi^{\alpha}(z) T_{\alpha\beta}^{a} \xi^{\beta}(z):, \tag{5.10}$$

Then the OPEs for the currents can be derived as follows. Using Wick's theorem, the operator product $:\xi^{\alpha}(z)\xi^{\beta}(z)::\xi^{\gamma}(w)\xi^{\delta}(w):$ can be expanded as

$$\begin{aligned}
:\xi^{\alpha}(z)\xi^{\beta}(z)::\xi^{\gamma}(w)\xi^{\delta}(w): = &-\langle\xi^{\alpha}(z)\xi^{\gamma}(w)\rangle :\xi^{\beta}(z)\xi^{\delta}(w): + \langle\xi^{\alpha}(z)\xi^{\delta}(w)\rangle :\xi^{\beta}(z)\xi^{\gamma}(w): \\
&+ \langle\xi^{\beta}(z)\xi^{\gamma}(w)\rangle :\xi^{\alpha}(z)\xi^{\delta}(w): - \langle\xi^{\beta}(z)\xi^{\delta}(w)\rangle :\xi^{\alpha}(z)\xi^{\gamma}(w): \\
&- \langle\xi^{\alpha}(z)\xi^{\gamma}(w)\rangle\langle\xi^{\beta}(z)\xi^{\delta}(w)\rangle + \langle\xi^{\alpha}(z)\xi^{\delta}(w)\rangle\langle\xi^{\beta}(z)\xi^{\gamma}(w)\rangle \\
&+ :\xi^{\alpha}(z)\xi^{\beta}(z)\xi^{\gamma}(w)\xi^{\delta}(w):.
\end{aligned} \tag{5.11}$$

Using Eq. (5.6), the first term can be expanded as

$$\begin{aligned}\langle\xi^\alpha(z)\xi^\gamma(w)\rangle : \xi^\beta(z)\xi^\delta(w) : &= \frac{\delta^{\alpha\gamma}}{2\pi(z-w)} : [\xi^\beta(w) + (z-w)\partial_w\xi^\beta(w)]\xi^\delta(w) : \\ &= \frac{\delta^{\alpha\gamma}}{2\pi(z-w)} : \xi^\beta(w)\xi^\delta(w) : + \frac{\delta^{\alpha\gamma}}{2\pi} : \partial_w\xi^\beta(w)\xi^\delta(w) : \\ &= \frac{\delta^{\alpha\gamma}}{2\pi(z-w)} : \xi^\beta(w)\xi^\delta(w) : + \text{ reg.} \end{aligned} \tag{5.12}$$

where we have Taylor expanded $\xi^\beta(z)$ in order to isolate the most singular term. The regular term $\frac{\delta^{\alpha\gamma}}{2\pi} : \partial_w\xi^\beta(w)\xi^\delta(w) :$ does not contribute any singularity to the OPE, but will be important when rewriting the kinetic term as chiral current-current interactions, which we will not explore here. Inserting this result into the current-current product, we have

$$\begin{aligned} J^a_-(z)J^b_-(w) &=: \xi^\alpha(z)T^a_{\alpha\beta}\xi^\beta(z) :: \xi^\gamma(w)T^b_{\gamma\delta}\xi^\delta(w) : \\ &= \frac{1}{2\pi(z-w)}[-T^a_{\alpha\beta}T^b_{\alpha\delta} : \xi^\beta(w)\xi^\delta(w) : + T^a_{\alpha\beta}T^b_{\gamma\alpha} : \xi^\beta(w)\xi^\gamma(w) : \\ &\qquad + T^a_{\alpha\beta}T^b_{\beta\delta} : \xi^\alpha(w)\xi^\delta(w) : - T^a_{\alpha\beta}T^b_{\gamma\beta} : \xi^\alpha(w)\xi^\gamma(w) :] \\ &\quad + \frac{-T^a_{\alpha\beta}T^b_{\alpha\beta} + T^a_{\alpha\beta}T^b_{\beta\alpha}}{4\pi^2(z-w)^2} + \text{ reg.} \\ &= \frac{2}{2\pi(z-w)} : \xi^\alpha(w)([T^a,T^b])_{\alpha\beta}\xi^\beta(w) : + \frac{2\,\mathrm{tr}(T^aT^b)}{4\pi^2(z-w)^2} + \text{ reg.} \\ &= \frac{\mathrm{i}f^{abc}}{\pi(z-w)}J^c_-(w) + \frac{\delta^{ab}}{4\pi^2(z-w)^2} + \text{ reg.} \end{aligned} \tag{5.13}$$

This is the OPE for the currents, from which we will derive the β functions later. Similarly, we have

$$J^a_+(\bar z)J^b_+(\bar w) = \frac{\mathrm{i}f^{abc}}{\pi(\bar z-\bar w)}J^c_+(\bar w) + \frac{\delta^{ab}}{4\pi^2(\bar z-\bar w)^2} + \text{ reg.} \tag{5.14}$$

Using the OPE, we can also derive the commutators of the currents $[J^a_-(\mathrm{i}x), J^b_-(\mathrm{i}y)]$ at an equal time. From Eq. (5.13), it seems that $J^a_-(\mathrm{i}x)J^b_-(\mathrm{i}y) = J^b_-(\mathrm{i}y)J^a_-(\mathrm{i}x)$ and

the commutator would be zero. However, we should be careful when $y \to x$, because the OPE is singular and we encounter the situation of infinity minus infinity. In order to avoid this infinity, we regularize the OPE slightly in the temporal direction,

$$\begin{aligned} J_-^a(\mathrm{i}x)J_-^b(\mathrm{i}y) &= \lim_{\varepsilon\to 0}\frac{\mathrm{i}f^{abc}}{\pi\mathrm{i}(x-y-\mathrm{i}\varepsilon)}J^c(\mathrm{i}y) - \frac{\delta^{ab}}{4\pi^2(x-y-\mathrm{i}\varepsilon)^2} + \text{ reg.} \\ J_-^b(\mathrm{i}y)J_-^a(\mathrm{i}x) &= \lim_{\varepsilon\to 0}\frac{\mathrm{i}f^{bac}}{\pi\mathrm{i}(y-x-\mathrm{i}\varepsilon)}J^c(\mathrm{i}x) - \frac{\delta^{ab}}{4\pi^2(y-x-\mathrm{i}\varepsilon)^2} + \text{ reg.} \\ &= \lim_{\varepsilon\to 0}\frac{\mathrm{i}f^{abc}}{\pi\mathrm{i}(x-y+\mathrm{i}\varepsilon)}J^c(\mathrm{i}y) - \frac{\delta^{ab}}{4\pi^2(x-y+\mathrm{i}\varepsilon)^2} + \text{ reg.}, \end{aligned} \tag{5.15}$$

where we again Taylor expanded $J^c(\mathrm{i}x)$ at y in the last line and shifted the reg. terms. Using the identities

$$\lim_{\varepsilon\to 0}\frac{1}{x-\mathrm{i}\varepsilon} - \frac{1}{x+\mathrm{i}\varepsilon} = 2\pi\mathrm{i}\delta(x) \tag{5.16}$$

$$\lim_{\varepsilon\to 0} -\frac{1}{(x-\mathrm{i}\varepsilon)^2} + \frac{1}{(x+\mathrm{i}\varepsilon)^2} = 2\pi\mathrm{i}\delta'(x), \tag{5.17}$$

we have the following current algebras

$$[J_-^a(\mathrm{i}x), J_-^b(\mathrm{i}y)] = 2\mathrm{i}f^{abc}J^c(\mathrm{i}y)\delta(x-y) + \frac{1}{2\pi}\delta^{ab}\delta'(x-y) + \text{ reg.}, \tag{5.18}$$

and similarly

$$[J_+^a(-\mathrm{i}x), J_+^b(-\mathrm{i}y)] = 2\mathrm{i}f^{abc}J^c(-\mathrm{i}y)\delta(x-y) - \frac{1}{2\pi}\delta^{ab}\delta'(x-y) + \text{ reg.}. \tag{5.19}$$

Eqs. (5.18) and (5.19) are known as the Kac-Moody algebra at level 1 [74, 75]. The Kac-Moody algebra at arbitrary level k is

$$[J_\mp^a(\pm\mathrm{i}x), J_\mp^b(\pm\mathrm{i}y)] = 2\mathrm{i}f^{abc}J^c(\pm\mathrm{i}y)\delta(x-y) \pm \frac{k}{2\pi}\delta^{ab}\delta'(x-y) + \text{ reg.}. \tag{5.20}$$

As a side note, one might want to derive a current algebra simply from the Majorana fermion commutators Eq. (5.8), i.e.,

$$[\xi_\pm^T T^a \xi_\pm(x), \xi_\pm^T T^b \xi_\pm(y)] = 2\xi_\pm^T [T^a, T^b]\xi_\pm(y)\delta(x-y). \tag{5.21}$$

However, this only gives the first terms in Eqs. (5.18) and (5.19) but not the second $\delta'(x-y)$ term, which is an anomalous term and is sometimes referred to as a Schwinger term [76, 74, 77]. It is a c-number and mathematically can be viewed as a central extension of Eq. (5.21). It appears only for a system of an infinite number of particles and vanishes for any finite system [77, 78].

5.2 The β functions

At leading order, the β functions are related to the OPE coefficients [78, 79, 80]. In this section, we will show and use this fact to derive the β functions. The idea is to expand the partition function in the couplings, and then use OPE to recast the second-order current interactions in the form of the first-order one and renormalize the coupling. This calculation is equivalent to a one-loop renormalization.

In order to use the OPEs, we will use the Hamiltonian formulation and note that the interaction is given by

$$H_{\text{int}} = \int \mathrm{d}x \sum_a \lambda \; J_+^a J_-^a. \tag{5.22}$$

Instead of this interaction, let us start with a more general anisotropic interaction

$$H_{\text{int}} = \int \mathrm{d}x \sum_a \lambda_a J_+^a J_-^a. \tag{5.23}$$

In the interaction picture, the partition function can be written as

$$\begin{aligned} Z &= T \exp\Big(- \int_{-\infty}^{\infty} \mathrm{d}t H_{\text{int}} \Big) = T \exp\Big(- \int \mathrm{d}t \mathrm{d}x \sum_a \lambda_a J_+^a J_-^a \Big) \\ &= 1 - \sum_a \lambda_a \int \mathrm{d}t \mathrm{d}x J_+^a J_-^a + \sum_{a,b} \lambda_a \lambda_b \int_{t_1 > t_2} \mathrm{d}t_1 \mathrm{d}x_1 \mathrm{d}t_2 \mathrm{d}x_2 J_+^a(\bar{z}_1) J_-^a(z_1) J_+^b(\bar{z}_2) J_-^b(z_2) + \cdots \end{aligned} \tag{5.24}$$

where T is the time order operator and $z_i = t_i + \mathrm{i}x_i$. Using the OPE in Eqs. (5.13)

and (5.14) we can rewrite the last integrand as

$$J_+^a(\bar{z}_1)J_+^b(\bar{z}_2)J_-^a(z_1)J_-^b(z_2) = \frac{\mathrm{i}f^{abc}}{\pi(\bar{z}_1-\bar{z}_2)}J_+^c(\bar{z}_2)\frac{\mathrm{i}f^{abd}}{\pi(z_1-z_2)}J_-^d(z_2)$$
$$= \frac{-f^{abc}f^{abd}}{\pi^2|z_1-z_2|^2}J_+^c(\bar{z}_2)J_-^d(z_2). \tag{5.25}$$

Then using the integral

$$\int_{t>0}\mathrm{d}t\mathrm{d}x\frac{1}{t^2+x^2} = \pi\ln\frac{L}{a}, \tag{5.26}$$

where L is the IR cutoff and a is the UV cutoff, we can perform the integration over t_1 and x_1,

$$\int_{t_1>t_2}\mathrm{d}t_1\mathrm{d}x_1\mathrm{d}t_2\mathrm{d}x_2\frac{-f^{abc}f^{abd}}{\pi^2|z_1-z_2|^2}J_+^c(\bar{z}_2)J_-^d(z_2) = -\frac{1}{\pi}f^{abc}f^{abd}\ln\frac{L}{a}\int\mathrm{d}t_2\mathrm{d}x_2J_+^c(\bar{z}_2)J_-^d(z_2). \tag{5.27}$$

This implies that the couplings λ_a at scale L is related to the coupling at scale a by

$$\lambda_a(L) = \lambda_a(a) + \frac{1}{\pi}\ln\frac{L}{a}\sum_{b,c}(f^{abc})^2\lambda_b\lambda_c, \tag{5.28}$$

from which we can read the β function

$$\frac{\mathrm{d}\lambda_a}{\mathrm{d}\ln L} = \frac{1}{\pi}\sum_{b,c}(f^{abc})^2\lambda_b\lambda_c, \tag{5.29}$$

or in terms of the energy scale μ defined by $\mu = \frac{1}{L}$,

$$\frac{\mathrm{d}\lambda_a}{\mathrm{d}\ln\mu} = -\frac{1}{\pi}\sum_{b,c}(f^{abc})^2\lambda_b\lambda_c. \tag{5.30}$$

In the case of our lattice model, we set $\lambda_a = \lambda$ for all a. Then we have

$$\frac{\mathrm{d}\lambda}{\mathrm{d}\ln\mu} = -\frac{1}{\pi}\sum_{b,c}(f^{abc})^2\lambda^2. \tag{5.31}$$

The factor $\sum_{b,c}(f^{abc})^2$ is related to the Killing form,

$$\sum_{b,c}(f^{abc})^2 = -\operatorname{tr}(T^{aT}_{\mathbf{adj}}T^a_{\mathbf{adj}}) = \operatorname{tr}(T^a_{\mathbf{adj}}T^a_{\mathbf{adj}}) = g^{aa}, \tag{5.32}$$

and in the case of SO(N), we have $g^{aa} = \frac{N-2}{2}$. See Appendix C for more details. In our theory, T^a is the generator of the O($2N_f$) symmetry, and we have

$$\frac{\mathrm{d}\lambda}{\mathrm{d}\ln\mu} = -\frac{N_f-1}{\pi}\lambda^2. \tag{5.33}$$

This result is consistent with the literature for the Gross-Neveu model [51, 81]. In particular, it vanishes for $N_f = 1$, because in this case, the Gross-Neveu interaction is proportional to the Thirring interaction, which has the full chiral symmetry, see Eq. (4.10).

5.3 Lattice correlation functions in the free theory

In this section, we will derive the correlation functions of lattice fermion bilinears in a free theory. From Eq. (3.29) we know that the lattice fermion bilinears are related to currents and masses in the continuum through

$$\begin{aligned}\mathcal{O}^a_j := \frac{1}{2a}\gamma^\alpha_j T^a_{\alpha\beta}\gamma^\beta_j &\approx J^a_+(aj) + J^a_-(aj) + (-1)^j\xi^{\alpha T}\mathcal{C}T^a_{\alpha\beta}\xi^\beta(aj)\\ &= J^a_+(aj) + J^a_-(aj) + (-1)^j 2\xi^\alpha_+ T^a_{\alpha\beta}\xi^\beta_-(aj).\end{aligned} \tag{5.34}$$

In order to derive the correlation functions of $\mathcal{O}^a_j\mathcal{O}^b_k$, we first need to determine the OPE of them. We already know the current-current OPEs, i.e., the current algebra, but we still need to calculate the current-fermion OPEs, and mass-mass OPEs.

Since the currents commute with fermions with opposite chirality, in order to determine the current-mass OPEs, it is sufficient to calculate the current-fermion OPEs $J^a_-(z)\xi_-(w)$.

5.3.1 Current-fermion OPEs

Using Wick's theorem, we have

$$:\xi_-^\alpha(z)\xi_-^\beta(z):\xi_-^\gamma(w) = -\langle\xi_-^\alpha(z)\xi_-^\gamma(w)\rangle\xi_-^\beta(z) + \xi_-^\alpha(z)\langle\xi_-^\beta(z)\xi_-^\gamma(w)\rangle + :\xi_-^\alpha(z)\xi_-^\beta(z)\xi_-^\gamma(w):, \tag{5.35}$$

and with Eq. (5.6), the first term can be expanded as

$$\begin{aligned}\langle\xi_-^\alpha(z)\xi_-^\gamma(w)\rangle\xi_-^\beta(z) &= \frac{\delta^{\alpha\gamma}}{2\pi(z-w)}[\xi_-^\beta(w) + (z-w)\partial_w\xi_-^\beta(w)] \\ &= \frac{\delta^{\alpha\gamma}}{2\pi(z-w)}\xi_-^\beta(w) + \text{ reg.}\end{aligned} \tag{5.36}$$

Therefore we have

$$J_-^a(z)\xi_-^\alpha(w) =: \xi_-^\beta(z)T^a_{\beta\gamma}\xi_-^\gamma(z):\xi_-^\alpha(w) = \frac{1}{\pi(z-w)}\xi_-^\beta(w)T^a_{\beta\alpha} + \text{ reg.}, \tag{5.37}$$

and similarly

$$J_+^a(\bar{z})\xi_+^\alpha(\bar{w}) = \frac{1}{\pi(\bar{z}-\bar{w})}\xi_+^\beta(\bar{w})T^a_{\beta\alpha} + \text{ reg.}. \tag{5.38}$$

These relations show that $\xi_\pm^\alpha$ are Kac-Moody primary fields. It will also be useful later to reverse the operators, giving

$$\xi_-^\alpha(z)J_-^a(w) = \frac{1}{\pi(z-w)}T^a_{\alpha\beta}\xi_-^\beta(w) + \text{ reg.}, \tag{5.39}$$

$$\xi_+^\alpha(\bar{z})J_+^a(\bar{w}) = \frac{1}{\pi(\bar{z}-\bar{w})}T^a_{\alpha\beta}\xi_+^\beta(\bar{w}) + \text{ reg.}. \tag{5.40}$$

5.3.2 Mass-mass OPEs

Again, due to that fermions with different chirality commute with each other, the mass-mass OPEs are simply

$$\begin{aligned}\xi_+^\alpha(\bar z)\xi_-^\beta(z)\xi_+^\gamma(\bar w)\xi_-^\delta(w) &= -\langle\xi_+^\alpha(\bar z)\xi_+^\gamma(\bar w)\rangle : \xi_-^\beta(z)\xi_-^\delta(w) : -\langle\xi_-^\beta(z)\xi_-^\delta(w)\rangle : \xi_+^\alpha(\bar z)\xi_+^\gamma(\bar w) : \\ &\quad - \langle\xi_+^\alpha(\bar z)\xi_+^\gamma(\bar w)\rangle\langle\xi_-^\beta(z)\xi_-^\delta(w)\rangle \\ &= -\frac{\delta^{\alpha\gamma}}{2\pi(\bar z-\bar w)} : \xi_-^\beta(z)\xi_-^\delta(w) : -\frac{\delta^{\beta\delta}}{2\pi(z-w)} : \xi_+^\alpha(\bar z)\xi_+^\gamma(\bar w) : \\ &\quad - \frac{\delta^{\alpha\gamma}\delta^{\beta\delta}}{4\pi^2|z-w|^2} + \text{reg.}. \end{aligned} \tag{5.41}$$

5.3.3 OPE of lattice fermion bilinears

Now we are ready to calculate the OPE of lattice fermion bilinears, which can be expanded as

$$\begin{aligned}\mathcal{O}_j^a\mathcal{O}_k^b &\approx \big(J_+^a(aj)+J_-^a(aj)+(-1)^j 2\xi_+^\alpha T_{\alpha\beta}^a\xi_-^\beta(aj)\big)\big(J_+^b(ak)+J_-^b(ak)+(-1)^k 2\xi_+^\alpha T_{\alpha\beta}^b\xi_-^\beta(ak)\big) \\ &= J_+^a(aj)J_+^b(ak)+J_-^a(aj)J_-^b(ak)+(-1)^k(J_+^a(aj)+J_-^a(aj))2\xi_+^\alpha T_{\alpha\beta}^b\xi_-^\beta(ak) \\ &\quad + (-1)^j 2\xi_+^\alpha T_{\alpha\beta}^a\xi_-^\beta(aj)(J_+^b(ak)+J_-^b(ak)) + (-1)^{j+k}4\xi_+^\alpha T_{\alpha\beta}^a\xi_-^\beta(aj)\xi_+^\gamma T_{\gamma\delta}^b\xi_-^\delta(ak)\end{aligned} \tag{5.42}$$

The OPEs we need are current-current OPEs,

$$J_-^a(aj)J_-^b(ak) = \frac{\mathrm{i}f^{abc}}{\mathrm{i}\pi a(j-k)}J_-^c(ak) - \frac{\delta^{ab}}{4\pi^2a^2(j-k)^2} + \text{ reg.}, \tag{5.43}$$

$$J_+^a(aj)J_+^b(ak) = \frac{\mathrm{i}f^{abc}}{-\mathrm{i}\pi a(j-k)}J_+^c(ak) - \frac{\delta^{ab}}{4\pi^2a^2(j-k)^2} + \text{ reg.}, \tag{5.44}$$

current-mass OPEs,

$$J_-^a(aj)\xi_+^\alpha T_{\alpha\beta}^b\xi_-^\beta(ak) = \frac{-1}{\mathrm{i}\pi a(j-k)}\xi_+^\alpha T_{\alpha\gamma}^b T_{\gamma\beta}^a\xi_-^\beta(ak) + \text{ reg.}, \tag{5.45}$$

$$J_+^a(aj)\xi_+^\alpha T_{\alpha\beta}^b\xi_-^\beta(ak) = \frac{1}{-\mathrm{i}\pi a(j-k)}\xi_+^\alpha T_{\alpha\gamma}^a T_{\gamma\beta}^b\xi_-^\beta(ak) + \text{ reg.}, \tag{5.46}$$

mass-current OPEs,

$$\xi_+^\alpha T_{\alpha\beta}^b \xi_-^\beta(aj) J_-^a(ak) = \frac{1}{\mathrm{i}\pi a(j-k)} \xi_+^\alpha T_{\alpha\gamma}^b T_{\gamma\beta}^a \xi_-^\beta(ak) + \text{ reg.}, \tag{5.47}$$

$$\xi_+^\alpha T_{\alpha\beta}^b \xi_-^\beta(aj) J_+^a(ak) = \frac{1}{\mathrm{i}\pi a(j-k)} \xi_+^\alpha T_{\alpha\gamma}^a T_{\gamma\beta}^b \xi_-^\beta(ak) + \text{ reg.}, \tag{5.48}$$

and finally, mass-mass OPEs,

$$\begin{aligned}\xi_+^\alpha T_{\alpha\beta}^a \xi_-^\beta(aj) \xi_+^\gamma T_{\gamma\delta}^b \xi_-^\delta(ak) &= \frac{(T^aT^b)_{\beta\delta}}{-2\pi\mathrm{i}a(j-k)} : \xi_-^\beta(ak)\xi_-^\delta(ak) : + \frac{(T^aT^b)_{\beta\delta}}{2\pi\mathrm{i}a(j-k)} : \xi_+^\alpha(ak)\xi_+^\gamma(ak) : \\ &\quad + \frac{\mathrm{tr}(T^aT^b)}{4\pi^2a^2(j-k)^2} + \text{reg.} \\ &= \frac{\mathrm{i}f^{abc}}{4\pi\mathrm{i}a(j-k)}(J_+^c(ak) - J_-^c(ak)) + \frac{\delta^{\alpha\beta}}{8\pi^2a^2(j-k)^2} + \text{reg.}\end{aligned} \tag{5.49}$$

Inserting these results back in Eq. (5.42), we have

$$\begin{aligned}\mathcal{O}_j^a \mathcal{O}_k^b \approx (1-(-1)^{j-k})\Big(\frac{f^{abc}}{\pi a(j-k)}(J_-^c(ak) - J_+^c(ak)) - \frac{\delta^{ab}}{2\pi^2a^2(j-k)^2}\Big) \\ + ((-1)^j - (-1)^k)\frac{2}{\mathrm{i}\pi a(j-k)} \xi_+^\alpha \{T^a, T^b\}_{\alpha\beta} \xi_-^\beta(ak) + \text{reg.},\end{aligned} \tag{5.50}$$

which implies the following the correlation function

$$\langle \mathcal{O}_j^a \mathcal{O}_k^b \rangle \approx -\frac{(1-(-1)^{j-k})\delta^{ab}}{2\pi^2a^2(j-k)^2}. \tag{5.51}$$

From this correlation function, we observe that the correlation is zero when $r := j-k$ is even. In Fig. 5.1, we compare this correlation function with a density matrix renormalization group (DMRG) simulation of the free lattice model using ITensor [82]. In the DMRG calculation, we set the lattice size to be 1000 with an open boundary condition. We indeed see the correlation vanishes when r is even. Furthermore, the correlation at odd r is also quite close to the DMRG result, considering that we only keep leading terms in the lattice operator $\mathcal{O}_j^a$, and that there is no fitting parameter.

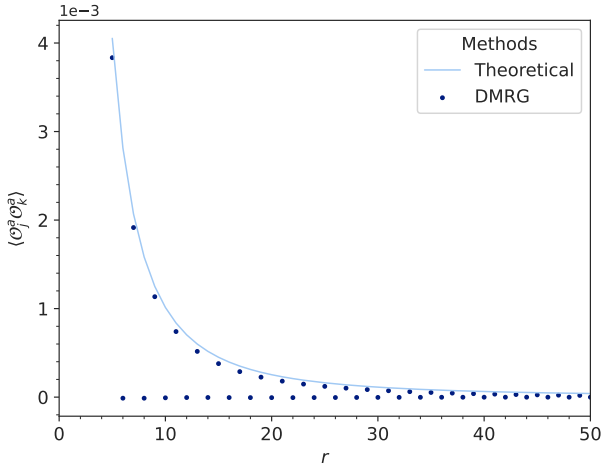

FIGURE 5.1: Correlation functions of lattice fermion bilinears in a free lattice theory.

5.3.4 The dimer operator

An interesting operator that we will study later is the dimer operator defined as

$$\mathcal{D}_j^a := \frac{1}{2}(\mathcal{O}_j^a \mathcal{O}_{j+1}^a - \mathcal{O}_{j-1}^a \mathcal{O}_j^a). \tag{5.52}$$

Using Eq. (5.50), we have

$$\mathcal{O}_j^a \mathcal{O}_{j+1}^a = -\frac{1}{\pi^2 a^2} - \frac{8(-1)^j}{\mathrm{i}\pi a} \xi_+^\alpha (T^a)^2_{\alpha\beta} \xi_-^\beta (aj) + \text{higher orders in } a, \tag{5.53}$$

and therefore

$$\mathcal{D}_j^a = -\frac{8(-1)^j}{\mathrm{i}\pi a} \xi_+^\alpha (T^a)^2_{\alpha\beta} \xi_-^\beta (aj) + \text{higher orders in } a. \tag{5.54}$$

Using Eq. (5.41), we can easily calculate the OPE of the dimer operators in a free theory,

$$\begin{aligned}
\mathcal{D}_j^a \mathcal{D}_k^b &= -\frac{64(-1)^{j-k}}{\pi^2 a^2} \xi_+^\alpha (T^a)^2_{\alpha\beta} \xi_-^\beta (aj) \xi_+^\gamma (T^b)^2_{\gamma\delta} \xi_-^\delta (ak) + \text{higher orders in } a \\
&= \frac{64(-1)^{j-k}}{\pi^2 a^2} \Big(\frac{1}{-2\pi \mathrm{i} a(j-k)} (: \xi_-^\alpha(z) (T^{a2} T^{b2})_{\alpha\beta} \xi_-^\beta(w) : - : \xi_+^\alpha(z) (T^{a2} T^{b2})_{\alpha\beta} \xi_+^\beta(w) :) \\
&\quad + \frac{\mathrm{tr}(T^{a2} T^{b2})}{4\pi^2 a^2 |j-k|^2} \Big) + \text{higher orders in } a,
\end{aligned} \tag{5.55}$$

and therefore we obtain

$$\langle \mathcal{D}_j^a \mathcal{D}_k^b \rangle = (-1)^{j-k} \frac{16 \operatorname{tr}(T^{a2} T^{b2})}{\pi^4 a^4 |j-k|^2} + \text{higher orders in } a. \tag{5.56}$$

This result will be used in the next section to compare with the results from bosonization.

5.4 Non-abelian bosonization

It turns out that the current algebras Eq. (5.20) can be generalized to arbitrary compact Lie groups. Although not all of them have a fermionic realization [83], they can all be realized as certain Wess-Zumino-Witten (WZW) models [74, 75]. The action of a WZW model is

$$S[g] = \frac{1}{4\lambda^2} \int \mathrm{d}^2 x \operatorname{tr}(\partial_\mu g^{-1} \partial^\mu g) + \frac{\mathrm{i}k}{24\pi} \int \mathrm{d}^3 y \varepsilon^{\mu\nu\rho} \operatorname{tr}(g^{-1} \partial_\mu g g^{-1} \partial_\nu g g^{-1} \partial_\rho g), \tag{5.57}$$

where $g(x) \in G$ is a group-valued field. This model is sometimes called a G_k WZW theory, where k is the level. While the first term in the action is an integration over space-time taken to be $\mathbb{S}^2$, the second term involves an integration over a 3-disk whose boundary is the $\mathbb{S}^2$. This requires smooth continuation of the g field to the interior of $\mathbb{S}^2$, which is possible for an arbitrary field configuration only if $\pi_2(G) \cong 0$. This condition is actually true for any simple compact Lie group. Furthermore, the second term S_{WZW} counts the winding number of $\mathbb{S}^3$ over the group G, being non-trivial only when

$$\pi_3(G) \ncong 0. \tag{5.58}$$

In fact, $\pi_3(G) \cong \mathbb{Z}$ for any simple compact Lie group. In order for the partition function to not depend on the continuation of the g field inside $\mathbb{S}^2$, k can only take integer values. This theory has chiral $G_+ \times G_-$ symmetry, under which $g \to L g R^{-1}$, where $L \in G_+$ and $R \in G_-$.

It turns out that when $k \neq 0$, the theory will flow to $\lambda^2 = 4\pi/k$, which is a CFT in the IR. At this fixed point, the currents satisfy Eq. (5.18) [74, 75]. When $G \cong \mathrm{SO}(2N_f)$ and $k = 1$, this CFT is equivalent to the N_f-flavor free Dirac fermion theory, or equivalently, $2N_f$-flavor free Majorana fermion theory, known as non-abelian bosonization [74, 75]. The currents of these two theories map directly to each other, and the mass terms in the fermionic theory map to the field g in the bosonic theory as follows [74, 75],

$$\mathrm{i}\xi_+^\alpha \xi_-^\beta \leftrightarrow -M g^{\alpha\beta}, \tag{5.59}$$

or more conveniently,

$$\xi_+^\alpha T^a_{\alpha\beta} \xi_-^\beta \leftrightarrow \mathrm{i}M g^{\alpha\beta} T^a_{\alpha\beta} = -\mathrm{i}M \,\mathrm{tr}(gT^a) \tag{5.60}$$

Since $\xi_\pm^\alpha$ are Kac-Moody primary fields (see Eq. (5.37)), the fields g are also Kac-Moody primary fields, whose scaling dimension h_g can be inferred from the Knizhnik-Zamolodchikov equation [75, 84, 85],

$$h_g = \frac{c_2'(g)}{k + h^\vee}, \tag{5.61}$$

where $c_2'(g)$ and $h^\vee$ are the quadratic Casimir number and dual Coxeter number respectively, which are defined carefully in Appendix C. In particular, for $k = 1$, we have

$$h_g = \begin{cases} \frac{(N^2-1)/N}{1+N} = \frac{N-1}{N} & \text{for } g \in \mathrm{SU}(N), \\ \frac{N-1}{1+N-2} = 1 & \text{for } g \in \mathrm{SO}(N), \end{cases} \tag{5.62}$$

and g is assumed to be in the defining representations. We see that when $k = 1$ and $g \in \mathrm{SO}(2N_f)$, corresponding to free fermions, $h_g \equiv 1$ for any N_f, which is consistent with the scaling dimension of mass terms in a free fermion theory (see Eq. (5.41)).

5.5 The case of $N_f = 2$ with SO(4) symmetry

As we explained in the last chapter, in the case of $N_f = 2$ with SO(4) symmetry, we have more independent interactions, and Eq. (5.22) can be further split into

$$H_{\text{int}} = \int \mathrm{d}x \ \lambda_s J^i_{s+} J^i_{s-} + \lambda_c J^i_{c+} J^i_{c-}, \tag{5.63}$$

where $J^i_{s\pm} = \frac{1}{2}\xi^\alpha_\pm A^i_{s\alpha\beta}\xi^\beta_\pm$ and $J^i_{c\pm} = \frac{1}{2}\xi^\alpha_\pm A^i_{c\alpha\beta}\xi^\beta_\pm$. In the case of $\lambda_s = \lambda_c = 2\lambda$, we go back to the original interaction

$$2\lambda J^i_{s+} J^i_{s-} + 2\lambda J^i_{c+} J^i_{c-} = \lambda J^a_+ J^a_-, \tag{5.64}$$

which is invariant under O(4). Using the results we derived in the previous sections, we have the following OPEs,

$$J^i_{s,c-}(z) J^j_{s,c-}(w) = \frac{\mathrm{i}\varepsilon^{ijk}}{2\pi(z-w)} J^k_{s,c-}(w) + \frac{\delta^{ij}}{8\pi^2(z-w)^2} + \text{ reg.} \tag{5.65}$$

$$J^i_{s,c+}(\bar{z}) J^j_{s,c+}(\bar{w}) = \frac{\mathrm{i}\varepsilon^{ijk}}{2\pi(\bar{z}-\bar{w})} J^k_{s,c+}(\bar{w}) + \frac{\delta^{ij}}{8\pi^2(\bar{z}-\bar{w})^2} + \text{ reg.}, \tag{5.66}$$

where the different factors are due to a different normalization of the Lie algebra generators $\frac{1}{2}A^i_s$ and $\frac{1}{2}A^i_c$ defined in Chapter 4. As we discussed earlier, these OPEs imply that for general anisotropic interactions

$$H_{\text{int}} = \int \mathrm{d}x \ \lambda^i_s J^i_{s+} J^i_{s-} + \lambda^i_c J^i_{c+} J^i_{c-}, \tag{5.67}$$

we have the following beta functions,

$$\frac{\mathrm{d}\lambda^i_{s,c}}{\mathrm{d}\ln\mu} = -\frac{1}{4\pi}\sum_{i,k} (\varepsilon^{ijk})^2 \lambda^j_{s,c}\lambda^k_{s,c}, \tag{5.68}$$

and in the isotropic case $\lambda^i_{s,c} = \lambda_{s,c}$, we have

$$\frac{\mathrm{d}\lambda_{s,c}}{\mathrm{d}\ln\mu} = -\frac{1}{2\pi}\lambda^2_{s,c}. \tag{5.69}$$

Furthermore, in the case of $\lambda_s = \lambda_c = 2\lambda$, it can be easily seen that this result is consistent with the general beta function Eq. (5.33) at $N_f = 2$.

5.5.1 Bosonization

When studying the correlation functions, it is convenient to bosonize the theory, and in this case, the isomorphism $\mathrm{SO}(4) \cong \mathrm{SU}(2) \times \mathrm{SU}(2)/\mathbb{Z}_2$ allows insight into the SU(2) WZW theory. From the discussion near Eq. (4.19), we know that an SO(4) transformation on the Majorana fermions $\xi \mapsto O\xi$ can be identified as spin $\mathrm{SU}(2)_s$ and charge $\mathrm{SU}(2)_c$ transformations on the Dirac fermions $\Psi \mapsto g\Psi h^{-1}$, where $g \in \mathrm{SU}(2)_s$, $h \in \mathrm{SU}(2)_c$, and Ψ is defined in terms of ξ as

$$\Psi = \begin{pmatrix} \xi^1 - \mathrm{i}\xi^2 & -\xi^3 - \mathrm{i}\xi^4 \\ \xi^3 - \mathrm{i}\xi^4 & \xi^1 + \mathrm{i}\xi^2 \end{pmatrix}, \tag{re 4.19}$$

and $O = \mathrm{e}^{\mathrm{i}\theta_i A_s^i + \mathrm{i}\phi_i A_c^i}$ corresponds to $(g, h) = (\mathrm{e}^{\mathrm{i}\frac{\theta_i}{2}\sigma^i}, \mathrm{e}^{\mathrm{i}\frac{\phi_i}{2}\sigma^i})$. Now the bosonization of the mass terms is

$$\xi_+^\alpha A_{s\alpha\beta}^i \xi_-^\beta \leftrightarrow -M \operatorname{tr}(O\mathrm{i}A_s^i) = -\frac{M}{2} \operatorname{tr}(g\mathrm{i}\sigma^i) \operatorname{tr} h, \tag{5.70}$$

$$\xi_+^\alpha A_{c\alpha\beta}^i \xi_-^\beta \leftrightarrow -M \operatorname{tr}(O\mathrm{i}A_c^i) = -\frac{M}{2} \operatorname{tr} g \operatorname{tr}(h\mathrm{i}\sigma^i). \tag{5.71}$$

The bosonized theory enjoys almost the same symmetries as the fermionic one, except that (g, h) and $(-g, -h)$ should be identified, because we have written the bosonized theory with an $\mathrm{SU}(2)_s \times \mathrm{SU}(2)_c$ symmetry rather than SO(4). This means that observables in the fermionic theory will always be mapped into terms that do not violate this identification. For example, $\operatorname{tr} g$ itself is not an observable, but $(\operatorname{tr} g)^2$, $\operatorname{tr} g \operatorname{tr} h$ are. Besides, the chiral symmetries of S_{WZW} in each sector are SO(4) instead of $\mathrm{SU}(2)_+ \times \mathrm{SU}(2)_-$. Also note that under spin-charge flip symmetry $g \leftrightarrow h$.

5.5.2 Spin correlation

The lattice spin operator $\mathcal{S}_j^i$ is bosonized to

$$\begin{aligned} \mathcal{S}_j^i := \frac{1}{4a} \gamma_j^\alpha A_{s\alpha\beta}^i \gamma_j^\beta &= J_{+s}^i(aj) + J_{s-}^i(aj) + (-1)^j \xi_+^\alpha A_{s\alpha\beta}^i \xi_-^\beta(aj). \\ &\leftrightarrow J_{+s}^i(aj) + J_{s-}^i(aj) - (-1)^j \frac{M}{2} \operatorname{tr}(g\mathrm{i}\sigma^i) \operatorname{tr} h. \end{aligned} \tag{5.72}$$

First let us understand the OPE of $\mathcal{S}^i_j$ at $\lambda_s = \lambda_c = 0$ in this bosonized language. The current-current OPEs and current-mass OPEs are purely dictated by the symmetry of the theory, which must be identical to the fermionic theory. On the other hand, the correlation function of the mass terms, i.e., the WZW primary fields g and h, need to be treated separately. From Eq. (5.62), we know the conformal dimensions of g and h are

$$h_g = h_h = \frac{1}{2}, \tag{5.73}$$

which is as expected because $h_g + h_h = h_O = 1$. Then from the SU(2) invariance, we have

$$\langle \mathrm{tr}(g(aj)\mathrm{i}\sigma^i)\,\mathrm{tr}(g(ak)\mathrm{i}\sigma^j)\rangle = \frac{C\delta^{ij}}{a|j-k|}, \tag{5.74}$$

$$\langle \mathrm{tr}\, g(aj)\,\mathrm{tr}\, g(ak)\rangle = \frac{C}{a|j-k|}, \tag{5.75}$$

and similarly for h. Therefore

$$\begin{aligned}\langle \xi^\alpha_+ A^i_{s\alpha\beta}\xi^\beta_-(aj)\xi^\gamma_+ A^j_{s\gamma\delta}\xi^\delta_-(ak)\rangle &= \frac{M^2}{4}\langle \mathrm{tr}(g(aj)\mathrm{i}\sigma^i)\,\mathrm{tr}(g(ak)\mathrm{i}\sigma^j)\rangle\langle \mathrm{tr}\, h(aj)\,\mathrm{tr}\, h(ak)\rangle \\ &= \frac{M^2C^2\delta^{ij}}{4a^2(j-k)^2}.\end{aligned} \tag{5.76}$$

On the other hand, from Eq. (5.49) we know

$$\langle \xi^\alpha_+ A^i_{s\alpha\beta}\xi^\beta_-(aj)\xi^\gamma_+ A^j_{s\gamma\delta}\xi^\delta_-(ak)\rangle = \frac{1}{4\pi^2a^2(j-k)^2}, \tag{5.77}$$

which implies $MC = 1/\pi$.

All the results up to here are already known in the free fermionic theory. So what do we gain by bosonizing the theory? It turns out that the bosonic theory will help us gain more insights into the interacting theory. As we can see in the current algebra, the spin current and charge current commute. Furthermore, we also saw from the β

function in the interacting theory that λ_s and λ_c do not mix. Actually, the bosonic language makes this "spin-charge separation" manifest, because the theory becomes two copies of $\mathrm{SU}(2)_1$ WZW theory.

Now let us discuss how this "spin-charge separation" helps us understand the interacting theory. From the β functions in Eq. (5.69), we know that $\lambda_{s,c}$ are relevant when they are positive, and irrelevant when they are negative. If we set $\lambda_s = 0$ and $\lambda_c > 0$, the charge sector will be gapped at low energy, while the spin sector is still gapless. The interaction $\lambda_c J^i_{c+} J^i_{c-}$ breaks the chiral symmetry in the charge sector $\mathrm{SU}(2)_{c+} \times \mathrm{SU}(2)_{c-}$ down to the diagonal $\mathrm{SU}(2)_c$ symmetry and a discrete chiral symmetry, under which $h \to -h$ (or equivalently, $g \to -g$). The mass gap in the charge sector implies that this discrete chiral symmetry must be spontaneously broken. Therefore we expect the corresponding WZW field h to develop a non-zero vacuum expectation value (VEV), which breaks the chiral symmetries but preserves the diagonal $\mathrm{SU}(2)_c$ symmetry,

$$\langle h_{\alpha\beta} \rangle = K \delta_{\alpha\beta}. \tag{5.78}$$

Therefore

$$\langle \mathcal{S}^i_j \mathcal{S}^i_k \rangle = -\frac{1}{4\pi^2 a^2 (j-k)^2} + \frac{(-1)^{j-k} M K^2}{4\pi a |j-k|}. \tag{5.79}$$

5.5.3 Dimer correlation

Recall that the general dimer operator was defined in Eq. (5.52). For convenience, we further define the dimer operator associated with $\mathcal{S}^3$ as

$$\mathcal{D}_j := \mathcal{D}^3_j = \frac{1}{2}(\mathcal{S}^3_j \mathcal{S}^3_{j+1} - \mathcal{S}^3_{j-1} \mathcal{S}^3_j). \tag{5.80}$$

The continuum limit of the dimer operator was given in Eq. (5.54), leading to

$$\mathcal{D}_j = -\frac{(-1)^j}{\mathrm{i}2\pi a} \xi^\alpha_+ \xi^\alpha_-(aj) + \text{higher orders in } a, \tag{5.81}$$

where we have inserted $T^a = \frac{1}{2}A_s^i$ and used $(\frac{1}{2}A_s^i)^2_{\alpha\beta} = \frac{1}{16}\delta_{\alpha\beta}$. Notice that in terms of Dirac fermions, the dimer operator is a chiral mass term

$$\mathcal{D}_j = -\frac{(-1)^j}{2\pi a}\bar{\psi}^\alpha \mathrm{i}\gamma^3\psi^\alpha(aj) + \text{higher orders in } a. \tag{5.82}$$

Upon bosonization, we have

$$\mathcal{D}_j = -(-1)^j \frac{M}{2\pi a}\,\mathrm{tr}\, g\,\mathrm{tr}\, h(aj) + \text{higher orders in } a. \tag{5.83}$$

Comparing this with the oscillating part of $\mathcal{S}_j^i$ in Eq. (5.72),

$$\mathcal{S}^i_{j,\mathrm{osc}} := -(-1)^j \frac{M}{2}\,\mathrm{tr}(g\mathrm{i}\sigma^i)\,\mathrm{tr}\, h, \tag{5.84}$$

we see that $\mathcal{S}^i_{j,\mathrm{osc}}$ and $\pi a\mathcal{D}_j$ form a 4-component vector representation of the $\mathrm{SU}(2)_{s+}\times$ $\mathrm{SU}(2)_{s-}$ symmetry [86, 87]. Therefore when $\lambda_s = 0$ (the $\mathrm{SU}(2)_{s+} \times \mathrm{SU}(2)_{s-}$ symmetry is unbroken), the correlation function of $\pi a\mathcal{D}_j$ should be identical with $\mathcal{S}^i_{j,\mathrm{osc}}$. Indeed, we can check that when $\lambda_s = \lambda_c = 0$,

$$\langle \mathcal{D}_j\mathcal{D}_k\rangle = (-1)^{j-k}\frac{1}{(2\pi^2a^2)^2(j-k)^2} + \cdots, \tag{5.85}$$

which is consistent with Eq. (5.56). On the other hand, when $\lambda_s = 0$ and $\lambda_c > 0$, we have

$$\langle \mathcal{D}_j\mathcal{D}_k\rangle = (-1)^{j-k}\frac{MK^2}{4(\pi a)^3|j-k|} + \cdots. \tag{5.86}$$

The identification of $\mathcal{S}^i_{j,\mathrm{osc}}$ and $\pi a\mathcal{D}_j$ as a 4-component vector under the $\mathrm{SU}(2)_{s+} \times$ $\mathrm{SU}(2)_{s-}$ symmetry at $\lambda_s = 0$ will be checked very precisely in the numerical results in Chapter 7.

5.5.4 Logarithmic corrections to the correlation functions

When $\lambda_s < 0$ and $\lambda_c > 0$, although the coupling λ_s is marginally irrelevant, it has logarithmic corrections to the correlation functions. These corrections are crucial

when we fit the numerical results away from the critical point in Chapter 7. Therefore we will derive these corrections now. We begin with the β-function of the marginal coupling λ_s

$$\frac{\mathrm{d}\lambda_s}{\mathrm{d}\ln r} = \frac{\lambda_s^2}{2\pi}, \tag{5.87}$$

which is the same as Eq. (5.69) except that we have replaced the energy scale μ with a length scale r. Integrating this equation, we obtain

$$\frac{1}{\lambda_s(r)} - \frac{1}{\lambda_{s0}} = -\frac{1}{2\pi}\ln\frac{r}{r_0}, \tag{5.88}$$

where λ_{s0} is the coupling at some short distance length scale r_0. Note that the solution $\lambda_s(r)$ above is meaningful for very large values of r only when $\lambda_{s0} < 0$, i.e., the coupling $\lambda_s(r)$ is marginally irrelevant. When $\lambda_{s0} > 0$ the coupling $\lambda_s(r)$ diverges at $r = r_0\,\mathrm{e}^{2\pi/\lambda_{s0}}$, which is the remnant of the Landau pole of perturbation theory and signals new physics at long distances due to the formation of a fermion mass.

For convenience, let us denote the leading WZW terms of $\mathcal{S}^3$ and $\mathcal{D}$ as

$$\varphi_{\mathcal{S}} := \mathrm{tr}(g\mathrm{i}\sigma^i)\,\mathrm{tr}\,h, \quad \varphi_{\mathcal{D}} := \mathrm{tr}\,g\,\mathrm{tr}\,h, \tag{5.89}$$

and the correlation functions at coupling λ_s as

$$G_i(\lambda_s(r), r) := \langle\varphi_i(0)\varphi_i(r)\rangle \text{ for } i = \mathcal{S}, \mathcal{D}. \tag{5.90}$$

The notation $G_i(\lambda_s(r), r)$ highlights the fact that the correlation functions depend on r both explicitly and implicitly through $\lambda_s(r)$. We note that $G_i(\lambda_s(r), r)$ satisfies the following RG equation:

$$\frac{\mathrm{d}\ln G_i(\lambda_s(r), r)}{\mathrm{d}\ln r} = -2\big(h_i + \gamma_i(\lambda_s(r))\big), \tag{5.91}$$

where h_i is the conformal dimension of φ_i at the critical point, and $\gamma_i(\lambda_s(r))$ is the anomalous dimension of φ_i induced by the marginal perturbation. Integrating this equation, we get

$$\ln\frac{G_i(\lambda_s(r), r)}{G_i(\lambda_{s0}, r_0)} = \int_{r_0}^{r} -2(h_i + \gamma_i(\lambda_s(r')))\mathrm{d}\ln r', \tag{5.92}$$

from which we can derive the correlation functions in the presence of the marginal perturbation once we know $\gamma_i(\lambda_s(r))$.

In CFT the conformal dimension h_i of the operator φ_i is related to the finite size energy $E_i = 2\pi h_i/L$ of the state $|\varphi_i\rangle$ through the state-operator correspondence [88]. Then the anomalous dimension γ_i of the operator is related to the change of this energy due to the marginal operator. In our case, to leading order in λ_s, this leads to the expression [89],

$$\gamma_i(\lambda_s) = \frac{b_i}{2\pi}\lambda_s + O(\lambda_s^2), \tag{5.93}$$

where

$$\begin{aligned} b_i &= \int \mathrm{d}x\ \langle\varphi_i|J^j_{s+}J^j_{s-}(x)|\varphi_i\rangle \\ &= \frac{1}{2}\int \mathrm{d}x\ \langle\varphi_i|(J^j_{s+}+J^j_{s-})^2 - J^j_{s+}J^j_{s+} - J^j_{s-}J^j_{s-}|\varphi_i\rangle \\ &= \frac{1}{2}(s_{\mathrm{tot}}(s_{\mathrm{tot}}+1) - s_L(s_L+1) - s_R(s_R+1)). \end{aligned} \tag{5.94}$$

In the above formula, $s_L = s_R = 1/2$ for both spin and dimer states, but s_{tot} are different. The values of b_i can be calculated for both spin and dimer fields, which are tabulated in Table 5.1 below.

Table 5.1: h_i and b_i for the WZW fields φ_i.

WZW fields	s_{tot}	s_L	s_R	b_i	h_i
$\varphi_{\mathcal{S}} = \mathrm{tr}\, h\, \mathrm{tr}\, g\sigma^i$	1	1/2	1/2	1/4	1/2
$\varphi_{\mathcal{D}} = \mathrm{tr}\, h\, \mathrm{tr}\, g$	0	1/2	1/2	−3/4	1/2

Inserting these values of b_i and $\lambda_s(r)$ (given in Eq. (5.88)) into Eq. (5.93), we can compute $\gamma_i(\lambda_s(r))$. Substituting this into Eq. (5.92) we get

$$\frac{G_S(\lambda(r), r)}{G_S(\lambda_{s0}, r_0)} = \frac{r_0}{r}\left(1 - \frac{\lambda_{s0}}{2\pi}\ln\frac{r}{r_0}\right)^{\frac{1}{2}}, \tag{5.95}$$

$$\frac{G_D(\lambda(r), r)}{G_D(\lambda_{s0}, r_0)} = \frac{r_0}{r}\left(1 - \frac{\lambda_{s0}}{2\pi}\ln\frac{r}{r_0}\right)^{-\frac{3}{2}}. \tag{5.96}$$

Similar expressions have been derived earlier in the context of spin chains [90, 91] and verified numerically [90]. Note again that for a fixed value of λ_{s0} but large values of r, the above expressions make sense only when $\lambda_{s0} \leq 0$, i.e., when we are in the conformal phase as already mentioned above. On the other hand, when r is in a fixed range but $\lambda_{s0} \to 0$, the above expressions give us the leading corrections to conformal behavior on both sides of the critical point.

We could perform a similar analysis in the massive phase. However, in the massive phase, the anomalous dimension Eq. (5.93) obtained in the conformal phase cannot be completely correct. Besides, like the β-function, it was derived in perturbation theory, so there could be non-perturbative corrections due to the mass scale M. In particular if we assume the correlation function to the leading order is of the form $G_i(r) \sim \mathrm{e}^{-\alpha_i M r}$, this would contribute additional non-perturbative terms to the anomalous dimension $\gamma_i(\lambda_s)$. For example, if we assume

$$\lambda_s(r) = -\frac{2\pi}{\ln Mr} \tag{5.97}$$

as a possible definition for the RG invariant mass scale M, then it is easy to see that

$$\gamma_i(\lambda_s) = \frac{b_i}{2\pi}\lambda_s + \frac{\alpha_i}{2}\ \mathrm{e}^{-2\pi/\lambda_s} + O(\lambda_s^2). \tag{5.98}$$

Since we are only deriving corrections to $G(r)$ due to the marginal interaction perturbatively, we will ignore such non-perturbative effects. Then, Eqs. (5.95) and (5.96) can still be used in the massive phase near the critical point except that we will find $\lambda_{s0} > 0$ and r is constrained to be such that $\lambda_{s0}/2\pi \ln(r/r_0) < 1$.

6

Physics in Two Spatial Dimensions

In this chapter, we will study the physics of the continuum theory corresponding to our lattice model in two spatial dimensions. From our analysis in Chapter 4, we know that up to quartic interactions, the most general continuum Euclidean Lagrangian that preserves the symmetries of our lattice model can be written as

$$\mathcal{L} = \bar{\psi}^{\alpha}\gamma^{\mu}\partial_{\mu}\psi^{\alpha} - \frac{g_{\mathbf{adj}}^2}{2}\sum_a (M_{\mathbf{adj}}^a)^2 - \frac{g_3^2}{2}(\bar{\psi}^{\alpha}\mathrm{i}\gamma^3\psi^{\alpha})^2 - \frac{g_5^2}{2}(\bar{\psi}^{\alpha}\mathrm{i}\gamma^5\psi^{\alpha})^2 - \frac{g_{35}^2}{2}(\bar{\psi}^{\alpha}\mathrm{i}\gamma^3\gamma^5\psi^{\alpha})^2, \tag{6.1}$$

where $\alpha = 1, 2, \cdots, N_f$. $M_{\mathbf{adj}}^a = \xi^T(A^a \otimes \mathcal{C})\xi$ are the adjoint mass terms with A^a, $a = 1, \cdots, \binom{2N_f}{2}$ forming a basis of all anti-symmetric Hermitian matrices and satisfy $\mathrm{tr}(A^a A^b) = \frac{1}{2}\delta^{ab}$. Further imposing the $\mathrm{SO}(2)_R$ symmetry coming from lattice rotation, we should require $g_3^2 = g_5^2$. We are interested in understanding the ground state properties and the quantum critical behavior of the theory in Eq. (6.1) when tuning the three couplings $g_{\mathbf{adj}}^2$, $g_3^2 = g_5^2$ and g_{35}^2. Further imposing the $\mathrm{SO}(2)_R$ symmetry coming from lattice rotation, we should require $g_3^2 = g_5^2$. However, unlike in one spatial dimension, where we could use the powerful CFT and bosonization techniques

to understand the physics by perturbing any CFT, in two spatial dimensions, we can only resort to perturbations to the free theory.

In three space-time dimensions, near the free fermion fixed point, all four-fermion interactions are irrelevant because they have mass dimension 4, making it hard to perform a perturbative calculation. However, it is possible to go to a dimension where the interactions are marginal, perform a perturbative calculation, and then extrapolate to the original dimension. This technique is known as ε-expansion [92], which is a double expansion in ε, the deviation from the dimension where the interactions are marginal, and the couplings. In our four-fermion field theories, one can begin with two space-time dimensions and perform a $2+\varepsilon$ expansion. There is another type of ε-expansion often employed to analyze four-fermion theories, where auxiliary bosons are introduced to convert the Gross-Neveu interactions into Gross-Neveu-Yukawa (GNY) interactions. The GNY interactions are marginal in four space-time dimensions, and in this case one performs a $4-\varepsilon$ expansion. Under RG, all possible terms allowed by the symmetries of the theory will be generated, and in four space-time dimensions, the kinetic terms for the bosons and quartic boson self-interactions become marginal and must be taken into account.

It is also possible to perform a perturbative calculation in an arbitrary dimension, given that the fermion flavor number N_f is large, which is known as a large N_f expansion. Since all the fermion loops are enhanced by a factor of N_f, the diagrams containing fermion loops should be summed over systematically, leading to summing over the "bubble chain" diagrams. The physical observables are calculated in powers of $1/N_f$. Although our theory has $N_f = 2$, which is not large, we can at least compare the result with the large N_f limit of ε expansion for consistency check.

In the $N_f \to \infty$ limit, the partition function can also be evaluated exactly using the saddle point approximation, which corresponds to summing over all one-fermion-loop diagrams, and we can calculate the effective action and effective potential.

In this approach, the quantum fluctuation of the fermion bilinears is completely ignored. However, it can still help us obtain useful information about how the fermion bilinears condense as a function of the couplings, and therefore understand the phase structures.

In this chapter, we will focus mainly on the theory with $N_f = 2$, where we have some results from the Monte Carlo simulation to reduce the possible interactions. As we discussed in Section 4.2.4, when $N_f = 2$ with SO(4) symmetry the interaction $(M^a_{\mathbf{adj}})^2$ splits into two independent interactions $2(M^i_s)^2$ and $2(M^i_c)^2$, where $M^i_s = \frac{1}{2}\xi^T A^i_s \otimes \mathcal{C}\xi$, $M^i_c = \frac{1}{2}\xi^T A^i_c \otimes \mathcal{C}\xi$. In terms of Dirac fermions, they can be written as

$$M^i_s = \frac{1}{2}\bar{\psi}\sigma^i\psi, \quad M^3_c = -\frac{1}{2}\bar{\psi}\psi,$$
$$M^1_c = \frac{1}{2}(\psi_1^T\mathcal{C}\psi_2 + \bar{\psi}_2\mathcal{C}\bar{\psi}_1^T), \quad M^2_c = -\frac{\mathrm{i}}{2}(\psi_1^T\mathcal{C}\psi_2 - \bar{\psi}_2\mathcal{C}\bar{\psi}_1^T). \tag{6.2}$$

The numerical study of our lattice model, presented in the next chapter, suggests that by tuning the lattice coupling, there is a second-order phase transition from a free Dirac fermion phase to a phase where either M^i_s or M^i_c develops a VEV. This result implies that the SO(4) symmetry spontaneously breaks to either $\mathrm{SU}(2)_s$ or $\mathrm{SU}(2)_c$ [1]. Since the other fermion mass bilinears do not develop VEVs, it might be sufficient to focus on the RG flow in the subspace that only includes $(M^i_s)^2$ and $(M^i_c)^2$. Assuming this to be true, in this chapter, we will focus on the continuum Lagrangian (which we refer to as the SO(4) Gross-Neveu model),

$$\mathcal{L} = \bar{\psi}^\alpha\gamma^\mu\partial_\mu\psi^\alpha - \frac{g_s^2}{2}(M^i_s)^2 - \frac{g_c^2}{2}(M^i_c)^2. \tag{6.3}$$

In our lattice model with $U = 0$, the continuum model must have spin-charge flip symmetry, forcing $g_s^2 = g_c^2$. However, when $U \neq 0$, this symmetry is broken and the two couplings can be different.

[1] In the condensed matter literature, when M^i_s develops a VEV, the system is said to be in an AFM order, when $M^{1,2}_c$ develops a VEV, the system is said to be in a superconducting order, and when M^3_c develops a VEV, the system is said to be in a CDW order.

In the next section, we will compute the one-loop field effective potential for Eq. (6.3) which shows that at large coupling, either $\mathrm{SU}(2)_s$ or $\mathrm{SU}(2)_c$ is spontaneously broken, as suggested by the Monte Carlo results. Later we will compute the RG flow diagrams in $4-\varepsilon$ expansion and large N expansion.

6.1 The mean-field effective potential

In this section, we will study the phase structure of the SO(4) Gross-Neveu model Eq. (6.3) by calculating the effective potential of the fermion bilinears as a function of the four-fermion couplings. In order to do so, we rewrite the four-fermion theory by introducing bosonic fields that couple to fermion bilinears. We then derive the effective potential of the bosonic fields by integrating out the fermions, which is equivalent to a one-loop calculation. In order to simplify the calculation, we assume the bosonic field to be a constant in space-time. This assumption is naturally justified in the large N_f limit, where the bosonic field is a sum of many fermion bilinears, and thus their fluctuations are negligible. This effective potential then gives us information about how the fermion bilinears condense as a function of the couplings. To introduce the calculation, we first consider a simple example and calculate the effective potential of the traditional Ising Gross-Neveu model. Later we extend it to the SO(4) Gross-Neveu model Eq. (6.3).

6.1.1 The Ising Gross-Neveu model

The Ising Gross-Neveu model is defined through the Lagrangian

$$\mathcal{L} = \bar{\psi}^\alpha \gamma^\mu \partial_\mu \psi^\alpha - \frac{g^2}{2} (\bar{\psi}^\alpha \psi^\alpha)^2. \tag{6.4}$$

In order to calculate the effective potential, we first rewrite the partition function in an equivalent form

$$Z = \int D\psi D\bar{\psi} D\phi \ \mathrm{e}^{-S[\psi,\bar{\psi},\phi]}, \tag{6.5}$$

where

$$S[\psi, \bar{\psi}, \phi] = \int \mathrm{d}^d x \bar{\psi}^\alpha \gamma^\mu \partial_\mu \psi^\alpha + \frac{1}{2g^2}\phi^2 + \phi \bar{\psi}^\alpha \psi^\alpha, \tag{6.6}$$

where we have introduced a non-dynamical real scalar field ϕ, and we will choose $d = 3$ as the space-time dimensions. It can be easily seen that if we perform the Gaussian integral over the non-dynamical field ϕ, we get back to the partition function of the Ising Gross-Neveu model.

Our goal is to find the ground state expectation value of ϕ as a function of the coupling g. To find this, we can integrate out the fermions and obtain the one-loop effective action for the bosonic fields, which is given by

$$S_{\text{eff}}[\phi] = -\log \mathrm{Det}(\not{\partial} + \phi) + \int \mathrm{d}^d x \ \frac{1}{2g^2}\phi^2. \tag{6.7}$$

To find the ground state expectation value of ϕ, we need to minimize the effective potential $V_{\text{eff}}[\phi]$ as a functional of ϕ. It is usually challenging to compute $V_{\text{eff}}[\phi]$, especially if the fluctuations of ϕ field cannot be neglected. Here we use a mean-field analysis where such fluctuations are neglected, i.e., ϕ is assumed to be a constant, which can also be justified in the large N_f limit. Then we can compute the determinant in the basis of momentum eigenstates to obtain

$$S_{\text{eff}}[\phi] = -\log \mathrm{Det}(-i\not{k} + \phi) + \int \mathrm{d}^d x \ \frac{1}{2g^2}\phi^2. \tag{6.8}$$

Since $\det \gamma^5 = 1$ and $\{\not{k}, \gamma^5\} = 0$, we have

$$\mathrm{Det}(i\not{k} + \phi) = \mathrm{Det}\, \gamma^5 (i\not{k} + \phi)\gamma^5 = \mathrm{Det}(-i\not{k} + \phi), \tag{6.9}$$

which implies

$$\mathrm{Det}(i\not{k} + \phi) = \mathrm{Det}((\not{k})^2 + \phi^2)^{\frac{1}{2}} = \mathrm{Det}(k^2 \mathbb{1}_4 + \phi^2)^{\frac{1}{2}} = \mathrm{Det}(k^2)\, \mathrm{Det}(1 + \frac{\phi^2}{k^2})^2. \tag{6.10}$$

Using the fact that $\log \mathrm{Det}\, O = \mathrm{Tr} \log O$ for an operator O, we obtain

$$S_{\text{eff}}[\phi] = -\log \mathrm{Det}(k^2) - 2\, \mathrm{Tr} \log \left(1 + \frac{\phi^2}{k^2}\right) + \int \mathrm{d}^d x \ \frac{1}{2g^2}\phi^2. \tag{6.11}$$

Note that $\log \mathrm{Det}(k^2)$ is independent of ϕ and therefore only contributes a constant shift to the effective potential and can be ignored. Therefore we get

$$V_{\text{eff}}[\phi] = -S_d \int_0^\Lambda \mathrm{d}k^2 \; k^{d-2} \log\Big(1 + \frac{\phi^2}{k^2}\Big) + \frac{1}{2g^2}\phi^2, \tag{6.12}$$

where $S_d := \frac{2}{(4\pi)^{d/2}\Gamma(d/2)}$ is the loop integral factor. When $d = 3$, the integral in the equation above does not seem to have an IR divergence. However, the effective potential is not analytical at $\phi = 0$, and to see this, we have to introduce an IR cutoff Λ_{IR}. Then we have

$$\begin{aligned}\int_{\Lambda_{\text{IR}}}^\Lambda \mathrm{d}k^2 \; k \log\Big(1 + \frac{\phi^2}{k^2}\Big) &= -\frac{2\pi}{3}|\phi^3| + \frac{4}{3}\phi^3 \tan^{-1}\frac{\phi}{k} + \frac{4}{3}k\phi^2 + \frac{2}{3}k^3 \log\Big(1 + \frac{\phi^2}{k^2}\Big)\Big|_{\Lambda_{\text{IR}}}^\Lambda \\ &= \frac{4}{3}\phi^3 \tan^{-1}\frac{\phi}{\Lambda} - \frac{4}{3}\phi^3 \tan^{-1}\frac{\phi}{\Lambda_{\text{IR}}} + \frac{4}{3}\Lambda\phi^2 + \frac{2}{3}\Lambda^3 \log\Big(1 + \frac{\phi^2}{\Lambda^2}\Big),\end{aligned}$$

where we have dropped terms that vanish when $\Lambda_{\text{IR}} \to 0$. Using

$$\lim_{\Lambda_{\text{IR}} \to 0} \phi^3 \tan^{-1}\frac{\phi}{\Lambda_{\text{IR}}} = \frac{\pi}{2}|\phi|^3, \tag{6.13}$$

we obtain

$$\frac{1}{S_d}V_{\text{eff}}[\phi] = \frac{1}{2S_d g^2}\phi^2 - \frac{4}{3}\phi^3 \tan^{-1}\frac{\phi}{\Lambda} + \frac{2\pi}{3}|\phi|^3 - \frac{4}{3}\Lambda\phi^2 - \frac{2}{3}\Lambda^3 \log\Big(1 + \frac{\phi^2}{\Lambda^2}\Big), \tag{6.14}$$

which is not analytic at $\phi = 0$. In Fig. 6.1 we plot this potential at $S_d \Lambda g^2 = 5$. and observe that the effective potential is indeed non-analytic at $\phi = 0$. There is an interesting lesson to learn about the perturbative expansion and the $|\phi|^3$ term. Assuming $\phi < \Lambda_{\text{IR}}$, we could have used the Taylor expansion within the integrand to obtain

$$\int_{\Lambda_{\text{IR}}}^\Lambda \mathrm{d}k^2 \; k \log\Big(1 + \frac{\phi^2}{k^2}\Big) = \sum_{n=1}^\infty \Big(-2\frac{(-1)^n}{n} \int_{\Lambda_{\text{IR}}}^\Lambda \mathrm{d}k \; \frac{1}{k^{2n-2}}\Big)\phi^{2n}. \tag{6.15}$$

The expansion on the right can be identified as the summation over all one-loop diagrams with $2n$ external legs ϕ. However, except for $n = 1$, each term in the expansion

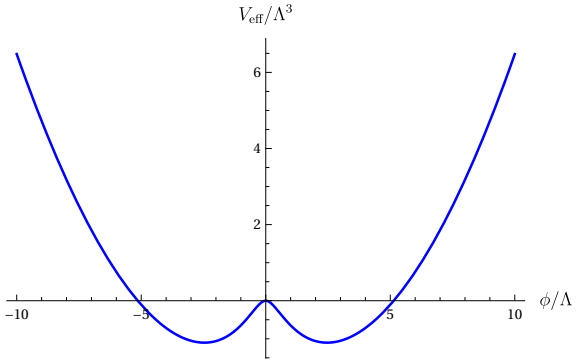

FIGURE 6.1: Effective potential of the Gross-Neveu Model at $S_d \Lambda g^2 = 5$.

is IR divergent. Furthermore, in this perturbative expansion, all the diagrams have even numbers of the ϕ field, and we would not be able to see the $|\phi|^3$ term. In this sense, we can think of $|\phi|^3$ as a non-perturbative effect.

Having seen this connection to the diagram expansion, we can see this issue clearer in terms of perturbative expansion of $\phi^3 \tan^{-1} \frac{\phi}{\Lambda_{\text{IR}}}$ in different limits

$$\phi^3 \tan^{-1} \frac{\phi}{\Lambda_{\text{IR}}} = \begin{cases} \frac{\pi}{2}|\phi|^3 & \text{when } \phi \gg \Lambda_{\text{IR}}, \\ \frac{1}{\Lambda_{\text{IR}}}\phi^4 - \frac{1}{3\Lambda_{\text{IR}}^3}\phi^6 + \cdots & \text{when } \phi \ll \Lambda_{\text{IR}}. \end{cases} \tag{6.16}$$

In the effective potential, we assumed $\phi \gg \Lambda_{\text{IR}}$, and we are able to see the $|\phi|^3$ term, while in the perturbative expansion, we assumed $\phi \ll \Lambda_{\text{IR}}$, and what we see are the IR divergences. Therefore, it is reasonable to attribute these divergences in the perturbative expansion to the wrong limit we assume in perturbation theory. This observation is also related to the rationale behind renormalized perturbation theory: a finite term at lower order may look infinite at a higher one, and this is why we usually use the counter-terms at the tree level to cancel the divergences at one loop.

Now let us find the minimum of the effective potential. Solving the equation

$$0 \stackrel{!}{=} \frac{1}{S_d} V'_{\text{eff}}[\phi] = 4\phi^2 \tan^{-1} \frac{\Lambda}{\phi} + \Big(\frac{1}{S_d g^2} - 4\Lambda\Big)\phi. \tag{6.17}$$

We see that there is a trivial solution at $\phi = 0$, and two non-trivial solutions at

$\phi = \pm\phi_0$, where $\phi_0 > 0$ satisfies

$$\frac{\phi_0}{\Lambda}\tan^{-1}\frac{\Lambda}{\phi_0} = 1 - \frac{1}{4S_d\Lambda g^2}. \tag{6.18}$$

Furthermore,

$$\begin{aligned}\frac{1}{S_d}V''_{\text{eff}}[\phi] &= -\frac{4\Lambda}{1+\Lambda^2/\phi^2} + 8\phi\tan^{-1}\frac{\Lambda}{\phi} + \frac{1}{S_d g^2} - 4\Lambda \\ &= \begin{cases} -4\Lambda(1-\frac{1}{4S_d\Lambda g^2}) & \text{when } \phi = 0 \\ -\frac{4\Lambda}{1+\Lambda^2/\phi_0^2} + 4\phi_0\tan^{-1}\frac{\Lambda}{\phi_0} & \text{when } \phi = \phi_0. \end{cases}\end{aligned} \tag{6.19}$$

Therefore $\phi = 0$ is a stable fixed point when $4S_d\Lambda g^2 \le 1$, and becomes unstable when $4S_d\Lambda g^2 > 1$. On the other hand, since $x\tan^{-1}\frac{1}{x}$ has values between 0 and 1, and is monotonic for $x > 0$, we know that there are non-trivial solutions at $\phi = \pm\phi_0$ only when $4S_d\Lambda g^2 \ge 1$, and therefore we can define $g_0^2 = \frac{1}{4S_d\Lambda}$ as the critical point. It can be easily checked that the solutions $\phi = \pm\phi_0$ are always stable when they exist. In Fig. 6.2, we plot the order parameter ϕ_0 as a function of $S_d g^2$.

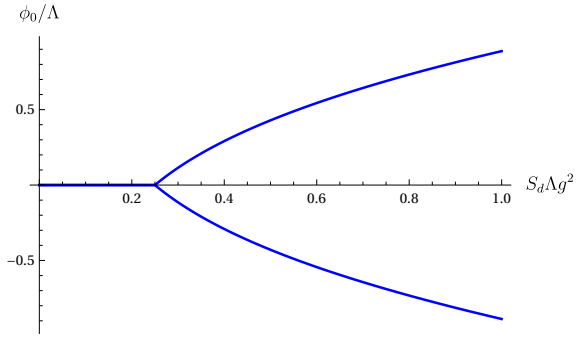

FIGURE 6.2: The order parameter ϕ_0/Λ of the Ising Gross-Neveu Model as a function of $S_d\Lambda g^2$.

In the $g \to g_{0+}$ limit, ϕ_0 is small. Using $\lim_{x\to 0}\tan\frac{1}{x} \approx \frac{\pi}{2}\frac{x}{|x|}$, we have

$$\frac{\pi}{2}\frac{|\phi_0|}{\Lambda} \approx 1 - \frac{1}{4S_d\Lambda g^2} \implies |\phi_0| \approx \frac{1}{2\pi S_d}\left(\frac{1}{g_0^2} - \frac{1}{g^2}\right) = \frac{1}{2\pi S_d}\frac{g^2 - g_0^2}{g_0^4}, \tag{6.20}$$

from which we can read the critical exponent $\frac{1}{2}(1+\eta)\nu =: \beta = 1$, where β is the critical exponent of the order parameter defined as $|\phi_0| \propto (g^2 - g_0^2)^\beta$, agreeing with

our leading order result from large N in Section 6.3. Notice that $\beta = 1$ can also be understood from the existence of a $|\phi|^3$ term in the effective potential.

6.1.2 The SO(4) *Gross-Neveu model*

We now extend the above calculation to the four-fermion theory of interest to us, the SO(4) Gross-Neveu model given by Eq. (6.3). Similar to the Ising Gross-Neveu model, in order to calculate the effective potential, we need to introduce six scalar fields $\vec{\phi}_s$ and $\vec{\phi}_c$. As before, when calculating the effective potential, we will treat these scalar fields as constants in space and time. Then using the spin $\mathrm{SU}(2)_s$ and charge $\mathrm{SU}(2)_c$ symmetry, we can always rotate $\vec{\phi}_s$ and $\vec{\phi}_c$ such that $\phi_s^{1,2} \equiv \phi_c^{1,2} \equiv 0$. Therefore it is sufficient to only consider the third components of spin and charge interactions, and for simplicity, we will denote them by ϕ_s and ϕ_c in this section. Now the action can be written as

$$S[\psi, \bar{\psi}, \phi_s, \phi_c] = -\int \mathrm{d}^d x \; \bar{\psi}^\alpha \gamma^\mu \partial_\mu \psi^\alpha + \frac{1}{2g_s^2}\phi_s^2 + \frac{1}{2g_c^2}\phi_c^2 \\ + \phi_s(\bar{\psi}^1\psi^1 - \bar{\psi}^2\psi^2) + \phi_c(\bar{\psi}^1\psi^1 + \bar{\psi}^2\psi^2). \tag{6.21}$$

Integrating out the fermions as before, we obtain

$$S_{\text{eff}}[\phi_s, \phi_c] = -\log \mathrm{Det} \begin{pmatrix} -i\not{k} + \phi_+ & \\ & -i\not{k} + \phi_- \end{pmatrix} + \int \mathrm{d}^d x \; \frac{1}{2g_s^2}\phi_s^2 + \frac{1}{2g_c^2}\phi_c^2, \tag{6.22}$$

where $\phi_\pm := \phi_c \pm \phi_s$. We observe that the fermion matrix is block-diagonal, and each block would be the same as the Ising Gross-Neveu model if we replace ϕ with $\phi_\pm$. This motivates us to define

$$V_d[\phi] := -S_d \int_0^\Lambda \mathrm{d}k^2 \; k^{d-2} \log\Big(1 + \frac{\phi^2}{k^2}\Big), \tag{6.23}$$

and then we have the following effective potential for ϕ_s and ϕ_c,

$$V_{\text{eff}}[\phi_s, \phi_c] = V_3[\phi_+] + V_3[\phi_-] + \frac{1}{2g_s^2}\phi_s^2 + \frac{1}{2g_c^2}\phi_c^2, \tag{6.24}$$

where from the previous subsection, we know that

$$\frac{1}{S_d}V_3[\phi] = -\frac{4}{3}\phi^3 \tan^{-1}\frac{\phi}{\Lambda} + \frac{2\pi}{3}|\phi|^3 - \frac{4}{3}\Lambda\phi^2 - \frac{2}{3}\Lambda^3 \log\Big(1+\frac{\phi^2}{\Lambda^2}\Big), \tag{6.25}$$

and

$$\frac{1}{S_d}V_3'[\phi] = 4\phi^2 \tan^{-1}\frac{\Lambda}{\phi} - 4\Lambda\phi. \tag{6.26}$$

As before, the minima of the effective potential can be obtained using the following equations:

$$0 \stackrel{!}{=} \frac{1}{S_d}\frac{\partial V_{\text{eff}}[\phi_s,\phi_c]}{\partial \phi_\pm} = \frac{1}{S_d}\Big(V_3'[\phi_\pm] + \frac{1}{2g_s^2}\phi_\pm + \big(\frac{1}{4g_c^2} - \frac{1}{4g_s^2}\big)(\phi_+ + \phi_-)\Big). \tag{6.27}$$

When $2g_s^2 = 2g_c^2 = g^2$, we see that $\phi_\pm$ satisfy independent equations, which are the same as Eq. (6.17), and therefore the solutions are given by $\phi_\pm = 0$ and $\phi_\pm = \pm\phi_0$, where $\phi_0 > 0$ satisfies

$$\frac{\phi_0}{\Lambda}\tan^{-1}\frac{\Lambda}{\phi_0} = 1 - \frac{1}{8S_d\Lambda g_s^2}. \tag{6.28}$$

From the discussion in the previous subsection, we know that when $8S_d\Lambda g_s^2 \le 1$, $\phi_\pm = 0$ is the only solution. On the other hand, when $8S_d\Lambda g_s^2 > 1$, $\phi_\pm = 0$ is no longer stable, and the true minima are at $\phi_\pm = \pm\phi_0$. Note that the signs are not correlated, and we have four degenerate minima corresponding to $(\phi_s,\phi_c) = (\pm\phi_0, 0)$ and $(\phi_s,\phi_c) = (0,\pm\phi_0)$.

When $g_s > g_c$, these minima are no longer degenerate. Intuitively, since g_s is larger, the potential $\frac{1}{2g_s^2}\phi_s^2$ is lower, and the spin broken phase is preferable, as expected. See Fig. 6.3 for an illustration of this potential in the unbroken phase at $S_d\Lambda g_s^2 = S_d\Lambda g_c^2 = 0.1$ and $S_d\Lambda g_s^2 = 0.1, S_d\Lambda g_c^2 = 0.05$, and Fig. 6.4 for an illustration of this potential in the broken phase at $S_d\Lambda g_s^2 = S_d\Lambda g_c^2 = 5$ and $S_d\Lambda g_s^2 = 5, S_d\Lambda g_c^2 = 2.5$. The critical exponent $\beta = 1$ is the same as the Ising Gross-Neveu model.

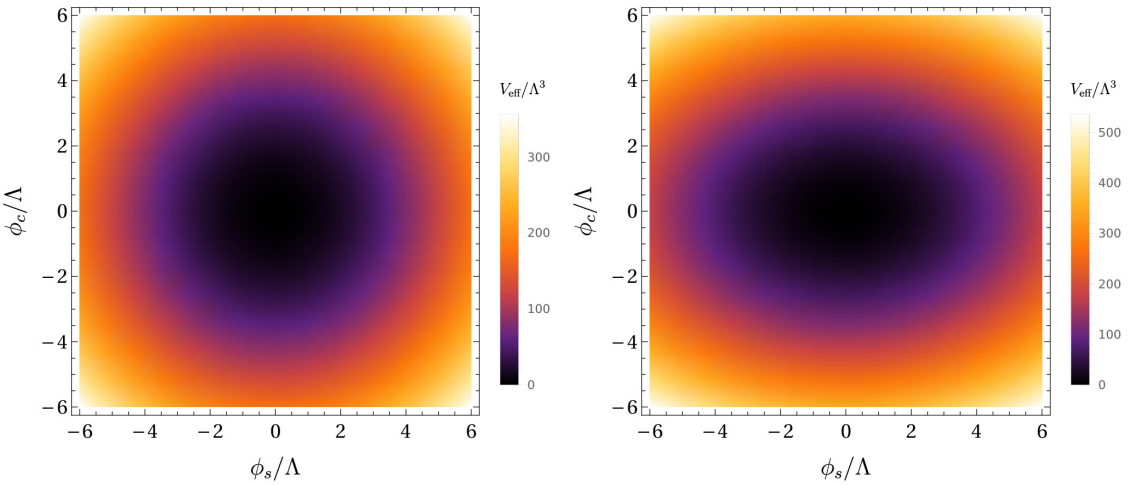

(a) $S_d\Lambda g_s^2 = S_d\Lambda g_c^2 = 0.1$ (b) $S_d\Lambda g_s^2 = 0.1$, $S_d\Lambda g_c^2 = 0.05$

FIGURE 6.3: The effective potential of the SO(4) Gross-Neveu model in the unbroken phase.

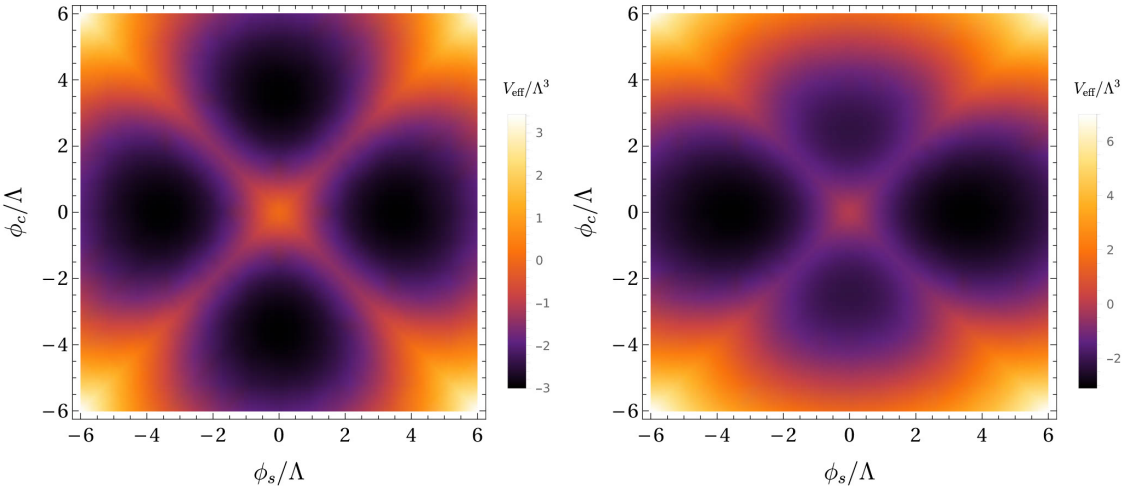

(a) $S_d\Lambda g_s^2 = S_d\Lambda g_c^2 = 5$ (b) $S_d\Lambda g_s^2 = 5$, $S_d\Lambda g_c^2 = 2.5$

FIGURE 6.4: The effective potential of the SO(4) Gross-Neveu model in the broken phase.

6.2 $4-\varepsilon$ expansion

In this section, we would like to understand the RG flow and critical properties of the SO(4) GNY model by calculating the loop expansions near four space-time dimensions. In four space-time dimensions, the kinetic terms of the scalar fields are marginal and will be generated dynamically, giving rise to a GNY theory. We will compute the β functions and the anomalous dimensions of various operators at one-loop order using standard perturbation theory in $4-\varepsilon$ dimensions. As before, we will first outline the calculation using the Ising GNY model and later extend it to the SO(4) GNY model.

In the following, we will perform our calculation using renormalized perturbation theory. The fields and couplings with subscript 0 are the bare ones, while those without subscript 0 are the renormalized ones.

6.2.1 The Ising GNY model

We begin by considering the Ising GNY model, whose Lagrangian is given by

$$\mathcal{L} = \bar{\psi}_0 \gamma^\mu \partial_\mu \psi_0 + \frac{1}{2}\partial_\mu \phi_0 \partial^\mu \phi_0 + \frac{1}{2} m_0^2 \phi_0^2 + \frac{1}{4!}\lambda_0 \phi_0^4 + g_0 \phi_0 \bar{\psi}_0 \psi_0, \tag{6.29}$$

where we have suppressed the flavor index α for simplicity, and the path integral is

$$Z = \int D\psi_0 D\bar{\psi}_0 D\phi_0 \ \ \mathrm{e}^{-\int \mathrm{d}^{4-\varepsilon} x \mathcal{L}[\psi_0, \bar{\psi}_0, \phi_0]}. \tag{6.30}$$

In $4-\varepsilon$ dimension, the bare fields and couplings have dimensions $[\psi_0] = \frac{3-\varepsilon}{2}$, $[\phi_0] = \frac{2-\varepsilon}{2}$, $[\lambda_0] = \varepsilon$ and $[g_0] = \frac{\varepsilon}{2}$, and the renormalized Lagrangian can be written as

$$\begin{aligned}
\mathcal{L} &= Z_\psi \bar{\psi} \gamma^\mu \partial_\mu \psi + \frac{1}{2} Z_\phi \partial_\mu \phi \partial^\mu \phi + \frac{1}{2} Z_\phi m_0^2 \phi^2 + \frac{1}{4!} Z_\phi^2 \lambda_0 \phi^4 + Z_\phi^{1/2} Z_\psi g_0 \phi \bar{\psi} \psi \\
&=: \bar{\psi} \gamma^\mu \partial_\mu \psi + \frac{1}{2}\partial_\mu \phi \partial^\mu \phi + \frac{1}{2} m^2 \phi^2 + \frac{1}{4!} m^\varepsilon \lambda \phi^4 + m^{\varepsilon/2} g \phi \bar{\psi} \psi \\
&\quad + \delta_\psi \bar{\psi} \gamma^\mu \partial_\mu \psi + \frac{1}{2}\delta_\phi \partial_\mu \phi \partial^\mu \phi + \frac{1}{2}\delta_m \phi^2 + \frac{1}{4!} m^\varepsilon \delta_\lambda \phi^4 + m^{\varepsilon/2} \delta_g \phi \bar{\psi} \psi,
\end{aligned} \tag{6.31}$$

where we define

$$Z_\psi = 1 + \delta_\psi, \quad Z_\phi = 1 + \delta_\phi, \quad Z_\phi m_0^2 = m^2 + \delta_m,$$
$$Z_\phi^2 \lambda_0 = m^\varepsilon(\lambda + \delta_\lambda), \quad Z_\phi^{1/2} Z_\psi g_0 = m^{\varepsilon/2}(g + \delta_g), \tag{6.32}$$

and introduce the renormalized couplings m, g and λ. The counter terms δ_i are formal series in the renormalized couplings. In the minimal subtraction scheme, they are determined order by order by canceling the divergent part of the renormalized theory at one loop higher. The free propagator in the momentum space can be read as

$$\int \mathrm{d}^{4-\varepsilon}x \ \langle \psi^\alpha(x)\bar{\psi}^\beta(0)\rangle \, \mathrm{e}^{\mathrm{i}kx} = \frac{\delta^{\alpha\beta}}{-i\not{k}} = \frac{i\not{k}\delta^{\alpha\beta}}{k^2},$$
$$\int \mathrm{d}^{4-\varepsilon}x \ \langle \phi(x)\phi(0)\rangle \, \mathrm{e}^{\mathrm{i}kx} = \frac{1}{k^2 + m^2}. \tag{6.33}$$

Mass and wave function renormalization

The relevant one-loop Feynman diagrams that help us compute the mass and wave function renormalizations are shown in Fig. 6.5, where the dashed lines denote the boson fields, and the solid lines denote the fermion fields.

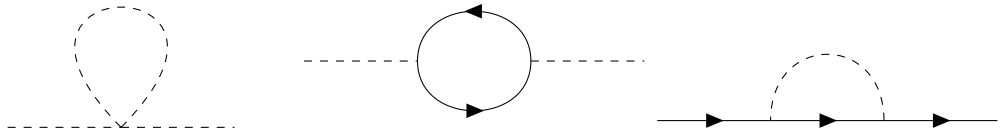

(a) Boson loop $M_{\phi b}$ (b) Fermion loop $M_{\phi f}$ (c) Self-energy loop M_ψ

FIGURE 6.5: One-loop diagrams that contribute to mass and field renormalizations.

At one loop Fig. 6.5a does not depend on the external momenta, and therefore it only contributes to δ_m but not δ_ϕ. We have

$$\frac{1}{4} m^\varepsilon (-\lambda) \phi\phi\overbrace{\phi\phi}\phi = \lambda M_{\phi b}\phi^2, \tag{6.34}$$

where

$$M_{\phi b}(p^2) = \frac{-m^\varepsilon}{4} \int \frac{\mathrm{d}^{4-\varepsilon}k}{(2\pi)^{4-\varepsilon}} \frac{1}{k^2 + m^2} =: \frac{-m^\varepsilon}{4} I_1(4 - \varepsilon, m^2) = \frac{m^2}{4} \frac{S_d}{\varepsilon}. \tag{6.35}$$

Here the integrals $I_1(d, m^2)$, and the following integrals $I_2(d, m^2)$ and $I_3^\mu(d, p, m^2)$ are defined and calculated in Appendix D. This divergence should be canceled by the counter-term δ_m,

$$-\frac{1}{2}\delta_m + \frac{m^2\lambda}{4}\frac{S_d}{\varepsilon} \implies \delta_m = \frac{m^2\lambda}{2}\frac{S_d}{\varepsilon}. \tag{6.36}$$

The two-point fermion loop (vacuum polarization) in Fig. 6.5b contributes to δ_ϕ,

$$\frac{1}{2}m^\varepsilon g^2(\phi\bar{\psi}\psi)(\phi\bar{\psi}\psi) = g^2 N_f M_{\phi f}(p^2)\phi^2, \tag{6.37}$$

where

$$M_{\phi f}(p^2) = -\frac{m^\varepsilon}{2}\int \frac{\mathrm{d}^{4-\varepsilon}k}{(2\pi)^{4-\varepsilon}}\frac{\mathrm{tr}(\mathrm{i}\not{k}\mathrm{i}(\not{k}+\not{p}))}{k^2(k+p)^2} = \frac{m^\varepsilon}{2}\int \frac{\mathrm{d}^{4-\varepsilon}k}{(2\pi)^{4-\varepsilon}}\frac{4(k^2+k\cdot p)}{k^2(k+p)^2}$$

$$= 2m^\varepsilon(I_1(4-\varepsilon,0) + p_\mu I_3^\mu(4-\varepsilon,-p,0) = -p^2\frac{S_d}{\varepsilon}. \tag{6.38}$$

This divergence should be canceled by the counter-term δ_ϕ,

$$-\frac{1}{2}p^2\delta_\phi - p^2 N_f g^2\frac{S_d}{\varepsilon} = 0 \implies \delta_\phi = -2N_f g^2\frac{S_d}{\varepsilon}. \tag{6.39}$$

The self-energy loop in Fig. 6.5c is given by

$$m^\varepsilon g^2(\phi\bar{\psi}\psi)(\phi\bar{\psi}\psi) = g^2 M_\psi(p^2)\bar{\psi}\psi, \tag{6.40}$$

where

$$M_\psi(p^2) = m^\varepsilon\int \frac{\mathrm{d}^{4-\varepsilon}k}{(2\pi)^{4-\varepsilon}}\frac{\mathrm{i}\not{k}}{k^2}\frac{1}{(k-p)^2+m^2} = m^\varepsilon\mathrm{i}\gamma_\mu I_3^\mu(4-\varepsilon,p,m) = \mathrm{i}\not{p}\frac{S_4}{2\varepsilon}. \tag{6.41}$$

This divergence should be canceled by the counter term δ_ψ, i.e.,

$$i\delta_\psi\not{p} + \mathrm{i}\not{p}g^2\frac{S_d}{2\varepsilon} = 0 \implies \delta_\psi = -\frac{g^2}{2}\frac{S_d}{\varepsilon}. \tag{6.42}$$

Renormalization of interaction vertices

The one-loop Feynman diagrams that renormalize the interaction vertices are shown in Fig. 6.6. Since the interactions do not contain derivatives, we can set external

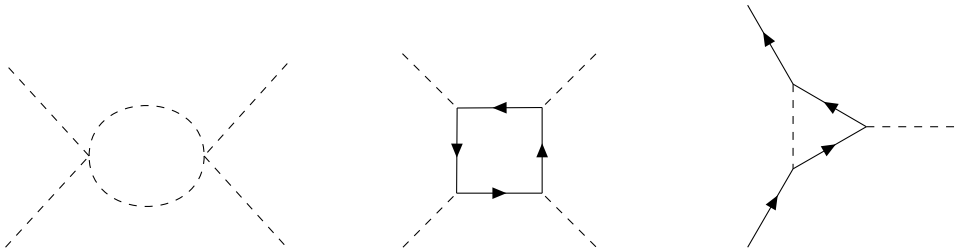

(a) Boson loop V_b (b) Fermion loop V_f (c) Triangle diagram $V_\triangle$

FIGURE 6.6: One-loop diagrams that contribute to the renormalization of interaction vertices.

momenta to zero in all the following calculations. In order to determine δ_λ, we need to calculate the divergent part of the boson loop in Fig. 6.6a and the divergent part of the fermion loop in Fig. 6.6b. The boson loop integral is given by

$$\frac{1}{16}m^{2\varepsilon}(-\lambda)^2(\phi\phi\overbrace{\phi\phi)(\phi\phi}\phi\phi) = \lambda^2 V_b\phi^4, \tag{6.43}$$

where

$$V_b = \frac{m^{2\varepsilon}}{16}\int\frac{\mathrm{d}^{4-\varepsilon}k}{(2\pi)^{4-\varepsilon}}\frac{1}{(k^2+m^2)^2} = \frac{m^{2\varepsilon}}{16}I_2(4-\varepsilon,m^2) = \frac{m^\varepsilon}{16}\frac{S_d}{\varepsilon}. \tag{6.44}$$

The fermion loop integral is

$$\frac{1}{4}m^{2\varepsilon}(-g)^4(\phi\bar\psi\overbrace{\psi)(\phi\bar\psi}\psi)(\phi\bar\psi\overbrace{\psi)(\phi\bar\psi}\psi) = N_f g^4 V_f\phi^4, \tag{6.45}$$

where

$$V_f = -\frac{m^{2\varepsilon}}{4}\int\frac{\mathrm{d}^{4-\varepsilon}k}{(2\pi)^{4-\varepsilon}}\frac{\mathrm{tr}(i\not{k})^4}{(k^2)^4} = -\frac{m^{2\varepsilon}}{4}\int\frac{\mathrm{d}^{4-\varepsilon}k}{(2\pi)^{4-\varepsilon}}\frac{4}{(k^2)^2} = -m^{2\varepsilon}I_2(4-\varepsilon,0) = -m^\varepsilon\frac{S_d}{\varepsilon}. \tag{6.46}$$

Therefore

$$-\frac{1}{4!}m^\varepsilon\delta_\lambda + S_d\frac{m^\varepsilon\lambda^2}{16\varepsilon} - S_d\frac{m^\varepsilon N_f g^4}{\varepsilon} = 0 \implies \delta_\lambda = \Big(\frac{3\lambda^2}{2} - 24N_f g^4\Big)\frac{S_d}{\varepsilon}. \tag{6.47}$$

Similarly, δ_g is determined by the divergent part of the triangle diagram in Fig. 6.6c,

$$m^{3\varepsilon/2}(-g)^3(\phi\bar\psi\overbrace{\psi)(\phi\bar\psi}\psi)(\phi\bar\psi\psi) = g^3 V_\triangle\phi\bar\psi\psi, \tag{6.48}$$

where

$$V_{\triangle} = -m^{3\varepsilon/2}\int \frac{\mathrm{d}^{4-\varepsilon}k}{(2\pi)^{4-\varepsilon}}\frac{(i\not{k})^2}{(k^2)^2}\frac{1}{k^2} = m^{3\varepsilon/2}\int \frac{\mathrm{d}^{4-\varepsilon}k}{(2\pi)^{4-\varepsilon}}\frac{1}{(k^2)^2} = m^{3\varepsilon/2}I_2(4-\varepsilon,0) = m^{\varepsilon/2}\frac{S_d}{\varepsilon}. \tag{6.49}$$

Therefore

$$-m^{\varepsilon/2}\delta_g + g^3 m^{\varepsilon/2}\frac{S_d}{\varepsilon} = 0 \implies \delta_g = g^3\frac{S_d}{\varepsilon}. \tag{6.50}$$

β functions and RG flows

We are now ready to compute the β functions for the two marginal couplings λ and g, defined as

$$\beta_\lambda = m\frac{\partial\lambda}{\partial m}, \qquad \beta_{g^2} = m\frac{\partial g^2}{\partial m}, \tag{6.51}$$

each of which will be a function of g^2, λ, ε and N_f in general. We compute them using the relations between the bare couplings and the renormalized couplings at the one-loop order we derived above, which are given by

$$\begin{aligned} m^{-\varepsilon}\lambda_0 = Z_\phi^{-2}(\lambda+\delta_\lambda) &= \Big(1+4N_f g^2\frac{S_d}{\varepsilon}\Big)\Big(\lambda+\Big(\frac{3\lambda^2}{2}-24N_f g^4\Big)\frac{S_d}{\varepsilon}\Big) \\ &= \lambda+\Big(\frac{3\lambda^2}{2}-24N_f g^4+4N_f g^2\lambda\Big)\frac{S_d}{\varepsilon}, \end{aligned} \tag{6.52}$$

$$\begin{aligned} m^{-\varepsilon}g_0^2 = Z_\psi^{-2}Z_\phi^{-1}(g^2+2g\delta_g) &= \Big(1+g^2\frac{S_d}{\varepsilon}\Big)\Big(1+2N_f g^2\frac{S_d}{\varepsilon}\Big)\Big(g^2+2g^4\frac{S_d}{\varepsilon}\Big) \\ &= g^2+(2N_f+3)g^4\frac{S_d}{\varepsilon}. \end{aligned} \tag{6.53}$$

The bare couplings can be viewed as functions of m, λ and g^2, i.e., $\lambda_0(m,\lambda,g^2)$ and $g_0^2(m,\lambda,g^2)$. Now we use the fact that the bare couplings are scale-invariant, i.e., they cannot depend on m,

$$m\frac{\mathrm{d}}{\mathrm{d}m}\lambda_0 = m\frac{\partial}{\partial m}\lambda_0+\beta_\lambda\frac{\partial}{\partial\lambda}\lambda_0+\beta_{g^2}\frac{\partial}{\partial g^2}\lambda_0 = 0, \tag{6.54}$$

$$m\frac{\mathrm{d}}{\mathrm{d}m}g_0^2 = m\frac{\partial}{\partial m}g_0^2+\beta_\lambda\frac{\partial}{\partial\lambda}g_0^2+\beta_{g^2}\frac{\partial}{\partial g^2}g_0^2 = 0 \tag{6.55}$$

Then inserting Eqs. (6.52) and (6.53) into these equations one can derive the β functions. In general, bare couplings λ_{i0}, $i = 1, \cdots, n$ satisfy the equation

$$m^{-\varepsilon}\lambda_{i0} = \lambda_i + f_i(\lambda_1, \cdots, \lambda_n)/\varepsilon \tag{6.56}$$

up to one loop. Then we can take the derivative with respect to m on both sides to obtain the following n linear equations for the β functions,

$$0 = m^{1-\varepsilon}\frac{\mathrm{d}}{\mathrm{d}m}\lambda_{i0} = \varepsilon\lambda_i + f_i + \sum_j \Big(\delta_{ij} + \frac{1}{\varepsilon}\frac{\partial f_i}{\partial \lambda_j}\Big)\beta_{\lambda_j}. \tag{6.57}$$

Since up to one loop terms of order $O(\frac{1}{\varepsilon^2})$ will be dropped, we can compute the inverse of the matrix $(\delta_{ij} + \frac{1}{\varepsilon}\frac{\partial f_i}{\partial \lambda_j})$ as simply $(\delta_{ij} - \frac{1}{\varepsilon}\frac{\partial f_i}{\partial \lambda_j})$, and the β functions can be solved as

$$\beta_{\lambda_i} = -\sum_j \Big(\delta_{ij} - \frac{1}{\varepsilon}\frac{\partial f_i}{\partial \lambda_j}\Big)(\varepsilon\lambda_j + f_j) = -\varepsilon\lambda_i - f_i + \sum_j \lambda_j \frac{\partial f_i}{\partial \lambda_j}. \tag{6.58}$$

At one loop, $f_i(\lambda_1, \cdots, \lambda_n)$ is usually a homogeneous function of degree 2, in which case we simply have

$$\beta_{\lambda_i} = -\varepsilon\lambda_i + f_i. \tag{6.59}$$

We can use this general strategy to obtain

$$\beta_{g^2} = -\varepsilon g^2 + S_d(2N_f + 3)g^4, \tag{6.60}$$

$$\beta_\lambda = -\varepsilon\lambda + S_d\Big(\frac{3\lambda^2}{2} - 24N_f g^4 + 4N_f g^2\lambda\Big). \tag{6.61}$$

These β functions help us understand the RG flow of the marginal couplings, which is shown in Fig. 6.7. The zeros of the β functions give us information about the fixed points of these flows. For example, in Fig. 6.7, the red one is the Gross-Neveu fixed point, while the green one at $\lambda > 0$ is the Wilson-Fisher fixed point. The presence of a stable fixed point suggests the existence of a quantum critical point in the lattice theory that can be reached by fine-tuning the single relevant parameter of the field theory, namely the boson mass, to zero.

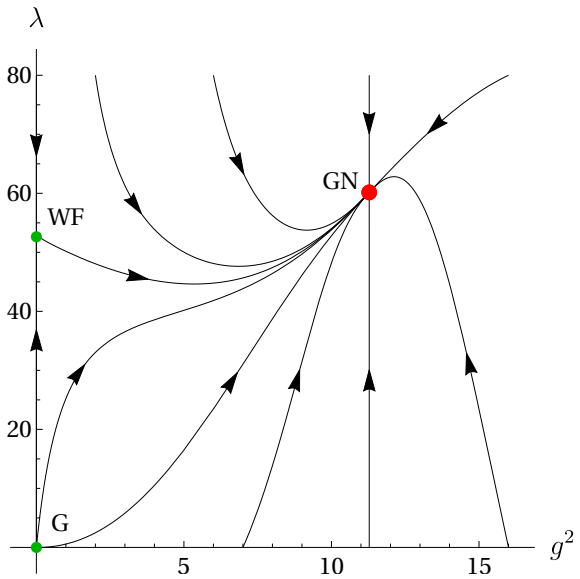

FIGURE 6.7: The flow diagram of g^2 and λ in the Ising GNY model.

At one loop, β_g^2 is independent of λ, and we can solve $\beta_{g^2} = 0$ first. There is a trivial solution at $g^2 = 0$, which is an unstable Gaussian fixed point, and a non-trivial stable fixed point at

$$g^2 = \frac{\varepsilon}{S_d(2N_f + 3)}. \tag{6.62}$$

Inserting this non-trivial solution of g^2 into β_λ, we obtain $\beta_\lambda = \frac{\varepsilon^2}{S_d} f_\lambda(\frac{S_d}{\varepsilon}\lambda, N_f)$, where

$$\begin{aligned} f_\lambda(x, N_f) &= -x + \frac{3x^2}{2} - \frac{24N_f}{(2N_f+3)^2} + \frac{4N_f}{2N_f+3}x \\ &= \frac{3x^2}{2} + \frac{4N_f - \frac{9}{N_f}}{4N_f + \frac{9}{N_f} + 12}x - \frac{24}{4N_f + \frac{9}{N_f} + 12}. \end{aligned} \tag{6.63}$$

Notice that in this form, it is clear that $f_\lambda(x, N_f)$ has a very interesting symmetry at one-loop order, i.e.,

$$f_\lambda(-x, \frac{9}{4N_f}) = f_\lambda(x, N_f). \tag{6.64}$$

This symmetry implies that there is an interesting duality between small N_f and large N_f at the stable fixed point of g^2: if one knows the flow diagram of λ at N_f,

then the flow diagram at $\frac{9}{4N_f}$ is almost identical, except that the fixed point at λ goes to $-\lambda$, and the direction of the flow is reversed. For example, in the limit $N_f \to 0$, the fermions decouple from the bosons, and the Gaussian fixed point $\lambda = 0$ is an unstable fixed point; this implies that in the limit $N_f \to \infty$, the Gaussian fixed point $\lambda = 0$ remains a fixed point, but becomes stable.

Solving $\beta_\lambda = 0$, we obtain two fixed points, and the stable one is given by

$$\lambda = \frac{\varepsilon}{3S_d}\left(1 - \frac{4N_f - 2\sqrt{(N_f + 33/2)^2 - 270}}{2N_f + 3}\right) \xrightarrow{N_f \to \infty} \frac{12\varepsilon}{S_d(2N_f + 3)}, \tag{6.65}$$

which indeed agrees with our observation that $\lambda = 0$ is a stable fixed point in the limit $N_f \to \infty$. Notice that this fixed point exists for all values of N_f and is referred to as the Ising GNY fixed point [64]. Several lattice studies have been done to explore this fixed point [93, 94, 95, 96, 43, 44].

Anomalous dimensions and critical exponents

At the non-trivial fixed point, the scaling dimensions of the fields ϕ and ψ can be different from their canonical dimensions of the free theory, and the corrections to the canonical dimensions are usually referred to as anomalous dimensions. The anomalous dimensions of the fields can be computed through the relations

$$\eta_\phi = m\frac{\mathrm{d}}{\mathrm{d}m}\ln Z_\phi = \beta_{g^2}\frac{1}{Z_\phi}\frac{\mathrm{d}}{\mathrm{d}g^2}(1 - 2N_f g^2\frac{S_d}{\varepsilon}) = 2S_d N_f g^2, \tag{6.66}$$

$$\eta_\psi = m\frac{\mathrm{d}}{\mathrm{d}m}\ln Z_\psi = S_d\frac{g^2}{2}. \tag{6.67}$$

Similarly, the bare mass m_0^2 can also have a different scaling dimension, which can be computed through the relation

$$\eta_m = \frac{m^2}{m_0^2}m\frac{\mathrm{d}}{\mathrm{d}m}\frac{m_0^2}{m^2} = \frac{m^2}{m_0^2}\beta_\lambda\frac{\partial}{\partial\lambda}\frac{m_0^2}{m^2} + \beta_{g^2}\frac{\partial}{\partial g^2}\frac{m_0^2}{m^2}. \tag{6.68}$$

Using the relation

$$m_0^2 = Z_\phi^{-1}(m^2 + \delta_m) = m^2\Big(1 + 2N_f g^2\frac{S_d}{\varepsilon} + \frac{\lambda}{2}\frac{S_d}{\varepsilon}\Big), \tag{6.69}$$

we can calculate

$$\eta_m = -S_d\Big(2N_f g^2 + \frac{\lambda}{2}\Big). \tag{6.70}$$

η_m is related to the correlation length critical exponent through the relation

$$\nu^{-1} = \eta_m + 2 = 2 - S_d\Big(2N_f g^2 + \frac{\lambda}{2}\Big). \tag{6.71}$$

The critical exponents η_ϕ, η_ψ, and ν^{-1} can be used to characterize a quantum critical point. In particular, at the stable Ising GNY fixed point, we insert the critical values of g^2 and λ given in Eqs. (6.62) and (6.65), and we have

$$\eta_\phi = \frac{2N_f\varepsilon}{2N_f+3}, \quad \eta_\psi = \frac{\varepsilon}{2(2N_f+3)}, \quad \nu^{-1} = 2 - \varepsilon - \frac{3\varepsilon}{2N_f+3}, \tag{6.72}$$

where we have taken the large N_f limit for ν^{-1}.

6.2.2 The SO(4) *GNY model*

We now extend the analysis of the Ising GNY model to the SO(4)-GNY model whose bare Lagrangian is given by

$$\begin{aligned}\mathcal{L} &= \bar{\psi}_0^\alpha \gamma^\mu \partial_\mu \psi_0^\alpha + g_{s0}\vec{\phi}_{0s}\cdot 2\vec{M}_{0s} + g_{c0}\vec{\phi}_{0c}\cdot 2\vec{M}_{0c} \\ &+ \sum_{a=s,c}\left(\frac{1}{2}\partial_\mu\vec{\phi}_{0a}\cdot\partial^\mu\vec{\phi}_{0a} + \frac{1}{2}m_{a0}^2\vec{\phi}_{0a}\cdot\vec{\phi}_{0a} + \frac{1}{4!}\lambda_{a0}(\vec{\phi}_{0a}\cdot\vec{\phi}_{0a})^2\right) + \frac{1}{12}\lambda_{sc0}(\vec{\phi}_{0s}\cdot\vec{\phi}_{0s})(\vec{\phi}_{0c}\cdot\vec{\phi}_{0c}).\end{aligned} \tag{6.73}$$

Here $\vec{M}_{0s}$ and $\vec{M}_{0c}$ are the adjoint spin and charge mass terms introduced in Eq. (6.2) but written in terms of the bare fields. There are seven independent parameters: two boson mass terms m_{c0}, m_{s0} which are relevant, and five marginal couplings including two GNY couplings g_{c0}, g_{s0} and three boson quartic self couplings $\lambda_{s0}, \lambda_{c0}$ and λ_{sc0}. In general, the theory has an SO(4) symmetry, but if we set $g_{c0} = g_{s0}$, $m_{c0} = m_{s0}$, and $\lambda_{s0} = \lambda_{c0}$, we have an additional spin-charge flip symmetry making the theory invariant under O(4) transformations. Thus if we require the theory to be O(4) invariant, there is only one relevant parameter and three marginal couplings.

Similar to the Ising GNY model, we begin with the renormalized Lagrangian in $4-\varepsilon$ dimension given by

$$\begin{aligned}
\mathcal{L} &= Z_\psi \bar{\psi}^\alpha \gamma^\mu \partial_\mu \psi^\alpha + g_{s0} Z_s^{1/2} Z_\psi \vec{\phi}_s \cdot 2\vec{M}_s + g_{c0} Z_c^{1/2} Z_\psi \vec{\phi}_c \cdot 2\vec{M}_c \\
&+ \sum_{a=s,c} \left(\frac{1}{2} Z_a \partial_\mu \vec{\phi}_a \cdot \partial^\mu \vec{\phi}_a + \frac{1}{2} Z_a m_{a0}^2 \vec{\phi}_a \cdot \vec{\phi}_a + \frac{1}{4!} Z_a^2 \lambda_{a0} (\vec{\phi}_a \cdot \vec{\phi}_a)^2 \right) + \frac{1}{12} Z_s Z_c \lambda_{sc0} (\vec{\phi}_s \cdot \vec{\phi}_s)(\vec{\phi}_c \cdot \vec{\phi}_c) \\
&= \bar{\psi}^\alpha \gamma^\mu \partial_\mu \psi^\alpha + m^{\varepsilon/2} g_s \vec{\phi}_s \cdot 2\vec{M}_s + m^{\varepsilon/2} g_c \vec{\phi}_c \cdot 2\vec{M}_c \qquad (6.74) \\
&+ \sum_{a=s,c} \left(\frac{1}{2} \partial_\mu \vec{\phi}_a \cdot \partial^\mu \vec{\phi}_a + \frac{1}{2} m_a^2 \vec{\phi}_a \cdot \vec{\phi}_a + \frac{1}{4!} m^\varepsilon \lambda_a (\vec{\phi}_a \cdot \vec{\phi}_a)^2 \right) + \frac{1}{12} m^\varepsilon \lambda_{sc} (\vec{\phi}_s \cdot \vec{\phi}_s)(\vec{\phi}_c \cdot \vec{\phi}_c) \\
&+ \delta_\psi \bar{\psi}^\alpha \gamma^\mu \partial_\mu \psi^\alpha + m^{\varepsilon/2} \delta_{g_s} \vec{\phi}_s \cdot 2\vec{M}_s + m^{\varepsilon/2} \delta_{g_c} \vec{\phi}_c \cdot 2\vec{M}_c \\
&+ \sum_{a=s,c} \left(\frac{1}{2} \delta_a \partial_\mu \vec{\phi}_a \cdot \partial^\mu \vec{\phi}_a + \frac{1}{2} \delta_{m_a} \vec{\phi}_a \cdot \vec{\phi}_a + \frac{1}{4!} m^\varepsilon \delta_a (\vec{\phi}_a \cdot \vec{\phi}_a)^2 \right) + \frac{1}{12} m^\varepsilon \delta_{sc} (\vec{\phi}_s \cdot \vec{\phi}_s)(\vec{\phi}_c \cdot \vec{\phi}_c),
\end{aligned}$$

where

$$Z_\psi = 1 + \delta_\psi, \quad Z_a = 1 + \delta_a, \quad Z_a m_{a0}^2 = m_a^2 + \delta_{m_a}, \qquad (6.75)$$

$$g_{a0} Z_a^{1/2} Z_\psi = m^{\varepsilon/2} (g_a + \delta_{g_a}),\ Z_a^2 \lambda_{a0} = m^\varepsilon (\lambda_a + \delta_a),\ Z_s Z_c \lambda_{sc0} = m^\varepsilon (\lambda_{sc} + \delta_{sc}),$$

and ϕ_s^i, $i = 1, \cdots, N_s$, ϕ_c^i, $i = 1, \cdots, N_c$, and $\alpha = 1, \cdots, N_f$. Although in the SO(4) GNY model we have $N_s = N_c = 3$ and $N_f = 2$, in the following we will not fix them in order to keep track of their contributions.

Although the SO(4) GNY Lagrangian looks more complicated than the Ising GNY Lagrangian, the relevant Feynman diagrams are almost identical to those shown in Figs. 6.5 and 6.6, with some minor differences. For example, in Fig. 6.5a, when the external lines are ϕ_s, the loop can be either ϕ_s or ϕ_c. Furthermore, due to the charge interactions containing $\psi\psi$ and $\bar{\psi}\bar{\psi}$ terms, the fermion number is not conserved, and the possibility of flipping the directions of the fermion propagators needs to be considered separately.

Mass and wave function renormalization

In this case, the boson loops that contribute to the renormalization of $(\phi_s^i)^2$ are of three types

$$\frac{1}{6}m^{\varepsilon}(-\lambda_s)\phi_s^i\phi_s^i\overbrace{\phi_s^j\phi_s^j}\phi_s^j = \frac{2}{3}\lambda_s M_{\phi b}\phi_s^i\phi_s^i, \tag{6.76}$$

$$\frac{1}{12}m^{\varepsilon}(-\lambda_s)\phi_s^i\phi_s^i\phi_s^i\overbrace{\phi_s^j\phi_s^j} = \frac{1}{3}\lambda_s N_s M_{\phi b}\phi_s^i\phi_s^i, \tag{6.77}$$

$$\frac{1}{12}m^{\varepsilon}(-\lambda_{sc})\phi_s^i\phi_s^i\phi_s^i\overbrace{\phi_c^j\phi_c^j} = \frac{1}{3}\lambda_{sc} N_c M_{\phi b}\phi_s^i\phi_s^i. \tag{6.78}$$

Therefore

$$\delta_{m_{s,c}} = \frac{m_{s,c}^2}{6}\big((N_{s,c}+2)\lambda_{s,c} + N_{c,s}\lambda_{sc}\big)\frac{S_d}{\varepsilon}. \tag{6.79}$$

In order to determine δ_s, it is sufficient to look at the component ϕ_s^3, which couples to the fermions in the same way as the Ising GNY model, and therefore

$$\delta_{s,c} = -2N_f g_{s,c}^2\frac{S_d}{\varepsilon}. \tag{6.80}$$

δ_ψ is enhanced by the number of bosons,

$$\delta_\psi = -\frac{N_s g_s^2 + N_c g_c^2}{2}\frac{S_d}{\varepsilon}. \tag{6.81}$$

Renormalization of interaction vertices

In order to determine δ_s, δ_c and δ_{sc}, we need to calculate the divergent part of the boson loop (Fig. 6.6a) and the divergent part of the fermion loop (Fig. 6.6b). The Feynman rules for the spin vertex, charge vertex and spin-charge vertex are

$$-\frac{\lambda_s}{3}(\delta_{ij}^s\delta_{kl}^s + \delta_{ik}^s\delta_{jl}^s + \delta_{il}^s\delta_{jk}^s), \tag{6.82}$$

$$-\frac{\lambda_c}{3}(\delta_{ij}^c\delta_{kl}^c + \delta_{ik}^c\delta_{jl}^c + \delta_{il}^c\delta_{jk}^c), \tag{6.83}$$

$$-\frac{\lambda_{sc}}{3}(\delta_{ij}^s\delta_{kl}^c + \delta_{ik}^s\delta_{jl}^c + \delta_{il}^s\delta_{jk}^c) + s \leftrightarrow c. \tag{6.84}$$

The spin loop which renormalizes the spin vertex contains the following contribution from two spin vertices,

$$\frac{\lambda_s^2}{9}(\delta_{ij}^s\delta_{kl}^s+\delta_{ik}^s\delta_{jl}^s+\delta_{il}^s\delta_{jk}^s)(\delta_{kl}^s\delta_{mn}^s+\delta_{km}^s\delta_{ln}^s+\delta_{kn}^s\delta_{lm}^s)$$

$$=\frac{\lambda_s^2}{9}((N_s+4)\delta_{ij}^s\delta_{mn}^s+2\delta_{im}^s\delta_{jn}^s+2\delta_{in}^s\delta_{jm}^s), \tag{6.85}$$

Summing over all the three channels we have

$$\frac{\lambda_s^2}{9}(N_s+8)(\delta_{ij}^s\delta_{mn}^s+\delta_{im}^s\delta_{jn}^s+\delta_{in}^s\delta_{jm}^s), \tag{6.86}$$

which gives a factor of $\frac{N_s+8}{9}$ compared with the Ising GNY model.

The charge loop which renormalizes the spin vertex contains the following contribution from two spin-charge vertices,

$$\frac{\lambda_{sc}^2}{9}(\delta_{ij}^s\delta_{kl}^c+\delta_{ik}^s\delta_{jl}^c+\delta_{il}^s\delta_{jk}^c)(\delta_{kl}^c\delta_{mn}^s+\delta_{km}^c\delta_{ln}^s+\delta_{kn}^c\delta_{lm}^s)=\frac{\lambda_{sc}^2}{9}N_c\delta_{ij}^s\delta_{mn}^s \tag{6.87}$$

Summing over all the three channels we have

$$\frac{\lambda_{sc}^2}{9}N_c(\delta_{ij}^s\delta_{mn}^s+\delta_{im}^s\delta_{jn}^s+\delta_{in}^s\delta_{jm}^s), \tag{6.88}$$

Therefore the boson loop contribution to δ_s is

$$\delta_{sb}=\Big(\frac{N_s+8}{9}\lambda_s^2+\frac{N_c}{9}\lambda_{sc}^2\Big)\frac{3}{2}\frac{S_d}{\varepsilon}. \tag{6.89}$$

Using the spin-charge flip symmetry, we have

$$\delta_{cb}=\Big(\frac{N_c+8}{9}\lambda_c^2+\frac{N_s}{9}\lambda_{sc}^2\Big)\frac{3}{2}\frac{S_d}{\varepsilon}. \tag{6.90}$$

The spin loop which renormalizes the spin-charge vertex contains the product of a spin vertex and a charge vertex,

$$\frac{\lambda_s\lambda_{sc}}{9}(\delta_{ij}^s\delta_{kl}^s+\delta_{ik}^s\delta_{jl}^s+\delta_{il}^s\delta_{jk}^s)(\delta_{kl}^s\delta_{mn}^c+\delta_{km}^s\delta_{ln}^c+\delta_{kn}^s\delta_{lm}^c)=\frac{\lambda_s\lambda_{sc}}{9}(N_s+2)\delta_{ij}^s\delta_{mn}^c. \tag{6.91}$$

Summing over all the three channels we have

$$\frac{\lambda_s\lambda_{sc}}{9}(N_s+2)(\delta^s_{ij}\delta^c_{mn}+\delta^s_{im}\delta^c_{jn}+\delta^s_{in}\delta^c_{jm}+s\leftrightarrow c). \tag{6.92}$$

and similarly for the charge loop. Finally, the spin-charge loop for the spin-charge vertex is

$$\begin{aligned}&\frac{\lambda^2_{sc}}{9}(\delta^s_{ij}\delta^c_{kl}+\delta^s_{ik}\delta^c_{jl}+\delta^s_{il}\delta^c_{jk}+s\leftrightarrow c)(\delta^s_{kl}\delta^c_{mn}+\delta^s_{km}\delta^c_{ln}+\delta^s_{kn}\delta^c_{lm}+s\leftrightarrow c)\\ &=\frac{\lambda^2_{sc}}{9}(2\delta^s_{im}\delta^c_{jn}+2\delta^s_{in}\delta^c_{jm}+s\leftrightarrow c).\end{aligned} \tag{6.93}$$

Summing over all the three channels, we have

$$\frac{4\lambda^2_{sc}}{9}(\delta^s_{ij}\delta^c_{mn}+\delta^s_{im}\delta^c_{jn}+\delta^s_{in}\delta^c_{jm}+s\leftrightarrow c). \tag{6.94}$$

Therefore the boson loop contribution to δ_{sc} is

$$\delta_{scb}=\Big(\frac{N_s+2}{9}\lambda_s\lambda_{sc}+\frac{N_c+2}{9}\lambda_c\lambda_{sc}+\frac{4}{9}\lambda^2_{sc}\Big)\frac{3}{2}\frac{S_d}{\varepsilon}. \tag{6.95}$$

The fermion loops for the spin and charge vertices are the same as the Gross-Neveu-Yukawa model, but the fermion loop for the spin-charge vertex is enhanced by a factor of $\frac{4!}{2!2!\times 2}=3$. Putting the boson loops and fermion loops together, we have

$$\delta_s=\big((N_s+8)\lambda^2_s+N_c\lambda^2_{sc}\big)\frac{S_d}{6\varepsilon}-24N_f g_s^4\frac{S_d}{\varepsilon}, \tag{6.96}$$

$$\delta_c=\big((N_c+8)\lambda^2_c+N_s\lambda^2_{sc}\big)\frac{S_d}{6\varepsilon}-24N_f g_c^4\frac{S_d}{\varepsilon}, \tag{6.97}$$

$$\delta_{sc}=\big((N_s+2)\lambda_s\lambda_{sc}+(N_c+2)\lambda_c\lambda_{sc}+4\lambda^2_{sc}\big)\frac{S_d}{6\varepsilon}-72N_f g_s^2 g_c^2\frac{S_d}{\varepsilon}. \tag{6.98}$$

Similarly, we can determine δ_{g_s} and δ_{g_c} using the divergent parts of the triangle diagrams (Fig. 6.6c). For example, when we calculate the renormalization of the $\phi^3_s\bar{\psi}^1\psi^1$ vertex, all the six bosons can be the internal boson lines. It can be easily

seen that when the internal boson is ϕ_s^3, the result is the same as the 1-flavor case, and when the internal boson is $\phi_s^{1,2}$, the result has a minus sign,

$$m^{3\varepsilon/2}(-g_s)^2(\overbrace{\phi_s^1\bar{\psi}^1\psi^2}\overbrace{(-\phi_s^3\bar{\psi}^2\psi^2)}\overbrace{(\phi_s^1\bar{\psi}^2}\psi^1) = -g_s^3 V_f\phi^4. \tag{6.99}$$

On the other hand, the contributions from the charge bosons ϕ_c^i are all the same as ϕ_s^3 by the $\mathrm{SU}(2)_c$ symmetry. Therefore we have

$$\delta_{g_s} = (-g_s^3 + 3g_s g_c^2)\frac{S_d}{\varepsilon}, \tag{6.100}$$

$$\delta_{g_c} = (-g_c^3 + 3g_c g_s^2)\frac{S_d}{\varepsilon}. \tag{6.101}$$

β functions and RG flows

In order to determine the β functions, we focus on the five bare couplings, which are related to the renormalized couplings by

$$m^{-\varepsilon}\lambda_{s0} = \lambda_s + \frac{S_d}{\varepsilon}\Big(\frac{1}{6}\big((N_s+8)\lambda_s^2 + N_c\lambda_{sc}^2\big) - 24N_f g_s^4 + 4N_f g_s^2\lambda_s\Big), \tag{6.102}$$

$$\begin{aligned} m^{-\varepsilon}\lambda_{sc0} = \lambda_{sc} + \frac{S_d}{\varepsilon}\Big(\frac{1}{6}\big((N_s+2)\lambda_s\lambda_{sc} + (N_c+2)\lambda_c\lambda_{sc} + 4\lambda_{sc}^2\big) \\ - 72N_f g_s^2 g_c^2 + 4N_f(g_s^2+g_c^2)\lambda_{sc}\Big), \end{aligned} \tag{6.103}$$

$$m^{-\varepsilon}g_{s0}^2 = g_s^2 + \frac{S_d}{\varepsilon}\big((N_s+2N_f-2)g_s^4 + (N_c+6)g_s^2 g_c^2\big) \tag{6.104}$$

The couplings λ_{c0} and g_{c0}^2 can be obtained from λ_{s0} and g_{s0}^2 by replacing s with c. Since the one-loop corrections are all quadratic in the couplings λ and g^2, using Eqs. (6.56) and (6.59) we obtain

$$\beta_{g_s^2} = -\varepsilon g_s^2 + S_d\big((2N_f+1)g_s^4 + 9g_s^2 g_c^2\big), \tag{6.105}$$

$$\beta_{\lambda_s} = -\varepsilon\lambda_s + S_d\Big(\frac{1}{6}\big(11\lambda_s^2 + 3\lambda_{sc}^2\big) - 24N_f g_s^4 + 4N_f g_s^2\lambda_s\Big), \tag{6.106}$$

$$\beta_{\lambda_{sc}} = -\varepsilon\lambda_{sc} + S_d\Big(\frac{1}{6}\big(5(\lambda_s+\lambda_c)\lambda_{sc} + 4\lambda_{sc}^2\big) - 72N_f g_s^2 g_c^2 + 2N_f(g_s^2+g_c^2)\lambda_{sc}\Big), \tag{6.107}$$

where we have inserted $N_s = N_c = 3$. $\beta_{g_c^2}$ and β_{λ_c} can be obtained by replacing s with c in the above equations.

At one loop, we see that $\beta_{g_s^2}$ and $\beta_{g_s^2}$ do not depend on λ_s, λ_c and λ_{sc}, and therefore we can plot the RG flow diagram in the (g_s^2, g_c^2) plane, which is shown in Fig. 6.8.

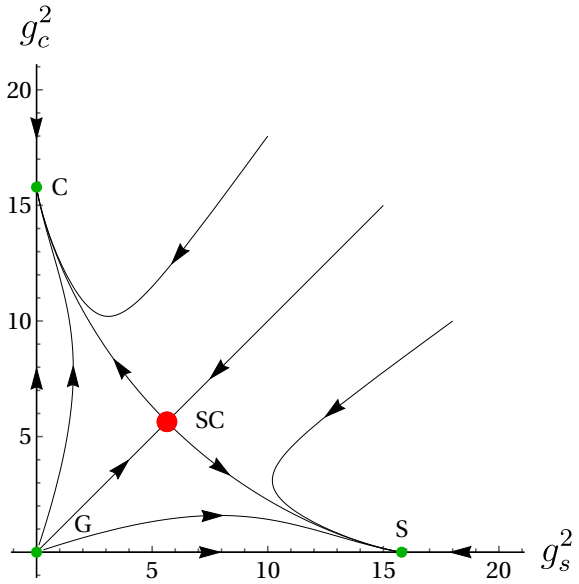

FIGURE 6.8: The flow diagram of g_s^2 and g_c^2 in the SO(4) GNY model.

The zeros of the beta function give fixed points of the RG flow. We see that in the (g_s^2, g_c^2) plane, there are four fixed points: $(0,0)$ is the unstable Gaussian fixed point, $(\frac{\varepsilon}{2S_d(N_f+5)}, \frac{\varepsilon}{2S_d(N_f+5)})$ is a spin-charge symmetric fixed point which is stable only on the symmetry axis. The other two fixed points, $(0, \frac{\varepsilon}{S_d(2N_f+1)})$ and $(\frac{\varepsilon}{S_d(2N_f+1)}, 0)$ are also stable fixed points, but arise only when the spin-charge symmetry is broken.

As far as we know, the previous work has ignored the spin-charge symmetric fixed point at

$$g_s^2 = g_c^2 = \frac{\varepsilon}{2S_d(N_f+5)} \tag{6.108}$$

This fixed point is not stable in the g_s^2 - g_c^2 plane, but it can be stable if protected by the spin-charge flip symmetry of the lattice model. Furthermore, there also has

to be a stable fixed point in the bosonic couplings at these critical values of g_s^2 and g_c^2. Substituting Eq. (6.108) into β_{λ_s} and $\beta_{\lambda_{sc}}$, and setting $\lambda_s = \lambda_c$, we obtain $\beta_{\lambda_s} = \frac{\varepsilon^2}{S_d} f_s(\frac{S_d}{\varepsilon}\lambda_s, \frac{S_d}{\varepsilon}\lambda_{sc}, N_f)$ and $\beta_{\lambda_{sc}} = \frac{\varepsilon^2}{S_d} f_{sc}(\frac{S_d}{\varepsilon}\lambda_s, \frac{S_d}{\varepsilon}\lambda_{sc}, N_f)$, where

$$\begin{aligned} f_s(x, y, N_f) &= -x + \frac{1}{6}\big(11x^2 + 3y^2\big) - \frac{6N_f}{(N_f+5)^2} + \frac{2N_f}{N_f+5}x \\ &= \frac{1}{6}\big(11x^2 + 3y^2\big) + \frac{N_f - \frac{25}{N_f}}{N_f + \frac{25}{N_f} + 10}x - \frac{6}{N_f + \frac{25}{N_f} + 10}, \end{aligned} \tag{6.109}$$

$$\begin{aligned} f_{sc}(x, y, N_f) &= -y + \frac{1}{6}\big(10xy + 4y^2\big) - \frac{18N_f}{(N_f+5)^2} + \frac{2N_f}{N_f+5}y \\ &= \frac{1}{6}\big(10xy + 4y^2\big) + \frac{N_f - \frac{25}{N_f}}{N_f + \frac{25}{N_f} + 10}y - \frac{18}{N_f + \frac{25}{N_f} + 10}. \end{aligned} \tag{6.110}$$

Notice that similar to the Ising GNY model, the functions f_s and f_{sc} also have an interesting symmetry

$$f_s(-x, -y, \frac{25}{N_f}) = f_s(x, y, N_f), \tag{6.111}$$

$$f_{sc}(-x, -y, \frac{25}{N_f}) = f_{sc}(x, y, N_f). \tag{6.112}$$

Similarly, this symmetry implies that there is an interesting duality between small N_f and large N_f: if we know the flow diagram at some value of N_f, then the flow diagram at $\frac{25}{N_f}$ is almost identical, except that the fixed points at $(\lambda_s, \lambda_{sc})$ move to $(-\lambda_s, -\lambda_{sc})$, and the direction of the flow is reversed. In the limit $N_f \to 0$, the fermions decouple with the boson, and the Gaussian fixed point $(\lambda_s, \lambda_{sc}) = (0, 0)$ is an unstable fixed point. This implies that in the limit $N_f \to \infty$, the Gaussian fixed point $(0, 0)$ is still a fixed point, but becomes stable. The RG flows of $\lambda_s = \lambda_c$ and λ_{sc} at $N_f = 0$ and $N_f = \infty$ are shown in Fig. 6.9, from which we can clearly see the duality between small N_f and large N_f: the positions of the fixed points are reversed, and the direction of the flow is also reversed.

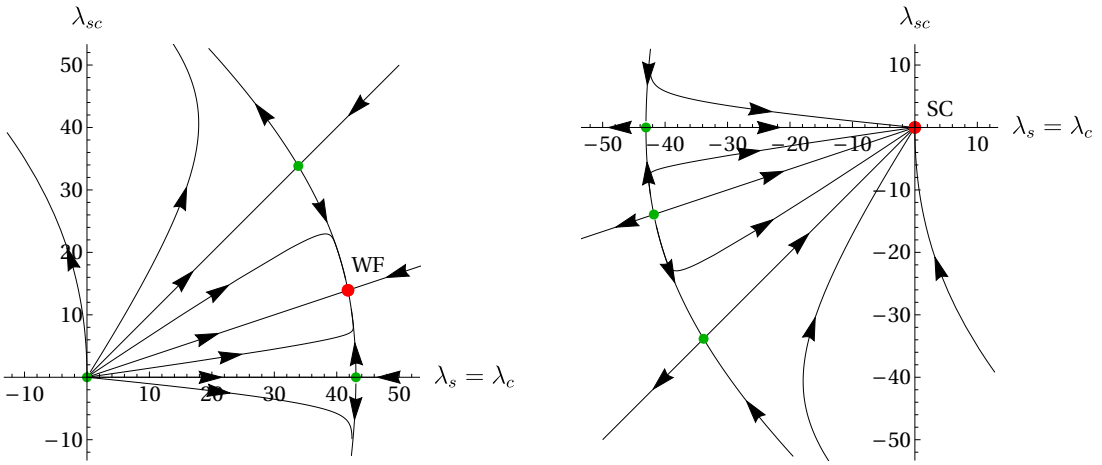

(a) $N_f = 0$ (b) $N_f = \infty$

FIGURE 6.9: RG flow of $\lambda_s = \lambda_c$ and λ_{sc} at the critical value of $g_s^2 = g_c^2 = \frac{\varepsilon}{2S_d(N_f+5)}$. The red dots indicate fixed points.

The number of solutions for the equations $\beta_{\lambda_s} = \beta_{\lambda_{sc}} = 0$ depend on N_f. When $0 \leq N_f \lesssim 0.016$, there is a stable fixed point in $(\lambda_s, \lambda_{sc})$; when $0.016 \lesssim N_f \lesssim 1.48$, there are two fixed points, but none of them are stable; when $1.48 \lesssim N_f \lesssim 16.83$, there are no fixed points; however, when $N_f \gtrsim 16.83$, there is again a stable fixed point, with the following asymptotic form as $N_f \to \infty$,

$$\lambda_s \sim \frac{6\varepsilon}{S_d(N_f+5)}, \quad \lambda_{sc} \sim \frac{18\varepsilon}{S_d(N_f+5)}, \tag{6.113}$$

which agrees with our earlier observation. A careful analysis of how the solutions of $\beta_{\lambda_s} = \beta_{\lambda_{sc}} = 0$ depend on N_f can also be found in [97].

Once we impose the spin-charge flip symmetry, the stable fixed point can be accessed by tuning only one parameter, the mass of the bosons $m_s = m_c$. It also implies that the lattice theory could have a second-order phase transition by tuning the only lattice interaction. Indeed, Monte Carlo results seem to show a continuous transition between the massless phase at small couplings and a massive phase at large couplings. However, it is important to point out that the stable fixed point does not exist for $N_f = 2$, which is the parameter in the lattice model. This is somewhat

disappointing, and we will discuss its implications in the next chapter.

Anomalous dimensions and critical exponents

The anomalous dimensions of the fields can be computed through the relations

$$\eta_{s,c} = m\frac{\mathrm{d}}{\mathrm{d}m}\ln Z_{s,c} = 2S_d N_f g_{s,c}^2 \tag{6.114}$$

$$\eta_\psi = m\frac{\mathrm{d}}{\mathrm{d}m}\ln Z_\psi = \frac{3S_d}{2}(g_s^2 + g_c^2). \tag{6.115}$$

Furthermore, using

$$m_{s0}^2 = Z_s^{-1}(m_s^2 + \delta_{m_s}) = m_s^2\Big(1 + \frac{S_d}{\varepsilon}\big(2N_f g_s^2 + \frac{1}{6}(5\lambda_s + 3\lambda_{sc})\big)\Big), \tag{6.116}$$

we can calculate the anomalous dimension of the mass,

$$\eta_{m_s} = \frac{m_s^2}{m_{s0}^2} m\frac{\mathrm{d}}{\mathrm{d}m}\frac{m_{s0}^2}{m_s^2} = -S_d\big(2N_f g_s^2 + \frac{1}{6}(5\lambda_s + 3\lambda_{sc})\big). \tag{6.117}$$

Therefore we have the correlation length critical exponent

$$\nu_{s,c}^{-1} = \eta_{m_{s,c}} + 2 = 2 - S_d\big(2N_f g_{s,c}^2 + \frac{1}{6}(5\lambda_{s,c} + 3\lambda_{sc})\big). \tag{6.118}$$

At the spin-charge symmetric fixed point, we have

$$\eta_{s,c} = \frac{N_f}{N_f+5}\varepsilon, \quad \eta_\psi = \frac{3}{2(N_f+5)}\varepsilon, \quad \nu^{-1} \sim 2 - \varepsilon - \frac{9}{N_f+5}\varepsilon, \tag{6.119}$$

where we have taken the large N_f limit for ν^{-1}. These critical exponents characterize the spin-charge symmetric quantum critical point.

6.3 Large N_f expansion

When calculating the effective potentials in Section 6.1, we completely ignored the fluctuations of the fermion bilinears, which can be justified in the $N_f \to \infty$ limit, because these fluctuations are suppressed as $1/\sqrt{N_f}$ (if different components are uncorrelated). When N_f is large but finite, it is possible to restore the fluctuations

of the fermion bilinears order by order in $1/N_f$. The strategy is similar to calculating the effective potential: integrating out the fermion degrees of freedom, and this will lead to an effective propagator for the boson. Since all the fermion loops are enhanced by a factor of N_f, the leading contribution in the large N_f limit comes from summing over the geometric series of the "bubble chain" diagrams [98], see Fig. 6.10. This effective propagator is of order $1/N_f$, and therefore loop calculation leads to a systematical expansion in $1/N_f$.

In this section, d denotes the space-time dimension, and we will work with a general $2 < d < 4$ dimension, where the kinetic terms of the boson fields and boson self-interactions are irrelevant. We will also evaluate the results at $d = 2 + \varepsilon$ and $d = 4 - \varepsilon$ to compare with the results from epsilon expansions. In the following, we will first perform the calculation using the Ising Gross-Neveu model, and later extend it to the SO(4) Gross-Neveu model.

6.3.1 The Ising Gross-Neveu model

From Eq. (6.6), we know that the Lagrangian of the Ising Gross-Neveu model in d space-time dimension can be written as

$$\mathcal{L} = \bar{\psi}\gamma^{\mu}\partial_{\mu}\psi + \frac{1}{2}m^{d-2}\phi^2 + g\phi\bar{\psi}\psi, \tag{6.120}$$

where ψ denotes N_f-flavor 4-component fermions. The path integral is then

$$Z = \int D\psi D\bar{\psi} D\phi \ \ \mathrm{e}^{-\int \mathrm{d}^d x \mathcal{L}[\psi,\bar{\psi},\phi]}. \tag{6.121}$$

In order to perform a semi-classical expansion, we require the Lagrangian to be proportional to N_f. Since there are N_f fermions, $\bar{\psi}\psi$ is already of order N_f. On the other hand, ϕ needs to scale as $\sqrt{N}$, $g \sim 1/\sqrt{N}$, and therefore it is convenient to rescale $g\phi \mapsto \phi$. In the large N_f limit, one integrates over the fermions and gets an effective action for ϕ. This would generate a non-local interaction for ϕ, which can

be captured by the effective non-local propagator [98]

$$\frac{1}{2v^2}\phi(-\partial^2)^{\frac{d}{2}-1}\phi. \tag{6.122}$$

In the $v^2 \to \infty$ limit, the original Lagrangian is recovered, and we will calculate the critical exponents in this limit. Setting the Lagrangian to be critical, i.e., $m = 0$, and redefining $\phi \mapsto v\phi$, we have the following alternative description of the renormalized Lagrangian at large N_f,

$$\begin{aligned}\mathcal{L} &= Z_\psi \bar{\psi}\gamma^\mu \partial_\mu \psi + \frac{1}{2}\phi(-\partial^2)^{d/2-1}\phi + Z_\psi v_0 \phi\bar{\psi}\psi \\ &=: \bar{\psi}\gamma^\mu\partial_\mu\psi + \frac{1}{2}\phi(-\partial^2)^{d/2-1}\phi + v\phi\bar{\psi}\psi + \delta_\psi\bar{\psi}\gamma^\mu\partial_\mu\psi + \delta_v\phi\bar{\psi}\psi.\end{aligned} \tag{6.123}$$

where we define

$$Z_\psi = 1 + \delta_\psi, \quad Z_\psi v_0 = v + \delta_v. \tag{6.124}$$

ϕ is not renormalized because we only allow local counter terms. The free propagator in the momentum space can be read as

$$\begin{aligned}\int \mathrm{d}^d x\ \langle \psi^\alpha(x)\bar{\psi}^\beta(0)\rangle\, \mathrm{e}^{\mathrm{i}kx} &= \frac{\delta^{\alpha\beta}}{-i\not{k}} = \frac{i\not{k}\delta^{\alpha\beta}}{k^2}, \\ \int \mathrm{d}^d x\ \langle \phi(x)\phi(0)\rangle\, \mathrm{e}^{\mathrm{i}kx} &= \frac{1}{(k^2)^{d/2-1}}.\end{aligned} \tag{6.125}$$

The effective boson propagator

In the large N_f expansion, all the fermion loops are enhanced by a factor of N_f, and therefore the leading order correction comes from summing over the geometric series of the bubble chain corrections to the ϕ-propagator, as shown in Fig. 6.10.

A single bubble is given by

$$\cdots\overbrace{(\phi\bar{\psi}\overbrace{\psi)v^2(\bar{\psi}\psi}\phi)}\cdots = \cdots\overbrace{\phi}v^2 N_f M_\phi(p^2)\overbrace{\phi}\cdots, \tag{6.126}$$

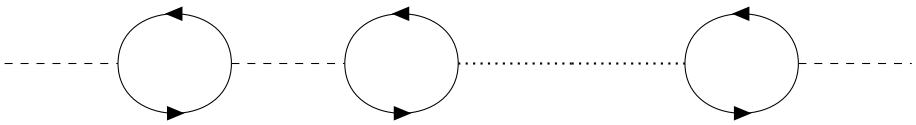

FIGURE 6.10: The bubble chain diagrams,

where

$$M_\phi(p^2) = -\int \frac{\mathrm{d}^d k}{(2\pi)^d} \frac{\mathrm{tr}(\mathrm{i}\not{k}\mathrm{i}(\not{k}+\not{p}))}{k^2(k+p)^2} = 4\int \frac{\mathrm{d}^d k}{(2\pi)^d} \frac{k^2+k\cdot p}{k^2(k+p)^2} = 4(I_1(d,0) + p_\mu I_3^\mu(d,-p,0)$$

$$= 2S_d \frac{\Gamma(\frac{d}{2})^3\Gamma(1-\frac{d}{2})}{\Gamma(d-1)} p^{d-2} = -S_d M_d p^{d-2}. \tag{6.127}$$

Here we have defined $M_d := -2\frac{\Gamma(\frac{d}{2})^3\Gamma(1-\frac{d}{2})}{\Gamma(d-1)}$. In particular, $M_{2+\varepsilon} = 4/\varepsilon$, $M_{4-\varepsilon} = 2/\varepsilon$. Summing over the geometric series, we get the effective propagator for the boson field in the large N_f limit,

$$\frac{1}{(p^2)^{d/2-1}} \sum_{n=0}^{\infty} \Big(\frac{v^2 N_f M_\phi(p^2)}{(p^2)^{d/2-1}}\Big)^n = \frac{1}{(p^2)^{d/2-1}} \frac{1}{1+v^2 N_f S_d M_d}. \tag{6.128}$$

Fermion wave function renormalization

The self-energy loop in Fig. 6.5c contributes to the fermion wave function renormalization,

$$v^2(\overbrace{\phi\bar\psi\psi)(\phi\bar\psi}\psi) = v^2 M_\psi(p^2)\bar\psi\psi, \tag{6.129}$$

where

$$(1+v^2 N_f S_d M_d) M_\psi(p^2) = \int \frac{\mathrm{d}^d k}{(2\pi)^d} \frac{\mathrm{i}\not{k}}{k^2} \frac{1}{(k-p)^{d-2}}$$

$$= \frac{\Gamma(d/2)}{\Gamma(d/2-1)} \int_0^1 \mathrm{d}u \int \frac{\mathrm{d}^d k}{(2\pi)^d} \frac{\mathrm{i}(\not{k}+u\not{p})u^{d/2-2}}{[k^2+u(1-u)p^2]^{d/2}}$$

$$= \mathrm{i}\not{p}\frac{S_d}{2}\frac{d-2}{2}\int_0^1 \mathrm{d}u \int_{\mu^2}^{\Lambda^2} \mathrm{d}k^2 \frac{u^{d/2-1}(k^2)^{d/2-1}}{[k^2+u(1-u)p^2]^{d/2}} \approx \mathrm{i}\not{p} S_d \frac{d-2}{d}\log\frac{\Lambda}{\mu},$$

$$\Longrightarrow\ M_\psi(p^2) = \mathrm{i}\not{p} S_d \frac{d-2}{d} \frac{\log\frac{\Lambda}{\mu}}{1+v^2 N_f S_d M_d}. \tag{6.130}$$

This divergence should be canceled by the counter term $i\delta_\psi \not{p}$, i.e.,

$$\delta_\psi = -v^2 S_d \frac{d-2}{d} \frac{\log \frac{\Lambda}{\mu}}{1 + v^2 N_f S_d M_d}. \tag{6.131}$$

Interaction renormalization

δ_v is determined by the divergent part of the triangle diagram in Fig. 6.6c,

$$(-v)^3 (\phi\bar{\psi}\overbrace{\psi})(\phi\bar{\psi}\overbrace{\psi})(\phi\bar{\psi}\psi) = v^3 V_\triangle \phi\bar{\psi}\psi, \tag{6.132}$$

where

$$(1 + v^2 N_f S_d M_d) V_\triangle = -\int \frac{\mathrm{d}^d k}{(2\pi)^d} \frac{(\mathrm{i}\not{k})^2}{(k^2)^2} \frac{1}{k^{d-2}} = \int \frac{\mathrm{d}^d k}{(2\pi)^d} \frac{1}{k^d} = \frac{S_d}{2} \int_{\mu^2}^{\Lambda^2} \mathrm{d}k^2 \frac{1}{k^2} = S_d \log \frac{\Lambda}{\mu},$$

$$\implies V_\triangle = S_d \frac{\log \frac{\Lambda}{\mu}}{1 + v^2 N_f S_d M_d}, \tag{6.133}$$

This divergence should be canceled by the counter term $-\delta_v$, i.e.

$$\delta_v = v^3 S_d \frac{\log \frac{\Lambda}{\mu}}{1 + v^2 N_f S_d M_d}. \tag{6.134}$$

The β function

Now we are ready to compute the β function of v. We know the bare coupling is related to the renormalized coupling as

$$v_0^2 = Z_\psi^{-2}(v^2 + 2v\delta_v) = v^2 + 2v^4 S_d \frac{2d-2}{d} \frac{\log \frac{\Lambda}{\mu}}{1 + v^2 N_f S_d M_d} =: v^2 + a v^4 \log \frac{\Lambda}{\mu}. \tag{6.135}$$

Then we have

$$\beta_{v^2} = a v^4 = v^4 \frac{4(d-1)}{d} \frac{S_d}{1 + v^2 N_f S_d M_d}. \tag{6.136}$$

The critical exponents

The anomalous dimension η_ψ is

$$\eta_\psi = \frac{\mathrm{d}}{\mathrm{d}\log\mu} \ln Z_\psi \approx \frac{\partial}{\partial \log \mu} \ln Z_\psi = v^2 \frac{d-2}{d} \frac{S_d}{1 + v^2 N_f S_d M_d}. \tag{6.137}$$

We are interested in the critical exponent in the limit $v^2 \to \infty$, which gives

$$\eta_\psi = \frac{d-2}{dN_f M_d}. \tag{6.138}$$

Similarly, in the limit $v^2 \to \infty$ we have

$$\beta_{v^2} = \frac{4(d-1)}{dN_f M_d} v^2, \tag{6.139}$$

from which we can read

$$\gamma_v = \frac{2(d-1)}{dN_f M_d}. \tag{6.140}$$

At leading order, the number of ϕ field is proportional to the number of vertices v, and we have

$$d_\phi = 1 - \gamma_v = 1 - \frac{2(d-1)}{dN_f M_d}. \tag{6.141}$$

Therefore

$$\eta_\phi = 4 - d - 2\gamma_v = 4 - d - \frac{4(d-1)}{dN_f M_d}. \tag{6.142}$$

The values of η_ψ and η_ϕ at $d = 2+\varepsilon$ and $d = 4-\varepsilon$ are shown in Table 6.1, which agree with the results from $2+\varepsilon$ and $4-\varepsilon$ expansions in the large N_f limit.

Table 6.1: Comparison of η_ψ and η_ϕ for the Ising Gross-Neveu model in $2+\varepsilon$, $4-\varepsilon$ and large N_f expansions.

Critical exponents	$2+\varepsilon$	large N_f at $2+\varepsilon$	$4-\varepsilon$	large N_f at $4-\varepsilon$
η_ψ	$\frac{(4N_f-1)\varepsilon^2}{2(4N_f-2)^2}$	$\frac{\varepsilon^2}{8N_f}$	$\frac{\varepsilon}{2(3+2N_f)}$	$\frac{\varepsilon}{4N_f}$
η_ϕ	$2-\varepsilon-\frac{\varepsilon}{2N_f-1}$	$2-\varepsilon-\frac{\varepsilon}{2N_f}$	$\varepsilon-\frac{3\varepsilon}{3+2N_f}$	$\varepsilon-\frac{3\varepsilon}{2N_f}$

6.3.2 The SO(4) *Gross-Neveu model*

Similarly, the renormalized critical Lagrangian for the SO(4) Gross-Neveu model in the large N_f limit is given by

$$\mathcal{L} = (1+\delta_\psi)\bar{\psi}\gamma^\mu\partial_\mu\psi + \sum_{a=s,c}\frac{1}{2}\vec{\phi}_a(-\partial^2)^{d/2-1}\vec{\phi}_a + (v_a+\delta_{v_a})\vec{\phi}_a\cdot\vec{M}_a. \tag{6.143}$$

Using the spin-charge flip transformation, we can translate results from spin into charge. Therefore we will focus on the spin sector in the following. It can be checked that the effective propagators of the spin bosons remain the same as the Ising Gross-Neveu model, except that v^2 is replaced with v_s^2,

$$\frac{1}{(p^2)^{d/2-1}}\frac{1}{1+v_s^2 N_f S_d M_d}. \tag{6.144}$$

The fermion wave function renormalization is enhanced by the boson numbers $N_s = N_c = 3$,

$$\delta_\psi = -S_d \log\frac{\Lambda}{\mu}\Big(\frac{v_s^2 N_s (d-2)/d}{1+v_s^2 N_f S_d M_d} + \frac{v_c^2 N_c (d-2)/d}{1+v_c^2 N_f S_d M_d}\Big). \tag{6.145}$$

Similar to determining Eqs. (6.100) and (6.101) in the $4-\varepsilon$ calculation, δ_{v_s} is of the form

$$\delta_{v_s} = S_d \log\frac{\Lambda}{\mu}\Big(\frac{-v_s^3}{1+v_s^2 N_f S_d M_d} + \frac{3 v_s v_c^2}{1+v_c^2 N_f S_d M_d}\Big). \tag{6.146}$$

The β functions

The bare coupling v_{s0}^2 is related to the renormalized couplings through

$$\begin{aligned} v_{s0}^2 = Z_\psi^{-2}(v_s^2 + 2 v_s \delta_{v_s}) &= v_s^2 + S_d \log\frac{\Lambda}{\mu}\Big(\frac{2v_s^4(N_s(d-2)/d-1)}{1+v_s^2 N_f S_d M_d} + \frac{2 v_s^2 v_c^2 (N_c(d-2)/d+3)}{1+v_c^2 N_f S_d M_d}\Big) \\ &=: v_s^2 + a_s v_s^3 \log\frac{\Lambda}{\mu} + b_c v_s^2 v_c^2 \log\frac{\Lambda}{\mu}. \end{aligned} \tag{6.147}$$

Then using relations similar to Eqs. (6.56) and (6.59), we have the following β function,

$$\beta_{v_s^2} = a_s v_s^4 + b_c v_s^2 v_c^2 = 4 S_d\Big(\frac{v_s^4 (d-3)/d}{1+v_s^2 N_f S_d M_d} + \frac{3 v_s^2 v_c^2 (d-1)/d}{1+v_c^2 N_f S_d M_d}\Big), \tag{6.148}$$

where we have inserted the values $N_s = N_c = 3$.

The critical exponents

The anomalous dimension η_ψ is

$$\eta_\psi = \frac{\mathrm{d}}{\mathrm{d}\log\mu}\ln Z_\psi \approx \frac{\partial}{\partial\log\mu}\ln Z_\psi = S_d\Big(\frac{v_s^2 N_s(d-2)/d}{1+v_s^2 N_f S_d M_d} + \frac{v_c^2 N_c(d-2)/d}{1+v_c^2 N_f S_d M_d}\Big). \tag{6.149}$$

We are interested in the critical exponent in the limit $v \to \infty$, which gives

$$\eta_\psi = \frac{(N_s+N_c)(d-2)}{dN_f M_d} = \frac{6(d-2)}{dN_f M_d}. \tag{6.150}$$

Similarly, in the limit $v_s^2, v_c^2 \to \infty$, we have

$$\beta_{v_s^2} = \frac{8(2d-3)}{dN_f M_d} v_s^2. \tag{6.151}$$

Therefore it can be read that

$$\gamma_{v_s} = \frac{4(2d-3)}{dN_f M_d}. \tag{6.152}$$

At leading order, the number of ϕ_s field is proportional to the number of vertices v_s, and therefore

$$\eta_{\phi_s} = 4 - d - 2\gamma_{v_s} = 4 - d - \frac{8(2d-3)}{dN_f M_d}. \tag{6.153}$$

The values of η_ψ and η_ϕ at $d = 4-\varepsilon$ are shown in Table 6.2, which agree with the results from $4-\varepsilon$ expansion in the large N_f limit.

Table 6.2: Comparison of η_ψ and η_ϕ for the SO(4) Gross-Neveu model in $4-\varepsilon$ and large N_f expansions.

Critical exponents	$4-\varepsilon$	large N_f at $4-\varepsilon$
η_ψ	$\frac{3\varepsilon}{2(N_f+5)}$	$\frac{3\varepsilon}{2N_f}$
η_ϕ	$\varepsilon - \frac{5\varepsilon}{N_f+5}$	$\varepsilon - \frac{5\varepsilon}{N_f}$

7

Numerical Results

In this chapter, we present some numerical results based on our lattice model described by the sum of Eq. (1.1) at $N_f = 2$ and Eq. (1.2), with two couplings κ and U, and confirm the analysis of the quantum critical behaviors in the previous chapters.

In the next section, we introduce the basic ideas behind the meron-cluster algorithm, which is an efficient Monte Carlo algorithm to simulate a class of Hamiltonian lattice fermions in principle in any dimension. Then we study the quantum critical behavior using this algorithm in one spatial dimension, by tuning the Hubbard coupling while fixing $\kappa \to \infty$. Besides, we also precisely locate the quantum critical point using the exact diagonalization method based on the spectrum of the $\mathrm{SU}(2)_1$ WZW model.

In two spatial dimensions, we study the phase transition at $U = 0$ by tuning κ. When κ is not infinite, the meron-cluster algorithm no longer works, but this parameter range can be studied using the fermion bag algorithm [43, 44]. This study was performed by Emilie Huffman.

7.1 The meron-cluster algorithm

The meron-cluster algorithm, first proposed by Chandrasekharan and Wiese [45], is a very efficient fermion Monte Carlo algorithm for simulating a class of fermionic models [46, 47]. In this section, instead of discussing the general algorithm, we will explain how it applies to our model with $N_f = 2$ and SO(4) symmetry. As we discussed in Section 2.2, the Hamiltonian

$$H_\kappa = -\sum_{\langle i,j\rangle} \exp\Big(\kappa\eta_{ij}\sum_{\alpha=1}^{2} c_i^{\alpha\dagger}c_j^{\alpha} + c_j^{\alpha\dagger}c_i^{\alpha}\Big), \tag{re 1.1}$$

has an O(4) symmetry, while the Hubbard Hamiltonian

$$H_U = U\sum_j \Big((n_j^1 - 1/2)(n_j^2 - 1/2) + 1/4\Big). \tag{re 2.23}$$

is odd under the spin-charge flip transformation, only symmetric under SO(4) transformations. We wish to study the model with the Hamiltonian $H = H_\kappa + H_U$.

In order to take advantage of the meron-cluster algorithm, we need to take the $\kappa \to \infty$ limit. In this case, the full Hamiltonian can be written as

$$H = -J\sum_{\langle i,j\rangle}\prod_{\alpha=1,2} H^{\alpha}_{\langle i,j\rangle} + H_U, \tag{7.1}$$

where $H^{\alpha}_{\langle i,j\rangle}$ is given by Eq. (2.22),

$$H^{\alpha}_{\langle i,j\rangle} = \eta_{ij}(c_i^{\alpha\dagger}c_j^{\alpha} + c_j^{\alpha\dagger}c_i^{\alpha}) - 2\Big(n_i^{\alpha} - \frac{1}{2}\Big)\Big(n_j^{\alpha} - \frac{1}{2}\Big) + \frac{1}{2}. \tag{7.2}$$

In order to compute quantities in our lattice model with the meron-cluster algorithm, we use the continuous-time formulation of the partition function [99, 100, 101, 102, 103, 104]

$$Z = \mathrm{Tr}\,\mathrm{e}^{-\beta H} = \sum_k \int \mathrm{d}t_k \cdots \mathrm{d}t_1 \sum_{[b]} J^k \ \mathrm{Tr}\left(H_{b_k}(t_k)\cdots H_{b_1}(t_1)\right), \tag{7.3}$$

where $H_b(t) = e^{tH_U} H^1_{\langle i,j\rangle} H^2_{\langle i,j\rangle} e^{-tH_U}$ is the bond operator associated with the bond $b = \langle i, j\rangle$ inserted at time t. The integrals over Euclidean time are always assumed to be time ordered such that $\beta > t_k > .... > t_2 > t_1 > 0$. The choice of H_b leads to a simple formula for the trace in the fermionic Hilbert space. In particular, it does not contain any determinants of large matrices, as in the traditional auxiliary field methods. Instead, it can be shown that

$$\mathrm{Tr}\left(H_{b_k}(t_k)\cdots H_{b_1}(t_1)\right) = \prod_i W(\ell_i), \tag{7.4}$$

where $\{\ell_1, \ell_2, ...\}$ is a set of loops and $W(\ell_i)$ is the weight associated with the loop ℓ_i [46]. The loops can be identified by introducing two parallel bonds for each H_b at an appropriate imaginary time, as is illustrated in Fig. 7.1. From the figure, we can see that these bonds naturally divide the lattice into disconnected loop clusters. When the trace over the fermionic Hilbert space is performed, each cluster gets a weight $W(\ell) = 2(1 \pm e^{-Us_\ell/2})$, where s_ℓ is the linear temporal size of the loop. The sign associated with each loop is given by $(-1)^{n_t+n_b/2+1}$, where n_t is the number of temporal winding, and n_b is the number of bonds. The fermionic nature of the problem is hidden in this sign. When $U = 0$, clusters with a negative sign (merons) are naturally forbidden. On the other hand, when U is very large, all clusters are allowed, and from the cluster representation, our model becomes identical to the Heisenberg spin-half chain [105, 106], which also agrees with our continuum analysis.

The quantum Monte Carlo method using the Metropolis-Hastings algorithm works as follows. We start with an empty configuration, and then for each update, we propose to add or subtract a bond with equal probability, accept it or not depending on the detailed balance. When adding a bond, we choose a random even site, a random time, and a random direction. If there is already a bond at the same location, we reject this proposal and go to the next update. If not, we further go through an accept/reject process based on the change in the Boltzmann weight of

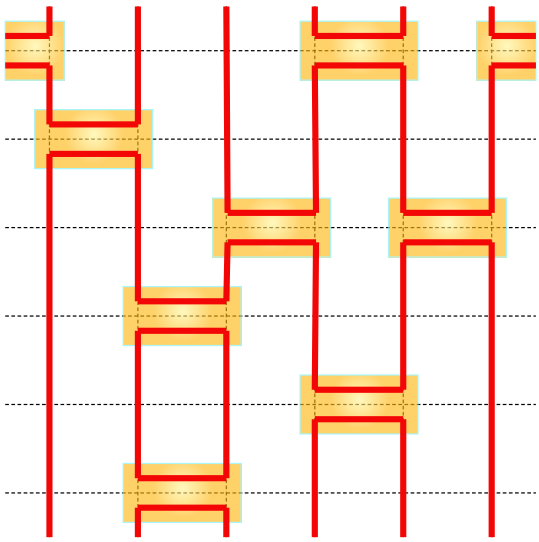

FIGURE 7.1: Illustration of a configuration of bonds that naturally divides space-time into loops.

the configuration. When subtracting a bond, we choose a random spatial site and choose one of the bonds connected to that site with equal probability and propose subtracting it. We again go through an accept/reject process based on the change in the Boltzmann weight of the configuration.

The Boltzmann weight of a configuration depends on the bond weight and the number of loops in the configuration. Furthermore, when a bond is added or subtracted, the number of loops always changes by 1. We can use this information to compute the probability of adding or subtracting a bond. For example, let us take the case of adding a bond that decreases the loop number by 1. The weights before (W_1) and after (W_2) adding the bond are

$$W_1 = 4W_0(1 \pm \mathrm{e}^{-\frac{U}{2}s_1})(1 \pm \mathrm{e}^{-\frac{U}{2}s_2}), \quad W_2 = \varepsilon J W_0 2(1 \pm \mathrm{e}^{-\frac{U}{2}(s_1+s_2)}), \tag{7.5}$$

and the transition probabilities are

$$P_{1\to 2} = \frac{\varepsilon}{V\beta 2d}, \quad P_{2\to 1} = \frac{1}{VN_b}, \tag{7.6}$$

where W_0 is the weight of the loops which do not change, s_i is the loop size of the

loop i, V is the volume of the lattice, ε is the unit time interval, and N_b is the number of bonds on this site after adding the bond. The ratio

$$\frac{W_2 P_{2\to 1}}{W_1 P_{1\to 2}} = \frac{2(1 \pm \mathrm{e}^{-\frac{U}{2}(s_1+s_2)})}{4(1 \pm \mathrm{e}^{-\frac{U}{2}s_1})(1 \pm \mathrm{e}^{-\frac{U}{2}s_2})} \frac{2d\beta J}{N_b} \tag{7.7}$$

is used to decide whether to accept an update or not. The quantity $\frac{N_b}{2d\beta J}$ can be thought of as bond density on a particular site and therefore tends to be a constant when we scale the lattice. Its value is usually of order 1; therefore $\frac{W_2}{W_1}$ is of order 1 when U is not very small.

7.2 Results in one spatial dimension

In this section, we will focus on the one dimensional version of the Hamiltonian in Eq. (7.1),

$$H = -J \sum_{\langle i,j \rangle} \prod_{\alpha=1,2} H^{\alpha}_{\langle i,j \rangle} + H_U. \tag{re 7.1}$$

We wish to study the physics of this model as a function of U. We will find a quantum phase transition in this model from a massive phase at small U to a critical phase at large U. We will first discuss the connection of this model to the continuum model we analyzed in Chapter 5, and then show the numerical results supporting our continuum analysis.

7.2.1 Connection to the continuum model

From the discussion in Section 4.1.4 and Section 5.5, we know that there are two independent interactions respecting the SO(4) symmetry, i.e., $\lambda_s J^i_{s+} J^i_{s-}$ and $\lambda_c J^i_{c+} J^i_{c-}$. Based on the β functions for λ_s and λ_c derived in Eq. (5.69), the RG flow diagram is shown in Fig. 7.2. The couplings are marginally relevant when $\lambda_{s,c} > 0$, and marginally irrelevant when $\lambda_{s,c} < 0$.

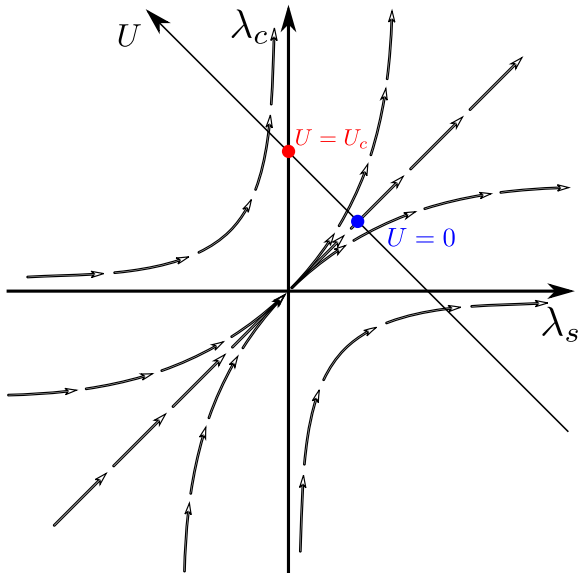

FIGURE 7.2: Phase diagram in the λ_s - λ_c plane.

We would like to know how the lattice Hamiltonian H in Eq. (7.1) fits into this continuum model. Due to the SO(4) symmetry, the lattice Hamiltonian H must describe the physics as some point in the (λ_s, λ_c) plane if we ignore irrelevant couplings. At $U = 0$, the Hamiltonian is spin-charge flip symmetric; therefore it must be on the $\lambda_c = \lambda_s$ line. Furthermore, from our numerical study, we know the Hamiltonian at $U = 0$ is massive with $\mathbb{Z}_2$ translation symmetry spontaneously broken, which is equivalent to a dimer condensate $\langle \mathcal{D}_j \rangle \neq 0$, known as a valence-bond solid (VBS) phase. From Eq. (5.82) we know that this corresponds to the condensation of the chiral mass in the fermion language. This degenerate ground state in the massive phase is expected from the Lieb-Schultz-Mattis theorem [32, 33, 34], which recently received a deeper understanding in terms of mixed 't Hooft anomaly [30, 25] of the U(1) charge symmetry and the $\mathbb{Z}_2^\chi$ discrete chiral symmetry and SPT phases [36, 38, 39]. This physics is also well known in terms of the Gross-Neveu model: the discrete chiral symmetry is spontaneously broken and the theory is asymptotically free. Therefore the lattice Hamiltonian at $U = 0$ must correspond to a theory with $\lambda_c = \lambda_s > 0$.

How do these parameters change when $U \neq 0$? We know that H_U is odd under the spin-charge flip transformation, and therefore when $U \neq 0$, the lattice model moves away from the $\lambda_c = \lambda_s$ line. Furthermore, when $U \to \infty$, we know the charge sector is completely gapped, and the system is equivalent to a Heisenberg spin-half chain, which was also seen from the meron-cluster algorithm directly in the previous section. Therefore when $U > 0$ our model must move away from the spin-charge flip symmetric axis towards the second quadrant where $\lambda_s < 0$ and $\lambda_c > 0$. This implies the existence of a quantum phase transition at some critical value $U = U_c$. When $U > U_c$, the low-energy physics of the Hamiltonian is described by the $\mathrm{SU}(2)_1$ WZW model perturbed by a marginally irrelevant coupling $\lambda_s < 0$; when $U = U_c$, we have $\lambda_s = 0$, and the low-energy physics is described exactly by the $\mathrm{SU}(2)_1$ WZW model without any marginal perturbation. This implies that at $U = U_c$, we should be able to see the $\mathrm{SU}(2)_{s+} \times \mathrm{SU}(2)_{s-}$ chiral symmetry, under which $\mathcal{S}^i_{j,\mathrm{osc}}$ and $\pi a \mathcal{D}_j$ forms a 4-component vector, as discussed in Section 5.5. This fact is confirmed precisely by the Monte Carlo simulation discussed below and will be used to precisely locate the critical point.

7.2.2 Monte Carlo results

We use the meron-cluster algorithm to compute the equal time spin and dimer correlation functions defined through the expressions

$$\tilde{G}_i(r) := \frac{1}{Z} \mathrm{Tr}\left(\mathrm{e}^{-\beta H} \mathcal{O}_i(r) \mathcal{O}_i(0) \right), \tag{7.8}$$

where $\mathcal{O}_i(r), i = \mathcal{S}^3, \mathcal{D}$ are the spin and dimer operators defined in Eqs. (5.72) and (5.80). The symbol r is used for the spatial lattice site j at some fixed time slice. We compute $\tilde{G}_i(r)$ at various lattice sizes and U, and in Fig. 7.3 we illustrate some of our results at $U = 0$, 0.5, 1 and 1.5 on a lattice of size $L = 128$. For clarity we focus on the region of $8 \leq r \leq 40$. Both correlation functions decrease expo-

nentially (with possible multiplicative power corrections) in r. The figure clearly shows a non-zero expectation value for the dimer order parameter $\langle \mathcal{D}_j(t) \rangle$ at $U = 0$, while there is no such expectation value for the spin operator, which means that for small values of U, the lattice model breaks the $\mathbb{Z}_2^\chi$ discrete chiral symmetry. Another important point to note is that the spin and dimer correlation functions also behave very differently, at least for small values of U but slowly begin to become similar by $U \approx 1.5$, signaling the enhanced $\mathrm{SU}(2)_{s+} \times \mathrm{SU}(2)_{s-}$ chiral symmetry.

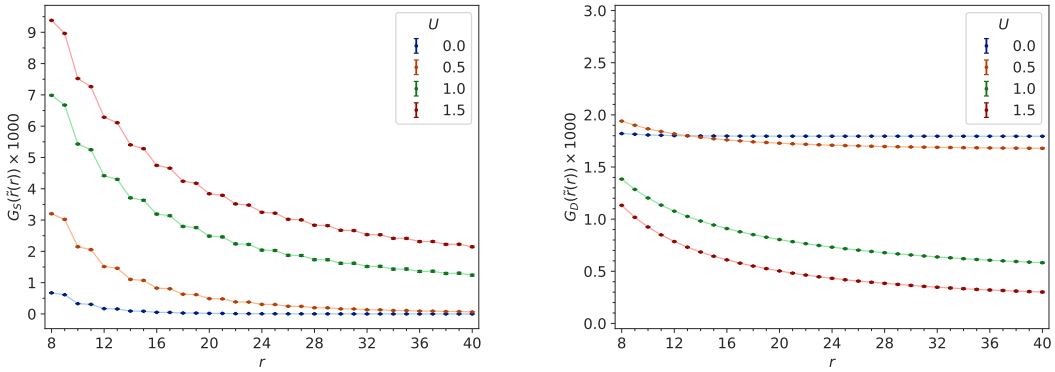

FIGURE 7.3: Spin correlation functions $G_{\mathcal{S}}(\tilde{r}(r))$ and dimer correlation functions $G_{\mathcal{D}}(\tilde{r}(r))$ as functions of r at $L = 128$ for $U = 0$, 0.5, 1.0 and 1.5.

Assuming we are in the vicinity of the critical point around $U \gtrsim 1.5$, we want to fit our MC data to Eqs. (5.95) and (5.96). However, since we work on a finite lattice with periodic boundary conditions, the correlation functions receive finite-size corrections. Fortunately, in the conformal phase, the finite size corrections can be obtained using the map from an infinite plane to a cylinder, which results in replacing r by

$$r \to \tilde{r} = \frac{L}{\pi} \sin \frac{\pi r}{L}, \tag{7.9}$$

where L is the spatial size [88, 91]. Furthermore, the spin correlation functions clearly show oscillating behavior due to the higher-order operators in the observable

with ferromagnetic behavior. Taking these corrections into account, we make the following ansatz for the lattice correlation functions at $U \gtrsim U_c$ on a finite lattice,

$$G_{\mathcal{S}}(\tilde{r}) = \frac{A_1}{\tilde{r}}\Big(1 - \frac{\tilde{\lambda}_0}{2\pi}\ln\tilde{r}\Big)^{\frac{1}{2}} - \frac{A_2(-1)^r}{\tilde{r}^2}, \tag{7.10}$$

$$G_{\mathcal{D}}(\tilde{r}) = \frac{B}{\tilde{r}}\Big(1 - \frac{\tilde{\lambda}_0}{2\pi}\ln\tilde{r}\Big)^{-\frac{3}{2}}, \tag{7.11}$$

where we have introduced a single fit parameter $\tilde{\lambda}_0 = \lambda_0/(1 + \frac{\lambda_0}{2\pi}\ln\tilde{r}_0)$, an RG invariant quantity that numerically equals the coupling measured at $\tilde{r}_0 = 1$ in the lattice unit. The critical point is obtained when $\tilde{\lambda}_0 = 0$. There are also precise asymptotic results for the spin and dimer correlation functions in the Heisenberg spin chain [91, 107, 108]:

$$G_{\mathcal{S}}(\tilde{r} \to \infty) = \frac{(\ln\tilde{r})^{\frac{1}{2}}}{(2\pi)^{3/2}\tilde{r}} - \frac{(-1)^r}{(2\pi)^2\tilde{r}^2}, \tag{7.12}$$

$$G_{\mathcal{D}}(\tilde{r} \to \infty) = \frac{(\ln\tilde{r})^{-\frac{3}{2}}}{(2\pi)^{3/2}\tilde{r}} + \frac{(-1)^r(\ln\tilde{r})^2}{6\pi^4\tilde{r}^4}, \tag{7.13}$$

and indeed they are consistent with Eqs. (7.10) and (7.11) in the $\tilde{r} \to \infty$ limit.

We have performed a combined fit for both $G_{\mathcal{S}}(\tilde{r})$ and $G_{\mathcal{D}}(\tilde{r})$ to the form Eqs. (7.10) and (7.11) at each fixed value of $U \geq 1.5$, tabulated in Table 7.1. Each of these is a four-parameter fit involving $A_1, A_2, B, \tilde{\lambda}_0$ and using all data from $L = 64$, 80, 96, 128 and $12 \leq r \leq 40$. As can be seen from these results, our data fit well to the form Eqs. (7.10) and (7.11) for all couplings in the range $1.5 \leq U \leq 2.0$. Since at the critical point we expect $\tilde{\lambda}_0 \approx 0$, applying conservative systematic errors related to the fitting procedures, we estimate $U_c = 1.75(5)$. At $U = 1.745$, we indeed find that $A_1/(\pi^2 B) \approx 1.004$ is very close to 1, which confirms the symmetry between $\mathcal{S}^i_{j,\mathrm{osc}}$ and $\pi a\mathcal{D}_j$ at the critical point.

In order to visualize that the correlation functions indeed obey the power law near the critical point, we plot them in log scale in Fig. 7.4. We only plot at even r

Table 7.1: Parameters in Eqs. (7.10) and (7.11) obtained by fitting the MC data for $U \gtrsim U_c = 1.75(5)$.

U	A_1	A_2	B	$\tilde{\lambda}_0$	χ^2_ν
1.5	0.0816(2)	0.0241(4)	0.007 47(4)	0.333(7)	0.55
1.6	0.0836(2)	0.0247(4)	0.007 66(4)	0.230(7)	0.69
1.7	0.0838(1)	0.0248(4)	0.008 18(3)	0.066(6)	1.10
1.745	0.0839(1)	0.0249(4)	0.008 47(3)	−0.019(6)	1.23
1.8	0.0852(1)	0.0253(3)	0.008 46(3)	−0.048(6)	1.10
1.9	0.0854(2)	0.0253(3)	0.008 90(5)	−0.195(9)	1.32
2.0	0.0871(2)	0.0257(3)	0.008 94(5)	−0.258(10)	0.78
2.5	0.0911(2)	0.0262(3)	0.009 82(6)	−0.670(11)	1.85
4.0	0.0997(2)	0.0268(3)	0.011 29(6)	−1.345(13)	1.90
∞	0.1110(2)	0.0269(2)	0.013 22(5)	−1.975(10)	9.68

to avoid distracting oscillation.

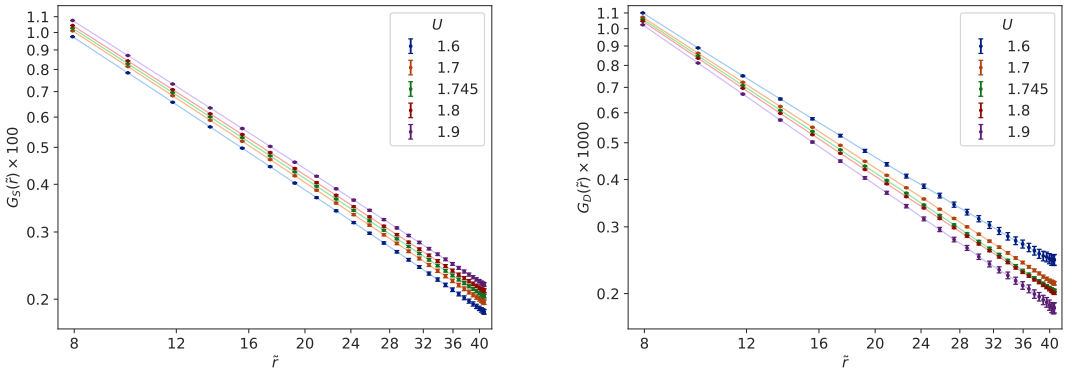

FIGURE 7.4: Spin correlation functions $G_{\mathcal{S}}(\tilde{r})$ and dimer correlation functions $G_{\mathcal{D}}(\tilde{r})$ as functions of $\tilde{r}$ at even r and $L = 128$ for $U = 1.6$, 1.7, 1.745, 1.8 and 1.9.

7.2.3 Exact diagonalization results

In order to confirm that our estimate for the critical point is reasonable, we also use an alternative idea outlined in [109], based on the low-energy physics of the WZW model (Eq. (5.57)) that emerges at the critical point. Since the WZW model is invariant under the $\mathrm{SU}(2)_{s+} \times \mathrm{SU}(2)_{s-}$ symmetry, the energy eigenstates can be

labeled with spin quantum numbers (s_L, s_R). It is known that the ground state has $(s_L, s_R) = (0, 0)$ with momentum 0, while the first excited state has $(s_L, s_R) = (\frac{1}{2}, \frac{1}{2})$ with momentum π [89], corresponding to the identity operator and primary WZW operators g under the state-operator correspondence. However, since the lattice model is only invariant under the diagonal $\mathrm{SU}(2)_s$ subgroup, the energy eigenstates on the lattice will only be labeled by the total spin s_{tot}. The four-fold degeneracy requires fine-tuning to the critical point where the singlet ($s_{\mathrm{tot}} = 0$) and the triplet ($s_{\mathrm{tot}} = 1$) state together form an $(s_L, s_R) = (\frac{1}{2}, \frac{1}{2})$ state. This observation suggests an alternative method to determine the critical point: we can compute the lowest five energy eigenvalues as a function of U using an exact diagonalization method and locate the coupling where the first excited state becomes four-fold degenerate for a fixed L. When L is finite, the critical coupling where the energies of these two total spin sectors cross can be referred to as a pseudo-critical point $U_c(L)$. This point turns into the true critical point as $L \to \infty$.

In order to implement the above idea, we computed the first five energy eigenvalues by diagonalizing the Hamiltonian on small lattices using the coordinate descent method [110, 111]. The behavior of the lowest five states as a function of U at $L = 14$ and $L = 16$ is plotted in Fig. 7.5. Note that only three eigenvalues are shown because the $s = 1$ states are threefold degenerate. We observe that in the broken phase (small U) the ground state and the first excited state turn out to be spin singlets with $s_{\mathrm{tot}} = 0$. The next three degenerate excited states form a triplet with $s_{\mathrm{tot}} = 1$. In contrast, when $U > U_c$, the triplet states have lower energy than the singlet state. We thus can determine $U_c(L)$ as the coupling where the triplet and singlet states cross, which are tabulated in Table 7.2 and plotted in Fig. 7.6 as a function of $1/L^2$. Based on Fig. 7.6 we can estimate $U_c(L) \approx 1.746(1)$, consistent with our estimate in the previous section and with the estimate using finite-size scaling in the conference proceeding [112].

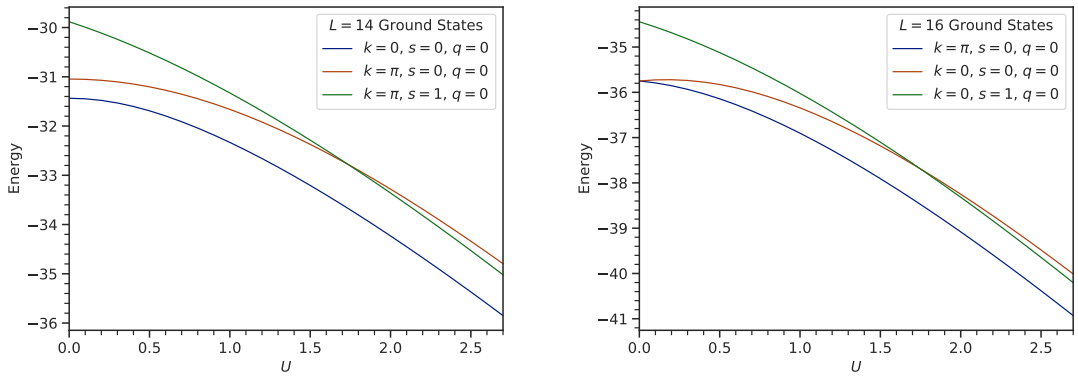

FIGURE 7.5: The plot of the lowest five energy eigenvalues obtained using an exact diagonalization method as a function of U at $L = 14$ and $L = 16$.

Table 7.2: Pseudo-critical couplings $U_c(L)$ as a function of L obtained using the exact diagonalization method.

L	$U_c(L)$	L	$U_c(L)$
4	2.539 823 88	6	1.266 992 59
8	1.860 358 76	10	1.688 343 26
12	1.757 261 71	14	1.735 292 71
16	1.745 085 77	18	1.743 089 79
20	1.745 025 94	22	1.745 311
24	1.745 996	26	1.746 393

This exact diagonalization result also confirms the degeneracy of the spectrum we proved in Theorem 1. Indeed, in Fig. 7.5 we observe that at $U = 0$ the ground state is degenerate at $L = 16$ which is a multiple of 4, but not at $L = 14$. Moreover, the difference between $L = 4n$ and $L = 4n + 2$ permeates even away from $U = 0$, and is observed in the dramatically different values of $U_c(L)$ when L is small: the degeneracy of the ground state and first excited state at $L = 4n$ pushes the first excited state downwards, resulting in a larger $U_c(L)$ than $L = 4n + 2$. However, the difference decreases rapidly as L increases, and both approach the true critical point as expected. Another peculiarity comes from the momentum quantum number k for the first five energy eigenstates. We note that k flips between π and 0 when

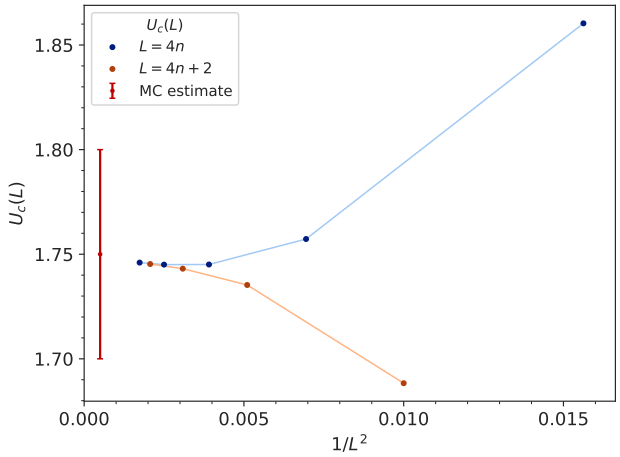

FIGURE 7.6: The plot of the behavior of the pseudo-critical coupling $U_c(L)$ as a function of $1/L^2$.

comparing $L = 4n$ with $4n + 2$. This is as expected because similar phenomena are also observed in the Heisenberg spin chain, with $k = 0$ for $L = 4n$ and $k = \pi$ for $L = 4n + 2$ [113]. The extra π phase in our model compared to the Heisenberg spin chain is due to the fermionic nature of our model, since there is an intrinsic extra minus sign when the system is translated by one site when $L = 2n$.

Using the exact diagonalization method, we have also confirmed that our model at $U = 0$ is indeed in a massive phase with spontaneously broken $\mathbb{Z}_2^X$ symmetry. In such a phase, the energy gap to the first excited state is expected to become exponentially small as L becomes large, but the gap to the second excited state remains non-zero as $L \to \infty$. We plot these gaps in Fig. 7.7, where the solid lines are exponential fits. From the figure, it can be clearly seen that the gaps of the first excited states close at $L \to \infty$ for both $L = 4n$ and $4n + 2$. At finite L, the former is identically zero, due to our theorem, while the latter closes exponentially. The gaps of the second excited states stay open for both $L = 4n$ and $4n + 2$.

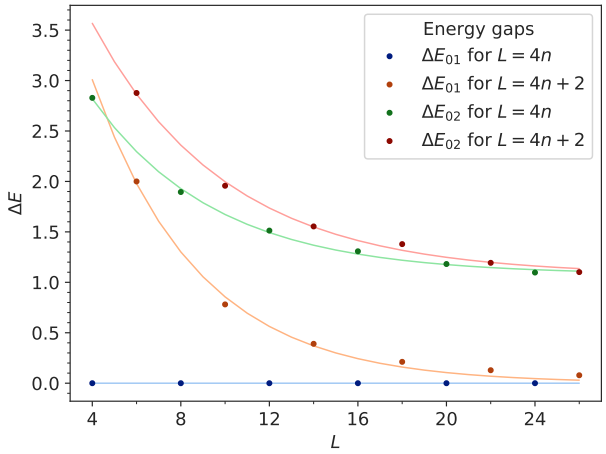

FIGURE 7.7: Scaling of energy gaps of the first and second excited states with the ground state at $U = 0$.

7.3 Results in two spatial dimensions

In this section, we will briefly discuss the results in two spatial dimensions at $U = 0$ obtained by Emilie Huffman using the fermion bag algorithm. Our goal is to put the results obtained within the perspective of the continuum analysis we developed in this dissertation. The Hamiltonian is given by

$$H_\kappa = -\sum_{\langle i,j \rangle} \exp\left(\kappa \eta_{ij} \sum_{\alpha=1}^{2} c_i^{\alpha\dagger} c_j^{\alpha} + c_j^{\alpha\dagger} c_i^{\alpha}\right). \tag{re 1.1}$$

which is O(4) symmetric and is defined on a two-dimensional square lattice. Recall that we have also defined $\mathbf{g} = 2\tanh\frac{\kappa}{2}$ as the coupling for convenience. As we will see in this section, this model has a quantum phase transition from a massless fermion phase to a massive fermion phase as we tune g from small to large values. In order to explore the quantum critical point, we need to study this model at finite κ, or equivalently, $\mathbf{g} < 2$, which is beyond the scope of the meron-cluster algorithm. Therefore, we need to resort to the fermion bag algorithm.

The fermion bag algorithm applies to all Hamiltonians that are made up of only

local terms whose fermionic degrees of freedom are exponentiated bilinears, which have particular simple cluster expansion using the Blankenbecler-Scalapino-Sugar (BSS) formula [114]. Although this is a limited family of systems, the algorithm is very efficient within its scope of applicability [43]. Using this algorithm, we can compute two correlation functions of order parameters,

$$C_S = 2\langle \mathcal{S}_i \mathcal{S}_j \rangle, \quad C_U = \langle \mathcal{U}_i \mathcal{U}_j \rangle, \tag{7.14}$$

where C_S measures the Néel order through the AFM spin order parameter $\mathcal{S}_i$, and C_U measures the breaking of the spin-charge flip symmetry through the order parameter $\mathcal{U}_i = (n_i^1 - \frac{1}{2})(n_i^2 - \frac{1}{2})$, which is a four-fermion operator that is odd under $\mathbb{Z}_2^{sc}$, but invariant under $\mathrm{SU}(2)_s \times \mathrm{SU}(2)_c$. In Eq. (7.14), $i = (0, 0)$ and $j = (L/2, 0)$ and we assume $L/2$ is even.

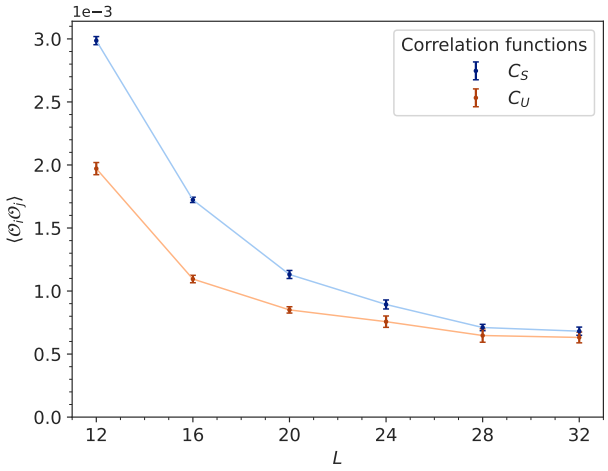

FIGURE 7.8: Finite-size scaling data for C_S and C_U using the fermion bag method for a coupling constant $\mathbf{g} = 1.6$.

We first discuss the nature of the massive phase in our lattice model. The result at $\mathbf{g} = 1.6$, being inside the massive phase, is shown in Fig. 7.8, from which we can see that as L becomes large, the data for both C_U and C_S seem to saturate to a finite value. Since C_U is non-zero in the thermodynamic limit, we can conclude

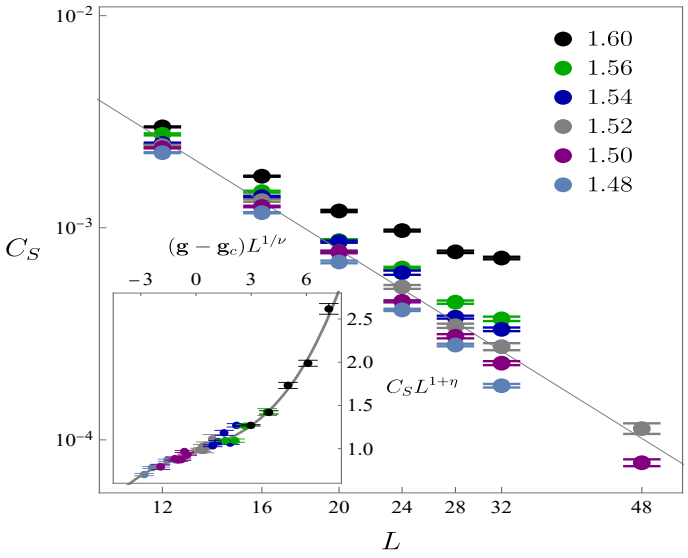

FIGURE 7.9: The main plot shows C_S as a function of L on a log-log scale up to $L = 48$ for various values of $\mathbf{g}$. The inset shows that the data collapsing.

that the spin-charge flip symmetry $\mathbb{Z}_2^{sc}$ is spontaneously broken. Furthermore, C_S being non-zero in the thermodynamic limit implies that the massive phase should have Néel order. These two observations imply that the system has to spontaneously choose between the charge and the spin sector, breaking $\mathbb{Z}_2^{sc}$, and forming either a Néel state or a superconductor-CDW state which breaks the corresponding SU(2) symmetry. This is precisely what we found through the effective potential analysis in Chapter 5.

Then we would like to study the nature of the phase transition between the massless phase at small g, usually referred to as the Dirac semi-metal phase, and the massive phase discussed above. In the main panel of Fig. 7.9, we plot C_S as a function of L at various values of U in the logarithmic scale. At large values of L, there is clear evidence that C_S converges to a non-zero constant at the coupling $\mathbf{g} = 1.6$ (massive phase), while it scales to zero at the coupling $\mathbf{g} = 1.48$ (Dirac semi-metal phase). At the critical coupling, we expect power law $C_S \propto L^{-(1+\eta)}$. For example, at $\mathbf{g} = 1.52$ the data fit well to $C_s = 0.67/L^{2.25}$, which suggests that $\mathbf{g} = 1.52$ could

be a quantum critical point. A multi-parameter scaling fit of all our data except for $L = 12$, to the form $C_S = L^{-(1+\eta)} f((g - g_c)\ L^{1/\nu})$ with $f(x) = f_0 + f_1 x + f_2 x^2 + f_3 x^3$ yields $\eta = 1.38(6)$, $\nu = 0.78(7)$, $\mathbf{g}_c = 1.514(8)$, $f_0 = 0.96(15)$, $f_1 = 0.073(26)$, $f_2 = 0.0012(43)$, $f_3 = 0.0026(32)$ with a $\chi^2_\nu = 1.25$. In the inset of Fig. 7.9 we show the scaling collapse of the data using the multi-parameter fit, providing strong evidence for a continuous quantum critical point.

Now we would like to compare these results with our $4-\varepsilon$ calculation in Chapter 6. Recall that the $4 - \varepsilon$ analysis finds a stable critical point only for $N_f < 0.016$ and $N_f > 16.83$, which suggests that there should not be any critical point at $N_f = 2$. The lack of a stable fixed point is often used as evidence that the lattice model may only have a weakly first-order transition, which is much harder to rule out. On the other hand, it is also possible that the $4-\varepsilon$ expansion up to one loop is not providing us with the complete story. Perhaps the window in N_f where a stable fixed point is present (i.e., $N_f < 0.016$ and $N_f > 16.83$) changes at higher loop orders. It is also possible that this window depends on ε in a non-trivial way that is beyond the reach of the $4 - \varepsilon$ calculation.

The large value of η obtained numerically as compared with our $4-\varepsilon$ calculation could be yet another evidence that the ε expansion might be unreliable. Note that when $\varepsilon = 0$, we always get $\eta = 0$, so the expansion is usually considered more reliable when η is small. Most other Monte Carlo results in three dimensions also find η large at the Gross-Neveu fixed point, but usually $\eta < 1$. However, examples of $\eta > 1$ have been observed at certain critical points previously [115, 116, 117].

8

Summary and Conclusions

In this dissertation, we developed a method to construct continuum QFTs that describe the long-distance physics near second-order quantum phase transitions in interacting lattice fermion models. Our work was inspired by the lattice fermion model Eq. (1.1), which is amenable to efficient Monte Carlo simulation without a sign problem. This model has an $\mathrm{O}(2N_f)$ internal symmetry, and we show how this symmetry constrains the continuum quantum field theories that describe the quantum critical behavior. We paid particular attention to the case of $N_f = 2$ with a weaker SO(4) symmetry, allowing a broken spin-charge flip symmetry, which is also the case where we performed numerical studies to compare the theoretical predictions.

In order to find the connection between the lattice models and the continuum QFTs near the quantum critical point, we employed a perturbative analysis near the free-fermion fixed point. We studied the continuum limit of the free fermion models, and analyzed all the possible four-fermion interactions allowed by the $\mathrm{O}(2N_f)$ symmetry near the free-fermion fixed point. We found that in one spatial dimension, there is only one independent interaction allowed by the symmetry, while in two

spatial dimensions, there are four independent interactions. In the case of $N_f = 2$ with an SO(4) symmetry, there is one more independent interaction in both cases, due to the breaking of the spin-charge flip symmetry.

We then analyzed these continuum QFTs using well-known techniques in the literature. In one spatial dimension, powerful tools such as CFT and bosonization allow us to perform a perturbative analysis near any CFT, helping us understand the phase structure and the correlation functions of the observables on the lattice. We found that by tuning the Hubbard coupling U, our model undergoes a second-order phase transition from a massive VBS phase to a massless critical phase, which can be described by the $\mathrm{SU}(2)_1$ WZW model with a marginal perturbation. The correlation functions from the Monte Carlo simulation agree pretty well with our theoretical prediction, allowing us to locate the quantum critical point. We also use exact diagonalization to locate the quantum critical point more precisely based on our knowledge of the spectrum of the $\mathrm{SU}(2)_1$ WZW model.

On the other hand, in two spatial dimensions, one has to resort to various perturbative techniques near the free-fermion fixed point. In particular, we calculate the effective potential of our theory, which is valid in the large N_f limit. Our effective potential indicates spontaneous breaking of the spin-charge flip symmetry in the strong coupling regime, resulting in an AFM order or a superconducting-CDW order but not both. This result is also verified by our numerical simulation using the fermion bag algorithm performed by Emilie Huffman. We also computed the β function and critical exponents using $4 - \varepsilon$ expansion and large N_f expansion. To the best of our knowledge, the spin-charge symmetric fixed point we discovered in our RG flow diagram has not been explored in the literature before.

There are several directions for future research. For example, we can perform a similar continuum analysis of the model on the Honeycomb lattice, which would be of interest in the condensed matter literature. We can also easily analyze all indepen-

dent four-fermion interactions with the more common U(N_f) symmetry. In fact, the special case of $N_f = 2$ in one spatial dimension was analyzed in [118]. Furthermore, we have included a $2 + \varepsilon$ calculation of the Ising-GN model in Appendix E, which can be extended to the O($2N_f$)-GN model. However, this requires a more careful analysis due to the difficulties arising from the generation of Thirring interactions.

Further exciting questions include investigating whether there are any deconfined quantum critical points or emergent symmetries in our model on a different lattice, because these phenomena have been observed in similar models [68]. We can also explore if the massive phase of our lattice model can be described by a non-linear sigma model with a Hopf term [119, 120]. The calculation would be similar to calculating the mean-field effective potential, but we can no longer treat the background scalar fields as constants in space-time.

Appendix A

Grassmann Coherent State Path Integral

In Chapter 3, we derived the continuum Hamiltonians of the lattice models in Eqs. (3.12) and (3.40), and stated that the continuum Lagrangians in Eqs. (3.13) and (3.41) can be obtained using Grassmann coherent state fermion path integral. In this appendix, we briefly outline the steps from a Hamiltonian of fermions to a Lagrangian using such a technique.

The continuum Hamiltonian of our lattice model $\mathcal{H}(\Psi^\dagger, \Psi)$ is normally ordered, where the fermion fields Ψ and $\Psi^\dagger$ are the usual fermion annihilation and creation operators satisfying the canonical anti-commutation relations. The imaginary-time partition function is then defined as

$$Z = \mathrm{Tr}\, \mathrm{e}^{-\beta \int \mathrm{d}^d x \mathcal{H}(\Psi^\dagger, \Psi)} \,. \tag{A.1}$$

The basic idea of turning it into a path integral can be traced back to Feynman's thesis [121], and it works as follows: we split $\mathrm{e}^{-\beta \int \mathrm{d}^d x \mathcal{H}(\Psi^\dagger, \Psi)}$ into small time steps, and insert a resolution of identity in terms of an (over-)complete set of coherent states $|\psi\rangle$ and $\langle\psi^\dagger|$, which are eigenstates of the $\Psi(x)$ and $\Psi^\dagger(x)$ operators. Then the operators $\Psi(x)$ and $\Psi^\dagger(x)$ can be replaced by their eigenvalues $\psi(x)$ and $\psi^\dagger(x)$,

which are completely independent Grassmann variables. The coherent states can be written down concretely as

$$|\psi\rangle = \mathrm{e}^{-\int \mathrm{d}^d x \psi(x)\Psi^\dagger(x)}\,|0\rangle, \quad \langle\psi^\dagger| = \langle 0|\,\mathrm{e}^{-\int \mathrm{d}^d x \Psi(x)\psi^\dagger(x)}\,. \tag{A.2}$$

and it can be checked that they are indeed eigenstates of $\Psi(x)$ and $\Psi^\dagger(x)$,

$$\Psi(x)|\psi\rangle = \psi(x)|\psi\rangle, \quad \langle\psi^\dagger|\Psi^\dagger(x) = \langle\psi^\dagger|\psi^\dagger(x). \tag{A.3}$$

The resolution of identity is given by [122],

$$\mathbb{1} = \int D\psi^\dagger D\psi\ |\psi\rangle\,\mathrm{e}^{-\int \mathrm{d}^d x \psi^\dagger(x)\psi(x)}\langle\psi^\dagger|, \tag{A.4}$$

and here, we emphasize that in the path integral, ψ is a function of space only.

Now we first split Eq. (A.1) into small steps,

$$Z = \mathrm{Tr}(\mathrm{e}^{-\varepsilon\int \mathrm{d}^d x \mathcal{H}(\Psi^\dagger,\Psi)})^N = \lim_{\varepsilon\to 0}\mathrm{Tr}\left(\mathbb{1} - \varepsilon\int \mathrm{d}^d x \mathcal{H}(\Psi^\dagger,\Psi)\right)^N, \tag{A.5}$$

where $\varepsilon N = \beta$. Inserting the resolution of identity Eq. (A.4) into each time step of the partition function, we have

$$Z = \lim_{\varepsilon\to 0}\int\prod_{i=0}^{N-1} D\psi_i^\dagger D\psi_i \langle\psi_{i+1}^\dagger|\Big(1-\varepsilon\int \mathrm{d}^d x\mathcal{H}(\Psi^\dagger,\Psi)\Big)|\psi_i\rangle\,\mathrm{e}^{-\int \mathrm{d}^d x\psi_i^\dagger(x)\psi_i(x)}, \tag{A.6}$$

where $\langle\psi_N^\dagger| = \langle -\psi_0^\dagger|$ due to the trace and anti-commutativity of the Grassmann variables. Each matrix element can be evaluated as

$$\begin{aligned}\langle\psi_{i+1}^\dagger|\Big(1-\varepsilon\int \mathrm{d}^d x\mathcal{H}(\Psi^\dagger,\Psi)\Big)|\psi_i\rangle &= \langle\psi_{i+1}^\dagger|\psi_i\rangle - \varepsilon\int \mathrm{d}^d x\mathcal{H}(\psi_{i+1}^\dagger,\psi_i)\langle\psi_{i+1}^\dagger|\psi_i\rangle \\ &= \mathrm{e}^{\int \mathrm{d}^d x\psi_{i+1}^\dagger(x)\psi_i(x)}\,\mathrm{e}^{-\varepsilon\int \mathrm{d}^d x\mathcal{H}(\psi_{i+1}^\dagger,\psi_i)},\end{aligned} \tag{A.7}$$

where we have used the fact that $\mathcal{H}(\Psi^\dagger,\Psi)$ is normally ordered in the first step, and $\langle\psi_{i+1}^\dagger|\psi_i\rangle = \mathrm{e}^{\int \mathrm{d}^d x\psi_{i+1}^\dagger(x)\psi_i(x)}$ in the second. Inserting these matrix elements back into

the partition function, we have

$$
\begin{aligned}
Z &= \lim_{\varepsilon\to 0}\int \prod_{i=0}^{N-1} D\psi_i^\dagger D\psi_i \, \mathrm{e}^{\int \mathrm{d}^d x \psi_{i+1}^\dagger(x)\psi_i(x)} \, \mathrm{e}^{-\varepsilon \int \mathrm{d}^d x \mathcal{H}(\psi_{i+1}^\dagger,\psi_i)} \, \mathrm{e}^{-\int \mathrm{d}^d x \psi_i^\dagger(x)\psi_i(x)} \\
&= \lim_{\varepsilon\to 0}\int \prod_{i=0}^{N-1} D\psi_i^\dagger D\psi_i \, \mathrm{e}^{\varepsilon \int \mathrm{d}^d x \partial_0\psi_i^\dagger(x)\psi_i(x)} \, \mathrm{e}^{-\varepsilon \int \mathrm{d}^d x \mathcal{H}(\psi_{i+1}^\dagger,\psi_i)} \\
&= \int D\psi^\dagger D\psi \, \mathrm{e}^{-\int_0^\beta \int \mathrm{d}^d x (\psi^\dagger \partial_0 \psi + \mathcal{H}(\psi^\dagger,\psi))} \\
&= \int D\psi^\dagger D\psi \, \mathrm{e}^{-\int \mathrm{d}^{d+1} x \mathcal{L}(\psi^\dagger,\psi)},
\end{aligned}
\tag{A.8}
$$

where ψ is a function of space-time in the path integral, and $\mathcal{L}(\psi^\dagger,\psi)$ is the Euclidean Lagrangian density

$$
\mathcal{L}(\psi^\dagger,\psi) = \psi^\dagger \partial_0 \psi + \mathcal{H}(\psi^\dagger,\psi). \tag{A.9}
$$

Appendix B

Various Definitions of Majorana Fermions

The term "Majorana fermion" is somewhat overloaded and sometimes can be confusing. For example, many times one can see the statement that there are no 4d Euclidean Majorana fermions [123, 124], but it is also possible to define them through analytical continuation from Minkowski space to Euclidean space [125]. Since this work uses them extensively, we will explain what people usually mean by Majorana fermions and how we use them carefully.

The simplest idea of Majorana fermion comes from that we can split a complex number into two real parts. This idea is most evident when we work with fermion creation/annihilation operators on the lattice, where the Majorana fermion operators γ_i^α are defined through

$$c_i = \frac{1}{2}(\gamma_i^1 - \mathrm{i}\gamma_i^2), \quad c_i^\dagger = \frac{1}{2}(\gamma_i^1 + \mathrm{i}\gamma_i^2). \tag{B.1}$$

The usual fermion commutation relations

$$\{c_i^\dagger, c_j\} = \delta_{ij}, \quad \{c_i, c_j\} = \{c_i^\dagger, c_j^\dagger\} = 0 \tag{B.2}$$

imply that the Majorana operators satisfy the Clifford algebra

$$\{\gamma_i^\alpha, \gamma_j^\beta\} = 2\delta_{ij}\delta_{\alpha\beta}\mathbb{1}. \tag{B.3}$$

In the continuum, however, the term "Majorana fermion" is less clear and can be used in different senses in different contexts. Mathematically, a Majorana fermion is related to real spin representations of the indefinite orthogonal group $\mathrm{O}(p,q)$, or equivalently, real representations of the even subalgebra of the Clifford algebra $\mathrm{Cl}(p,q)$. Physically, on the other hand, Majorana fermion is defined as an eigenstate of the charge conjugation operator, which flips the charge under a U(1) gauge field. Unfortunately, these two notions do not coincide, in particular, in the Euclidean signature. Therefore, we will briefly introduce both definitions and discuss what we mean by Majorana fermions in the following.

B.1 Mathematical Majorana fermions

In the mathematical sense, we are concerned about real spin representations of the even subalgebra of the Clifford algebra $\mathrm{Cl}(p,q)$. A complex, or Dirac representation of a Clifford algebra $\mathrm{Cl}(p,q)$ consists of a complex $2^{\lfloor d/2 \rfloor}$ dimensional vector space (the space of spinors), where $d = p + q$, and matrices γ^μ acting on this space and satisfying

$$\{\gamma^\mu, \gamma^\nu\} = 2\eta^{\mu\nu}\mathbb{1}, \quad \mu, \nu = 1, \cdots, d, \tag{B.4}$$

where η is a quadratic form of signature (p,q), with p plus signs and q minus signs. We also assume γ^μ to be unitary, i.e., $\gamma^{\mu\dagger}\gamma^\mu = \mathbb{1}$, which implies $\gamma^{\mu\dagger} = \eta^{\mu\mu}\gamma^\mu$ (no summation).

Then the $\mathfrak{so}(p,q)$ algebra is generated by

$$\sigma^{\mu\nu} = -\frac{\mathrm{i}}{4}[\gamma^\mu, \gamma^\nu], \tag{B.5}$$

or equivalently, the $\mathrm{SO}(p,q)$ group is generated by matrices of the form $\mathrm{e}^{\frac{\theta}{2}\gamma^\mu\gamma^\nu}$. Therefore we see that if we can choose the gamma matrices to be all real or all imaginary, then the $\mathrm{SO}(p,q)$ group is real (or more precisely, this representation of $\mathrm{SO}(p,q)$ is

real). Under a real $\mathrm{SO}(p,q)$ group, the complex spinors form a reducible representation, because the real and imaginary spinors will never mix. The real irreducible representation of the $\mathrm{SO}(p,q)$ group is known as Majorana spinors.

It is well known that the reality of γ^μ only depends on $p-q \pmod 8$, and γ^μ can be all real when $p-q \equiv 0,1,2 \pmod 8$, see, for example, [126] or Appendix B in [127]. If we redefine all γ^μ by multiplying an i, the metric $\eta^{\mu\nu}$ would flip sign, and therefore γ^μ can be all imaginary when $p-q \equiv 6,7,0 \pmod 8$. For example, for $\mathrm{Cl}(2,1)$, the gamma matrices can be chosen to be all real in the following way,

$$\gamma^1 = \sigma^1, \quad \gamma^2 = \sigma^3, \quad \gamma^3 = \mathrm{i}\sigma^2, \tag{B.6}$$

and for $\mathrm{Cl}(1,2)$, they can be chosen to be all imaginary,

$$\gamma^1 = \sigma^2, \quad \gamma^2 = \mathrm{i}\sigma^1, \quad \gamma^3 = \mathrm{i}\sigma^3. \tag{B.7}$$

This means we can have Majorana fermions when $p-q \equiv 0,1,2,6,7 \pmod 8$. However, not both cases are compatible with a mass term. If we are given the following massive Dirac equation

$$(\gamma^\mu \partial_\mu - m)\psi = 0, \tag{B.8}$$

In order to have real solutions, γ^μ has to be all real. In other words, when $p-q = 6,7 \pmod 8$, Majorana fermions must be massless and are sometimes called pseudo-Majorana fermions.

B.2 Physical Majorana fermion

In the physical sense, Majorana fermions are defined using charge conjugation [128, 129, 130]. In the following calculation, only transposes of the gamma matrices are used; therefore the signature of the metric is not important.[1] For concreteness, we

[1] Remember that we can change the signature of a Clifford algebra by putting appropriate i in the gamma matrices, which does not affect the symmetry or anti-symmetry property and does not change the commutation relations.

will work in the Euclidean signature. A free fermion with mass m moving in a U(1) background gauge field A_μ has the following Lagrangian,

$$\mathcal{L} = \bar{\psi}(\gamma^\mu \partial_\mu + \mathrm{i}\gamma^\mu A_\mu - m)\psi. \tag{B.9}$$

The field ψ satisfies the Dirac equation

$$(\gamma^\mu \partial_\mu + \mathrm{i}\gamma^\mu A_\mu - m)\psi = 0, \tag{B.10}$$

and the field $\bar{\psi}$ satisfies the equation

$$\bar{\psi}(-\gamma^\mu \partial_\mu + \mathrm{i}\gamma^\mu A_\mu - m) = 0. \tag{B.11}$$

Taking the transpose, we have

$$(-\gamma^{\mu T} \partial_\mu + \mathrm{i}\gamma^{\mu T} A_\mu - m)\bar{\psi}^T = 0. \tag{B.12}$$

If there exists an operator $\mathcal{C}_\pm$ satisfying

$$\mathcal{C}\gamma^\mu \mathcal{C}^{-1} = \lambda \gamma^{\mu T}, \tag{B.13}$$

where $\lambda = \pm 1$, then the equation of motion for ψ can be written as

$$\begin{aligned} (-\lambda^{-1}\mathcal{C}\gamma^\mu \mathcal{C}^{-1}\partial_\mu + \lambda^{-1}\mathrm{i}\mathcal{C}\gamma^\mu \mathcal{C}^{-1} A_\mu - m)\bar{\psi}^T = 0, \\ (\gamma^\mu \partial_\mu - \mathrm{i}\gamma^\mu A_\mu + \lambda m)\mathcal{C}^{-1}\bar{\psi}^T = 0. \end{aligned} \tag{B.14}$$

Therefore when $\lambda = -1$, $\mathcal{C}^{-1}\bar{\psi}^T$ satisfies the same Dirac equation as ψ but with an opposite charge, and can be identified as the anti-particle of ψ. In the case of $m = 0$ and $\lambda = 1$, $\mathcal{C}^{-1}\bar{\psi}^T$ can also be identified as the anti-particle of ψ. Then a physical Majorana fermion is defined as a fermion which is its own anti-particle, i.e., it satisfies

$$\mathcal{C}^{-1}\bar{\psi}^T = \kappa\psi \implies \bar{\psi} = \kappa\psi^T \mathcal{C}^T. \tag{B.15}$$

Inserting this back to the Lagrangian and remembering that Majorana fermions must carry zero charges under a U(1) gauge field, we have

$$\mathcal{L}_{\mathrm{Maj}} = \psi^T \mathcal{C}^T (\gamma^\mu \partial_\mu - m)\psi. \tag{B.16}$$

Due to the anti-commuting property of the Grassmann variables, we must have

$$\left(\mathcal{C}^T(\gamma^\mu\partial_\mu - m)\right)^T = -\mathcal{C}^T(\gamma^\mu\partial_\mu - m), \tag{B.17}$$

which implies

$$\mathcal{C}\gamma^\mu\mathcal{C}^{-1} = -\gamma^{\mu T}, \quad \mathcal{C}^T = -\mathcal{C}. \tag{B.18}$$

In the case of $m = 0$, we have another solution

$$\mathcal{C}\gamma^\mu\mathcal{C}^{-1} = \gamma^{\mu T}, \quad \mathcal{C}^T = \mathcal{C}. \tag{B.19}$$

As we promised, these conditions only involve transpose and are not sensitive to multiplying by an i, or equivalently, the signature of $\eta^{\mu\nu}$. In other words, this condition only depends on the value of $d = p+q$. $\mathcal{C}$ can be chosen to be the product of all symmetric γ^μ or the product of all anti-symmetric γ^μ depending on $d(\mathrm{mod}\,8)$. It turns out that $\mathcal{C}$ satisfying Eq. (B.18) only exists for $d \equiv 2, 3, 4 \pmod 8$, in which case we have Majorana fermions, while $\mathcal{C}$ satisfying Eq. (B.19) only exists for $d \equiv 0, 1, 2 \pmod 8$, in which case we have massless pseudo-Majorana fermions. [131].

Comparing with the mathematical definition of Majorana fermions, we see that they coincide in the Minkowski signature, but not in the Euclidean signature.

B.3 Majorana fermions with internal symmetry

In our case, we wish to split a Dirac fermion into two physical Majorana fermions and discuss the internal symmetry of the theory in the Euclidean signature.

Let us start with the following N_f flavor massless Euclidean Dirac Lagrangian,

$$\mathcal{L} = \sum_{\alpha=1}^{N_f} \bar{\psi}^\alpha\gamma^\mu\partial_\mu\psi^\alpha. \tag{B.20}$$

A Dirac fermion can be split into two Majorana fermions as [129]

$$\psi^\alpha = \xi^{2\alpha-1} - \mathrm{i}\xi^{2\alpha}, \quad \bar{\psi}^\alpha = \kappa\xi^{2\alpha-1T}\mathcal{C}^T + \mathrm{i}\kappa\xi^{2\alpha T}\mathcal{C}^T, \tag{B.21}$$

and the charge conjugation of ψ^α is nothing but $\mathcal{C}^{-1}\bar{\psi}^T = \kappa(\xi^{2\alpha-1} + \mathrm{i}\xi^{2\alpha})$. Then we have the Lagrangian

$$\mathcal{L} = \sum_{\alpha=1}^{2N_f} \xi^{\alpha T}\mathcal{C}^T\gamma^\mu\partial_\mu\xi^\alpha, \tag{B.22}$$

where $\mathcal{C}$ satisfies the Majorana condition Eq. (B.18) or the pseudo-Majorana condition Eq. (B.19) because we did not require a Majorana mass term. From the discussion in the last section, we know that this is possible when $d \equiv 0, 1, 2, 3, 4 \pmod 8$.

An important remark is that Eq. (B.21) should be merely viewed as a change of basis, rather than taking the real and imaginary part of ψ^α. There are three reasons for this statement:

1. In the Euclidean signature, ψ^α and $\bar{\psi}^\alpha$ should be viewed as independent fields, and therefore $\xi^{2\alpha-1}$ and $\xi^{2\alpha}$ are still complex fields.

2. If $\xi^{2\alpha-1}$ and $\xi^{2\alpha}$ are viewed as the real and imaginary part of ψ^α, they will mix under a complex space-time rotation, and it is impossible to define a single Majorana fermion, and

3. If $\xi^{2\alpha-1}$ and $\xi^{2\alpha}$ are viewed as the real and imaginary part of ψ^α, then under a space-time rotation $(\xi^{2\alpha-1} - \mathrm{i}\xi^{2\alpha}) \mapsto U(\xi^{2\alpha-1} - \mathrm{i}\xi^{2\alpha})$, which implies $(\xi^{2\alpha-1T} + \mathrm{i}\xi^{2\alpha T})\mathcal{C}^T \mapsto (\xi^{2\alpha-1T} + \mathrm{i}\xi^{2\alpha T})\mathcal{C}^T U^T$, and the Lagrangian is not invariant unless U is real.

The second and third points need a little more explanation. First, it is important to understand how $\xi^{2\alpha-1}$ and $\xi^{2\alpha}$ transform under $\psi^\alpha \mapsto \mathrm{i}\psi^\alpha$ from these two points of view. If $\xi^{2\alpha-1}$ and $\xi^{2\alpha}$ are viewed as the real and imaginary part of ψ^α, then $(\xi^{2\alpha-1} - \mathrm{i}\xi^{2\alpha}) \mapsto \mathrm{i}(\xi^{2\alpha-1} - \mathrm{i}\xi^{2\alpha})$ implies

$$\begin{pmatrix} \xi^{2\alpha-1} \\ \xi^{2\alpha} \end{pmatrix} \mapsto \begin{pmatrix} 0 & 1 \\ -1 & 0 \end{pmatrix} \begin{pmatrix} \xi^{2\alpha-1} \\ \xi^{2\alpha} \end{pmatrix} = \mathrm{i}\sigma^2 \begin{pmatrix} \xi^{2\alpha-1} \\ \xi^{2\alpha} \end{pmatrix}. \tag{B.23}$$

Therefore a complex space-time rotation will mix different flavors of Majorana fermions, and it is impossible to write down a space-time invariant single Majorana Lagrangian, contradicting the result in the previous section. Furthermore, Eq. (B.23) in turn implies $(\xi^{2\alpha-1T} + \mathrm{i}\xi^{2\alpha T}) \mapsto -\mathrm{i}(\xi^{2\alpha-1T} + \mathrm{i}\xi^{2\alpha T})$. Therefore under a space-time rotation $(\xi^{2\alpha-1} - \mathrm{i}\xi^{2\alpha}) \mapsto U(\xi^{2\alpha-1} - \mathrm{i}\xi^{2\alpha})$, $(\xi^{2\alpha-1T} + \mathrm{i}\xi^{2\alpha T})$ transforms as $(\xi^{2\alpha-1T} + \mathrm{i}\xi^{2\alpha T}) \mapsto (\xi^{2\alpha-1T} + \mathrm{i}\xi^{2\alpha T})U^\dagger$. More concretely, let $U = \mathrm{e}^{\frac{\theta}{2}\gamma^\mu\gamma^\nu}$, then

$$\begin{aligned}(\xi^{2\alpha-1T} + \mathrm{i}\xi^{2\alpha T})U^\dagger\mathcal{C}^T &= (\xi^{2\alpha-1T} + \mathrm{i}\xi^{2\alpha T})\,\mathrm{e}^{-\frac{\theta}{2}\gamma^\mu\gamma^\nu}\,\mathcal{C}^T \\ &= (\xi^{2\alpha-1T} + \mathrm{i}\xi^{2\alpha T})\mathcal{C}^T\,\mathrm{e}^{\frac{\theta}{2}(\gamma^\mu\gamma^\nu)^T} \\ &= (\xi^{2\alpha-1T} + \mathrm{i}\xi^{2\alpha T})\mathcal{C}^T U^T. \end{aligned} \tag{B.24}$$

This means the Lagrangian is only invariant when U is always real, and from the earlier discussion, we know this is not possible in 3d and 4d Euclidean space.

On the other hand, if $\xi^{2\alpha-1}$ and $\xi^{2\alpha}$ are viewed as complex fields, then $(\xi^{2\alpha-1} - \mathrm{i}\xi^{2\alpha}) \mapsto \mathrm{i}(\xi^{2\alpha-1} - \mathrm{i}\xi^{2\alpha})$ simply implies

$$\begin{pmatrix}\xi^{2\alpha-1} \\ \xi^{2\alpha}\end{pmatrix} \mapsto \begin{pmatrix}\mathrm{i}\xi^{2\alpha-1} \\ \mathrm{i}\xi^{2\alpha}\end{pmatrix}, \tag{B.25}$$

which means a complex space-time rotation will not mix different flavors of Majorana fermions, and it is possible to write down a space-time invariant single Majorana Lagrangian. Furthermore, under a complex space-time rotation $U = \mathrm{e}^{\frac{\theta}{2}\gamma^\mu\gamma^\nu}$,

$$\begin{aligned}(\xi^{2\alpha-1T} + \mathrm{i}\xi^{2\alpha T})U^T\mathcal{C}^T &= (\xi^{2\alpha-1T} + \mathrm{i}\xi^{2\alpha T})\,\mathrm{e}^{-\frac{\theta}{2}\gamma^{\mu T}\gamma^{\nu T}}\,\mathcal{C}^T \\ &= (\xi^{2\alpha-1T} + \mathrm{i}\xi^{2\alpha T})\mathcal{C}^T\,\mathrm{e}^{-\frac{\theta}{2}\gamma^\mu\gamma^\nu} \\ &= (\xi^{2\alpha-1T} + \mathrm{i}\xi^{2\alpha T})\mathcal{C}^T U^{-1}, \end{aligned} \tag{B.26}$$

and the Lagrangian is invariant for any space-time rotation U.

Notice that if we were in Minkowski signature, then $\xi^{2\alpha-1}$ and $\xi^{2\alpha}$ should be viewed as the real and imaginary part of ψ^α. However, this does not have the above

complications because the physical Majorana condition coincides with the mathematical Majorana condition, which means whenever we can write down a Majorana Lagrangian using the charge conjugation operator, we have a real representation of the Lorentz group.

Now we are ready to discuss the internal symmetry[2] of the Lagrangian Eq. (B.22). From the above discussion, we know that the space-time rotations do not mix Majorana flavors in both Euclidean and Minkowski signatures, and the symmetry of the Lagrangian is simply $\mathrm{O}(2N_f)$.

B.4 Majorana-Weyl fermions (Physical)

It is well known that Dirac fermion can also be split into Weyl fermions in even dimensions. When the Majorana condition is compatible (or in some sense, commutes) with the Weyl condition, we can have Majorana-Weyl fermions. Since Majorana-Weyl fermions are relevant to our two space-time dimension field theories, we will briefly discuss them here.

Weyl fermions exist because in even dimension d, we can always define a generalized "γ^5" as

$$\gamma^{d+1} = (-\mathrm{i})^{d/2}\gamma^1\gamma^2\cdots\gamma^d. \tag{B.27}$$

$(\gamma^{d+1})^2 = 1$ makes $\frac{1}{2}(1 \pm \gamma^{d+1})$ projectors, and $[\gamma^{d+1}, \sigma^{\mu\nu}]$ means the projectors are preserved by space-time rotations. Therefore the projectors project a Dirac fermion into two irreducible representations of the $\mathrm{O}(d)$ group, i.e., the Weyl fermions. A Majorana-Weyl fermion exists when the projectors project out half of the fields in the Lagrangian

$$\mathcal{L} = \sum_{\alpha=1}^{2N_f} \xi^{\alpha T}\mathcal{C}^T\gamma^\mu\partial_\mu\xi^\alpha. \tag{re B.22}$$

[2] In order to make our point clear, we will not consider the symmetry enhancement due to the existence of Weyl fermions in certain dimensions.

In other words, we need

$$\mathcal{C}^T \gamma^\mu \gamma^{d+1} = \gamma^{d+1T} \mathcal{C}^T \gamma^\mu. \tag{B.28}$$

Since $\{\gamma^{d+1}, \gamma^\mu\} = 0$, this condition can be reduced to

$$\mathcal{C} \gamma^{d+1} \mathcal{C}^{-1} = -\gamma^{d+1T}, \tag{B.29}$$

which is only possible when $d \equiv 2, 6 \pmod 8$ [130, 131]. Notice that this result does not depend on the signature of the metric as well. Together with the Majorana condition, we know a Majorana-Weyl fermion is only possible for $d \equiv 2 \pmod 8$. In our 2d field theory, we chose

$$\mathcal{C} = \sigma^1, \gamma^3 = \sigma^3, \tag{B.30}$$

which satisfies this condition.

Appendix C

Conventions of Lie Algebras

This appendix summarizes some conventions of the semi-simple compact Lie group G and its algebra $\mathfrak{g}$. We will use the "physicist" convention where all elements of $\mathfrak{g}$ can be represented by linear combinations of Hermitian matrices T_r^a (r labels irreps). Let Hermitian matrices T^a, $a = 1, \cdots, \dim(\mathfrak{g})$ be a basis of the defining representation of $\mathfrak{g}$ satisfying

$$\mathrm{tr}(T^a T^b) =: \frac{1}{2}\delta^{ab}. \tag{C.1}$$

Then the *structure constant* f^{abc} is defined as

$$[T^a, T^b] = \mathrm{i} f^{abc} T^c, \tag{C.2}$$

which is real because $\mathrm{i} f^{abc} T^c$ should be anti-Hermitian, and totally anti-symmetric because

$$f^{abc} = -2\mathrm{i}\,\mathrm{tr}([T^a, T^b]T^c). \tag{C.3}$$

The *adjoint representation* $T^a_{\mathbf{adj}}$ is defined as

$$(T^a_{\mathbf{adj}})_{bc} := -\mathrm{i} f^{abc}. \tag{C.4}$$

They form a representation because of the Jacobi identity

$$[T^a,[T^b,T^c]]-[T^b,[T^a,T^c]]=[[T^a,T^b],T^c]. \tag{C.5}$$

A *Killing form* on $\mathfrak{g}$ is a symmetric bilinear form defined as

$$g^{ab}:=\mathrm{tr}(T^a_{\mathbf{adj}}T^b_{\mathbf{adj}}), \tag{C.6}$$

and it is positive definite for simple compact Lie groups. In particular,

$$g^{ab}=\begin{cases} N\delta^{ab} & \text{for SU}(N),\\ \frac{N-2}{2}\delta^{ab} & \text{for SO}(N),\\ (N+1)\delta^{ab} & \text{for Sp}(N). \end{cases} \tag{C.7}$$

In these cases, we can define $g^{ab}=:g\delta^{ab}$. g_{ab} is defined to be the inverse of g^{ab}, i.e., $g_{ab}g^{bc}=\delta^c_a$. For convenience, let us also generalize this definition to an arbitrary irrep r,

$$g^{ab}_r:=\mathrm{tr}(T^a_rT^b_r), \tag{C.8}$$

and g_{rab} and g_r can be defined similarly.

The *quadratic Casimir operator* $C_2(r)$ for an irrep r is usually defined as

$$C_2(r):=g_{ab}T^a_rT^b_r=:c_2(r)\mathbb{1}_r, \tag{C.9}$$

where we have used the fact that $C_2(r)$ is always proportional to identity. Taking trace of both sides, we have

$$c_2(r)=\frac{1}{\dim(r)}g_{ab}\,\mathrm{tr}(T^a_rT^b_r)=\frac{1}{\dim(r)}g_{ab}g^{ab}_r=\frac{\dim(\mathfrak{g})}{\dim(r)}g^{-1}g_r. \tag{C.10}$$

Therefore, for defining representations, we have $c_2=\frac{\dim(\mathfrak{g})}{2\dim(r)}g^{-1}$, leading to

$$c_2=\begin{cases} \frac{N^2-1}{2N^2} & \text{for SU}(N),\\ \frac{N-1}{2(N-2)} & \text{for SO}(N),\\ \frac{2N+1}{4(N+1)} & \text{for Sp}(N), \end{cases} \tag{C.11}$$

and for adjoint representations, we simply have $c_2(\mathbf{adj})=\frac{\dim(\mathfrak{g})}{\dim(\mathfrak{g})}=1$.

In the above conventional Killing form, the squared length of the highest root is $\frac{1}{h^\vee}$, where $h^\vee$ is the dual Coxeter number and can be calculated as

$$h^\vee = \begin{cases} N & \text{for SU}(N), \\ N-2 & \text{for SO}(N), N \geq 4, \\ N+1 & \text{for Sp}(N). \end{cases} \tag{C.12}$$

In the field of physics and affine Lie algebra, it is usually convenient to normalize the Killing form as $g'^{ab} = \frac{1}{2h^\vee} g^{ab}$, such that the squared length of the maximal root is 2 [83], i.e.,

$$g'^{ab} = \begin{cases} \frac{1}{2}\delta^{ab} & \text{for SU}(N), \\ \frac{1}{4}\delta^{ab} & \text{for SO}(N), N \geq 4, \\ \frac{1}{2}\delta^{ab} & \text{for Sp}(N). \end{cases} \tag{C.13}$$

Now the quadratic Casimir operator is defined as

$$C_2'(r) := g'_{ab} T_r^a T_r^b =: c_2'(r) \mathbb{1}_r. \tag{C.14}$$

For the defining representation, we have

$$c_2' = \begin{cases} \frac{N^2-1}{N} & \text{for SU}(N), \\ N-1 & \text{for SO}(N), N \geq 4, \\ \frac{2N+1}{2} & \text{for Sp}(N), \end{cases} \tag{C.15}$$

while for the adjoint representation, we have

$$c_2'(\mathbf{adj}) = \begin{cases} 2N & \text{for SU}(N), \\ 2(N-2) & \text{for SO}(N), N \geq 4, \\ 2(N-1) & \text{for Sp}(N). \end{cases} \tag{C.16}$$

Appendix D

Divergent Loop Integrals

In this appendix, we calculate some divergent integrals used in Chapter 6. We will first review some general formulae, and then calculate these integrals. We will also discuss a formula used extensively in dimensional regularization.

D.1 Some general formulae

We will first simplify the loop integrals, which are usually of the form

$$\int \frac{\mathrm{d}^d k}{(2\pi)^d}\big(f_0(k^2) + k_\mu f_1(k^2) + k_\mu k_\nu f_2(k^2) + \cdots\big), \tag{D.1}$$

where we use k to denote both a d-dimensional vector and the length of this vector. The first integrand is rotationally invariant, and thus the d dimensional integral can be simplified to a one-dimensional integral,

$$\int \frac{\mathrm{d}^d k}{(2\pi)^d} f_0(k^2) = \int \frac{\frac{2\pi^{d/2}}{\Gamma(d/2)} k^{d-1}\mathrm{d}k}{(2\pi)^d} f_0(k^2) = \frac{S_d}{2}\int_0^\infty \mathrm{d}k^2\ (k^2)^{d/2-1} f_0(k^2), \tag{D.2}$$

where $S_d := \frac{2}{(4\pi)^{d/2}\Gamma(d/2)}$ is the loop integral factor. In particular, $S_2 = \frac{1}{2\pi}$ and $S_4 = \frac{1}{8\pi^2}$. The second integrand is odd in k, which vanishes upon integration.

Similarly, integration over the third integrand also vanishes unless $\mu = \nu$, which implies it is proportional to $\delta_{\mu\nu}$. Then taking trace over the indices, we arrive at

$$\int \frac{\mathrm{d}^d k}{(2\pi)^d} k_\mu k_\nu f_2(k^2) = \frac{\delta_{\mu\nu}}{d} \int \frac{\mathrm{d}^d k}{(2\pi)^d} k^2 f_2(k^2), \tag{D.3}$$

which reduces the integrand to the first type.

When the integrand contains a product of different propagators, one often uses the Feynman parametrization to simplify it

$$\frac{1}{A_1^{\alpha_1} \cdots A_n^{\alpha_n}} = \frac{\Gamma(\alpha_1 + \cdots + \alpha_n)}{\Gamma(\alpha_1) \cdots \Gamma(\alpha_n)} \int_0^1 \mathrm{d}u_1 \cdots \int_0^1 \mathrm{d}u_n \frac{\delta(1 - \sum_{k=1}^n u_k) u_1^{\alpha_1 - 1} \cdots u_n^{\alpha_n - 1}}{(\sum_{k=1}^n u_k A_k)^{\sum_{k=1}^n \alpha_k}}. \tag{D.4}$$

The most commonly used form is

$$\frac{1}{AB} = \int_0^1 \mathrm{d}u \frac{1}{[uA + (1-u)B]^2}, \tag{D.5}$$

using which we can write

$$\begin{aligned} \frac{1}{k^2(k+p)^2} &= \int_0^1 \mathrm{d}u \frac{1}{[(1-u)k^2 + u(k+p)^2]^2} \\ &= \int_0^1 \mathrm{d}u \frac{1}{[k^2 + 2uk \cdot p + up^2]^2} = \int_0^1 \mathrm{d}u \frac{1}{[(k'^2) + u(1-u)p^2]^2}, \end{aligned} \tag{D.6}$$

where $k' = k + up$.

Then almost all integrals can be reduced to the following form,

$$\int_0^\infty \mathrm{d}x \frac{x^{m-1}}{(x+a)^n} = \frac{\Gamma(m)\Gamma(n-m)}{\Gamma(n)} a^{m-n}, \tag{D.7}$$

which we will prove and discuss at the end of this appendix. Notice that this integral only converges when $0 < m < n$. However, in dimensional regularization, one often analytically continue m and n to the full complex planes through the gamma function, and the continuation contains poles at $m - n = 0, -1, -2, \cdots$. Recall that poles in the dimensional regularization correspond to logarithmic divergences in the cutoff

regularization, which contribute to the renormalization. On the other hand, the remaining infinite pieces in the original integral correspond to power divergences in the cutoff regularization, which does not affect RG flow. We will justify these claims at the end of this appendix.

D.2 Integrals used in the main text

Using the above formulae, we are ready to calculate the integrals $I_1(d, m^2)$, $I_2(d, m^2)$ and $I_3^\mu(d, p, m^2)$ used in the main text. The first integral is

$$I_1(d,m^2) := \int \frac{\mathrm{d}^d k}{(2\pi)^d}\frac{1}{k^2+m^2} = \frac{S_d}{2}\int \mathrm{d}x \frac{x^{d/2-1}}{x+m^2} = \frac{S_d}{2}\frac{\Gamma(\frac{d}{2})\Gamma(1-\frac{d}{2})}{\Gamma(1)} m^{d-2}$$
$$= \begin{cases} -\frac{S_2}{\varepsilon} m^{\varepsilon} & \text{for } d-2=\varepsilon \to 0, \\ -\frac{S_4}{\varepsilon} m^{2-\varepsilon} & \text{for } 4-d=\varepsilon \to 0. \end{cases} \tag{D.8}$$

The second one is

$$I_2(d,m^2) := \int \frac{\mathrm{d}^d k}{(2\pi)^d}\frac{1}{(k^2+m^2)^2} = \frac{S_d}{2}\int \mathrm{d}x \frac{x^{d/2-1}}{(x+m^2)^2} = \frac{S_d}{2}\frac{\Gamma(\frac{d}{2})\Gamma(2-\frac{d}{2})}{\Gamma(2)} m^{d-4}$$
$$= \begin{cases} \frac{S_2}{2} m^{\varepsilon-2} & \text{for } d-2=\varepsilon \to 0, \\ \frac{S_4}{\varepsilon} m^{-\varepsilon} & \text{for } 4-d=\varepsilon \to 0. \end{cases} \tag{D.9}$$

The third one is

$$I_3^\mu(d,p,m^2) := \int \frac{\mathrm{d}^d k}{(2\pi)^d}\frac{k^\mu}{k^2}\frac{1}{(k-p)^2+m^2} = \int_0^1 \mathrm{d}u \int \frac{\mathrm{d}^d k}{(2\pi)^d}\frac{k^\mu + u p^\mu}{[k^2+u(1-u)p^2+um^2]^2}$$
$$= p^\mu \int_0^1 \mathrm{d}u\; u I_2(d, u(1-u)p^2+um^2). \tag{D.10}$$

We will consider two cases:

$$I_3^\mu(d,p,0) = p^\mu p^{d-4}\frac{S_d}{2}\frac{\Gamma(\frac{d}{2})\Gamma(2-\frac{d}{2})}{\Gamma(2)}\int_0^1 \mathrm{d}u\; u[u(1-u)]^{\frac{d-4}{2}} \tag{D.11}$$
$$= p^\mu p^{d-4}\frac{S_d}{2}\frac{\Gamma(\frac{d}{2})\Gamma(2-\frac{d}{2})}{\Gamma(2)}\frac{\Gamma(\frac{d}{2})\Gamma(\frac{d}{2}-1)}{\Gamma(d-1)} = -p^\mu p^{d-4}\frac{S_d}{2}\frac{\Gamma(\frac{d}{2})^3\Gamma(1-\frac{d}{2})}{\Gamma(d-1)}$$

and

$$I_3^\mu(d,0,m^2) = p^\mu m^{d-4}\frac{S_d}{2}\frac{\Gamma(\frac{d}{2})\Gamma(2-\frac{d}{2})}{\Gamma(2)}\int_0^1 \mathrm{d}u\; u^{\frac{d-2}{2}} = p^\mu m^{d-4}\frac{S_d}{d}\Gamma(\frac{d}{2})\Gamma(2-\frac{d}{2}). \tag{D.12}$$

In particular, for $4-d=\varepsilon\to 0$, these two cases coincide, and we have

$$I_3^\mu(4-\varepsilon,p,m^2) = p^\mu m^\varepsilon \frac{S_d}{2\varepsilon}. \tag{D.13}$$

D.3 Proof and discussion of Eq. (D.7)

We first give a simple proof of Eq. (D.7) when $0<m<n$ using integration by part. Then we show that the analytical continuation of Eq. (D.7) to $n\le m$ is equivalent to removing the power divergences in the cutoff, and the poles of the analytical continuation correspond to logarithmic divergences in the cutoff. For convenience, we rescale $x\to ax$ and define $F(m,n)$

$$\int_0^\infty \mathrm{d}x\frac{x^{m-1}}{(x+a)^n} = a^{m-n}\int_0^\infty \mathrm{d}x\frac{x^{m-1}}{(x+1)^n} =: a^{m-n}F(m,n). \tag{D.14}$$

First, consider the case $0<m<n$, where the integral is convergent. Integrating by part, we have

$$\begin{aligned} F(m,n) &= \frac{1}{m-n}\int_0^\infty \frac{x^n}{(x+1)^n}\mathrm{d}x^{m-n} \\ &= \frac{1}{m-n}\frac{x^m}{(x+1)^n}\Big|_0^\infty - \frac{1}{m-n}\int_0^\infty x^{m-n}\mathrm{d}\Big(\frac{x}{x+1}\Big)^n. \end{aligned} \tag{D.15}$$

The first term vanishes when $0<m<n$. For the second term, we do a change of variable $t=\frac{x}{x+1}$,

$$\begin{aligned} -\frac{1}{m-n}\int_0^1 \Big(\frac{t}{1-t}\Big)^{m-n}\mathrm{d}t^n &= -\frac{n}{m-n}\int_0^1 \frac{t^{m-1}}{(1-t)^{m-n}}\mathrm{d}t \\ &= -\frac{n}{m-n}\mathrm{B}(m,n-m+1) \quad \text{when } 0<m<n+1 \\ &= \frac{\Gamma(m)\Gamma(n-m)}{\Gamma(n)}, \end{aligned} \tag{D.16}$$

where $\mathrm{B}(m,n) = \frac{\Gamma(m)\Gamma(n)}{\Gamma(m+n)}$ is the (mathematical) beta function. Therefore, we have

$$F(m,n) = \mathrm{B}(m, n-m) = \frac{\Gamma(m)\Gamma(n-m)}{\Gamma(n)} \quad \text{when } 0 < m < n. \tag{D.17}$$

Now let us consider the case $0 < n < m$, but $m-n$ is not an integer. In this case, the integral is divergent, and therefore we need to introduce a cutoff Λ. In order to emphasize the cutoff dependence, we define

$$F_\Lambda(m,n) := \int_0^\Lambda \mathrm{d}x \frac{x^{m-1}}{(x+1)^n}. \tag{D.18}$$

We would like to show that up to power divergences in Λ, Eq. (D.17) still holds. From Eqs. (D.15) and (D.16), we already know that

$$F_\Lambda(m,n) = \frac{1}{m-n}\frac{\Lambda^m}{(\Lambda+1)^n} - \frac{n}{m-n}\int_0^{\frac{\Lambda}{\Lambda+1}} \frac{t^{m-1}}{(1-t)^{m-n}}\mathrm{d}t. \tag{D.19}$$

Performing an integration by part again to the second term, we have

$$\begin{aligned}
-\frac{n}{m-n}\int_0^{\frac{\Lambda}{\Lambda+1}} \frac{t^{m-1}}{(1-t)^{m-n}}\mathrm{d}t &= \frac{1}{m-n}\int_0^{\frac{\Lambda}{\Lambda+1}} \frac{t^{m-1}}{(1-t)^{m-1}}\mathrm{d}(1-t)^n \\
&= \frac{1}{m-n}\frac{t^{m-1}}{(1-t)^{m-n-1}}\Big|_0^{\frac{\Lambda}{\Lambda+1}} - \frac{1}{m-n}\int_0^{\frac{\Lambda}{\Lambda+1}} (1-t)^n \mathrm{d}\Big(\frac{t}{1-t}\Big)^{m-1} \\
&= \frac{1}{m-n}\frac{\Lambda^{m-1}}{(\Lambda+1)^n} - \frac{m-1}{m-n}\int_0^\Lambda \frac{x^{m-2}}{(x+1)^n}\mathrm{d}x,
\end{aligned} \tag{D.20}$$

where we have changed the variable t back to x in the last step. Notice that the second term in the above equation is nothing but $-\frac{m-1}{m-n}F_\Lambda(m-1,n)$. Therefore we have the following recursion relation

$$F_\Lambda(m,n) = \frac{1}{m-n}\frac{\Lambda^m + \Lambda^{m-1}}{(\Lambda+1)^n} + \frac{m-1}{n-m}F_\Lambda(m-1,n). \tag{D.21}$$

Let s be the smallest integer such that $m - s < n$. Then applying Eq. (D.21)

recursively, we have

$$F_\Lambda(m,n) = \sum_{i=0}^{s-1} \frac{\Gamma(m)}{\Gamma(m-i)} \frac{\Gamma(n-m)}{\Gamma(n-m+i)} \frac{1}{m-i-n} \frac{\Lambda^{m-i}+\Lambda^{m-i-1}}{(\Lambda+1)^n}$$
$$+ \frac{\Gamma(m)}{\Gamma(m-s)} \frac{\Gamma(n-m)}{\Gamma(n-m+s)} F_\Lambda(m-s,n). \tag{D.22}$$

Now $F_\Lambda(m-s,n)$ is convergent when $\Lambda \to \infty$. Therefore using Eq. (D.17), we have

$$F(m,n) = \frac{\Gamma(m)\Gamma(n-m)}{\Gamma(n)} + \text{power divergences in } \Lambda. \tag{D.23}$$

We see that up to power divergences in Λ, $F(m,n)$ equals its analytical continuation from the region where it converges.

Finally, let us consider the case where $n > 0$ and $m - n = s$ is a non-negative integer. From previous discussion, we know that $F_\Lambda(m,n)$ is proportional to $F_\Lambda(m-s,n) = F_\Lambda(n,n)$ up to power divergences in Λ. It can be calculated that

$$\begin{aligned} F_\Lambda(n,n) &= \int_0^\Lambda \frac{x^n}{(x+1)^n} \mathrm{d}\log x \\ &= \frac{x^n \log x}{(x+1)^n}\Big|_0^\Lambda - \int_0^\Lambda \log x \ \mathrm{d}\Big(\frac{x}{x+1}\Big)^n \\ &= \frac{\Lambda^n \log\Lambda}{(\Lambda+1)^n} - n\int_0^{\frac{\Lambda}{1-\Lambda}} t^{n-1} \log\frac{t}{1-t} \mathrm{d}t. \end{aligned} \tag{D.24}$$

While the first term is logarithmically divergent, the second term is convergent when $n > 0$. On the other hand, from Eq. (D.17) we see that $F(n-\varepsilon,n) \propto \frac{1}{\varepsilon}+\text{reg}$. This suggests that the logarithmic divergence in $F_\Lambda(n,n)$ corresponds to the pole of $F(n-\varepsilon,n)$ at $\varepsilon = 0$. Adding the power divergences in Λ, we get back to $F_\Lambda(m,n)$. Therefore when $m-n$ is a non-negative integer, the logarithmic divergence in $F_\Lambda(m,n)$ corresponds to the pole of the analytical continuation of $F(m-\varepsilon,n)$ at $\varepsilon = 0$.

Appendix E

$2+\varepsilon$ Expansion

In this appendix, we will calculate the β function and the anomalous dimensions of the Ising GN model in $2+\varepsilon$ dimension using renormalized perturbation theory, which can be generalized to the SO(4). Similar to the $4-\varepsilon$ expansion, the fields and couplings with subscript 0 are the bare ones, and those without subscript 0 are the renormalized ones.

The Lagrangian of the Ising GN model is

$$\mathcal{L} = \bar{\psi}_0 \gamma^\mu \partial_\mu \psi_0 + m_0 \bar{\psi}_0 \psi_0 - \frac{g_0^2}{2} (\bar{\psi}_0 \psi_0)^2, \tag{E.1}$$

where we have suppressed the flavor index α for simplicity, and the path integral is

$$Z = \int D\psi_0 D\bar{\psi}_0 \ \mathrm{e}^{-\int \mathrm{d}^{2+\varepsilon} x \mathcal{L}[\psi_0, \bar{\psi}_0]}. \tag{E.2}$$

In $2+\varepsilon$ dimension, the bare fields and couplings have dimensions $[\psi_0] = \frac{1+\varepsilon}{2}$ and $[g_0^2] = -\varepsilon$. The renormalized Lagrangian can be written as

$$\begin{aligned}
\mathcal{L} &= Z_\psi \bar{\psi} \gamma^\mu \partial_\mu \psi + Z_\psi m_0 \bar{\psi} \psi - \frac{1}{2} Z_\psi^2 g_0^2 (\bar{\psi}\psi)^2 \\
&=: \bar{\psi} \gamma^\mu \partial_\mu \psi + m \bar{\psi} \psi - \frac{1}{2} m^{-\varepsilon} g^2 (\bar{\psi}\psi)^2 - \delta_\psi \bar{\psi} \gamma^\mu \partial_\mu \psi + \delta_m \bar{\psi} \psi - \frac{1}{2} m^{-\varepsilon} \delta_{g^2} (\bar{\psi}\psi)^2,
\end{aligned} \tag{E.3}$$

where we define

$$Z_\psi = 1 + \delta_\psi, \quad Z_\psi m_0 = m + \delta_m, \quad Z_\psi^2 g_0^2 = m^{-\varepsilon}(g^2 + \delta_{g^2}), \tag{E.4}$$

and introduce the renormalized couplings m, g. From the Lagrangian, we can read the free propagator in the momentum space

$$\int \mathrm{d}^{2+\varepsilon}x \ \langle \psi^\alpha(x)\bar{\psi}^\beta(0)\rangle \, \mathrm{e}^{\mathrm{i}kx} = \frac{\delta^{\alpha\beta}}{-i\not{k} + m} = \frac{(i\not{k} + m)\delta^{\alpha\beta}}{k^2 + m^2}. \tag{E.5}$$

Mass and wave function renormalization

At one loop order, the two-point fermion loop does not depend on the external momenta; therefore, it only contributes to δ_m but not δ_ψ. There are two types of contractions,

$$m^{-\varepsilon} g^2 \bar{\psi}^\alpha \overbrace{\psi^\alpha \bar{\psi}^\beta} \psi^\beta = g^2 N_f M_{-\circ} \bar{\psi}^\beta \psi^\beta, \tag{E.6}$$

where

$$M_{-\circ} = -m^{-\varepsilon} \int \frac{\mathrm{d}^{2+\varepsilon}k}{(2\pi)^{2+\varepsilon}} \frac{\mathrm{tr}(i\not{k} + m)}{k^2 + m^2} = -4m^{1-\varepsilon} I_1(2+\varepsilon, m^2) = 4m\frac{S_d}{\varepsilon}. \tag{E.7}$$

and

$$m^{-\varepsilon} g^2 \bar{\psi}^\alpha \psi^\alpha \overbrace{\bar{\psi}^\beta \psi^\beta} = g^2 M_{\bigcirc}^{ab} \bar{\psi}_a^\alpha \psi_b^\alpha, \tag{E.8}$$

where

$$M_{\bigcirc}^{ab} = m^{-\varepsilon} \int \frac{\mathrm{d}^{2+\varepsilon}k}{(2\pi)^{2+\varepsilon}} \frac{(i\not{k} + m)^{ab}}{k^2 + m^2} = -\frac{1}{4} M_{-\circ} \delta^{ab} = -m\frac{S_d}{\varepsilon}\delta^{ab}. \tag{E.9}$$

This divergence should be canceled by the counter term δ_m,

$$\delta_m = (4N_f - 1) m g^2 \frac{S_d}{\varepsilon}. \tag{E.10}$$

Interaction renormalization

In order to determine δ_{g^2}, we need to calculate the divergent part of the fermion loop. There are four inequivalent ways of contraction. The first contraction is

$$\frac{1}{2} m^{-2\varepsilon} g^4 (\overbrace{\bar{\psi}^\alpha \overbrace{\psi^\alpha \bar{\psi}^\beta} \psi^\beta}) (\overbrace{\bar{\psi}^\gamma \psi^\gamma} \bar{\psi}^\delta \psi^\delta) = g^4 N_f V_{\bigcirc} \bar{\psi}^\beta \psi^\beta \bar{\psi}^\delta \psi^\delta, \tag{E.11}$$

where

$$V_{\bigcirc} = -\frac{1}{2}m^{-2\varepsilon}\int\frac{\mathrm{d}^{2+\varepsilon}k}{(2\pi)^{2+\varepsilon}}\frac{\mathrm{tr}((i\not{k}+m)^2)}{(k^2+m^2)^2} = -\frac{1}{2}m^{-2\varepsilon}\int\frac{\mathrm{d}^{2+\varepsilon}k}{(2\pi)^{2+\varepsilon}}\frac{4(-k^2+m^2)}{(k^2+m^2)^2}$$

$$\overset{\lim}{=}_{\varepsilon\to 0}\frac{1}{2}m^{-2\varepsilon}\int\frac{\mathrm{d}^{2+\varepsilon}k}{(2\pi)^{2+\varepsilon}}\frac{4}{(k^2+m^2)} = 2m^{-2\varepsilon}I_1(2+\varepsilon,m^2) = -2m^{-\varepsilon}\frac{S_d}{\varepsilon}. \quad \text{(E.12)}$$

The second contraction is

$$m^{-2\varepsilon}g^4(\bar{\psi}^{\alpha}\psi^{\alpha}\bar{\psi}^{\beta}\psi^{\beta})(\bar{\psi}^{\gamma}\psi^{\gamma}\bar{\psi}^{\delta}\psi^{\delta}) = g^4V_{\triangle}^{ab}\bar{\psi}^{\beta}\psi^{\beta}\bar{\psi}_a^{\gamma}\psi_b^{\gamma}, \quad \text{(E.13)}$$

where

$$V_{\triangle}^{ab} = m^{-2\varepsilon}\int\frac{\mathrm{d}^{2+\varepsilon}k}{(2\pi)^{2+\varepsilon}}\frac{((i\not{k}+m)^2)^{ab}}{(k^2+m^2)^2} = -\frac{1}{2}V_{\bigcirc}\delta^{ab} = m^{-\varepsilon}\frac{S_d}{\varepsilon}\delta^{ab}. \quad \text{(E.14)}$$

The third contraction is

$$\frac{1}{2}m^{-2\varepsilon}g^4(\bar{\psi}^{\alpha}\psi^{\alpha}\bar{\psi}^{\beta}\psi^{\beta})(\bar{\psi}^{\gamma}\psi^{\gamma}\bar{\psi}^{\delta}\psi^{\delta}) = g^4V_{\square}^{abcd}\bar{\psi}_a^{\alpha}\psi_b^{\alpha}\bar{\psi}_c^{\beta}\psi_d^{\beta}, \quad \text{(E.15)}$$

where

$$V_{\square}^{abcd} = \frac{1}{2}m^{-2\varepsilon}\int\frac{\mathrm{d}^{2+\varepsilon}k}{(2\pi)^{2+\varepsilon}}\frac{(i\not{k}+m)^{ab}(-i\not{k}+m)^{cd}}{(k^2+m^2)^2}$$

$$= \frac{1}{4d}V_{\bigcirc}(\gamma^{\mu})^{ab}(\gamma^{\mu})^{cd} = -m^{-\varepsilon}\frac{S_d}{2d\varepsilon}(\gamma^{\mu})^{ab}(\gamma^{\mu})^{cd}, \quad \text{(E.16)}$$

and we have used Eq. (D.3). We see that this contraction results in a Thirring interaction. However, it is canceled by the fourth contraction

$$\frac{1}{2}m^{-2\varepsilon}g^4(\bar{\psi}^{\alpha}\psi^{\alpha}\bar{\psi}^{\beta}\psi^{\beta})(\bar{\psi}^{\gamma}\psi^{\gamma}\bar{\psi}^{\delta}\psi^{\delta}) = -g^4V_{\square}^{abcd}\bar{\psi}_a^{\alpha}\psi_b^{\alpha}\bar{\psi}_c^{\beta}\psi_d^{\beta}, \quad \text{(E.17)}$$

where the minus sign can be understood as that the fermion number flow is reversed in one of the propagators compared with the third contraction. However, this cancellation may not happen in more complex theories, for example, in the SO(4) GN model.

These divergences should be canceled by the counter terms δ_{g^2},

$$\frac{1}{2}\delta_{g^2} = (2N_f-1)g^4\frac{S_d}{\varepsilon}. \quad \text{(E.18)}$$

β functions

From the above calculation, we know that

$$m^{\varepsilon} g_0^2 = Z_\psi^{-2}(g^2 + \delta_{g^2}) = g^2 + 2(2N_f - 1)g^4 \frac{S_d}{\varepsilon}. \tag{E.19}$$

Then using Eq. (6.59) with ε replaced by $-\varepsilon$, we have

$$\beta_{g^2} = \varepsilon g^2 - 2(2N_f - 1)S_d g^4 = \varepsilon g^2 - \frac{(2N_f - 1)}{\pi} g^4. \tag{E.20}$$

This result agrees with Eq. (5.33) when $\varepsilon = 0$. The extra factor of 2 in front of N_f is because here we use four-component Dirac fermions rather than two. Solving the equation $\beta_{g^2} = 0$ gives the fixed point $g^2 = \frac{\pi\varepsilon}{2N_f - 1}$, which is a UV fixed point.

Anomalous dimensions and critical exponents

The anomalous dimension for the field ψ is

$$\gamma_\psi = \frac{1}{2} m \frac{\mathrm{d}}{\mathrm{d}m} \ln Z_\psi = 0. \tag{E.21}$$

Using

$$\frac{m_0}{m} = Z_\psi^{-1}(1 + \frac{\delta_m}{m}) = 1 + (4N_f - 1)g^2 \frac{S_d}{\varepsilon}, \tag{E.22}$$

we can calculate the anomalous dimension of the mass,

$$\gamma_m = \frac{m}{m_0} m \frac{\mathrm{d}}{\mathrm{d}m} \frac{m_0}{m} = \frac{m}{m_0} \beta_{g^2} \frac{\partial}{\partial g^2} \frac{m_0}{m} = \frac{(4N_f - 1)g^2}{2\pi}, \tag{E.23}$$

and $\gamma_{\bar\psi\psi} = -\gamma_m$. The correlation length critical exponent ν is

$$\nu = -\frac{1}{\beta'(g^2)} = -\frac{1}{\varepsilon - 2(2N_f - 1)g^2/\pi}. \tag{E.24}$$

At the fixed point $g^2 = \frac{\pi\varepsilon}{2N_f - 1}$, we have

$$\eta_{\bar\psi\psi} = d - 1 + \gamma_{\bar\psi\psi} = 2 - \frac{1}{4N_f - 2}\varepsilon, \quad \nu = \frac{1}{\varepsilon}. \tag{E.25}$$

Bibliography

[1] S. Sachdev, *Quantum Phase Transitions*. Cambridge University Press, 2 ed., 2011, 10.1017/CBO9780511973765.

[2] L. D. Landau, *On the theory of phase transitions*, *Zh. Eksp. Teor. Fiz.* **7** (1937) 19–32.

[3] L. Landau and E. Lifshitz, *Statistical Physics: Volume 5*. No. v. 5. Elsevier Science, 2013.

[4] K. G. Wilson and J. B. Kogut, *The Renormalization group and the epsilon expansion*, *Phys. Rept.* **12** (1974) 75–199.

[5] M. E. Fisher, *The renormalization group in the theory of critical behavior*, *Rev. Mod. Phys.* **46** (1974) 597–616.

[6] M. B. Hastings and X.-G. Wen, *Quasi-adiabatic continuation of quantum states: The Stability of topological ground state degeneracy and emergent gauge invariance*, *Phys. Rev. B* **72** (2005) 045141, [cond-mat/0503554].

[7] X. Chen, Z. C. Gu and X. G. Wen, *Local unitary transformation, long-range quantum entanglement, wave function renormalization, and topological order*, *Phys. Rev. B* **82** (2010) 155138, [1004.3835].

[8] X. G. Wen, *Topological Order in Rigid States*, *Int. J. Mod. Phys. B* **4** (1990) 239.

[9] X. Chen, Z.-C. Gu, Z.-X. Liu and X.-G. Wen, *Symmetry protected topological orders and the group cohomology of their symmetry group*, *Phys. Rev. B* **87** (2013) 155114, [1106.4772].

[10] A. Vishwanath and T. Senthil, *Physics of three dimensional bosonic topological insulators: Surface Deconfined Criticality and Quantized Magnetoelectric Effect*, *Phys. Rev. X* **3** (2013) 011016, [1209.3058].

[11] D. V. Else and C. Nayak, *Classifying symmetry-protected topological phases through the anomalous action of the symmetry on the edge*, *Phys. Rev. B* **90** (2014) 235137, [1409.5436].

[12] V. Ayyar and S. Chandrasekharan, *Massive fermions without fermion bilinear condensates*, *Phys. Rev. D* **91** (2015) 065035, [1410.6474].

[13] S. Catterall, *Fermion mass without symmetry breaking*, *JHEP* **01** (2016) 121, [1510.04153].

[14] V. Ayyar and S. Chandrasekharan, *Fermion masses through four-fermion condensates*, *JHEP* **10** (2016) 058, [1606.06312].

[15] Y.-Z. You, Y.-C. He, C. Xu and A. Vishwanath, *Symmetric Fermion Mass Generation as Deconfined Quantum Criticality*, *Phys. Rev. X* **8** (2018) 011026, [1705.09313].

[16] Y.-Z. You, Y.-C. He, A. Vishwanath and C. Xu, *From Bosonic Topological Transition to Symmetric Fermion Mass Generation*, *Phys. Rev. B* **97** (2018) 125112, [1711.00863].

[17] J. Wang and Y.-Z. You, *Symmetric Mass Generation*, 2204.14271.

[18] T. Senthil, A. Vishwanath, L. Balents, S. Sachdev and M. P. A. Fisher, *Deconfined Quantum Critical Points*, *Science* **303** (2004) 1490–1494, [cond-mat/0311326].

[19] T. Senthil, L. Balents, S. Sachdev, A. Vishwanath and M. P. A. Fisher, *Quantum criticality beyond the landau-ginzburg-wilson paradigm*, *Phys. Rev. B* **70** (Oct, 2004) 144407.

[20] T. Senthil and M. P. A. Fisher, *Competing orders, nonlinear sigma models, and topological terms in quantum magnets*, *Phys. Rev. B* **74** (Aug, 2006) 064405.

[21] A. Nahum, P. Serna, J. T. Chalker, M. Ortuño and A. M. Somoza, *Emergent SO(5) Symmetry at the Néel to Valence-Bond-Solid Transition*, *Phys. Rev. Lett.* **115** (2015) 267203, [1508.06668].

[22] C. Wang, A. Nahum, M. A. Metlitski, C. Xu and T. Senthil, *Deconfined quantum critical points: symmetries and dualities*, *Phys. Rev. X* **7** (2017) 031051, [1703.02426].

[23] J. McGreevy, *Generalized Symmetries in Condensed Matter*, 2204.03045.

[24] D. Gaiotto, A. Kapustin, N. Seiberg and B. Willett, *Generalized Global Symmetries*, *JHEP* **02** (2015) 172, [1412.5148].

[25] D. Gaiotto, A. Kapustin, Z. Komargodski and N. Seiberg, *Theta, Time Reversal, and Temperature*, *JHEP* **05** (2017) 091, [1703.00501].

[26] T. Lan, L. Kong and X.-G. Wen, *Theory of (2+1)-dimensional fermionic topological orders and fermionic/bosonic topological orders with symmetries*, *Phys. Rev. B* **94** (2016) 155113, [1507.04673].

[27] W. Ji and X.-G. Wen, *Categorical symmetry and noninvertible anomaly in symmetry-breaking and topological phase transitions*, *Phys. Rev. Res.* **2** (2020) 033417, [1912.13492].

[28] C.-M. Chang, Y.-H. Lin, S.-H. Shao, Y. Wang and X. Yin, *Topological Defect Lines and Renormalization Group Flows in Two Dimensions*, *JHEP* **01** (2019) 026, [1802.04445].

[29] X.-G. Wen, *Emergent anomalous higher symmetries from topological order and from dynamical electromagnetic field in condensed matter systems*, *Phys. Rev. B* **99** (2019) 205139, [1812.02517].

[30] G. 't Hooft, *Naturalness, chiral symmetry, and spontaneous chiral symmetry breaking*, *NATO Sci. Ser. B* **59** (1980) 135–157.

[31] C.-M. Jian, Z. Bi and C. Xu, *Lieb-Schultz-Mattis Theorem and its generalizations from the Perspective of the Symmetry Protected Topological phase*, *Phys. Rev. B* **97** (2018) 054412, [1705.00012].

[32] E. H. Lieb, T. Schultz and D. Mattis, *Two soluble models of an antiferromagnetic chain*, *Annals Phys.* **16** (1961) 407–466.

[33] M. Oshikawa, *Commensurability, excitation gap, and topology in quantum many-particle systems on a periodic lattice*, *Physical Review Letters* **84** (feb, 2000) 1535–1538.

[34] M. B. Hastings, *Lieb-Schultz-Mattis in higher dimensions*, *Phys. Rev. B* **69** (2004) 104431, [cond-mat/0305505].

[35] M. Cheng, M. Zaletel, M. Barkeshli, A. Vishwanath and P. Bonderson, *Translational Symmetry and Microscopic Constraints on Symmetry-Enriched Topological Phases: A View from the Surface*, *Phys. Rev. X* **6** (2016) 041068, [1511.02263].

[36] G. Y. Cho, S. Ryu and C.-T. Hsieh, *Anomaly Manifestation of Lieb-Schultz-Mattis Theorem and Topological Phases*, *Phys. Rev. B* **96** (2017) 195105, [1705.03892].

[37] M. Cheng, *Fermionic Lieb-Schultz-Mattis theorems and weak symmetry-protected phases*, *Phys. Rev. B* **99** (2019) 075143, [1804.10122].

[38] D. V. Else and R. Thorngren, *Topological theory of Lieb-Schultz-Mattis theorems in quantum spin systems*, *Phys. Rev. B* **101** (2020) 224437, [1907.08204].

[39] H. Tasaki, *The Lieb-Schultz-Mattis Theorem: A Topological Point of View*, 2202.06243.

[40] K. Binder, *Applications of monte carlo methods to statistical physics*, *Reports on Progress in Physics* **60** (1997) 487.

[41] E. Y. Loh, J. E. Gubernatis, R. T. Scalettar, S. R. White, D. J. Scalapino and R. L. Sugar, *Sign problem in the numerical simulation of many-electron systems*, *Phys. Rev.* **B41** (1990) 9301–9307.

[42] J. B. Kogut and L. Susskind, *Hamiltonian Formulation of Wilson's Lattice Gauge Theories*, *Phys. Rev. D* **11** (1975) 395–408.

[43] E. Huffman and S. Chandrasekharan, *Fermion bag approach to Hamiltonian lattice field theories in continuous time*, *Phys. Rev. D* **96** (2017) 114502, [1709.03578].

[44] E. Huffman and S. Chandrasekharan, *Fermion-bag inspired Hamiltonian lattice field theory for fermionic quantum criticality*, *Phys. Rev. D* **101** (2020) 074501, [1912.12823].

[45] S. Chandrasekharan and U.-J. Wiese, *Meron cluster solution of a fermion sign problem*, *Phys. Rev. Lett.* **83** (1999) 3116–3119, [cond-mat/9902128].

[46] S. Chandrasekharan, J. Cox, J. C. Osborn and U. J. Wiese, *Meron cluster approach to systems of strongly correlated electrons*, *Nucl. Phys.* **B673** (2003) 405–436, [cond-mat/0201360].

[47] S. Chandrasekharan and J. C. Osborn, *Kosterlitz-Thouless universality in a fermionic system*, *Phys. Rev. B* **66** (2002) 045113, [cond-mat/0109424].

[48] R. K. Kaul, R. G. Melko and A. W. Sandvik, *Bridging lattice-scale physics and continuum field theory with quantum Monte Carlo simulations*, *Ann. Rev. Condensed Matter Phys.* **4** (2013) 179, [1204.5405].

[49] I. F. Herbut, V. Juričić and B. Roy, *Theory of interacting electrons on the honeycomb lattice*, *Physical Review B* **79** (Feb, 2009) .

[50] E. Fermi, *An attempt of a theory of beta radiation. 1.*, *Z. Phys.* **88** (1934) 161–177.

[51] D. J. Gross and A. Neveu, *Dynamical Symmetry Breaking in Asymptotically Free Field Theories*, *Phys. Rev.* **D10** (1974) 3235.

[52] W. E. Thirring, *A Soluble relativistic field theory*, *Annals Phys.* **3** (1958) 91–112.

[53] I. F. Herbut, *Interactions and phase transitions on graphene's honeycomb lattice*, *Phys. Rev. Lett.* **97** (2006) 146401, [cond-mat/0606195].

[54] S. Sorella, Y. Otsuka and S. Yunoki, *Absence of a spin liquid phase in the hubbard model on the honeycomb lattice*, *Scientific Reports* **2** (Dec, 2012) .

[55] O. Vafek and A. Vishwanath, *Dirac Fermions in Solids: From High-Tc cuprates and Graphene to Topological Insulators and Weyl Semimetals*, *Ann. Rev. Condensed Matter Phys.* **5** (2014) 83–112, [1306.2272].

[56] J. A. Gracey, *Generalized Gross-Neveu universality class with non-abelian symmetry*, 2102.12767.

[57] S. Ryu, C. Mudry, C.-Y. Hou and C. Chamon, *Masses in graphenelike two-dimensional electronic systems: Topological defects in order parameters and their fractional exchange statistics*, *Physical Review B* **80** (Nov, 2009) .

[58] M. Gomes, R. S. Mendes, R. F. Ribeiro and A. J. da Silva, *Gauge structure, anomalies and mass generation in a three-dimensional Thirring model*, *Phys. Rev. D* **43** (1991) 3516–3523.

[59] S. Christofi, S. Hands and C. Strouthos, *Critical flavor number in the three dimensional Thirring model*, *Phys. Rev. D* **75** (2007) 101701, [hep-lat/0701016].

[60] L. Janssen and H. Gies, *Critical behavior of the (2+1)-dimensional Thirring model*, *Phys. Rev. D* **86** (2012) 105007, [1208.3327].

[61] B. H. Wellegehausen, D. Schmidt and A. Wipf, *Critical flavor number of the Thirring model in three dimensions*, *Phys. Rev. D* **96** (2017) 094504, [1708.01160].

[62] S. Hands, *Critical flavor number in the 2+1D Thirring model*, *Phys. Rev. D* **99** (2019) 034504, [1811.04818].

[63] A. W. Wipf and J. J. Lenz, *Symmetries of Thirring Models on 3D Lattices*, *Symmetry* **14** (2022) 333, [2201.01692].

[64] B. Rosenstein, B. Warr and S. H. Park, *Dynamical symmetry breaking in four Fermi interaction models*, *Phys. Rept.* **205** (1991) 59–108.

[65] J. Zinn-Justin, *Four fermion interaction near four-dimensions*, *Nucl. Phys. B* **367** (1991) 105–122.

[66] A. H. Castro Neto, F. Guinea, N. M. R. Peres, K. S. Novoselov and A. K. Geim, *The electronic properties of graphene*, *Rev. Mod. Phys.* **81** (2009) 109–162, [0709.1163].

[67] E. F. Huffman and S. Chandrasekharan, *Solution to sign problems in half-filled spin-polarized electronic systems*, *Phys. Rev. B* **89** (2014) 111101, [1311.0034].

[68] Z.-X. Li, S.-K. Jian and H. Yao, *Deconfined quantum criticality and emergent SO(5) symmetry in fermionic systems*, 1904.10975.

[69] S. L. Adler, *Axial vector vertex in spinor electrodynamics*, *Phys. Rev.* **177** (1969) 2426–2438.

[70] J. S. Bell and R. Jackiw, *A PCAC puzzle: $\pi^0 \to \gamma\gamma$ in the σ model*, *Nuovo Cim. A* **60** (1969) 47–61.

[71] K. Fujikawa, *Path Integral Measure for Gauge Invariant Fermion Theories*, *Phys. Rev. Lett.* **42** (1979) 1195–1198.

[72] K. Fujikawa, *Path Integral for Gauge Theories with Fermions*, *Phys. Rev. D* **21** (1980) 2848.

[73] A. A. Belavin, A. M. Polyakov and A. B. Zamolodchikov, *Infinite Conformal Symmetry in Two-Dimensional Quantum Field Theory*, *Nucl. Phys. B* **241** (1984) 333–380.

[74] E. Witten, *Nonabelian Bosonization in Two-Dimensions*, *Commun. Math. Phys.* **92** (1984) 455–472.

[75] V. G. Knizhnik and A. B. Zamolodchikov, *Current Algebra and Wess-Zumino Model in Two-Dimensions*, *Nucl. Phys.* **B247** (1984) 83–103.

[76] J. S. Schwinger, *Field theory commutators*, *Phys. Rev. Lett.* **3** (1959) 296–297.

[77] E. Fradkin, *Field Theories of Condensed Matter Physics*. Cambridge University Press, 2 ed., 2013, 10.1017/CBO9781139015509.

[78] A. Gogolin, A. Nersesyan and A. Tsvelik, *Bosonization and Strongly Correlated Systems*. Cambridge University Press, 2004.

[79] I. Affleck and A. W. W. Ludwig, *Critical theory of overscreened Kondo fixed points*, *Nucl. Phys. B* **360** (1991) 641–696.

[80] I. Affleck, *FIELD THEORY METHODS AND QUANTUM CRITICAL PHENOMENA*, in *Les Houches Summer School in Theoretical Physics: Fields, Strings, Critical Phenomena Les Houches, France, June 28-August 5, 1988*, pp. 0563–640, 1988.

[81] W. Wetzel, *Two Loop Beta Function for the Gross-Neveu Model*, *Phys. Lett. B* **153** (1985) 297–299.

[82] M. Fishman, S. R. White and E. M. Stoudenmire, *The ITensor software library for tensor network calculations*, 2020.

[83] P. Di Francesco, P. Mathieu and D. Senechal, *Conformal Field Theory*. Graduate Texts in Contemporary Physics. Springer-Verlag, New York, 1997, 10.1007/978-1-4612-2256-9.

[84] A. B. Zamolodchikov and V. A. Fateev, *Operator Algebra and Correlation Functions in the Two-Dimensional Wess-Zumino SU(2) x SU(2) Chiral Model*, *Sov. J. Nucl. Phys.* **43** (1986) 657–664.

[85] D. Gepner and E. Witten, *String Theory on Group Manifolds*, *Nucl. Phys.* **B278** (1986) 493–549.

[86] I. Affleck, *Field Theory Methods and Strongly Correlated Electrons*, pp. 1–13. Springer US, Boston, MA, 1990. 10.1007/978-1-4615-3802-8_1.

[87] A. M. Tsvelik, *Quantum Field Theory in Condensed Matter Physics*. Cambridge University Press, 2 ed., 2003, 10.1017/CBO9780511615832.

[88] J. L. Cardy, *Conformal invariance and universality in finite-size scaling*, *J. Phys. A* **17** (1984) L385–L387.

[89] I. Affleck, D. Gepner, H. J. Schulz and T. Ziman, *Critical Behavior of Spin S Heisenberg Antiferromagnetic Chains: Analytic and Numerical Results*, *J. Phys.* **A22** (1989) 511.

[90] S. Eggert, *Numerical evidence for multiplicative logarithmic corrections from marginal operators*, *Phys. Rev.* **B54** (1996) R9612, [cond-mat/9602026].

[91] I. Affleck, *Exact correlation amplitude for the heisenberg antiferromagnetic chain*, *Journal of Physics A: Mathematical and General* **31** (may, 1998) 4573–4581.

[92] K. G. Wilson and M. E. Fisher, *Critical exponents in 3.99 dimensions*, *Phys. Rev. Lett.* **28** (1972) 240–243.

[93] S. Chandrasekharan and A. Li, *Quantum critical behavior in three dimensional lattice Gross-Neveu models*, *Phys. Rev. D* **88** (2013) 021701, [1304.7761].

[94] Z.-X. Li, Y.-F. Jiang and H. Yao, *Solving the fermion sign problem in quantum Monte Carlo simulations by Majorana representation*, *Phys. Rev. B* **91** (2015) 241117, [1408.2269].

[95] L. Wang, M. Iazzi, P. Corboz and M. Troyer, *Efficient Continuous-time Quantum Monte Carlo Method for the Ground State of Correlated Fermions*, *Phys. Rev. B* **91** (2015) 235151, [1501.00986].

[96] S. Hesselmann and S. Wessel, *Thermal Ising transitions in the vicinity of two-dimensional quantum critical points*, *Phys. Rev. B* **93** (2016) 155157, [1602.02096].

[97] I. F. Herbut and M. M. Scherer, *SO(4) multicriticality of two-dimensional Dirac fermions*, 2206.04073.

[98] J. Zinn-Justin, *Quantum Field Theory and Critical Phenomena*. International series of monographs on physics. Clarendon Press, 2002.

[99] N. V. Prokof'ev and B. V. Svistunov, *Polaron problem by diagrammatic quantum monte carlo*, *Phys. Rev. Lett.* **81** (Sep, 1998) 2514–2517.

[100] A. N. Rubtsov, V. V. Savkin and A. I. Lichtenstein, *Continuous-time quantum monte carlo method for fermions*, *Phys. Rev. B* **72** (Jul, 2005) 035122.

[101] P. Werner, A. Comanac, L. de' Medici, M. Troyer and A. J. Millis, *Continuous-time solver for quantum impurity models*, *Phys. Rev. Lett.* **97** (Aug, 2006) 076405.

[102] M. Iazzi and M. Troyer, *Efficient continuous-time quantum monte carlo algorithm for fermionic lattice models*, *Physical Review B* **91** (Jun, 2015) .

[103] E. Burovski, E. Kozik, N. Prokof'ev, B. Svistunov and M. Troyer, *Critical temperature curve in bec-bcs crossover*, *Physical Review Letters* **101** (Aug, 2008) .

[104] O. Goulko and M. Wingate, *Thermodynamics of balanced and slightly spin-imbalanced fermi gases at unitarity*, *Phys. Rev. A* **82** (Nov, 2010) 053621.

[105] H. G. Evertz, G. Lana and M. Marcu, *Cluster algorithm for vertex models*, *Phys. Rev. Lett.* **70** (1993) 875–879, [cond-mat/9211006].

[106] B. Beard and U.-J. Wiese, *Simulations of discrete quantum systems in continuous Euclidean time*, *Phys. Rev. Lett.* **77** (1996) 5130–5133, [cond-mat/9602164].

[107] T. Hikihara, A. Furusaki and S. Lukyanov, *Dimer correlation amplitudes and dimer excitation gap in spin-$\frac{1}{2}$ xxz and heisenberg chains*, *Phys. Rev. B* **96** (Oct, 2017) 134429.

[108] T. Vekua and G. Sun, *Exact asymptotic correlation functions of bilinear spin operators of the heisenberg antiferromagnetic spin-$\frac{1}{2}$ chain*, *Phys. Rev. B* **94** (Jul, 2016) 014417.

[109] K. Okamoto and K. Nomura, *Fluid-dimer critical point in s = 12 antiferromagnetic heisenberg chain with next nearest neighbor interactions*, *Physics Letters A* **169** (1992) 433 – 437.

[110] Y. Li, J. Lu and Z. Wang, *Coordinatewise descent methods for leading eigenvalue problem*, *SIAM Journal on Scientific Computing* **41** (2019) A2681–A2716, [https://doi.org/10.1137/18M1202505].

[111] Z. Wang, Y. Li and J. Lu, *Coordinate descent full configuration interaction*, *Journal of Chemical Theory and Computation* **15** (2019) 3558–3569, [https://doi.org/10.1021/acs.jctc.9b00138].

[112] H. Liu, *Quantum Critical Phenomena in an $O(4)$ Fermion Chain*, in *37th International Symposium on Lattice Field Theory (Lattice 2019) Wuhan, Hubei, China, June 16-22, 2019*, 2019. 1912.11237.

[113] M. Karbach, K. Hu and G. Müller, *Introduction to the bethe ansatz ii*, *Computers in Physics* **12** (1998) 565–573, [https://aip.scitation.org/doi/pdf/10.1063/1.168740].

[114] R. Blankenbecler, D. J. Scalapino and R. L. Sugar, *Monte Carlo Calculations of Coupled Boson - Fermion Systems. 1.*, *Phys. Rev. D* **24** (1981) 2278.

[115] S. V. Isakov, R. G. Melko and M. B. Hastings, *Universal signatures of fractionalized quantum critical points*, *Science* **335** (Jan, 2012) 193–195.

[116] L. Janssen and I. F. Herbut, *Antiferromagnetic critical point on graphene's honeycomb lattice: A functional renormalization group approach*, *Physical Review B* **89** (May, 2014) .

[117] I. Boettcher and I. F. Herbut, *Superconducting quantum criticality in three-dimensional luttinger semimetals*, *Physical Review B* **93** (May, 2016) .

[118] H. Liu, S. Chandrasekharan and R. K. Kaul, *Hamiltonian models of lattice fermions solvable by the meron-cluster algorithm*, *Phys. Rev. D* **103** (2021) 054033, [2011.13208].

[119] A. G. Abanov and P. B. Wiegmann, *Theta terms in nonlinear sigma models*, *Nucl. Phys. B* **570** (2000) 685–698, [hep-th/9911025].

[120] A. G. Abanov, *Hopf term induced by fermions*, *Phys. Lett. B* **492** (2000) 321–323, [hep-th/0005150].

[121] R. P. Feynman, *The principle of least action in quantum mechanics*. PhD thesis, Princeton U., 1942. 10.1142/9789812567635_0001.

[122] R. Shankar, *Quantum Field Theory and Condensed Matter: An Introduction*. Cambridge University Press, 2017, 10.1017/9781139044349.

[123] J. Schwinger, *Euclidean Quantum Electrodynamics*, *Phys. Rev.* **115** (1959) 721–731.

[124] B. Zumino, *Euclidean Supersymmetry and the Many-Instanton Problem*, *Phys. Lett. B* **69** (1977) 369.

[125] K. Osterwalder and R. Schrader, *AXIOMS FOR EUCLIDEAN GREEN'S FUNCTIONS*, *Commun. Math. Phys.* **31** (1973) 83–112.

[126] P. G. O. Freund, *Introduction to Supersymmetry*. Cambridge Monographs on Mathematical Physics. Cambridge University Press, 1986, 10.1017/CBO9780511564017.

[127] J. Polchinski, *String Theory*, vol. 2 of *Cambridge Monographs on Mathematical Physics*. Cambridge University Press, 1998, 10.1017/CBO9780511618123.

[128] H. Nicolai, *A Possible constructive approach to (SUPER phi**3) in four-dimensions. 1. Euclidean formulation of the model*, *Nucl. Phys. B* **140** (1978) 294–300.

[129] T. Inagaki and H. Suzuki, *Majorana and Majorana-Weyl fermions in lattice gauge theory*, *JHEP* **07** (2004) 038, [hep-lat/0406026].

[130] C. Wetterich, *Spinors in euclidean field theory, complex structures and discrete symmetries*, *Nucl. Phys. B* **852** (2011) 174–234, [1002.3556].

[131] M. Stone, *Gamma matrices, Majorana fermions, and discrete symmetries in Minkowski and Euclidean signature*, 2009.00518.